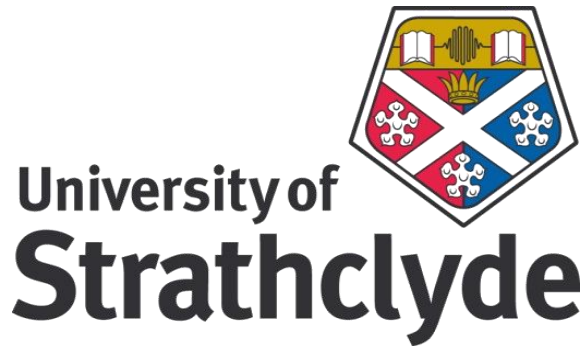

Strathclyde Institute of Pharmacy and Biomedical Sciences

Amorphous calcium phosphate nanocomplexes in dental film formulations

Mohammed Sabar AL-Lami

A thesis submitted to The University of Strathclyde in fulfilment of the requirements for the degree of Doctor of Philosophy

2012

Copyright statement

This thesis is the result of the author's original research. It has been composed by the author and has not been previously submitted for examination which has led to the award of a degree.

Signed: *Date:*

Acknowledgements

First of all I would like to thank Ministry of Higher Education and Scientific Research (Iraq) for sponsoring my scholarship

I express my deepest sense of gratitude and respectful regards to my first supervisor, Professor Clive G. Wilson for his valuable guidance, generous, patience and inspiring discussions and my sincere thanks to my second supervisor Dr. Chris van der Walls for his encouragement and support especially at first stage of the study.

I thankfully acknowledge to Eileen McBride and Lay Ean Tan for help, suggestions and comments during the stages of thesis.

I thank Dr. Chris Longbottom from College of Dentistry at the University of Dundee for kind providing of the teeth samples.

I would like to thank Dr. Fiona McInnes for DVS analysis

I would also like to thank Ahmed Saadi for LC-MS analysis of peptides and John Igoli for NMR studies.

Thanks are due to David Blatchford for CLSM and Paul Edward from the Department of Physics for EPMA imaging.

I would like to thank Dr. Laurence Tetley and Margaret Mullin from the University of Glasgow for SEM and TEM imaging

I would also like to thank Ryan Taylor and Scott McKellar for XRPD analysis and Simon Poland from IOP for fluorescence microscope imaging.

I am also thankful to Denise Gilmour for ICP analysis of calcium samples.

My deep thanks are going to my friends Giacomo Berretta and Mohammed Qadir for help and assistance in parts of thesis.

Thanks are due to Mrs. Anne Goudie and Miss. Catherine Dowdells for kind and ready to help anytime.

It is a pleasure to thank my friends Isam, Israa, Nabila, Jenifer, Gordon, Jessica, Rabbab, Munerah, Manal, Bilal, Nizar, Muhannad for warm atmosphere, understanding and the special moments of fun and relaxation.

Dedicated to the memory of my father Mr Sabar, who passed away on the 27th February 2009; To my mother and my loving wife.

Abstract

The present thesis concerns the exploration of novel amorphous calcium phosphate nanocomplexes stabilised by food grade additives. The concept is to generate a formulation to prevent dental caries through enamel remineralisation, supplementing the calcium and phosphate concentrations by delivery from an adhesive dental film dosage form.

A formulation containing calcium chloride, dibasic sodium phosphate and stabiliser in hydrochloric acid solution at a pH of 5 was complexed by pH adjustment to 7 in the presence of fractioned hydrolysed casein or negatively charged peptides. This allowed the formation of stabilised amorphous calcium phosphate nanocomplexes. An alternative method in which carboxymethyl cellulose with short chain length with measured molecular weight and degree of substitution, produced by acid hydrolysis, was similarly able to stabilise the amorphous calcium phosphate nanocomplex. The prepared amorphous calcium phosphate nanocomplexes were suitable for formulation into dental film dosage forms.

The prepared nanocomplexes were formulated into dental films based on hydroxy propyl methyl cellulose (HPMC) of various grades which formed hydrogels with good adhesive properties. The physical properties of the prepared films were characterised by texture analysis, tensile strength and structure and the calcium release was measured using film strips in a specially designed dissolution cell. The formulated dental films containing a mixture of 2% w/v E10M and 1% w/v F4M hydroxy propyl methylcellulose, loaded with 2 % w/v 4 hours acidic hydrolysed carboxy methylcellulose and hydrolysed casein, had a suitable release of calcium. The release pattern of the calcium was characterised using different diffusion/erosion models and was best described by a Higuchi mode with Fickian, non-Fickian and super case II transport kinetics depending on the type of ACP and the grade of HPMC used.

The effect of a biofilm generated on the tooth surface to make the substrate more hydrophobic was examined. The adhesion of 15% (w/v) HPMC-E10M hydrogel to enamel slabs was studied, and was found to be highly variable. The effect of ACP on

the culture of the biofilm using confocal laser scanning microscopy was investigated and a substantial inhibitory effect was obtained with 8% w/v ACP.

The remineralisation effect of preparations containing 2% w/v NGP-ACP, HC-ACP and acid hydrolysed CMC-ACP loaded into films formulated with a mixture of 2% w/v E10M and 1% w/v F4M hydroxy propyl methylcellulose was investigated. The method employed used scanning electron probe microanalysis to determine the elemental deposition of the calcium and phosphorus up to a depth of 400µm in enamel samples. Both 2% w/v 4h ahCMC-ACP and 2% w/v HC-ACP containing dental films showed an uptake of calcium and phosphate with uniform and constant deposition of the elements to a depth of 400µm into the enamel samples.

Chapter 1. Introduction

1.1 Cariology

1.1.1 Human adult dentition

Man has primary (deciduous) and secondary (permanent) dentitions. The first deciduous tooth erupts at about 6 months and the rest will have erupted by the end of the 3rd year of maturity. The first permanent tooth appears at six years old. the deciduous teeth exfoliated between 6 to 12 and the permanent dentition is completed when the 3rd molars appear at the age of 18-21 years. Twenty teeth, 5 in each jaw quadrant complete deciduous dentition, and 32 teeth, eight in each jaw quadrant complete permanent dentition.

There are three basic forms of tooth: the incisor, canine and the molars. They are shaped to assist with specific functions. The incisor has a cutting edge, the canine has cone end for tearing whilst the molar has a number of cusps for grinding (Figure 1.1).

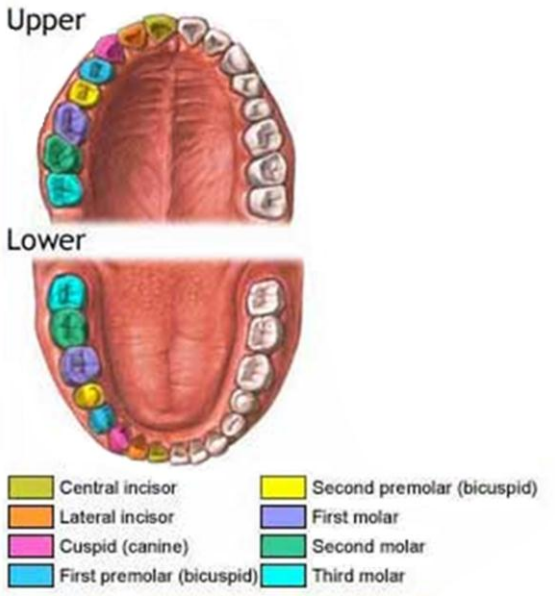

Figure 1.1: A permanent adult tooth forms in a 21-25 year old adult. From (Goforth, 2004).

The central pulp cavity of the tooth is surrounded by dentine with an opening, the apical foreman at, or close to its tip. The pulp consists of connective tissue with blood vessels to nourish the dentine and sensory nerves. The root is enveloped by the periodontal ligament, which is attached to the alveolar bone. The root cementum is thus separated from the osseous sachet by the connective tissue of periodontal ligament (Gray and Standring, 2005) (Figure 1.2a). The tooth body is composed of dentine, with up to a 2.5mm thickness cover of enamel (crown) with a very thin layer over the root of yellowish bone-like cementum (Figure 1.2b).

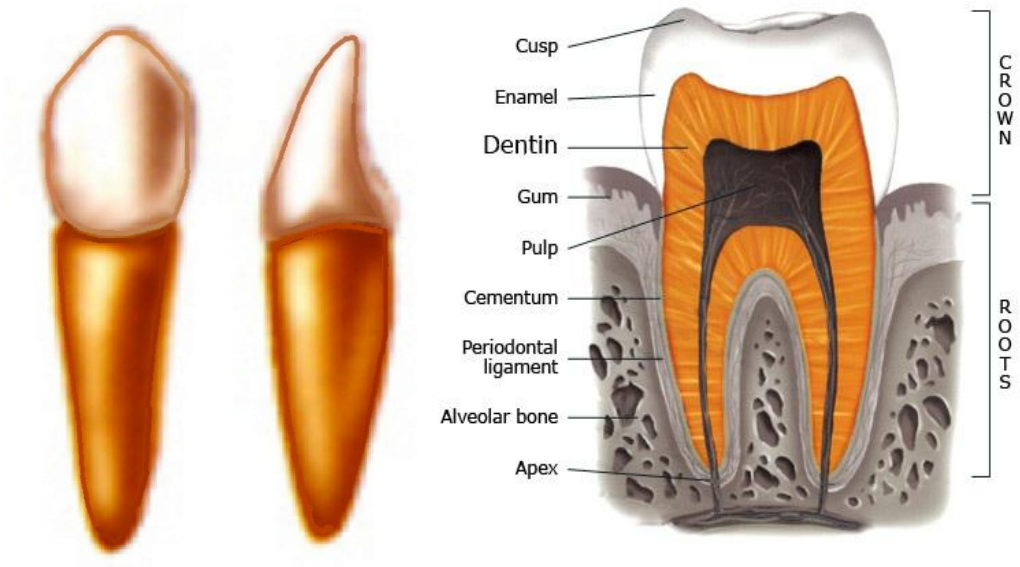

a - Canine tooth b - Longitudinal section of tooth

Figure 1.2: Tooth morphology and histology. From (Dentaire, 2011)

1.1.2 Enamel microstructure and biochemistry

Enamel is an extremely hard substance that coats the crown of the tooth. It is a totally mineralized tissue, composed of 95-96% w/w crystalline apatite, sometimes referred to as hydroxylapatite or hydroxyapatite. The organic materials, which compose less than 1% by mass, include amelogenins, enamelins and tuftelins, which are specific enamel proteins. The maximum thickness of enamel reaches 2.5 mm on the cusps, thinning at the cervical margins. The enamel does not have the ability to continue growing and it has a limited repair process, which occurs by remineralisation (Gray and Standring, 2005). Enamel is a non-cellular tissue mainly consisting of 80-90% v/v of carbonated calcium hydroxyapatite crystals and fluids as well as the proteins, which form the minority of its content. The crystals are arranged in a longitudinal array from the dentin to surface of the enamel. As shown in Figure 1.3-a and b, these crystals have intercrystalline spaces of hydration shell that reveals the electrical charge of crystals.

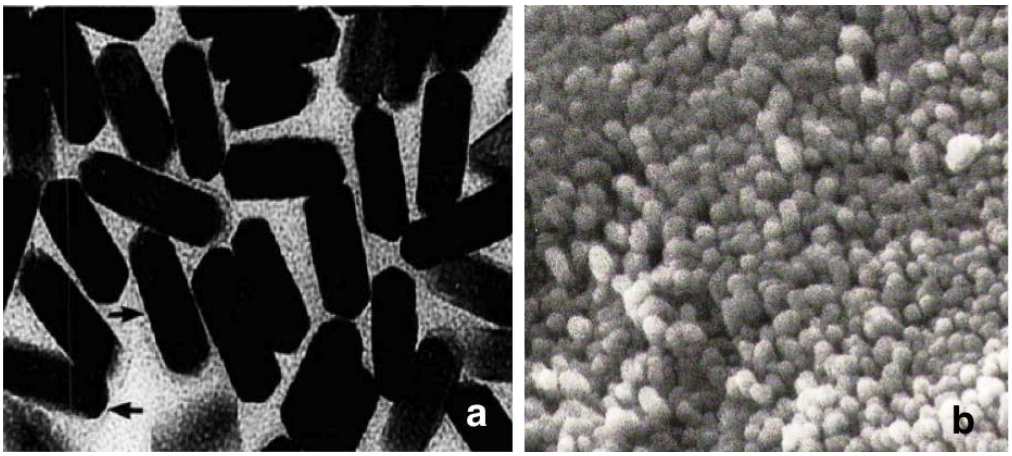

Figure 1.3: Enamel crystals. a - TEM of cross-sectioned crystallites from the mid portion of the maturation zone of rat incisor inner enamel. From (Warshawsky, 1989), b – SEM of tightly packed enamel crystals of smooth inter-rod enamel surface revealed after removal of proteins. From Thylstrup and Fejerskov (1994) .

An enamel prism consists of approximately 1000 crystals arranged in a form of a bundle which forms the basic unit of the structure. Cross section of these prisms shows spaces with circular to keyhole – shaped patterns, which are known as Tomes' processes pits. These are illustrated in Figure 1.4-a and b. At the surface of enamel, prisms deviate forming more inter-crystalline space, which provides the diffusion pathway. The density of the prisms determines the mineral content of the enamel, the density decreasing from the surface towards the dentine tissue. The inter-crystalline spaces and the mineral content determine the porosity of the enamel. The pores are filled with fluid and organic materials in a fashion proportion inversely related to the prism density. For example, a higher porosity with low mineral and high protein content is present in fissure enamel, probably as a result of poor prismatic packaging (Robinson *et al.*, 2000).

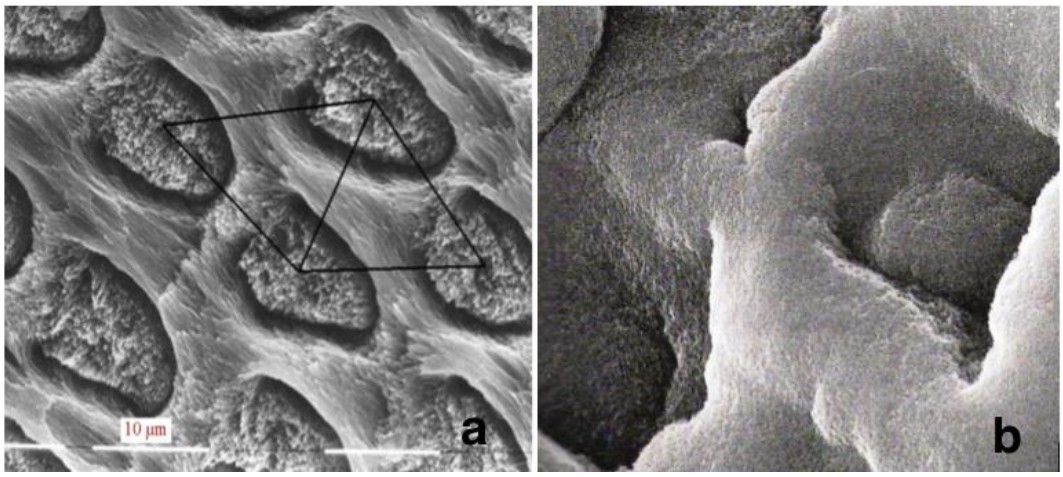

Figure 1.4: Enamel prisms. a- SEM of cross section of triangle enamel prisms (From (Fosse, 2002), b- SEM of a key-hole shape picture taken after removal of the proteins. From Thylstrup and Fejerskov (1994).

The inter-crystalline spaces are considered as the diffusion pathways within the enamel system. The exposure of enamel to the acids from plaque will dissolve or remove minerals, which decreases the mean crystal size. Consequently, the inter-crystalline spaces increase together with tissue porosity. Thus, quantitative measurement of tissue porosity can be utilized as a marker of enamel mineralization. Figure 1.4-b shows a single Tomes' processes pit at high magnification, showing the

variations in crystal packing. In the example, the crystal packing of the surface layer appears less dense at the base or the 'smooth' inter-rod enamel. Figure 1.5-a and b show the rows of Tomes' process pit of the enamel perikymata. Perikymata is the enamel on the sides of teeth that has been previously investigated to estimate the age of the tooth (Guatelli-Steinberg *et al.*, 2007). Higher magnification shows Tomes' processes pits as numerous openings in the enamel, the boundary of the additional layers being smooth. Small fissure or splits are evident between overlapping smooth layer and the Tomes' processes pits (Thylstrup and Fejerskov, 1994).

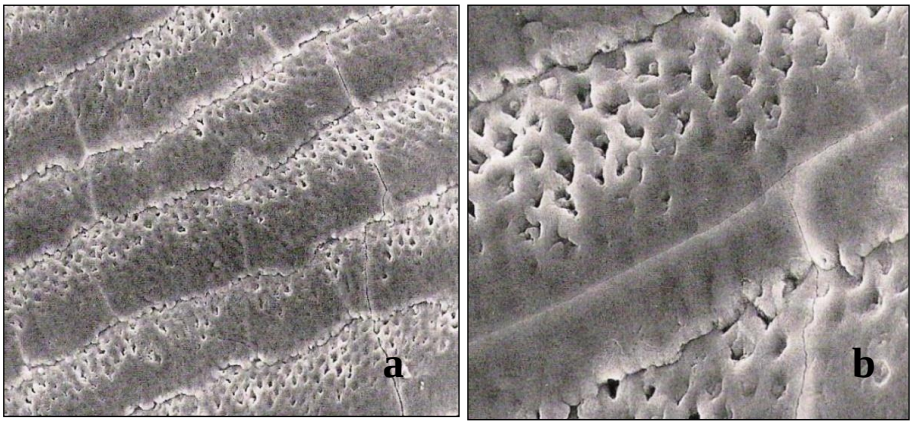

Figure 1.5: SEM- Perikymata and Tomes' processes pits. From Thylstrup and Fejerskov (1994).

1.1.2.1 **Hydroxyapatite**

The main component of solid enamel is the hydroxyapatite (HA) crystal. The empirical chemical formula of HA is $Ca_{10}(PO_4)_6(OH)_2$ and the acid dissolution process involves a calcium substitution reaction. The stoichiometry of the HA crystal is shown in Figure 1.6a and b. As can be seen it is composed of stacks of hexagonal plates, and each hexagonal plate consists of central hydroxyl ion surrounded by a triangle of three calcium ions and another one of three phosphate ions (Robinson *et al.*, 2000). However HA, rather like any other mineralized tissues, has a variety of conformational structure showing missing ions, especially calcium and hydroxyl ions. The expected ions are present at 25% less than the stoichiometric calculation of HA. Magnesium, sodium, fluoride and carbonate ions are frequently present in considerable quantities replacing the calcium and hydroxyl ions in the HA structure.

Thus, a more accurate stoichiometric HA would be $(Ca)_{10-x-y}(HPO_4)_V(HPO_4)_{6-x}(CO_3)_w(OH)_{2-x-y}$, where v+w=x (Robinson *et al.*, 2000). The calculated average components were $Ca_{9.48}Mg_{0.18}Na_{0.11}PO4_{5.67}(CO3)_{0.45}(OH)_{1.54}(H2O)_{0.46}$ according to Hendricks and Hill (1942).

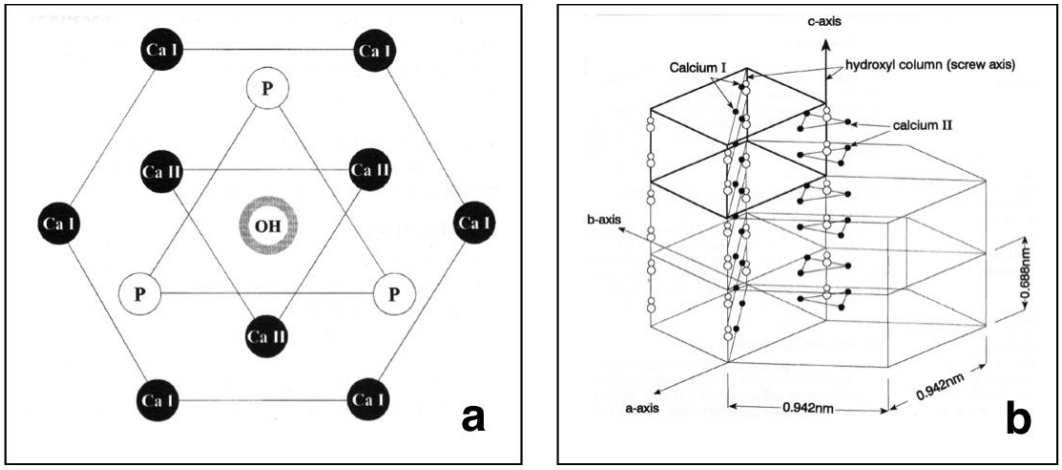

Figure 1.6: Hydroxyapatite planar hexagonal and crystal structure. From (Robinson *et al.*, 2000).

1.1.2.2 Proteins

One of the earlier quantitative analysis of the enamel components was reported in 1942 by Deakins who used pig teeth, examined during the calcification stage. Deakins found that as the inorganic component increases, the water and organic component decrease (Deakins, 1942). The results are summarised in Table 1-1. It was found that protein made up around 20% of the whole weight of the human foetal enamel. This protein is characterized by abnormal high concentration of the amino acid proline that approximates 25% of the total residues as shown in Table 1-2. The material contains the other amino acids that confirm its identity as a collagen. However, the analysis excludes the material from the class of keratins due to unusual high percentages of methionine and histidine (Eastoe, 1979). Eastoe first suggested the descriptor of amelogenins in 1965 (Eggert *et al.*, 1973). At the initial phase of mineralisation, proline and histidine are the major components of amelogenins; however, they are not conserved in mature enamel (Eastoe, 1979).

	Lowest Calcification, Density = 1.45, Very Soft			Highest Calcification, Density = 2.76*, Very Hard			Change In Volume
	mg./mm.^{3}	%	vol.**	mg./mm.^{3}	%	vol.**	
Inorganic	0.54	37	0.16	2.62	95	0.82	+0.66
Organic	0.27	19	0.20	0.05	1.8	0.04	-0.12
Water	0.64	44	0.64	0.12	4.3	0.12	-0.52
Total	1.45	100	1.00	2.79*	101.1	0.98	

* Value 2.76 obtained by flotation; 2.79 are the sum of the weights.
** The volume occupied by each constituent. This was found by assuming densities of 3.18 for inorganic and 1.31 for organic material.

Table 1-1: Enamel components during calcification in developing pig. From (Deakins, 1942).

Component [a]	Mr = 21000 – 28000 fractions	Mr = 12000 – 20000 fractions	Mr = 5000 – 10000 fractions
Aspartic acid	35	38	64
Threonine	33	31	36
Serine	34	43	71
Glutamic acid	235	220	140
Proline	304	287	203
Glycine	23	40	114
Alanine	41	37	58
Valine	41	32	28
Isoleucine	34	33	31
Leucine	110	117	117
Tyrosine	6	14	33
Phenylalanine	18	26	32
Histidine	76	60	34
Lysine	7	10	15
Arginine	4	11	19
Organic P	tr	0.20	0.64
Sialic acid	0.90	0.82	0.61
Galactosamine	0.17	0.26	0.40
Glucosamine	0.14	0.14	0.12
Total anthrone carbohydrate	8.2	8.6	19.2

Amino acids listed as residues/1000 (cysteine, methionine, tryptophan not determined); other components listed as percentages per unit of protein; Mr=relative molecular size; tr = trace.

Table 1-2 : Composition of 5 to 6 month foetal bovine amelogenins proteins isolated after guanidine HCl gel filtration chromatography. From (Termine *et al.*, 1980).

The second component of enamel proteins are termed enamelins and are found in the mature enamel. These were identified as separate from the amelogenins (Eastoe, 1979),which are the remnants of proteinases in the full-grown enamel after the completion of development (Smith, 1998). The percentage content of amelogenins and enamelins was found to be reduced in a foetal bovine enamel matrix during maturation. This reduction might be caused by an increase in proteolysis that accompanies enamel mineralization. In addition, glycosylated proteins were discovered in this enamel as shown by the composition of sialic, galactosamine and glucosamine in enamelins (Table 1-3). This carbohydrate content differentiates enamelins from the amelogenins (Termine *et al.*, 1980).

Component [a]	Mr = 42000 – 72000 fractions	Mr = 8000 – 30000 fractions
Aspartic acid	115	105
Threonine	67	62
Serine	77	136
Glutamic acid	150	144
Proline	166	176
Glycine	112	94
Alanine	56	32
Valine	33	16
Isoleucine	21	53
Leucine	23	15
Tyrosine	32	53
Phenylalanine	55	19
Histidine	25	16
Lysine	32	23
Arginine	36	48
Organic P	0.22	0.24
Sialic acid	4.71	2.82
Galactosamine	1.08	1.07
Glucosamine	3.24	2.58
Total anthrone carbohydrate	15.2	14.8
Amino acids listed as residues/1000 (cysteine, methionine, tryptophan not determined); other components listed as percentages per unit of protein; tr = trace.		

Table 1-3: Composition of 5- to 6-month foetal bovine enamelin proteins isolated after guanidine HC1 gel filtration chromatography. From (Termine *et al.*, 1980).

1.1.3 Demineralisation and remineralisation

1.1.3.1 Demineralisation of enamel

Dissolution of dental enamel or formation of caries is predominantly caused by lactic acid. The presence and involvement of other acids have been shown by investigations performed using saliva and other oral contents. These acids are present as mixtures in different ratios depending on inter-individual variation. Acids are produced by the fermentation of food debris trapped around the tooth surface and formation is influenced by diet. The resultant acidic medium with pH typically not lower than pH 4.5 due to buffers of saliva, plaque and even carious substances which have sufficient hydronium ions that are able to displace the cations from dental enamel, causing the decalcification (Koulourides and Buonocore, 1961).

The second factor in enamel dissolution is the concentration of the free forms of calcium, phosphate and fluoride. The ionic equilibrium between enamel and surrounding aqueous phase with regards to both hydroxyapatite and fluorapatite is illustrated as follows:

$$Ca_{10}(PO4)_6(OH)_2 \rightleftharpoons 10Ca^{2+} + 6PO_4^{3-} + 2OH^-$$

$$Ca_{10}(PO4)_6F_2 \rightleftharpoons 10Ca^{2+} + 6PO_4^{3-} + 2F^-$$

In normal circumstances, saliva (Larsen, 1975) is supersaturated with calcium, phosphate and fluoride as compared to apatite and plaque fluid (Margolis, 1990), which are responsible for enamel resistance and prevention of mineral loss. This is assisted by promotion of crystal growth on the surface of enamel or the formation of precipitates such as apatite, tri-calcium phosphate, octa-calcium phosphate and brushite ($CaHPO_4$, $2H_2O$) (Thylstrup and Fejerskov, 1994) (Thylstrup *et al.*, 1994) (Thylstrup *et al.*, 1994) (Thylstrup *et al.*, 1994).

The solubility of hydroxyapatite in an acidic medium provides the main weakness of dental enamel, in addition to its porosity. Lactic acid is a major metabolite of bacterial digestion of polysaccharide. It is sufficiently dissociated to lower the pH below 5.5 and consequently promote mineral dissolution beneath the bacterial

biofilm. The other source of acids comes from ingested soft drinks acidified with phosphoric and citric acids, which can have a pH of about 2.5 - for example colas (Barbour and Shellis, 2007).

The plaque fluid shows pH fluctuations due to the metabolic changes in the dental biofilm. These fluctuations result in innumerable cycles of mineral dissolution and deposition (Figure 1.7). The higher loss of minerals leads to increase in the pore size that is clinically associated with white or opaque spots on the diseased enamel (Fejerskov and Kidd, 2008) .

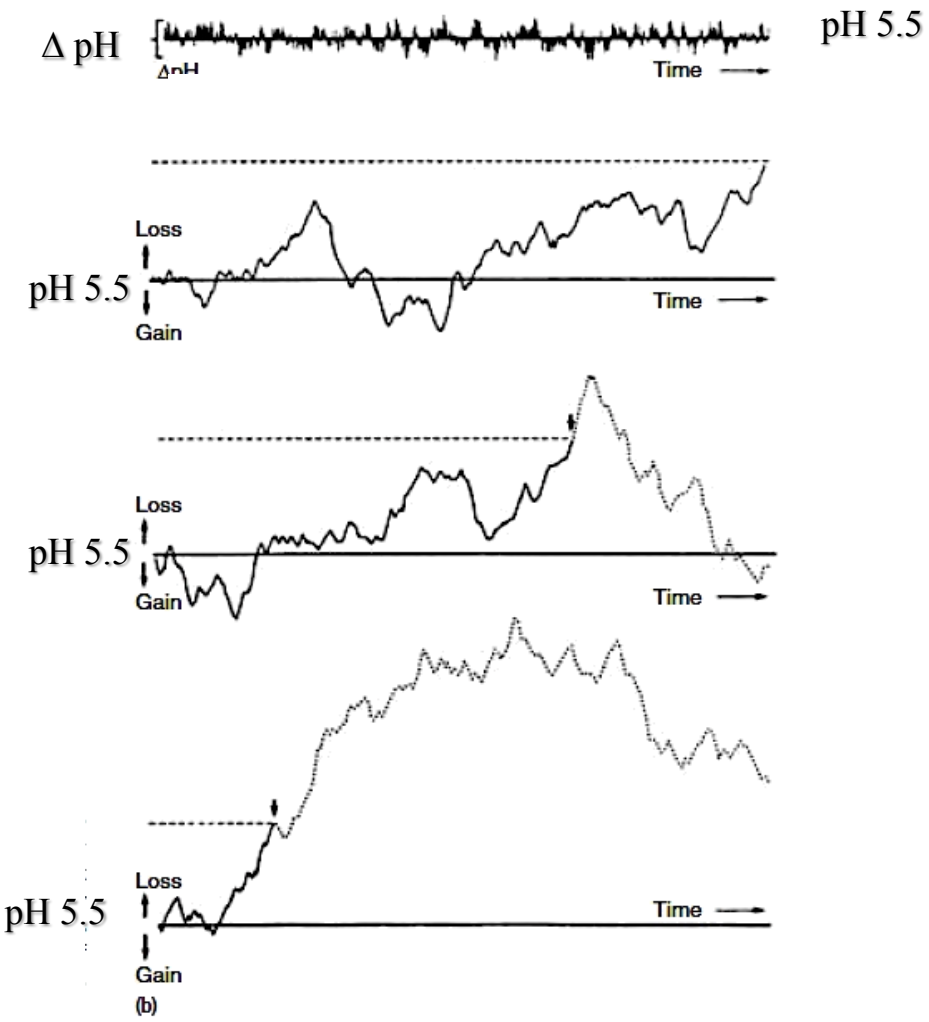

Figure 1.7: The cycles of mineral loss (upper) and gain (lower) in dental enamel surface that caused by pH fluctuations of dental plaques. Dotted lines represent a mineral loss characterised by clinically visible changes in enamel surface. From (Fejerskov and Kidd, 2008) .

Remineralisation of enamel

The enamel of a freshly erupted tooth is characterized by permeability down to around a depth of 200μm into the surface. The enamel is coated by a pellicle. Saliva can form a saturated solution containing calcium, phosphate and fluoride which results in the equilibration of tooth enamel via exchange between acid soluble components and acid insoluble components. Thus, carbonate and hydroxide will be replaced by fluoride, and in the presence of the minerals, a new fluoroapatite crystal will form that makes a mature enamel with a reduced porosity and permeability. An additional protection originates from a coating of a pellicle protein known as statherin that resists acidity as well as cariogenic microorganisms. The high concentration of calcium and phosphate in saliva, biofilms and artificial calcium containing oral solutions have a negative effect on enamel remineralisation, since a rapid precipitation of calcium phosphate on the enamel surface will block the pores. Moreover, calcium phosphate has low solubility at neutral pH, precipitates, and hence remineralisation is diminished (Garcia-Godoy and Hicks, 2008).

1.1.4 Dental Caries

Dental caries refers to a local destruction of the tooth surfaces as result of chemical etching, arising underneath the dental pellicle, by acidic metabolites. Theoretically, the carious lesion is present where a plaque grows. However, variation might be caused by dissimilarity in the chemical constituents of the plaque. The developed lesions can persist for a long time on the tooth surfaces that are protected from the mechanical effect of brushing, the tongue and chewing, these surfaces, such as fissure, grooves, contact area between adjacent teeth and gingival boundary (Fejerskov and Kidd, 2008).

Dental caries is a totally avoidable disorder (Zero, 2006). It is considered as a dynamic disease (Figure 1.8) of demineralisation caused by organic acids that come from a fermentable food consumed by the patient in the presence of bacteria and remineralisation that occurs by saliva throughout pH rising and elemental resourcing. Meals that are rich in carbohydrate and sugar are described as the most cariogenic,

however the others might be show a degree of cariogenic activity (Zero *et al.*, 2009). The permanent teeth have thicker enamel than that in the deciduous teeth. In addition permanent teeth have a more regular prismic macrostructure. Thus the permanent teeth are more susceptible to the remineralisation process (Oliveira *et al.*, 2010).

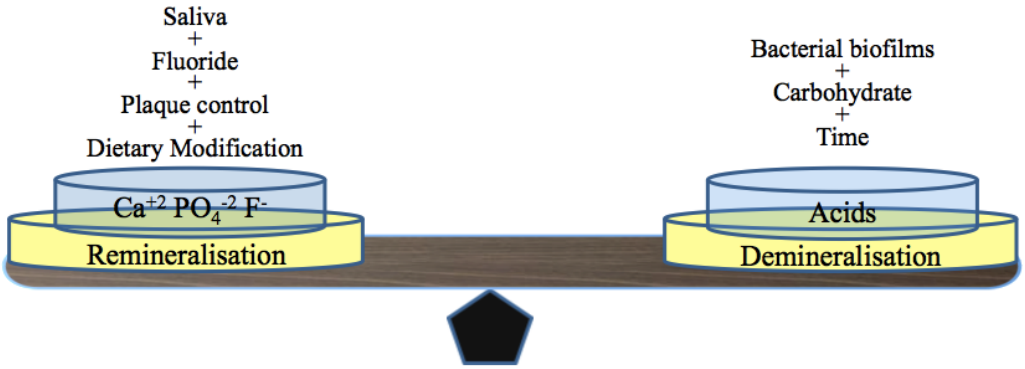

Figure 1.8: The dynamic processes of dental caries, demineralisation and remineralisation. Data obtained from (Selwitz *et al.*, 2007).

1.1.5 Treatment of caries

There are three strategies for dental caries treatment. The primary prevention involves identification and alteration of the initiative factors for caries; the secondary that considers preventive processes that arrest or reverse the caries processes and the tertiary treatment restores tooth cavitation and provides pain management (Whitaker, 2006). Chen and colleague identified a number of therapeutics to treat or arrest the dental enamel demineralization through inhibition of dental biofilm such as antibacterial agents, vaccines, probiotics and sugar substitutes. In addition, they identified agents that support the remineralisation process for examples, fluoride and casein (Chen and Wang, 2010).

1.2 Casein phosphopeptide amorphous calcium phosphate

1.2.1 Studies on casein derivatives as remineralising agents

Casein is a phosphopeptide that is present at an amount of 2.4-2.9% w/v in cow's milk. It is present as micellar complex of calcium, citrate and phosphate ions with a

very high molecular weight. Casein forms a very stable colloidal dispersion as result of its capability to form a stable negative charge at pH 6.6 in milk. The approximate isoelectric point of casein is 4.6 (Southward, 2008).

1.2.2 Casein fractions

The well-known fractions of casein are αs, β and κ. αs-casein is classified into the forms designated αs_1 and αs_2 and $\alpha s_1$is further divided into forms αs_0 and αs_1. They differ in the number of serine-phosphate groups. The αs and β caseins show a decrease in enamel dissolution as a result of their high binding properties toward hydroxyapatite. The binding action is directly proportional to the number of phosphoserine groups in each fraction (Reynolds, 1987). The percentages of bovine casein fractions (Figure 1.9) were measured recently by Bonizzi and colleagues. They demonstrated that α_{s1} and β caseins were the major fractions (Figure 1.10 and Figure 1.11) (Bonizzi *et al.*, 2009).

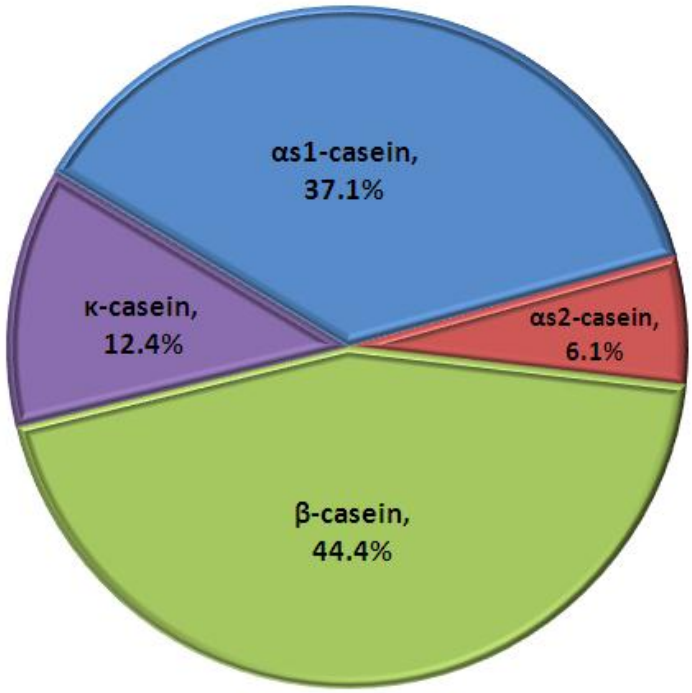

Figure 1.9: Percentages of bovine casein fractions in milk. Data obtained from (Bonizzi *et al.*, 2009).

ARG PRO LYS HIS PRO ILE LYS HIS GLN GLY LEU PRO GLN GLU VAL LEU ASN
GLU ASN LEU LEU ARG PHE PHE VAL ALA PRO PHE PRO GLN VAL PHE GLY LYS
GLU LYS VAL ASN GLU LEU SER LYS ASP ILE GLY PSE GLU PSE THR GLU ASP
GLN ALA MET GLU ASP ILE LYS GLN MET GLU ALA GLU PSE ILE PSE PSE PSE
GLU GLU ILE VAL PRO ASN PSE VAL GLU GLN LYS HIS ILE GLN LYS GLU ASP
VAL PRO SER GLU ARG TYR LEU GLY TYR LEU GLU GLN LEU LEU ARG LEU LYS
LYS TYR LYS VAL PRO GLN LEU GLU ILE VAL PRO ASN PSE ALA GLU GLU ARG
LEU HIS SER MET LYS GLU GLY ILE HIS ALA GLN GLN LYS GLU PRO MET ILE
GLY VAL ASN GLN GLU LEU ALA TYR PHE TYR PRO GLU LEU PHE ARG GLN PHE
TYR GLN LEU ASP ALA TYR PRO SER GLY ALA TRP TYR TYR VAL PRO LEU GLY
THR GLN TYR THR ASP ALA PRO SER PHE SER ASP ILE PRO ASN PRO ILE GLY
SER GLU ASN SER GLU LYS THR THR

Figure 1.10: The complete amino acids sequence of bovine αs1 casein. From (Kumosinski *et al.*, 1991)

ARG GLU LEU GLU GLU LEU ASN VAL PRO GLY GLU ILE VAL GLU PSE LEU PSE
PSE PSE GLU GLU SER ILE THR ARG ILE ASN LYS LYS ILE GLU LYS PHE GLN
PSE GLU GLU GLN GLN GLN THR GLU ASP GLU LEU GLN ASP LYS ILE HIS PRO
PHE ALA GLN THR GLN SER LEU VAL TYR PRO PHE PRO GLY PRO ILE PRO ASN
SER LEU PRO GLN ASN ILE PRO PRO LEU THR GLN THR PRO VAL VAL VAL PRO
PRO PHE LEU GLN PRO GLU VAL MET GLY VAL SER LYS VAL LYS GLU ALA MET
ALA PRO LYS HIS LYS GLU MET PRO PHE PRO LYS TYR PRO VAL GLN PRO PHE
THR GLU SER GLN SER LEU THR LEU THR ASP VAL GLU ASN LEU HIS LEU PRO
PRO LEU LEU LEU GLN SER TRP MET HIS GLN PRO HIS GLN PRO LEU PRO PRO
THR VAL MET PHE PRO PRO GLN SER VAL LEU SER LEU SER GLN SER LYS VAL
LEU PRO VAL PRO GLU LYS ALA VAL PRO TYR PRO GLN ARG ASP MET PRO ILE
GLN ALA PHE LEU LEU TYR GLN GLN PRO VAL LEU GLY PRO VAL ARG GLY PRO
PHE PRO ILE ILE VAL

Figure 1.11: The complete amino acids sequence of bovine β casein. From (Kumosinski *et al.*, 1993)

1.2.3 Preparation

1.2.3.1 Casein

The production methods of casein from whole milk are summarized in

Figure 1.12. The method of casein production utilises different precipitation processes. In the acid treatment method, a pH drop to 4.6 will fall to the isoelectric point of casein. This will be responsible for destruction of casein micelles and precipitation. In the alternative method, enzymatic digestion, destruction of the micelle also occurs. However, the mechanism is slightly different, k-casein is selectively cleaved, which results in the inability of the remaining casein to resist micelle destruction (Southward, 2008).

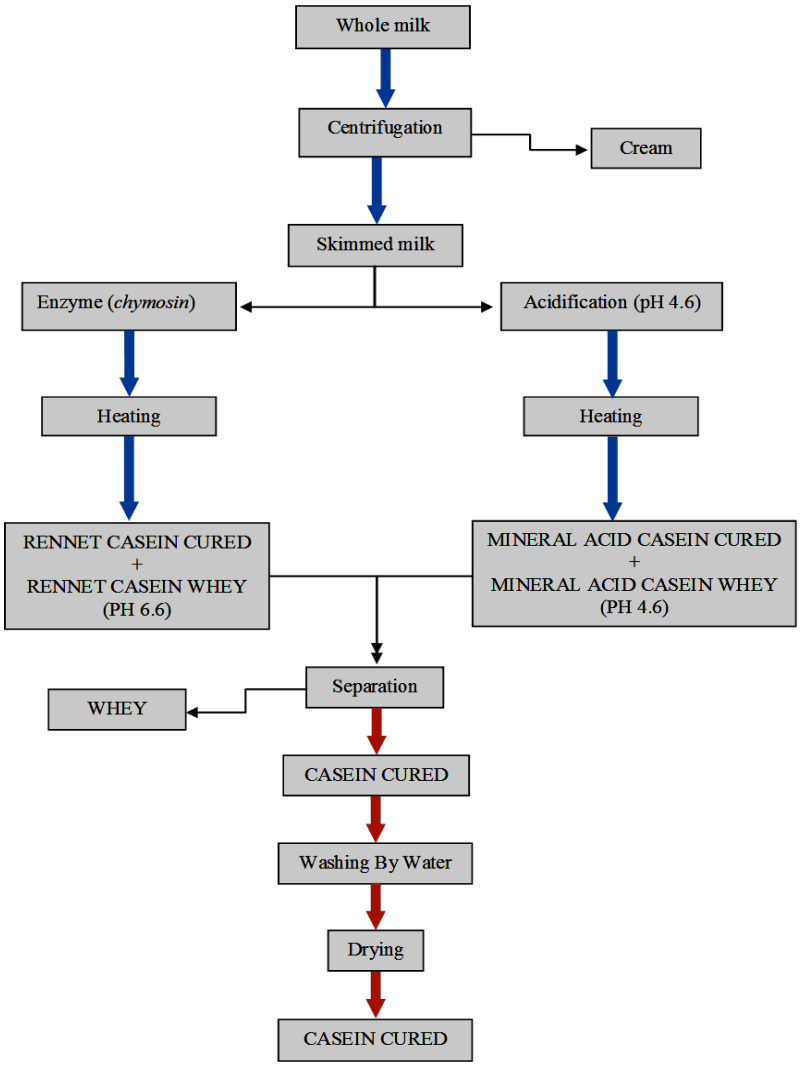

Figure 1.12: Flow diagram shows the production method of casein. Data obtained from Southward (2008).

1.2.3.2 Fractions of casein

Both basic techniques of casein production were utilized in the Reynolds studies to prepare casein fractions. Some modification with regard to the degree of pH change and type of enzymes resulted in the separation of fractions of casein. The first procedure for isolation of casein fractions from bovine milk casein was completed using a one hour enzymatic digestion by 1:50 ratio of trypsin to sodium caseinate in 20mM Tris-HCl and 2.5mM NaCl at pH 8.0 and 37° C. Separation of caseins were carried out using FPLC system using a (Mono Q 5/5) column with an eluent based on the solvent used in digestion. The extracts were washed and concentrated followed by analysis of the amino acids content. The resultant fractions were defined as T1 to T9 with their corresponding amino acids content and sequence as shown in Table 1-4.

Code	Amino acids content
T1	Glu-Met- Glu -Ala-Glu-Pse-Ile-Pse-Pse-Pse-Glu-Glu-Ile-Val-Pro-Asn-Pse-Val-Glu-Gln-Lys.
T2	Glu -Leu- Glu - Glu-Leu-Asn-Val-Pro-Gly-Glu-Ile-Val-Glu-Pse-Leu-Pse-Pse-Pse-Glu-Glu-Ser-Ile-Thr-Arg
T3	Asn-Thr-Met-Glu-His-Val-Pse-Pse-Pse-Glu-Glu-Ser-Ile-Ile-Pse-Gln-Glu-Thr-Tyr-Lys.
T4	Asn-Ala-Asn-Glu-Glu-Glu-Tyr-Ser-Ile-Gly-Pse-Pse-Pse-Glu-Glu-Pse-Ala-Glu-Val-Ala-Thr-Glu-Glu-Val-Lys
T5	Glu-Gln-Leu-Pse-Pth-Pse-Glu-Glu-Asn-Ser-Lys
T6	Asp-Ile-Gly-Pse-Glu-Pse-Thr-Glu-Asp-Gln-Ala-Met- Glu-Asp-Ile-Lys
T7	Val-Pro-Gln-Leu-GIn-Ile-Val-Pro-Asn-Pse-Ala-Glu-Glu-Arg
T8	Thr-Val-Asp-Met-Glu-Pse-Thr-Glu-VaI-Phe-Thr-Lys
T9	Leu-Pth-Glu-Glu-Lys

Table 1-4: Amino acids content and sequence of casein fractions. From (Reynolds, 1991).

For the second procedure, a modified pH routine was utilised for selective extraction of casein fractions from T1 to T5. Casein was digested in a similar to manner to that described in first procedure. The resultant product was acidified to pH 4.6 by HCl;

following this, 0.25% w/v $BaCl_2$ was added with precipitation with absolute ethanol and removal of formed precipitate. The dried precipitate was treated with one tenth by volume distilled water with alkali by adding NaOH for dissolution enhancement. Hydrochloric acid solution (1M) was added to adjust the pH to 3.5 followed by precipitation by means of the addition of an equal volume of acetone; the newly formed precipitate was separated and dried. The dried product was re-dissolved in water and acidified with HCl to pH 2 and the supernatant collected. The pH of the resultant solution was raised to pH 3.5 by addition of NaOH and re-precipitated by acetone. The precipitate was dissolved in water followed by an addition of H_2SO_4 to eliminate $BaSO_4$ as precipitate and supernatant isolated. The liquid extract was dialysed and spray dried. The resultant extract was a mixture of T1, T2, T3, T4 and T5 casein fractions (Reynolds, 1991).

1.2.4 Applications

1.2.4.1 Whole casein

Losee and colleagues examined the effects on casein of carious lesions (Losee *et al.*, 1957). The resultant weight difference of rat incisors, femurs and caries were used as parameters to measure the effect of casein. The result revealed that the only significant difference was seen in the caries lesion between control and test. However, in the protocol the diet was not controlled. Another study confirmed that casein could reduce caries in rat tooth enamel with scheduled feeding. A 2% w/v Sodium caseinate solution was as added into drinking water rather than being incorporated into the solid diet (Reynolds and del Rio, 1984) . The next illustration of anti-caries activity of casein was shown by a reduction of chocolate cariogenecity in a test that lasted for 58 day on rats with programmed feeding on chocolates contained 5.6 and 16.6%w/w casein (Reynolds and Black, 1987) (Reynolds *et al.*, 1987) (Reynolds *et al.*, 1987) (Reynolds *et al.*, 1987).

Reynolds and Black applied a more advanced technique to find and differentiate the capability of αs_1-casein and a tryptic digest of αs_1-casein to reduce enamel demineralization in bovine teeth. In this study, the intra oral appliance (Figure 1.13)

was introduced in order to expose the samples under normal physiological conditions. The sample slabs were prepared from enamel taken from a permanent bovine incisor crown and set into the intraoral appliances; the left side was used as control and the right side as test. Ten subjects wore the intra-oral appliances for ten days in each of four protocols. The appliances were set aside throughout food and drink intake.

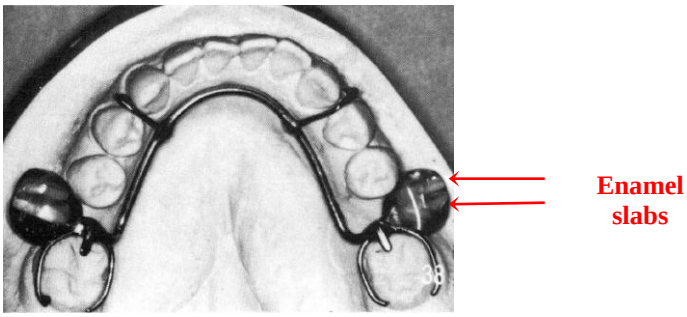

Figure 1.13:An intra-oral appliance showing buccal acrylic flanges with enamel slabs inset. From (Reynolds, 1987)

The protocols utilized are as illustrated in Table 1-5. In protocol 1, the appliances were incubated at 37^{o} C in corresponding solutions to examine the ability of 2% w/v sodium caseinate to counteract sugar enamel demineralization when it is combined within sugar-salt solution. Protocols 2, 3 and 4 were used to show that twice-daily exposure to caseins could counteract the effect of six times a day exposure to the sugar-salt solution.

Protocols	Left Side of Appliance	Right Side of Appliance
1*	Eight 20-minute exposures per day to solution A[a]	Eight 20-minute exposures per day to solution B§
2**	a. Six 20-minute exposures per day to solution A	a. Six 20-minute exposures per day to solution A
	b. Two 20-minute exposures per day to solution CII	b. Two 20-minute exposures per day to solution D¶
3**	a. Six 20-minute exposures per day to solution A	a. Six 20-minute exposures per day to solution A
	b. Two 20-minute exposures per day to solution C	b. Two 20-minute exposures per day to solution E∞
4**	a. Six 20-minute exposures per day to solution A	a. Six 20-minute exposures per day to solution A
	b. Two 20-minute exposures per day to solution C	b. Two 20-minute exposures per day to solution F[ψ]

* The appliances were immersed in the respective solutions for 20 min, on the hour, from 9 a.m. to 4 p.m.

** For protocols 2, 3, and 4, the first and fifth exposures were solutions C (on the left) and D, E, or F (on the right), respectively.

[a] Solution A: 3% (w/v) glucose, 3% sucrose, 20 mmol/L NaCl, 140 mmol/L KCl, 5 mmol/L $CaCl_2$, pH 7.0.

§ Solution B: 2% (w/v) sodium caseinate, 3% glucose, 3% sucrose, 20 mmol/L NaCl, 140 mmol/L KCl, 5 mmol/L $CaCl_2$, pH 7.0.

II Solution C: 20 mmol/L NaCl, 140 mmol/L KCI, 5mM $CaCl_2$, pH 7.0.

¶ Solution D: 2% (w/v) sodium caseinate, 20 mmol/L NaCl, 140 mmol/L KC1, 5 mmol/L $CaC1_2$, pH 7.0.

∞ Solution E: 2% (w/v) αs_1-casein, 20 mmol/L NaCl, 140 mmol/L KCl, 5 mmol/L $CaCl_2$, pH 7.0.

[ψ] Solution F: 2% (w/v) TD-casein (tryptic digest), 20 mmol/L NaCl, 140 mmol/L KCl, 5 mmol/L $CaC1_2$, pH 7.0.

Table 1-5: Protocols for intra-oral appliance experiments. From (Reynolds, 1987).

The slabs on the left side showed caries lesions, but not the slabs on the right side. The micro-hardness test reveals that the slabs on the right side were significantly different from the slabs on the left side in all protocols, as shown in Table 1-6. The plaque in the right side of the appliance has a significantly higher level of calcium and phosphate as compare to that on the left, which validates the cario-protective effect of αs1-casein. Demineralization is terminated by tryptic casein digest and casein as a result of the activity increasing the calcium and phosphate ions in the plaque. In addition, they showed acid resistance of the buffering action of

phosphoseryl, histidyl, glutamyl, and aspartyl residues and indirectly through plaque bacteria catabolism.

Protocols	Enamel Hardness*	
	Left	Right
1	234 ± 82(4)†	446 ± 121(4)
2	229 ± 94(4) ‡	508 ± 129(4)
3	175 ± 93(5) §	486 ± 151(5)
4	207 ± 97(4) ‡	482 ± 115(4)

* Knoop hardness number KHN (kg/mm2). Longitudinal plano-parallel sections were taken from the centre of each enamel slab. The sections were divided into ten segments, and each segment was hardness-tested at a depth of 70 µm from the surface. The values presented are means and standard deviations with number of subjects in parentheses. KHN of control sections at 70 µm was 484 + 123.
†Significantly lower ($p<0.05$) than right-side value analysed using the t test for paired comparisons.
‡$p<0.02$.
§ $p<0.0l$.

Table 1-6: Enamel micro-hardness data. From (Reynolds, 1987).

In 1989, Reynolds and Black reported the effect of sodium caseinate on confection cariogenecity. Rats were placed on a programmed feeding regimen for 52 days on a confection containing sodium caseinate equal to 1.6% and 5.3% w/w which represent the normal content of milky confection and the maximum palatable concentration, respectively. The outcome was not significantly different between the two groups, which indicated that casein had no anti-cariogenic effect at palatable dose (Reynolds and Black, 1989).

1.2.4.2 Casein phosphopeptide (CPP)

Reynolds established the anticariogenic casein-phosphopeptide invention in 1991. The patent mentions the methods of extraction and amino acid analysis of this phosphopeptide. Furthermore, a planar chemical form of the main cluster that is responsible for the anticariogenic effect was described, as shown in Figure 1.14. The inventor confirmed the anticariogenic action for this phosphopeptides using four different tests as illustrated in Table 1-7. In the exemplification of the patent, the

inventor described a series of examples for application of T1. Most common types of dentistry dosage forms were mentioned, as well as foods such as biscuits, confections, breads, cakes and soft drinks. Furthermore, he stated that the concentration of T1 in these preparations should range from 0.01 to 10 % w/w.

	Type of test	Results
1	Hydroxyapatite dissolution	T1-T5* were showed 32% decrease in dissolution and T6-T9 were showed a much less activity.
2	Intra oral caries test	T1 (αs_1-casein) showed anticariogenic effect, acid buffer capacity and elevation of Ca and PO_4 ion in plaque. (Reynolds, 1987).
3	Intra-oral remineralisation	T1was showed 57% return mineral loss compare with 13% for saliva
4	Plaque pH fall	T1 was showed to stable pH at 6.7
* Casein phosphopeptides from table 1-4		

Table 1-7: Tests applied on casein-phosphopeptides.

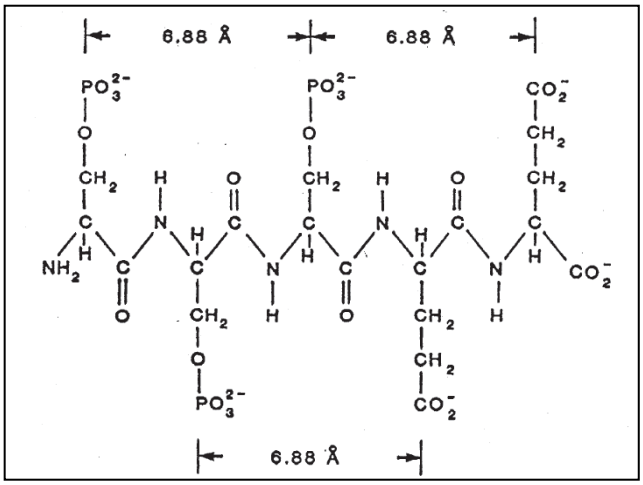

Figure 1.14: Structural formula of Pse-Pse-Pse-Glu-Glu pentapeptide cluster. From (Reynolds, 1991).

1.2.4.3 CPP stabilized amorphous calcium phosphate (CPP-ACP)

The interaction between casein phosphopeptide αS_1-casein (59-79) and mineral ions in amorphous calcium phosphate was analysed using NMR spectroscopy. The NMR

spectrum analyses show that αS_1-casein (59-79) has systemic coil skeleton of rounds and circles with specific binding orientation toward minerals (Cross *et al.*, 2005a). An investigation was carried out to show that CPP-CP has anti-cariogenic effect on the rat tooth and to evaluate its action against fluoride, non-phosphorylated tryptic-casein and synthetic octapeptide contain the cluster (Figure 1.14) similar to that present in αs1 casein and β-casein.100μL of different solutions (Table 1-8) were administered directly into the molar teeth of animals, two times a day for 50 days.

Group	Number of animals	Treatment [a]
1	24	Milli-Q Water
2	12	0.1% w/v CPP[e], 6.0 mmol/L $CaCl_2$, 3.6 mmol/L sodium phosphate, pH 7.0[b]
3	12	0.2% w/v CPP, 12.0 mmol/L $CaCl_2$, 7.2 mmol/L sodium phosphate, pH 7.0[b]
4	24	0.5% w/v CPP, 30.0 mmol/L $CaCl_2$, 18.0 mmol/L sodium phosphate, pH 7.0[b]
5	12	1.0% w/v CPP, 60.0 mmol/L $CaCl_2$, 36.0 mmol/L sodium phosphate, pH 7.0[b]
6	12	0.5% w/v CPP, 30 mmol/L $CaCl_2$, 18.0 mmol/L sodium phosphate, pH 7.0 plus 26.3 mmol/L sodium fluoride[b]
7	24	26.3 mmol/L sodium fluoride (500 ppm F)
8	12	0.5% w/v NPP[C], pH 7.0
9	12	0.18% w/v synthetic octapeptide[d], 22.5 mmol/L $CaCl_2$, 13.5 mmol/L sodium phosphate, pH 7.0[b]

a-Each solution was applied to the molar teeth of the animals twice daily for the experimental period.
b-These concentrations of calcium and phosphate at pH 7.0 are close to the maximum level sequestered by the phosphopeptides at each respective concentration.
c -NPP indicates the non-phosphorylated peptide fraction of a tryptic digest of casein defined in Table 2.
d-This molar concentration of the synthetic peptide [Ac-Glu-Ser(P)-Ile-Ser(P)-Ser(P)-Ser(P)-Glu-Glu-NHMe]corresponds to the molar concentration of 0.5% w/v CPP.
e-CPP indicates the sodium salt of the casein phosphopeptides.

Table 1-8: Experimental groups. From Reynolds *et al.* (1995)

The assessment of caries in smooth surfaces and fissures was used as an indicator for the measurements of the effect of solutions on the animal; molar caries. The scoring systems were those used by Keyes (1958) and König KG(1958) for smooth surface and fissure, respectively. The results obtained are as shown in Table 1-9. The CPP-CP significantly reduces caries incidence in a dose-responsive fashion, with 1.0% CPP-CP producing 55% and 46% reductions in smooth surface and fissure caries incidence, respectively, similar to that of 500 ppm F. There were additive anti-cariogenic effects of CPP-CP and F, since animals receiving 0.5% CPP-CP plus 500ppm F had significantly lower caries incidence than those animals receiving either CPP-CP or fluoride alone. In addition, the outcomes indicated that the synthetic octapeptide-calcium phosphate complex significantly reduced caries activity. In contrast, the tryptic digest of casein with the selectively removed phosphopeptides showed no anticariogenic incidence.

	Group treatment	Caries score			
		Smooth surface		Fissure	
		E	T	B	C
1	H20	33.9 ± 3.0^{a}	10.8 ± 1.2^{a}	6.6 ± 1.2^{a}	4.2 ± 1.3^{a}
2	0.1 % CPP-CP[h]	29.2 ± 1.4^{b}	9.1 ± 0.8^{b}	$5.3 \pm 0.8^{b,f}$	2.9 ± 1.1^{b}
3	0.2% CPP-CP	$26.3 \pm 1.6^{b,c}$	7.7 ± 1.2^{c}	$4.9 \pm 0.7^{b,c}$	2.3 ± 0.9^{b}
4	0.5% CPP-CP	19.1 ± 2.4^{d}	$6.4 \pm 0.9^{d,f}$	$4.1 \pm 1.1^{c,d}$	1.4 ± 1.0^{c}
5	1.0% CPP-CP	15.4 ± 2.4^{e}	$5.8 \pm 1.0^{d,e}$	3.9 ± 1.0^{d}	1.1 ± 0.9^{c}
6	0.5% CPP-CP + F	14.7 ± 1.8^{e}	4.6 ± 1.2^{e}	2.7 ± 0.8^{e}	0.6 ± 0.5^{c}
7	F- 500 ppm	18.9 ± 2.5d	$6.2 \pm 0.9^{d,f}$	3.7 ± o.9[d]	1.0 ± 0.9^{c}
8	0.5% NPP	31.9 ± 3.2^{a}	$10.1 \pm 1.4^{a,b}$	6.8 ± 1.4^{a}	4.1 ± 1.3^{a}
9	0.18% Octa-CP[i]	24.2 ± 2.7^{c}	$7.3 \pm 0.9^{c,f}$	$4.8 \pm 1.1^{c,f}$	2.2 ± 1.3^{b}

a-f Significantly different ($p < 0.05$) from all other values not similarly marked in column. Mean ± SD (n = 12 or 24).
h Casein-phosphopeptide calcium-phosphate complex.
i Synthetic-octapeptide calcium-phosphate complex.

Table 1-9: Caries data obtained. From Reynolds *et al.* (1995).

The effects of different concentrations and pH of CPP-CP solutions on anti-cariogenicity were investigated on enamel slabs prepared from human third molars by Reynolds (Reynolds, 1997) . The slabs were demineralised by incubation in 40mL of 0.1 mol/L lactic acid, 500mg/L hydroxyapatite, and 20g/L carbopol C907 at pH 4.8 and 37º C for 4 days. The samples were then remineralised for 2days in two sets of CPP-CP solutions. The first set contained 0.1, 0.5 or 1.0% w/v CPP-CP at pH 7 and the second set 0.5%w/v CPP-CP at pH 7, 7.5, 8, 8.5 or 9. The first set was used to discover the effect of the concentration of CPP-ACP administered on remineralisation. The other was utilised to inspect the effect of increasing pH on remineralisation, which decreased the concentrations of free calcium and phosphate ions and increased the level of CPP-bound ACP. It was found that the highest levels of minerals for bound and free phases were gained at pH 7 and 1% w/v CPP-CP concentration.

The results, shown in Table 1-10 and Table 1-11 reveal that the extent and rate of remineralisation were directly proportional to the concentration of CPP-CP. In addition, the remineralisation was attributed to an increase in concentration of free and bound calcium phosphate in the solutions. Moreover the solution of 0.5% CPP pH 7.0 (RC) replaced mineral at a significantly faster rate than the other.

Remineralising solutions	% Remineralisation	Rate of Remineralisation moles HA/m^2/s x 10^{-8}
0.1% CPP pH 7.0 (RB)	43.6 ± 18.9[b]	2.2 ± 1.5[b]
0.5%CPP pH 7.0 (RC)	51.6 ± 20.8	3.5 ± 1.6
1.0%CPP pH 7.0 (RA)	63.9 ± 20.1	3.9 ± 0.8
a-Mean ± standard deviation (n = 10). b- Significantly different from other values in the column not similarly marked ($p < 0.05$).		

Table 1-10: Effect of CPP-CP concentration on remineralisation of enamel subsurface lesions. From (Reynolds, 1997).

Remineralising solution	% Remineralisation	Rate of Remineralisation moles $HA/m^2/s \times 10^{-8}$
0.5% CPP pH 7.0 (RC)	$51.6 \pm 20.8^{a,b}$	3.5 ± 1.6^{c}
0.5% CPP pH 7.5 (RD)	28.6 ± 8.0	2.7 ± 1.0
0.5% CPP pH 8.0 (RE)	22.7 ± 14.9	1.5 ± 1.2
0.5% CPP pH 8.5 (RF)	19.0 ± 11.8	2.2 ± 0.8
0.5% CPP pH 9.0 (RG)	28.1 ± 12.0	1.7 ± 0.8

a Mean ± standard deviation (n = 10).
b Significantly different from other values in the column not similarly marked.
c Significantly different to RE, RF, and RG ($p < 0.05$).

Table 1-11: Effect of CPP solution pH on remineralisation of enamel subsurface lesion. From (Reynolds, 1997)

Kanekanian and colleagues studied the effect of calcium concentration on the hydroxyapatite dissolution using calcium enriched CPP and calcium reduced CPP as alternatives to CPP, in addition to tryptic casein and sodium caseinate (Kanekanian *et al.*, 2008). The effect of concentration is shown in Figure 1.15 and Figure1.16. The profiles demonstrate that all the caseins had a protective action, which was directly proportional to the concentration used. The lowest effect was found for the sodium caseinate whilst CPP + Ca and CPP – Ca, produced similar to each other.

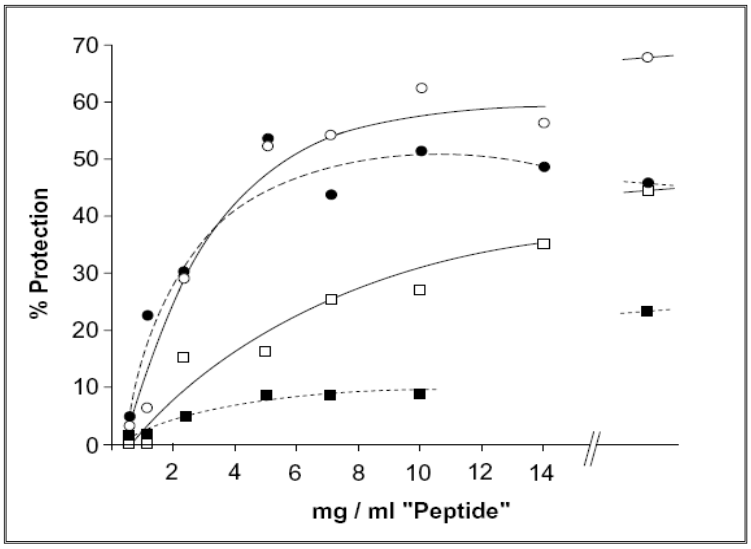

Figure 1.15: Inhibition of hydroxyapatite with unbound Ca solubilisation by acidic buffer at pH 4.2. Calcium-saturated CPP, ○–○; calcium-reduced CPP, ●–●; tryptic casein, □–□; sodium caseinate,■–■. From (Kanekanian *et al.*, 2008).

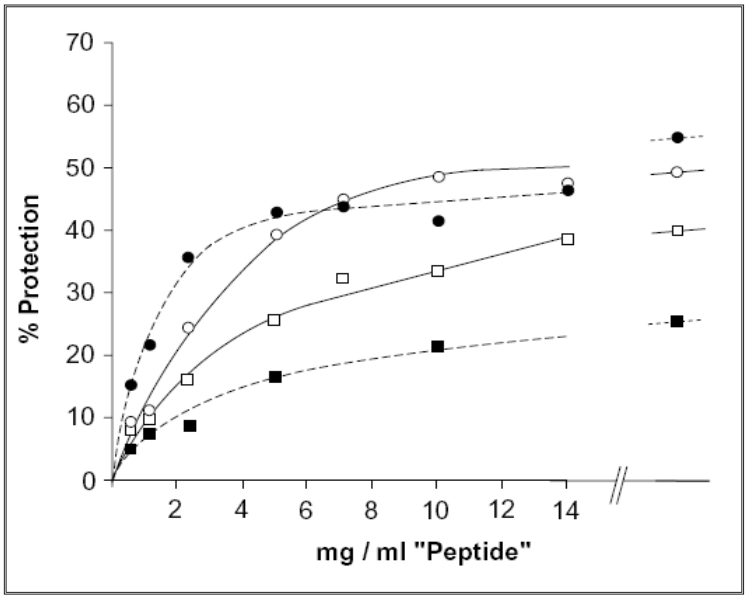

Figure1.16: Inhibition of hydroxyapatite free from unbound Ca solubilisation by acidic buffer at pH 4.2. Calcium-saturated CPP, ○–○; calcium-reduced CPP, ●–●; tryptic casein, □–□; sodium caseinate, ■–■. From (Kanekanian *et al.*, 2008).

1.2.4.3.1 Sugar–free chewing gums

A report published in 2001 described a sugar-free chewing gum as carrier for the CPP-ACP (casein phosphopeptide - amorphous calcium phosphate) and was examined for *in situ* on human enamel remineralisation (Shen *et al.*, 2001). Three cohorts of 10 volunteers wore a palatal appliance holding enamel slabs and were treated with four preparations containing CPP-ACP. The subjects chewed the preparation for 20 minutes, 4 times a day for 14 days. The additives used were sorbitol and xylitol. The remineralisation of the enamel was found to be dose-dependent as shown in Figure 1.17 and independent on the type of additives used.

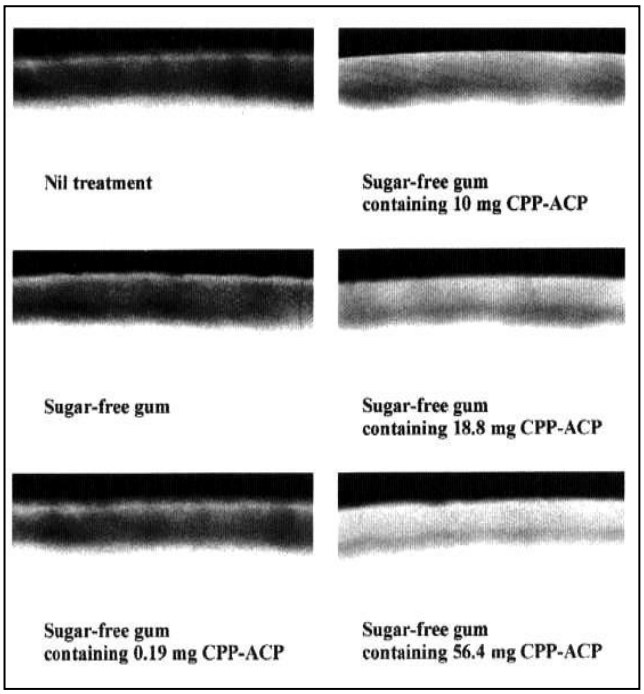

Figure 1.17: Microradiographic image for the effect of CPP-ACP on enamel subsurface lesions. From (Shen *et al.*, 2001).

Recaldent™ gums containing CPP-ACP produced the maximum level of enamel subsurface lesion remineralisation as compared to those gums contained $CaCO_3$ with and without $CaHPO_4$. Furthermore, the plaque alkali extract had 81% of total CPP and the percentage residence was equal to 3.5 times greater than the baseline (Reynolds *et al.*, 2003). The enamel resistance to acid challege was studied by exposing control and test enamel samples to acidic solution for 8 and 16h after sugar-free gum chewing for 20min 4 times a day for 14 days. The sugar-free gum used in the test contained 18.8mg CPP-ACP, against a placebo control. It was found that the ability of CPP-ACP to produce remineralisation was approximately double that produced by the control sugar-free gum. Demineralisation after 8 and 16h acid exposure was 65.4-88% for control and 30.5-41.8% for CPP-ACP, respectively. It was found that beneath the remineralised zone, for both control and test there remineralised an narrow zone of demineralisation as shown in Figure 1.18 (Iijima *et al.*, 2004).

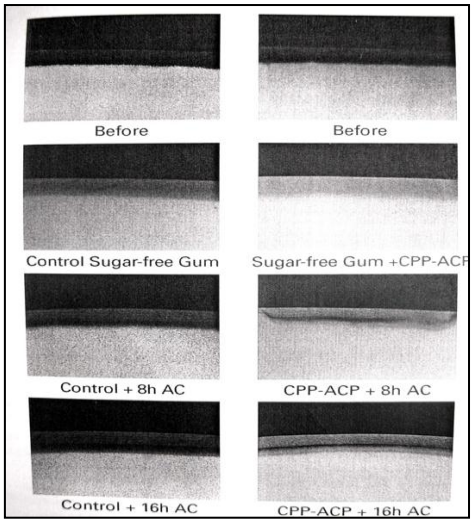

Figure 1.18: Microradiograph of enamel subsurface lesion before and after 8 and 16h challenge. From (Iijima *et al.*, 2004).

The effect of acidity on the remineralisation action of sugar-free chewing gum with and without citric acid has been further investigated by chewing for 20 minutes for 14 days, 4 times a day followed by 16 h acid treatment using Carbopol containing buffers of lactic acid and calcium phosphate (White, 1987). The treatment was carried out with three chewing gums. The first preparation contained 18.8mg CPP-ACP and 20mg citric acid, the second contained only 20mg citric acid and the third was a control containing neither ingredient. The data shown in Table 1-12 highlights that the resistance to acid demineralisation was significantly greater ($p<0.05$) for a chewing gum containing CPP-ACP (Cai *et al.*, 2007).

Gum Type	% Remineralisation before acid challenge	% Remineralisation after acid challenge	Difference in % of remineralisation
Neutral	9.4 ± 1.2^{a}	-2.8 ± 1.9^{a}	-12 ± 1.5^{b}
Citric acid	2.6 ± 1.3^{a}	-11.7 ± 1.6^{a}	-14.3 ± 2.0^{b}
CPP-ACP and Citric acid	13.0 ± 2.2^{a}	2.9 ± 1.8^{a}	-10.1 ± 1.2^{b}
a – All values were significantly different from each other ($p<0.05$) b – All values were significantly different from each other ($p<0.01$)			

Table 1-12: Remineralisation data of sugar-free chewing gums. From (Cai *et al.*, 2007).

A recent clinical trial examined the effect of sugar-free gum containing CPP-ACP nanocomplex. This trial lasted for 2 years and enrolled more than 2500 subjects. The result indicated that there is a significant difference between control and CPP-ACP nanocomplex containing sugar-free gums (Morgan *et al.*, 2008).

1.2.4.3.2 Sugar-free lozenges

The inclusion effect of CPP-ACP into sugar-free lozenges on the enamel remineralisation was determined by measuring the percent remineralised sub-surface enamel lesions after lozenge intake 4 times daily for 14 days. 10 subjects who consumed 4 different types of lozenge in succession wore the palatal appliances holding enamel slabs. The results obtained confirm that lozenges containing CPP-ACP provide a dose dependent increase in remineralisation (Cai *et al.*, 2003).

1.2.4.3.3 Solutions

A mouth rinse was applied to examine the action of CPP-ACP in solution dosage forms in 2003. The mouth rinses used were deionised water, non-stabilized calcium phosphate solution and 2 and 4 % Recaldent™ mouthrinse solutions. Rinsing was carried out using 15mL for 30 seconds, 3 times a day for 4 days. The result shown in Figure 1. demonstrate that the plaque calcium and phosphate levels were not increased after exposure to non-stabilized calcium phosphate solution. In contrast, significant rises in these two ions were seen after exposure to mouth rinse solutions containing CPP-ACP, which were directly proportional to the concentration of CPP-ACP in the preparation (Reynolds *et al.*, 2003).

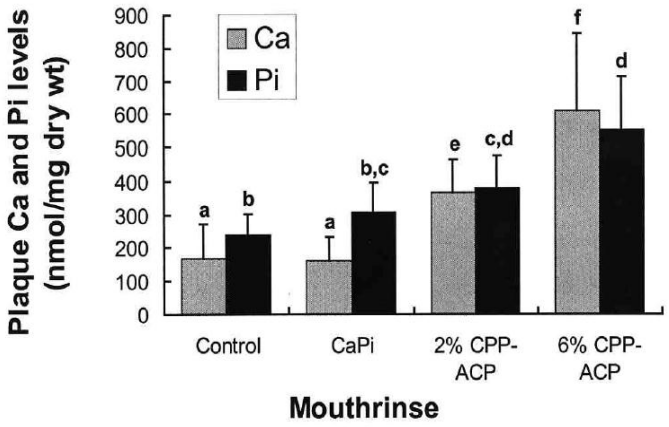

Figure 1.19: Plaque Calcium and inorganic phosphate levels after rinsing with non-stabilized calcium phosphate and CPP-ACP mouth rinse solutions. From (Reynolds *et al.*, 2003).

Powerade^{TM} sport drink has been utilized as an *in vitro* challenge to determine the reduction in demineralisation produced by CPP-ACP. Enamel slabs were incubated in solutions for 30 minutes and the lesion depth measured. Solutions and erosion lesion depth used are listed in Table 1-13. It was shown that the erosion lesion depth decreased with an increase in CPP-ACP concentration. In addition, this study suggested that 0.125%w/v was the maximum palatable concentration for oral solution (Ramalingam et al., 2005).

	Solutions	Depth of erosion (kA) mean (±SD), n=15
1	Powerade	38.70±5.60*
2	Powerade + 0.063% CPP-ACP	17.98±3.05*
3	Powerade + 0.09% CPP-ACP	4.31±0.64**
4	Powerade + 0.125% CPP-ACP	3.35±1.65**
5	Powerade + 0.25% CPP-ACP	1.94±0.65**
6	Double deionised water	2.53±0.67**
*Mean values, which differed with statistical significance. ** Mean values, which were not statistical significantly different.		

Table 1-13: Lesion depth for test solutions and deionised water. From Ramalingam *et al.* (2005).

A second *in vitro* study was reported by Cochrane's group (Cochrane *et al.*, 2008). This study examined the ionic effect of 2% w/v CPP-ACP and CPP-ACFP solutions on enamel remineralisation. Two sets of enamel slabs were examined at six different pH values: 4.5, 5, 5.5, 6, 6.5, and 7. Demineralised enamel slabs were suspended in 2mL of the prepared solutions at 37º C for 10 days with daily solution replacement. The collected data are summarized in Table 1-14 and Table 1-15. CPP-ACFP showed a remineralisation effect as shown in Table 1-14, which is confirmed by images in Figure 1.20. In addition, the maximum remineralisation effect was obtained at pH 5.5, at which the ratio of free to bound for Ca, PO_4 and F approached unity, as shown in Table 1-15. The authors highlighted that CPP-ACFP has higher remineralisation potential than CPP-ACP with a remineralisation rate equal twice than achieved previously (Cochrane *et al.*, 2008). The data for effect of pH on remineralisation concur with results obtained previously by Reynolds (Reynolds, 1997).

Treatment	pH	% Remineralisation	Rate (10^{-8}) mole apatite/m^2/s
2% CPP-ACP	4.5	10.3±3.3	1.4±0.9
	5	18.4±9.2	2.4±1.1
	5.5	41.8±8.5	5.7±1.4[a]
	6	26.7±8.4	3.7±1.3
	6.5	19.9±6.1	2.4±0.9
	7	15.0±3.5	2.0±0.6
2% CPP-ACFP	4.5	29.2±10.0	3.4±1.2
	5	40.0±11.2	4.4±1.7
	5.5	57.7±8.4	7.3±1.5[b]
	6	30.7±8.7	4.5±1.4
	6.5	20.8±5.8	2.6±0.8
	7	17.6±1.8	2.2±0.9
a-Significantly different to all other CPP-ACP values in the same column ($p<0.05$) b-Significantly different to all other CPP-ACFP values in the same column ($p<0.05$)			

Table 1-14: *In vitro* effect of pH on percentage and rate of enamel lesion remineralisation with CPP-ACP and CPP-ACFP solutions. (Cochrane *et al.*, 2008).

Treatment	pH	Free			CPP-bound		
		mM Calcium	mM Phosphate	mM Fluoride	mM Calcium	mM Phosphate	mM Fluoride
2% CPP-ACP[a]	4.5	60.0±1.6[c]	35.7±0.1		4.5±1.9	4.3±1.5	
	5	41.5±1.5	26.5±0.1		23.0±1.8	13.4±1.5	
	5.5	21.4±0.4	12.8±0.1		43.1±1.1	27.1±1.5	
	6	11.9±0.3	7.11±0.25		52.6±1.1	32.8±1.6	
	6.5	5.67±0.07	3.95±0.07		58.8±1.0	36.0±1.5	
	7	2.62±0.04	2.41±0.04		61.9±1.0	37.5±1.5	
2% CPP-ACFP[b]	4.5	54.0±1.4	33.4±0.2	0.68±0.05	24.1±2.2	14.8±1.3	11.7±0.3
	5	36.9±0.6	24.6±03	1.16±0.09	41.2±1.8	23.6±1.3	11.3±0.3
	5.5	18.5±0.1	13.5±0.7	1.54±0.12	59.6±1.7	34.6±1.5	10.9±0.3
	6	8.74±0.14	6.33±0.03	1.54±0.06	69.4±1.7	41.8±1.3	10.9±0.3
	6.5	4.51±0.07	3.96±0.16	1.60±0.06	73.6±1.6	44.2±1.3	10.8±0.3
	7	2.21±0.04	2.61±0.07	1.58±0.13	76.0±1.6	45.6±1.3	10.8±0.3

a-Total concentration Ca and PO_4 was 64.5±1.0 and 40.0±1.5 mmol/L, respectively.
b-Total concentration Ca, PO_4 and F was 78.1±1.6, 48.2±1.3 and 12.4±0.3mmol/L, respectively.
c-Mean ±SD

Table 1-15: Effect of pH on free and CPP bound Ca, PO4 and F ions in CPP-ACP and CPP-ACFP remineralisation solutions. From (Cochrane *et al.*, 2008).

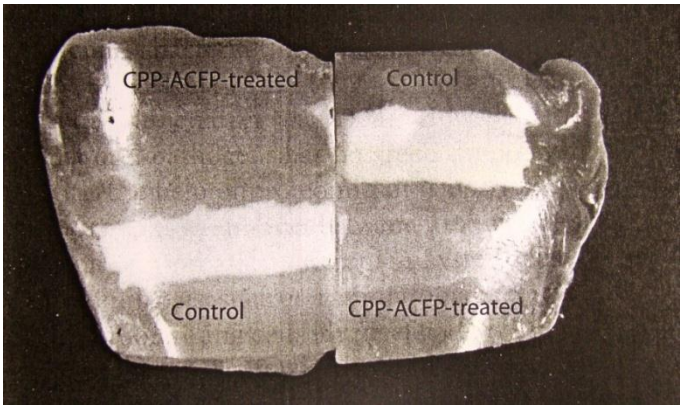

Figure 1.20: Representative images of enamel subsurface lesion treated with 2% w/v CPP-ACFP solution at pH 5.5. From (Cochrane *et al.*, 2008).

1.2.4.3.4 Tooth paste

Kumar and colleagues have described a comparison of mousse and toothpaste supernatants using similar experimental designs to those described previously. A carious lesion with depth of 120-200μm was generated on permanent teeth by immersing in a demineralising solution. The samples were then allocated to groups and exposed to 5 different types of treatment. The treatment schedule was immersing for 3 times a day for 3 hours in demineralising solution, with an intermittent 2 hours of twice daily exposure to remineralising solutions for 10 days. The samples were treated with test treatments listed in Table 1-16 at each transfer.

Groups	Treatment
A	Supernatant of fluoridated toothpaste 1100ppm as positive control for 60s.
B	Non-fluoridated toothpaste as negative control.
C	Supernatant of Tooth Mousse™ contained CPP-ACP used as toothpaste for 60s.
D	Topical coating of Tooth Mousse™ contained CPP-ACP used for 3m.
E	Topical coating of Tooth Mousse™ contained CPP-ACP used for 3m after treated for 60 s. with supernatant of fluoridated toothpaste.

Table 1-16: Test treatments. Data obtained from (Kumar *et al.*, 2008).

As shown in Figure 1.21, a significant reduction in lesion depth was demonstrated for treatments A, C, D and E. However, the lesion was significantly increased in treatment B. In addition, it was concluded that CPP-ACP containing Tooth Mousse™ gave the maximum remineralising action when applied after brushing with fluoridated toothpaste (Kumar *et al.*, 2008).

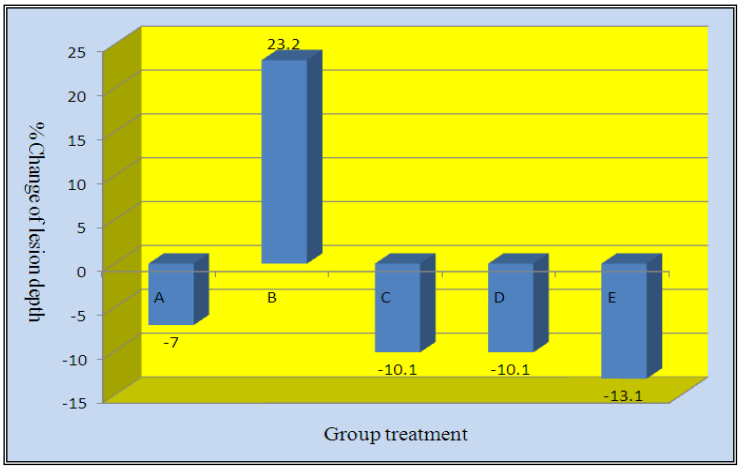

Figure 1.21: Means of percentages change in lesion depth (μ) after five treatments. According to data obtained from (Kumar *et al.*, 2008).

1.3 Effect of various forms of calcium phosphate on remineralisation

Five treatments were compared to examine the effect of various forms of calcium phosphate added to CPP-ACP on remineralisation of pre-lesion bovine enamel slabs. 4 treatment groups with 20min chewing four times a day for 14 days and a no-treatment control were compared as listed in Table1-17. There was no significant difference among groups suggesting the use of chewing gums do not provide an additional remineralisation benefit. In addition, the 4.4% gain of remineralisation with chewing gum containing 0.7% CPP-ACP differ from previous results obtained by Shen and colleagues (Shen *et al.*, 2001). The possible reason suggested for the difference in outcomes was the different slab location in the palatal appliances (Schirrmeister *et al.*, 2007).

	Compounds	Gum type
Group 1	Dicalcium phosphate 3.9%, Calcium gluconate 1.8%, Calcium lactate 0.45% and sodium carbonate 0.45%	Sugar substitutes, gum baseflavours,E422, hydrolysed milk protein, water and phenylanalnine
Group 2	Dicalcium phosphate 3.9%, Calcium gluconate 1.8%, Calcium lactate 0.45% and sodium carbonate 0.45%	Sugar substitutes, gum base, flavours, E422, hydrolysed milk protein, water, phenylanalnine and Zinc citrate.
Group 3	CPP-ACP 0.7% and Calcium carbonate	Sugar substitutes, gum base, flavours, E414, E472, Sodium stearate, E171, E903 and phenylanalnine.
Group 4	No Calcium	Sugar substitutes, gum base, flavours, E414, E422, Sodium stearate, E171, E903 and phenylanalnine.
Group 5 Control	No chewing gum	

Table1-17: Gum types and compounds. From (Schirrmeister *et al.*, 2007).

1.4 Research objectives

The main objective of this thesis was to study the preparation and formulation of ACP nanocomplexes stabilised by food grade additives into a suitable dental dosage form for potential use in enamel remineralisation. To achieve this goal, the ACP stabilised by tryptic digest of casein phosphopeptides had to be prepared and investigated for mechanism of stabilisation. Following on from this initial work an alternative means of stabilisation had to be investigated. The following specific aims were performed in order to accomplish the stated objectives:

In the first instance extraction and peptide analysis of CPP and negatively charged ionizable peptides (NGP) from sodium casein and hydrolysed casein were performed. Following this ACP stabilised by CPP, NGP and unfractionated hydrolysed casein were all prepared and characterised in Chapter 2 of this thesis.

Chapter 3 focuses on the cellulosic polymers that enable the stabilisation of ACP nanocomplexes, via the presence of the negatively charged ionizable carboxyl group. The preparation of ACP stabilised by polymer selected to be the most suitable is also discussed. In addition to this, characterisation of the prepared ACP was carried out to determine the amorphous state and the nano size range of the colloidal particles.

The next phase of the study looked at the pre-formulation analysis of the prepared ACP for the calcium content and pH-solubility. In addition, a method of calcium determination using a calcium ion selective electrode was validated. The final stage of chapter 4 focuses on the formulation and characterisation of the adhesive dental film dosage form containing ACP, in addition to investigating the calcium release analysis.

Chapter 5 describes the investigation of the inhibitory effect of the prepared ACP on the orally relevant biofilm. The biofilm thickness was used as a marker of the effect of the ACP and was determined using confocal microscopy.

The final part of the thesis describes the investigation of the remineralisation performance of the dental films selected based on the results that had been obtained from the previous studies. The remineralisation study was carried out on human dental enamel blocks and the counts of calcium and phosphorus deposition on the cross-

sectioned enamel surface were used as a marker of the depth of remineralisation and determined using electron probe microanalysis.

Chapter 2. Preparation of ACP nanocomplexes stabilised by negatively charged ionisable peptides (NGP) in food-grade hydrolysed casein and unfractionated hydrolysed casein.

2.1 Introduction

The formation of calcium phosphate in buffered electrolyte solutions occurs in a sequence of three events: primary deposition of amorphous calcium phosphate (ACP) followed by transformation to seed crystals and then enlargement of these crystals (Termine and Posner, 1970). The time required to convert the amorphous form into the crystal form is affected by solution conditions including pH, temperature, ionic strength, the ratio of calcium to phosphate ions and the starting concentrations. The stability of the amorphous state has been found to be enhanced by the presence of poly L-glutamate, casein, phosvitin and polyacrylate as well as by the addition of minute amount of electrolytes such as magnesium, pyrophosphate, carbonate and fluoride (Termine *et al,* 1970). Casein phosphopeptides have been used to stabilise the ACP at nanometre sizes from solutions with a low content of salts, in the presence of β-(1→25) bovine casein at pH values rising from 5.5 to 6.7 with the addition of urea and urease. An analytical confirmation has been made to determine the presence of ions and free peptide in dynamic exchange with nanocomplexes (Holt *et al.*, 1996). Core to shell modelling of the ACP stabilised by β-casein (1→25) was characterised by Holt and colleagues (Holt *et al.*, 1998) as $CaHPO_4 \cdot 2H_2O$ units of 2.30±0.05 nm in the core surrounded by 49 ± 4 CPP chains forming a shell with an outer radius of 4.04 ± 0.15 nm as shown in Figure 2-1.

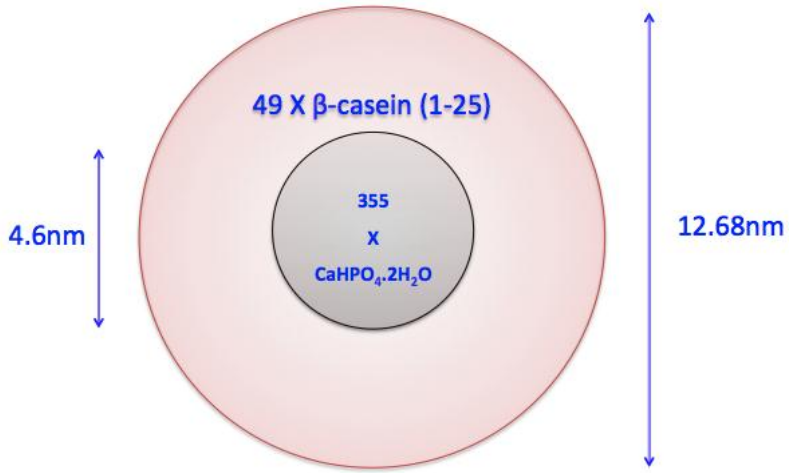

Figure 2-1: A plot of ACP stabilised by ß-casein (1-25) shows the dimensions of the core of 355 molecules of $CaHPO_4$. $2H_2O$ surrounded by a shell of 49 peptides.

The synthetic polymer polyethylene glycol mol wt 10,000 Daltons (PEG10000) has been reported to stabilise ACP. A solution of calcium chloride (0.1M) and PEG in a specific concentration ratio was prepared and left overnight followed by the addition of tribasic sodium phosphate (0.133M) at 5° C with stirring for 30 minutes. The lack of crystallinity of the prepared amorphous calcium phosphate was confirmed by X-ray diffraction analysis (Li *et al.*, 2003). Silcock and his colleagues studied the enhancement of calcium loading of hydrolysed casein, which was carried out with a partial cross linking of the glutamyl / lysyl residues of casein (4.5% w/w) treating the preparation with the enzyme transglutamase for various time periods followed by calcium and phosphate loading. The remineralisation efficiency of enamel by these complexes was confirmed (Silcock *et al.*, 2009).

2.1.1 Objectives:

The objective of the present study was to use negatively charged ionizable peptides (NGP) and hydrolysed casein as alternatives to CPP to stabilise amorphous calcium phosphate during the isolation and LC-MS analysis of CPP and NGP those extracted from sodium casein and hydrolysed casein, respectively. The ACP nanocomplexes prepared from NGP and unfractionated hydrolysed casein were then characterised.

2.2 Materials and methods

2.2.1 Materials

Bovine casein sodium salt, trypsin from porcine pancreas (1,000-2,000 BAEE units/mg solid, lot#039K013), tris (hydroxymethyl) aminomethane, calcium chloride dihydrate, disodium hydrogen phosphate, hydrochloric acid, acetone and ethanol were purchased from Sigma-Aldrich (UK). Enzymatically-hydrolysed casein-CE90CPP (lot# 10461008) was kindly provided by DMV International (USA).

2.2.2 Preparation of casein phosphopeptides from sodium casein

The first attempt to prepare casein phosphopeptides in our laboratory followed the same procedure employed by (Reynolds, 1991) and (Reynolds *et al.*, 1994), as shown in figure 2-2 with modifications using calcium chloride instead of barium chloride. The precipitation step was completed in chilled acetone as an alternative to sulphuric acid. The percent yield was recorded.

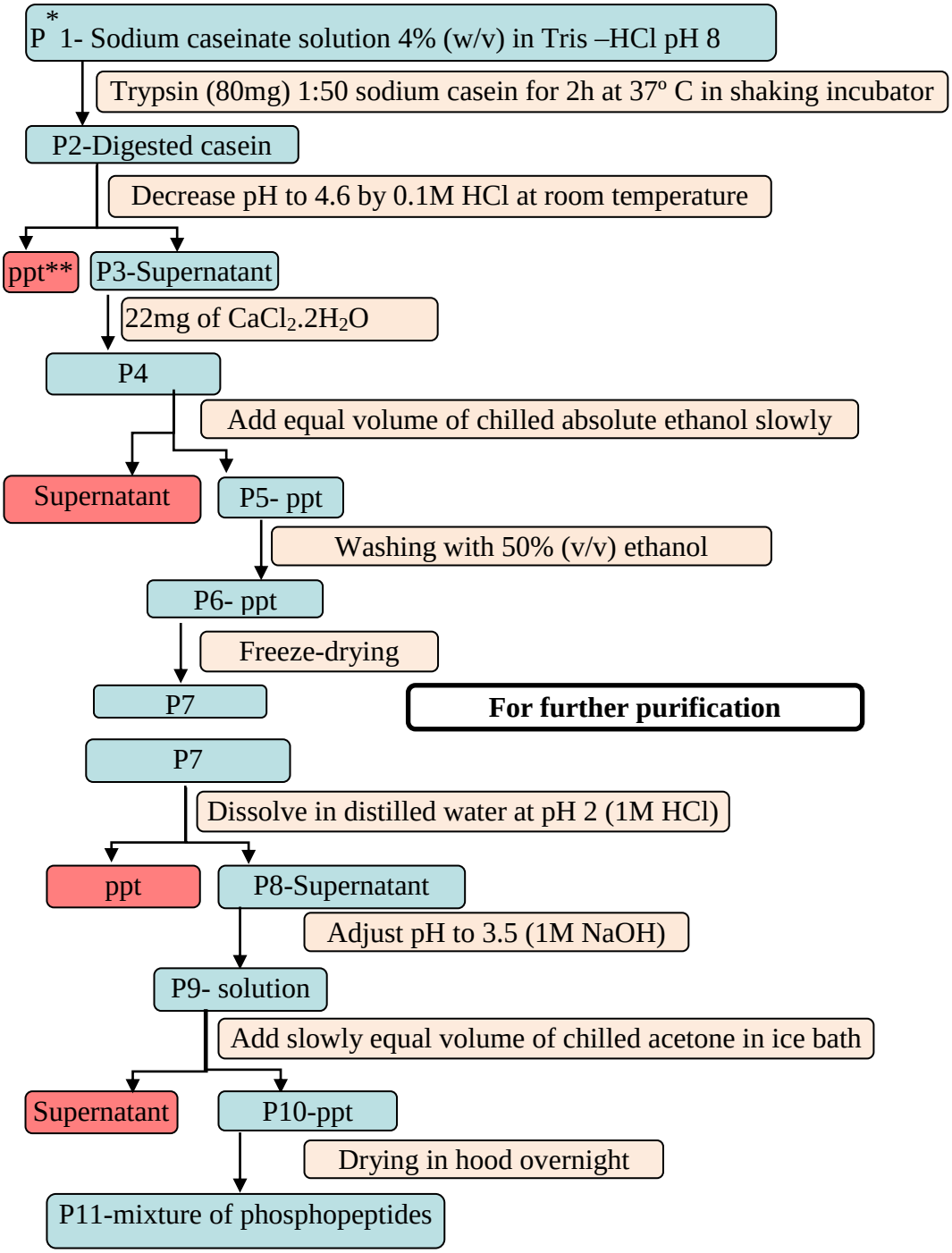

* Product number
** Precipitate

Figure 2-2: Flow diagram illustrating the isolation procedure of casein phosphopeptides from sodium caseinate using calcium chloride instead of barium chloride. The precipitation step was completed in chilled acetone as an alternative to sulphuric acid.

In order to increase the product yield, further modification was made by increasing the amount of trypsin and time of digestion to 18 hours. In addition, the amount of calcium chloride was increased as a result of a calculation based on the molecular weight of α and β casein fractions (25 kDa), rather than the whole molecule of casein (520 kDa) as shown in equation 2.1. Furthermore, the product P6 was directly transferred to the purification step without freeze-drying. The percent yield was recorded and the sample was taken for analysis using LC-MS spectrophotometry.

$A = 20 \times (B/C) \times$ mol weight of $CaCl_2.2H_2O$ ------- Equation 2.1

Where A is the amount required of calcium chloride in the preparation of P4, 20 as a twenty-fold molar ratio that was used, while B is the weight of sodium casien and C is the molecular weight of the used sodium caseinate (520 kDa) or casein fraction (25kDa). Further modifications were applied to increase the yield as shown in results section 2.3.1. The time of digestion was extended to 36 hours and acetone was used instead of ethanol, with the final procedure as shown in figure 2-3. The percentage yield was recorded and the samples were subjected to analysis using LC-MS spectrophotometry.

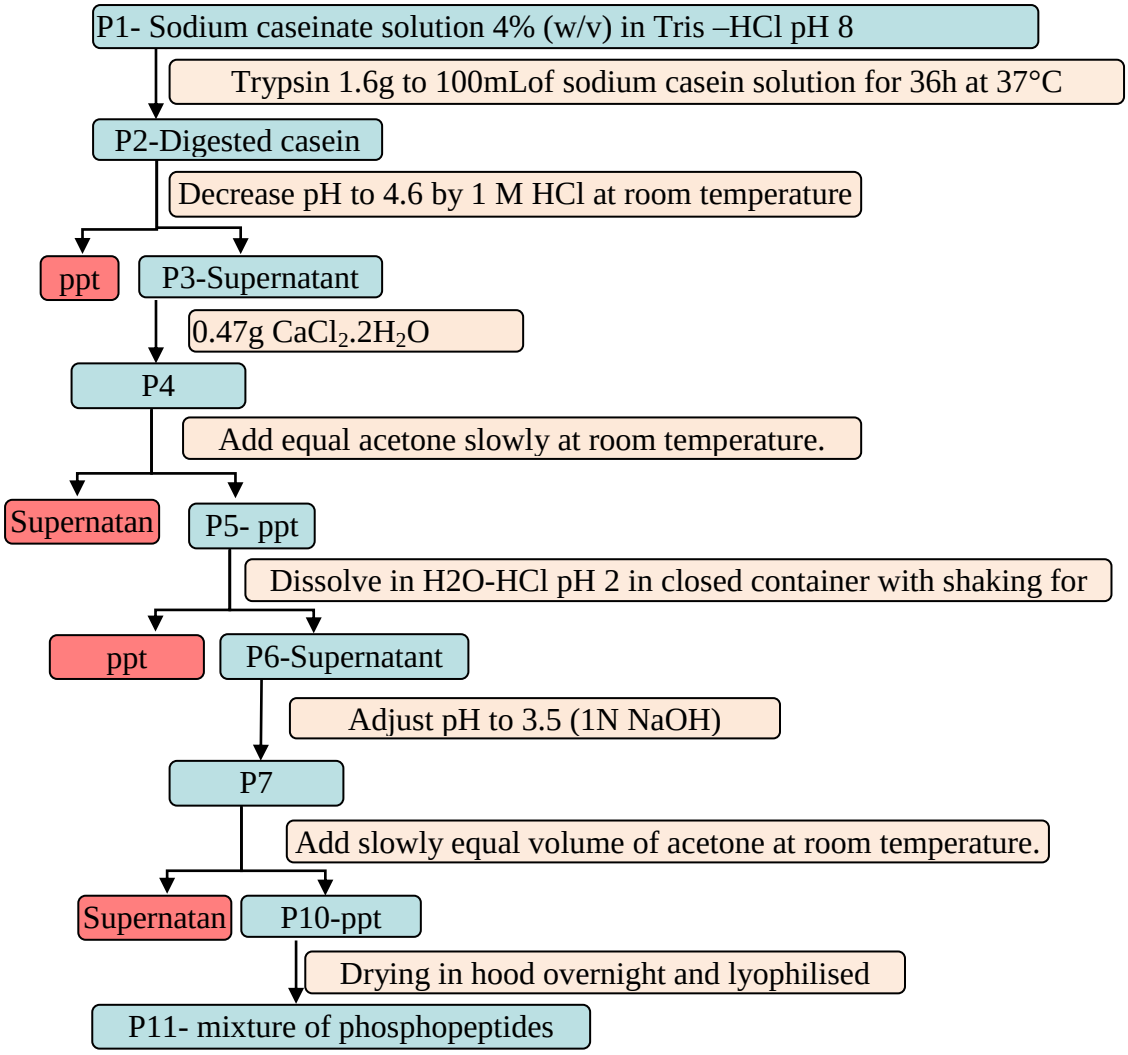

Figure 2-3: Flow diagram illustrating the isolation procedure of casein phosphopeptides from sodium caseinate using the modified method

2.2.3 Extraction of NGP from hydrolysed casein (HC)

A 4 % (w/v) of HC in distilled water solution was used to isolate NGP with the adapted procedure as shown in figure 2-4. The product obtained was weighed and subjected to analysis using LC-MS spectrophotometry.

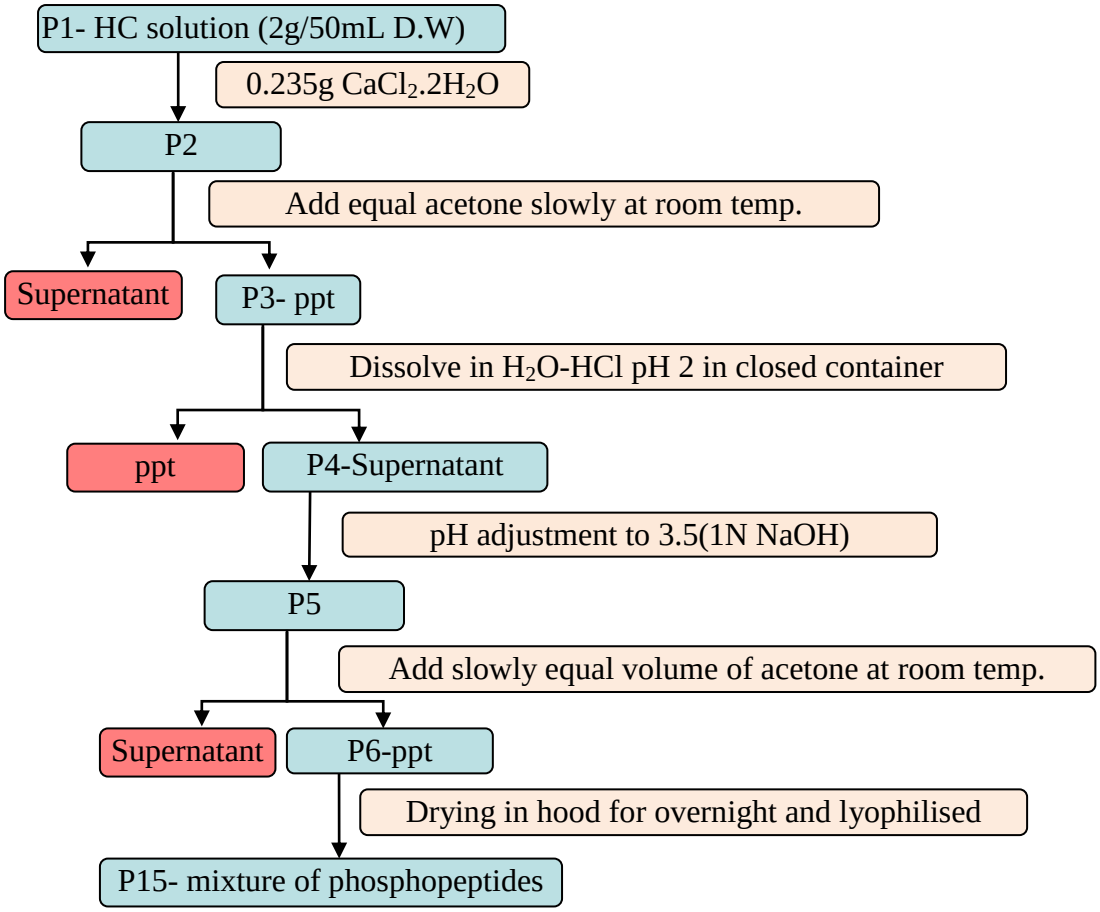

Figure 2-4: Flow diagram illustrating the isolation procedure of NGP from HC

2.2.4 LC-MS Analysis of CPP and NGP products

A Finnigan LTQ iontrap mass spectrometer coupled with a Fourier transform-Orbitrap (Thermo Electron Corporation) was connected to a HPLC System. The HPLC unit was equipped with Finnigan Surveyor autosampler Plus and a Finnigan Surveyor MS pump. A ZIC-HILIC® column (5µm, 200 Å, 150×4.6mm; HICHROM, UK) was used. The flow rate used was 0.5mL.min^{-1} for chromatographic separation and analysis of the isolated peptides. Samples of the prepared CPP and NGP were prepared in Milli-Q water at concentration of 6mg/mL. Gradient elution was used with solution A, which consisted of 0.1% v/v formic acid in acetonitrile and solution B, 0.1% formic acid v/v in Milli-Q water were used. UV monitoring at 214nm and 280nm were used for channel A and channel B respectively according to the data obtained from the sample spectra for the UV scan.

Gradient and isocratic elution procedures shown in table 2-1 were used for optimisation, which was subsequently employed to analyse the prepared CPP and NGP. The mass peaks obtained were then matched with their corresponding peptides.

	Method	Concentrations of A		Time (min)	
1	Isocratic	90%		60	
2	Isocratic	85%		60	
3	Isocratic	80%		60	
4	Isocratic	75%		60	
5	Isocratic	70%		60	
6	Isocratic	65%		60	
7	Gradient	90-60%	60%	20	20-60
8	Gradient	90-60%		30	
9	Gradient	90-60%		40	

Table 2-1: LC-MS elution methods

2.2.5 Preparation of CPP-ACP, NGP-ACP and HC-ACP

2.2.5.1 Preparation of CPP-ACP and NGP-ACP

The preparation method used was adapted from Cross and colleagues (Cross *et al.*, 2005b). The prepared CPP and NGP were dissolved at a concentration of 50mg/5mL in Milli-Q water. Calcium dichloride dihydrate and disodium hydrogen phosphate dodecahydrate in molar ratio of 1.67 [1.25mL from each (0.5M $CaCl_2.2H_2O$ and 0.3M $Na_2HPO_4.12H_2O$)] were added separately by syringe pump (WU-74900-05 Cole-Parmer UK) at a rate of 7.5mL h^{-1} to the solutions adjusted to pH 9.0 with 0.5M NaOH (figure 2-5). Samples of colloid were analysed for particle size determination. Half of the ACP produced was then isolated by microfiltration through a 30,000 molecular weight cut off VIVASPIN 20 Sartorius filter and washed 3 times with 2 volumes of Milli-Q water to remove free calcium and phosphate ions. The purified fraction and the remaining half were then freeze dried. The purified fraction obtained from the isolation process was referred to as isolated ACP in the rest of this thesis. The crude fraction, which did not go through the purification process, is hereafter referred to as unpurified ACP.

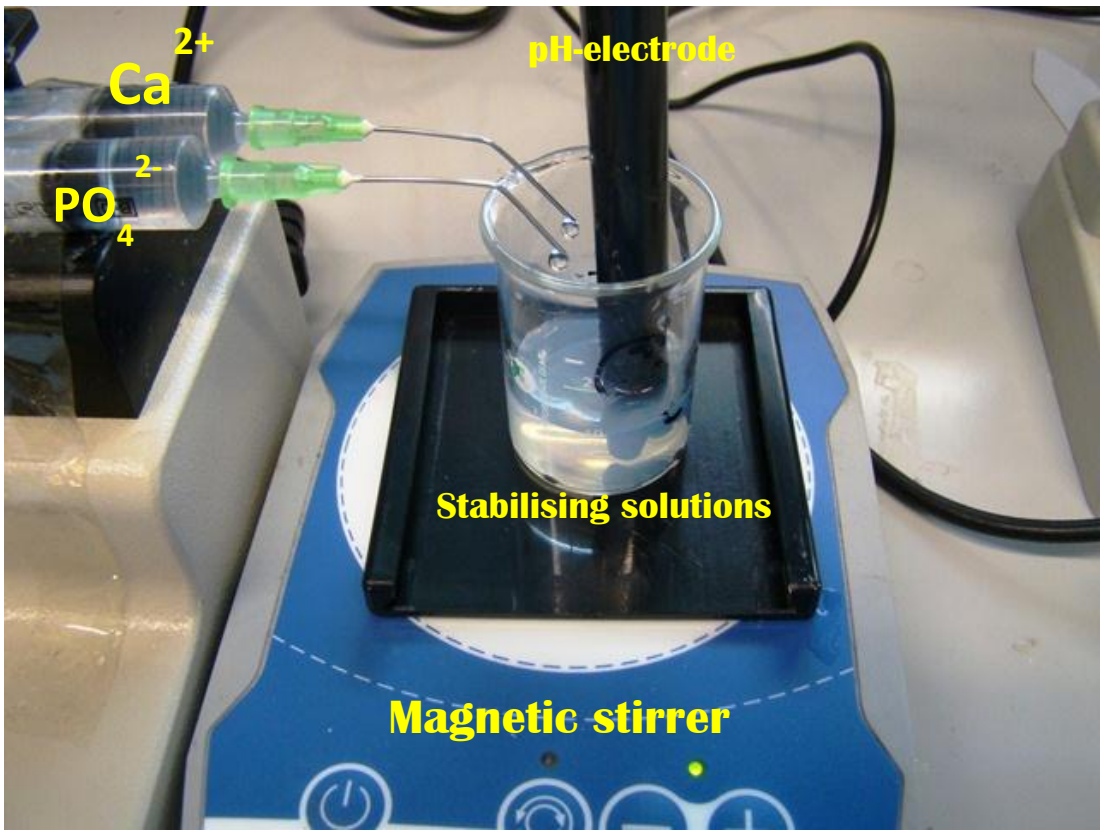

Figure 2-5: Preparation of ACP by the gradual addition of calcium chloride and disodium hydrogen phosphate solutions into a solution containing the stabilising agent.

2.2.5.2 Method modification of NGP-ACP preparation

In order to reduce the prolonged instrument use in the preparation of NGP-ACP, a modification was performed by the addition of $Na_2HPO_4.12H_2O$ to the NGP solution containing $CaCl_2.2H_2O$ at pH 5. The pH was raised gradually to 7 using 0.5M NaOH to complex the calcium phosphate. The final isolated preparation and also the unpurified NGP-ACP were then freeze-dried. These products were used later (sections 2.3.3 and 4.3.2) to study the effect of the isolation step on the properties of the prepared ACP.

2.2.5.3 Preparation of HC-ACP (final modification).

Following the isolation of NGP from HC as detailed in 2.2.3, HC (1 g) was dissolved in 10mL Milli-Q water and 2.125 mL of each of the stock solutions 0.5M $CaCl_2.2H_2O$ and 0.3M $Na_2HPO_4.12H_2O$ were added.

2.2.6 Characterisation of the prepared ACP

2.2.6.1 Particle size analysis

Dynamic light scattering (DLS) using a Zetasizer (NanoZS, Malvern-UK) was used for particle size measurement of the prepared colloids and freeze dried ACP. Freeze dried ACP samples were prepared by the reconstitution of 10mg in 1 mL of Milli-Q water. Samples were pooled into a 1.5 mL polystyrene semi-micro cuvette. Three consecutive measurements were taken for each sample.

2.2.6.2 Solid state form analysis of NGP-ACP and HC-ACP

To confirm the lack of crystallinity, X-Ray powder diffraction analysis was carried out on samples of the prepared NGP-ACP and HC-ACP samples that had been stored for longer than one month. Samples were held in 0.7mm glass capillary tubes and the source of radiation used was CuK alpha 1 on a Bruker D8 diffractometer. The data were collected for a theta scale of 2-34.

2.2.6.3 Scanning and transmission electron microscopy imaging

Scanning electron microscopy (JEOL 6400 SEM-Japan) was used to image NGP-ACP and HC-ACP. Powders were dusted on 10 mm aluminium stubs with double sided copper tape and coated with gold using a sputter coating system (Polaron SC 515).

Transmission electron microscopy (Leo 912AB TEM-Germany) images were obtained by methylamine vanadate (Nanovan®) negative staining of NGP-ACP and HC-ACP colloidal samples on carbon-coated grids with a 300 mesh.

2.2.6.4 Thermal stability study

Thermal gravimetric analysis (TGA) of the prepared NGP-ACP and HC-ACP was carried out to identify temperature ranges that were suitable for differential scanning calorimetry (DSC). Experiments were conducted using a Mettler Toledo TGA/SDTA 851e and Mettler Toledo DSC 8222e using STARSW 8.10 software. Samples of approximately 2–5 mg were placed in an alumina or aluminium pans sealed with a pinhole in the lid. The rate of heating used was 10 ° C min^{-1} from 0 to 750 ° C in TGA and from 0-300° C in DSC.

2.2.6.5 Dynamic vapour sorption (DVS) analysis

Samples of approximately 10-13 mg were subjected to two controlled cycles of changing relative humidity using a DVS apparatus (SMS-UK), beginning with an initial drying phase at 0% RH, followed by 2 cycles of increasing to 95% RH in 10% steps, followed by desorption from 95 to 0% RH in same decrements at constant temperature of 25º C. The records of sample mass change with correspond RH were collected and transferred into profiles using DVS analysis suite for Microsoft Excel 2010.

2.2.7 Statistical analysis

The particle sizes of the prepared CPP-ACP, NGP-ACP and HC-ACP were statistically analysed using one-way ANOVA on Minitab V.16 to find out the effect of stabilising agents on the size of the produced nanocomplexes.

2.3 Results

2.3.1 Preparation of CPP from sodium casein and NGP from hydrolysed casein

The calculated theoretical content of CPP in sodium casein was equal to 12% (w/w). The yield of products was found to increase with modification of the procedures and percentages recovered from the calculated CPP were 1.3%, 15.16% and 69.16% (w/w). However, the percentage yield of NGP from HC was 8.5% (w/w). The prepared CPP from second and third attempts and NGP were subjected to peptide content analysis.

2.3.2 LC-MS Analysis of CPP and NGP

The ZIC-HILIC® column employs hydrophilic interaction liquid chromatography that is suggested to be a suitable technique to separate polar compounds especially peptides. The collected peaks of MS with m/z +2 from the corresponding methods used are listed in table 2-2, and method 4 was selected for content analysis of the peptides because it resolved the highest number of peaks.

Method	Method	m/z +2 Peaks
1	Isocratic 90%	1484 and 1177
2	Isocratic 85%	1484 and 1177
3	Isocratic 80%	1444, 1484, 1177
4	Isocratic 75%	1562, 1496, 1484, 1444, 1246, 1177, 1137 and 1079
5	Isocratic 70%	1496, 1484, 1444, 1246, 1177 and 1079
6	Isocratic 65%	1496, 1484, 1444, 1246, 1177, 1137 and 1079
7	Gradient 90-60% (20)	1496, 1484, 1444, 1373, and 1177
8	Gradient 90-60% (30)	1496, 1484, 1444, 1373, and 1177
9	Gradient 90-60% (40)	1496, 1484, 1444, and 1177

Table 2-2: MS peaks with m/z +2 from the corresponding methods of 60 minutes elution time.

Table **2-3** identifies the presence of m/z peaks for CPP produced from second and third batches in addition to NGP. Figure 2-6 shows an example of HPLC and mass peaks for β-casein (1-24)4P. The results obtained for the NGP did not reveal αS2

casein (1-23) and αS1 casein (59-79) fractions. Furthermore, the presence of de-monophosphorylated and de–diphosphorylated CPP and NGP indicates that the trypsin contained alkaline phosphatase enzymes.

Peptides	Observed	Calculated	m/z +2
β-casein (1-25)4P	3123.28	3123.26	1562.14
αS2 casein (1-23)4P	2990.16	2990.08	1496.07
β-casein (1-24)4P	2967.16	2967.16	1484.09
β-casein (1-24)3P	2887.22	2886.18	1444.11
β-casein (1-24)2P	2807.24	2805.24	1404.12
αS1 casein (59-79)5P	2721.92	2721.91	1361.46*
Not identified	2703.91		1352.95**
αS1 casein (59-79)4P	2641.96	2640.93	1321.48
αS2 casein (2-20)4P	2491.8	2491.82	1246.41
αS2 casein (2-20)3P	2411.86	2410.83	1206.43
αS1casein (73-91)1P	2363.86	2364.10	1182.43
αS1casein (33-52)2P	2353.88	2352.98	1177.44
αS1casein (33-52)1P	2273.92	2273.00	1137.46
β-casein (32-47)1P	2061.84	2060.82	1031.42
αS1casein (115-119)1P	671.24	671.23	671.24***

*_in CPP

**_in NGP

***_(m/z+1)

Table 2-3: Peptides identified in CPP and NGP with Isocratic 75% for 60 minutes elution time.

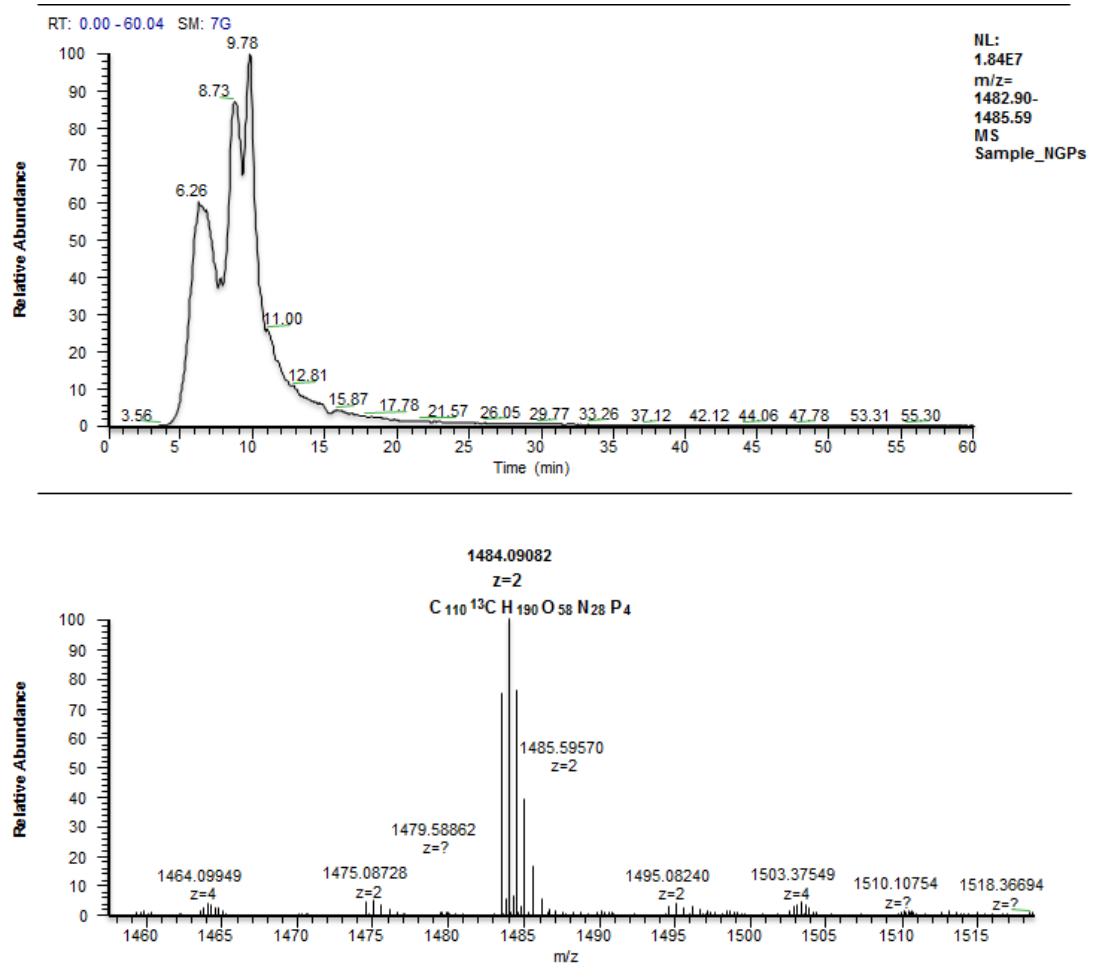

Figure 2-6: HPLC (upper) and LC-MS (lower) chromatograms of isolated peptides in CPP.

2.3.3 Characterisation of the prepared ACP

The prepared isolated NGP-ACP and HC-ACP had different appearances as shown in figure 2-7, HC-ACP was characterised as a structure of shiny flakes whilst NGP-ACP was light friable latex easy broken to a free-flowing powder with a spatula. In contrast, the unpurified ACP showed a harder matrix structure, especially that prepared from HC-ACP as shown in figure 2-8.

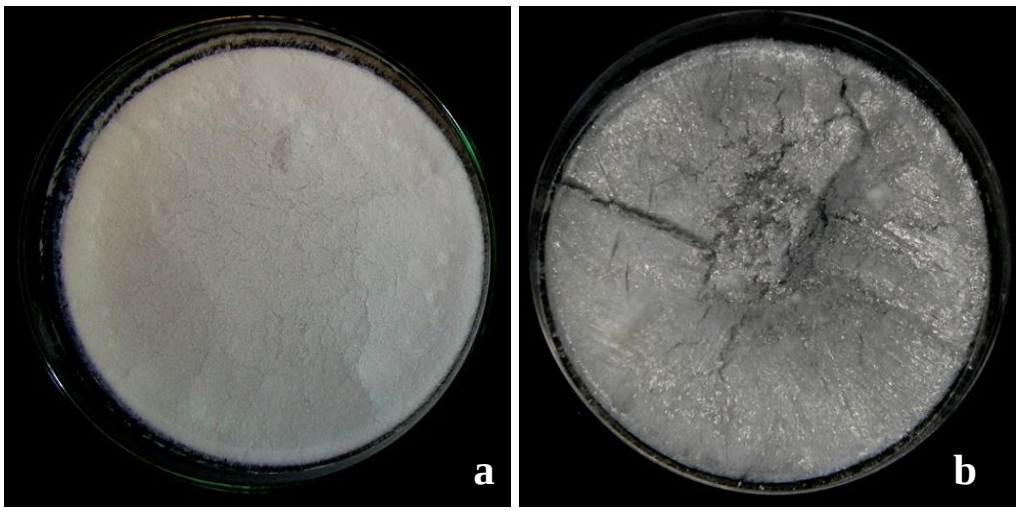

Figure 2-7: Photographic images of the freeze dried isolated NGP-ACP (a) and HC-ACP (b)

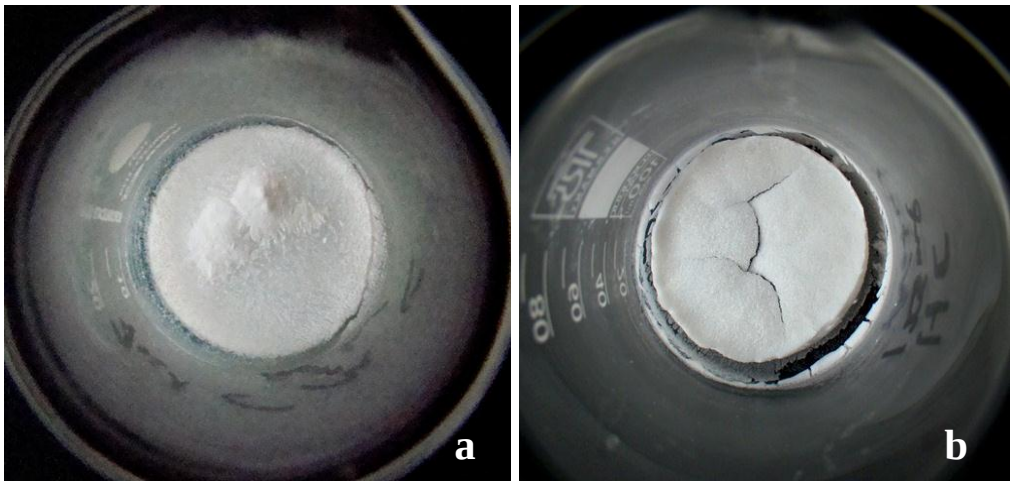

Figure 2-8: Photographic images of the freeze dried unpurified NGP-ACP (a) and HC-ACP (b)

The production yield was studied by analysis of the effect of the isolation step on the percent of yields obtained of NGP-ACP and HC-ACP. The total weight of ACP produced was calculated (equation 2.2) based on the weight of stabilising agent used, as demonstrated in figure 2-9. For example from 1g of NGP the product average yield was 2.84g of unpurified NGP-ACP.

$$Total\ weight\ of\ prepared\ ACP = \frac{Weight\ of\ freeze\ dried\ ACP}{Weight\ of\ protein\ used} \quad \ldots. \quad \text{Equation 2.2}$$

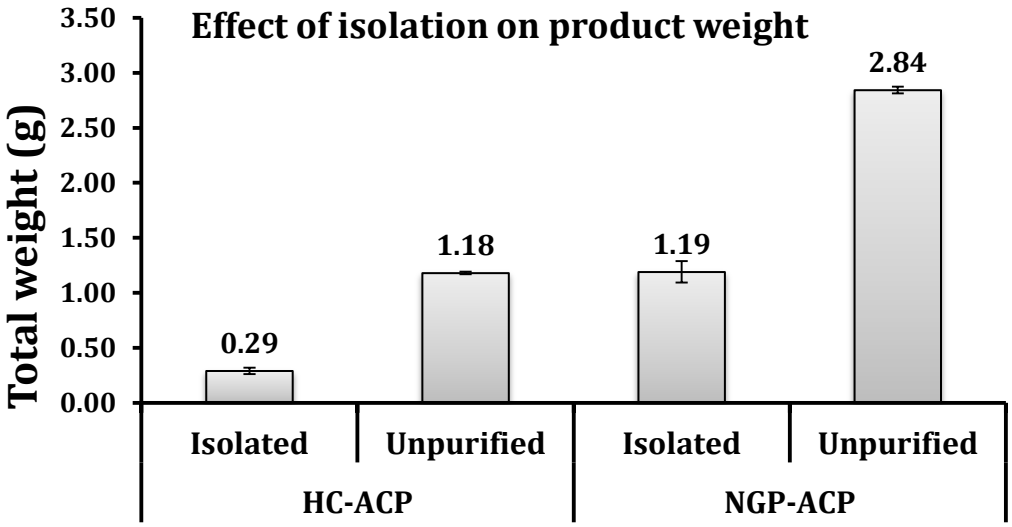

Figure 2-9: Total weight of ACP produced showing an effect of the isolation process on the weight of NGP-ACP and HC-ACP produced, mean ±SEM (n=3).

2.3.3.1 Particle size analysis

Particle distribution curves by % intensity, volume and number were plotted from the particle size analysis of the prepared colloids. The CPP-ACP, NGP-ACP and HC-ACP colloids showed polydispersity as shown in figure 2-10, figure 2-11 and figure 2-12 respectively. Figure 2-13 shows averages of smallest particle size 228nm in the prepared CPP-ACP, 40nm for NGP-ACP and 79nm for HC-ACP colloids. Freeze dried ACP showed variable size measurements from batch to batch.

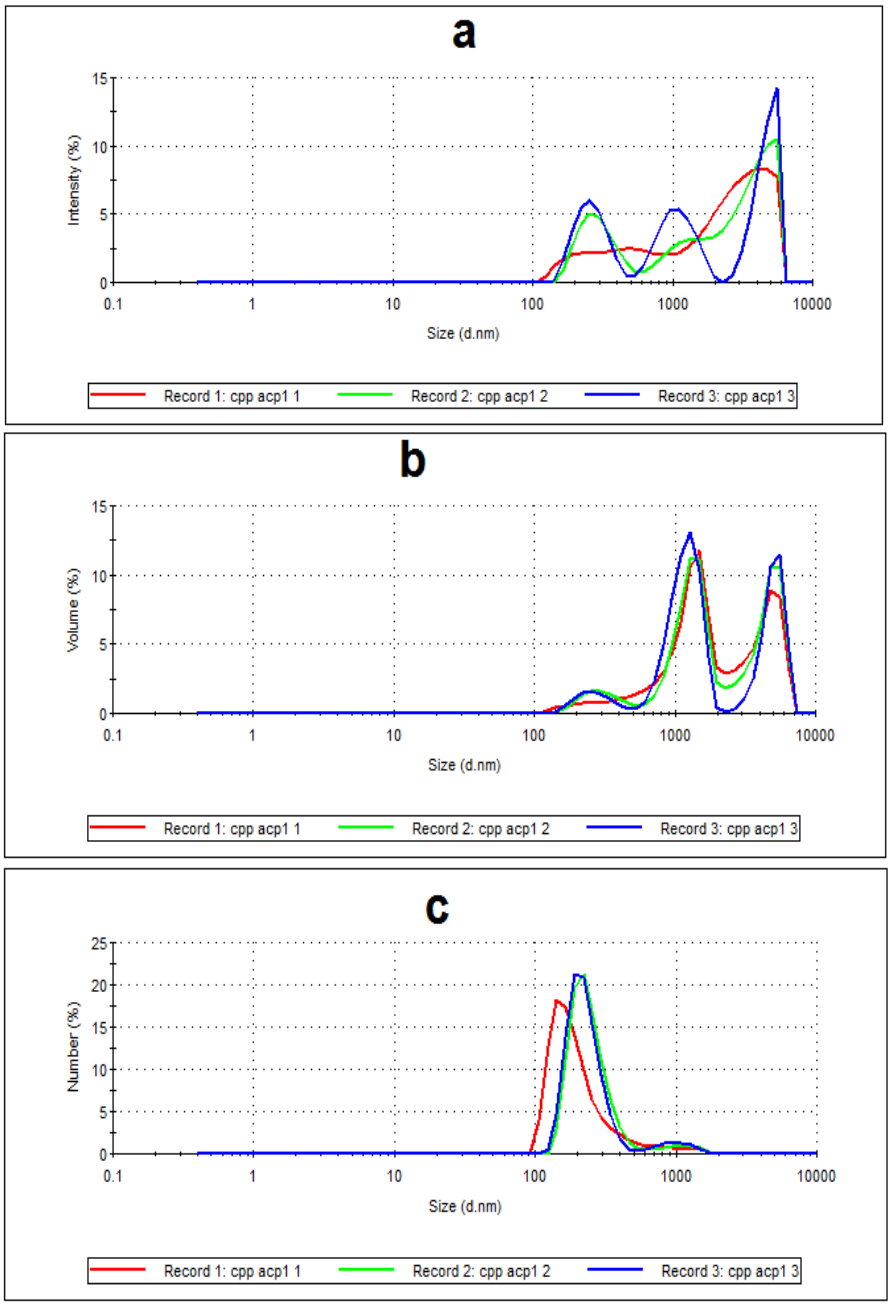

Figure 2-10: Particle size distribution curves of CPP-ACP:
a-Intensity %, b-Volume % and c- Number %

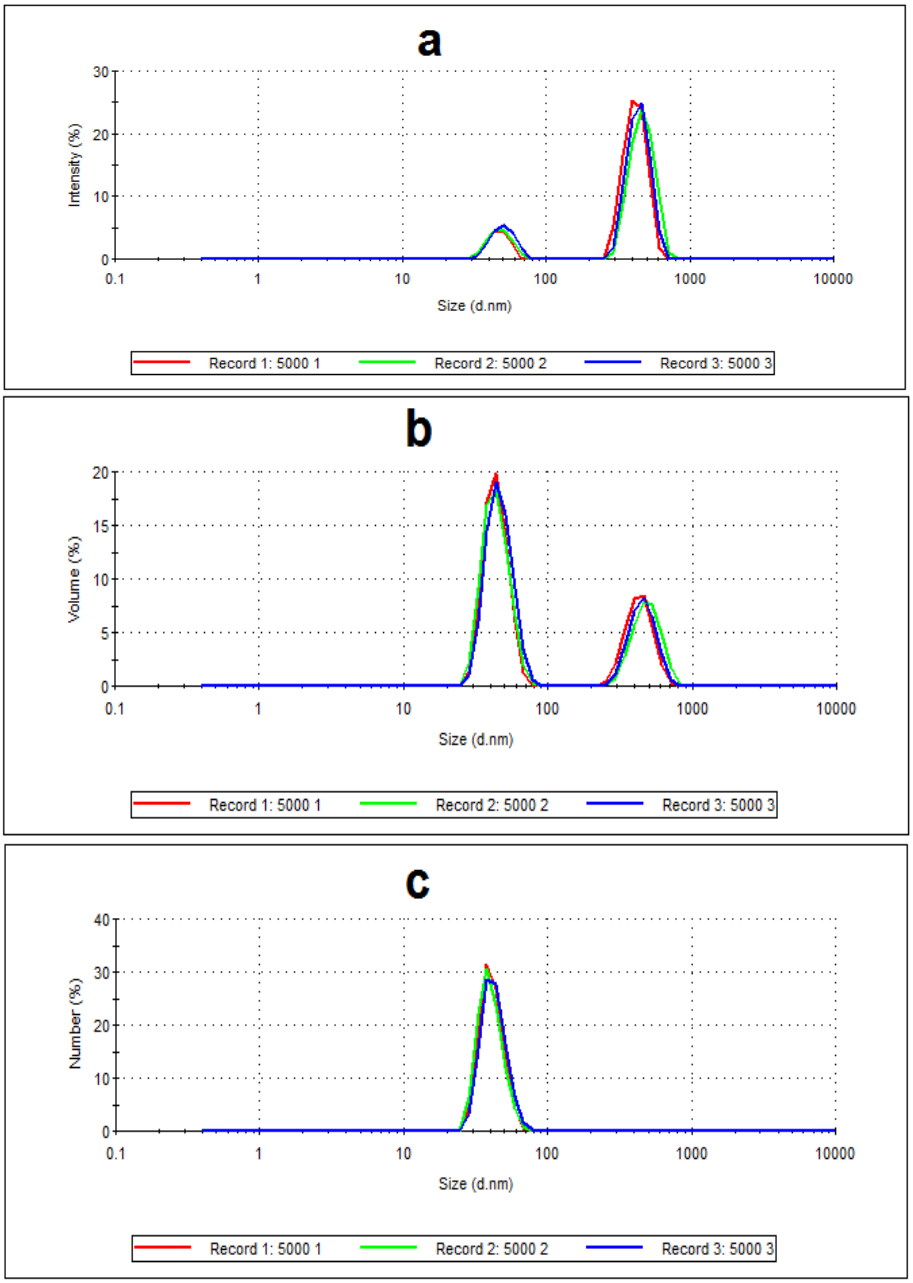

Figure 2-11: Particle size distribution curves of NGP-ACP: a-Intensity %, b-Volume % and c- Number %

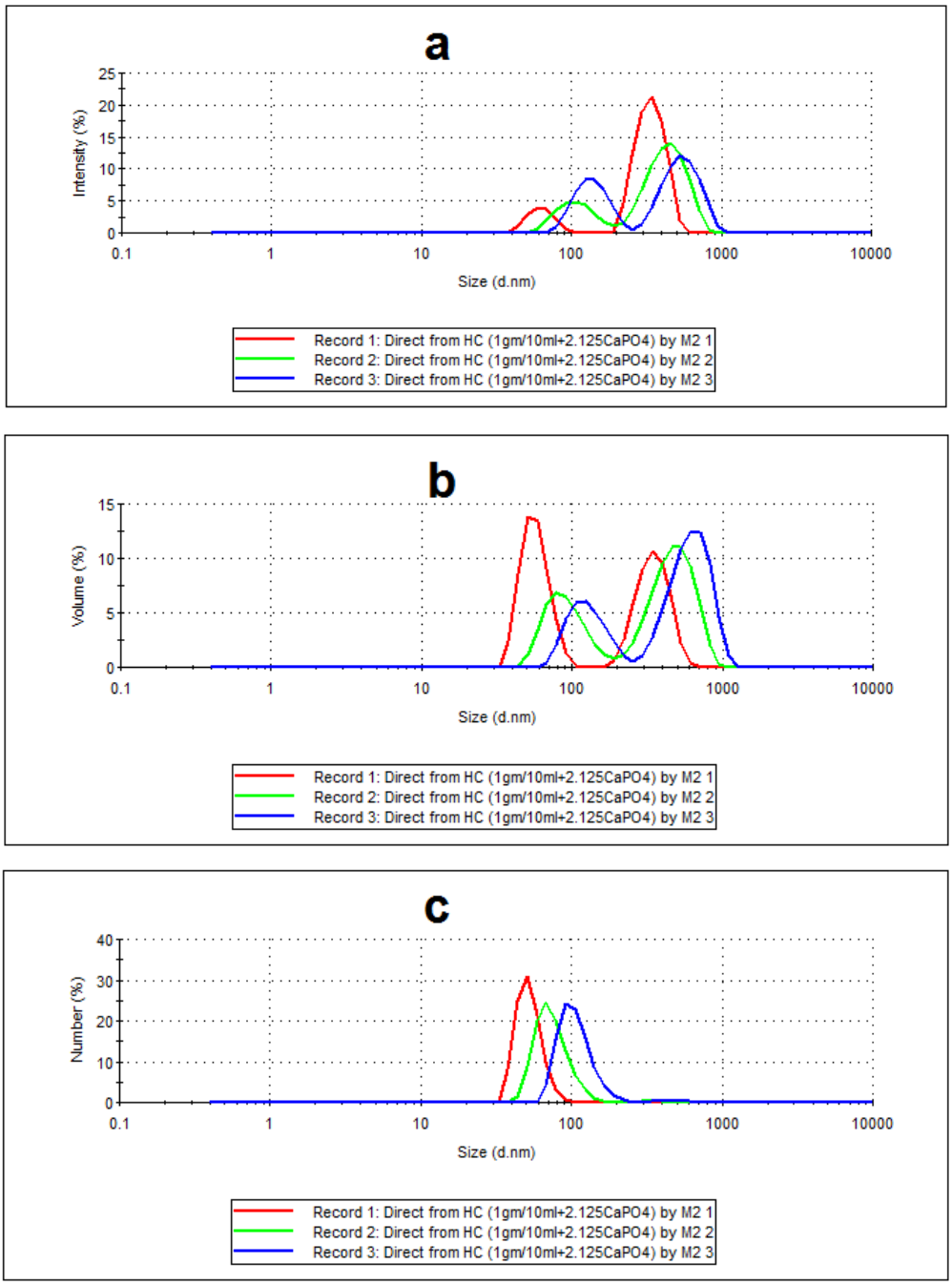

Figure 2-12: Particle size distribution curves of HC-ACP: a-Intensity %, b-Volume % and c- Number %

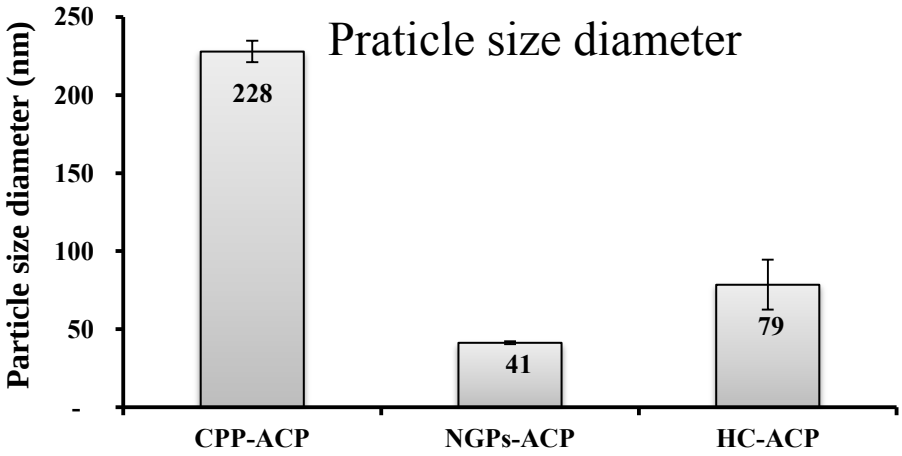

Figure 2-13: Mean particle size (±SEM) of of prepared ACP (n=3) based on % number distribution.

2.3.3.2 Solid state form analysis

Figure 2-14 shows the X-ray diffraction chromatogram of the prepared NGP-ACP, which confirmed the lack of sharp, distinct peaks of crystallinity in the prepared forms of the ACP.

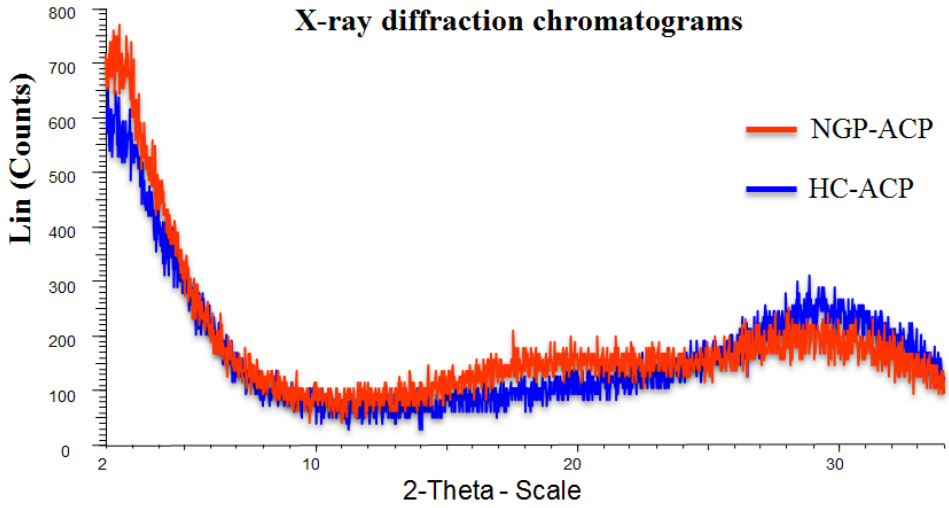

Figure 2-14: X-ray diffraction of the isolated freeze dried NGP-ACP and HC-ACP. Both chromatograms demonstrate the normal characteristics of an amorphous complex.

2.3.3.3 Scanning and transmission electron microscopy imaging

The SEM images of freeze dried NGP-ACP prepared by the original method are shown in figure 2-15 and figure 2-16. The figures show the effect of packing and absence of crystals due to filtration in the isolation step, while figure 2-17 shows the SEM images of the freeze-dried ACP prepared by the modified method, which revealed large particles, possibly encapsulated ACP complexes.

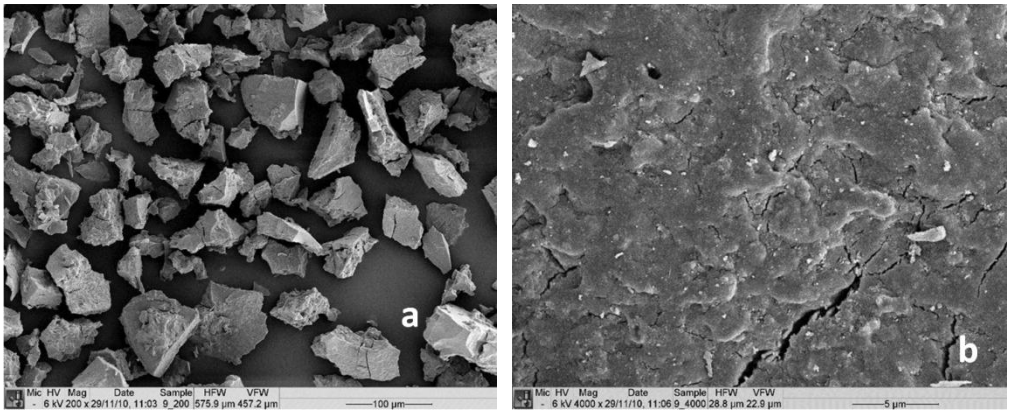

Figure 2-15: SEM images of isolated NGP-ACP: a-200x and b-4000x

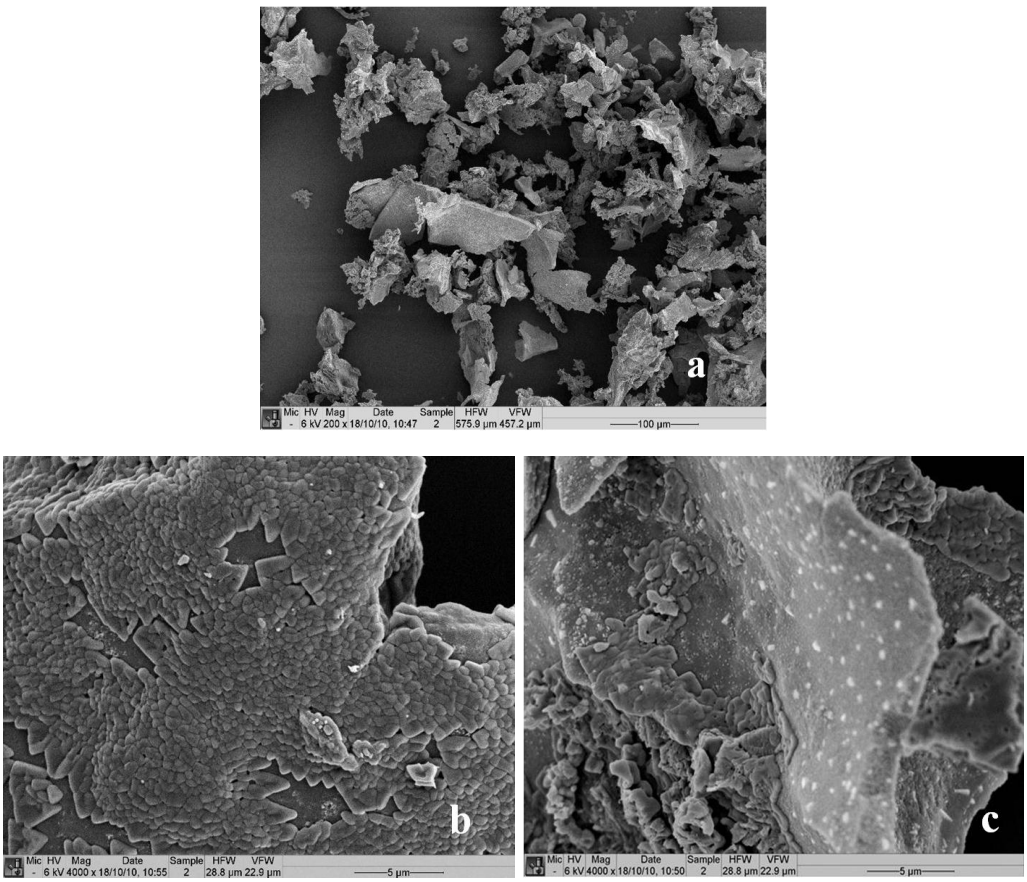

Figure 2-16: SEM images of unpurified freeze dried NGP-ACP: a-200x, b-4000x and c-4000x. The images b and c were captured at different positions on the field.

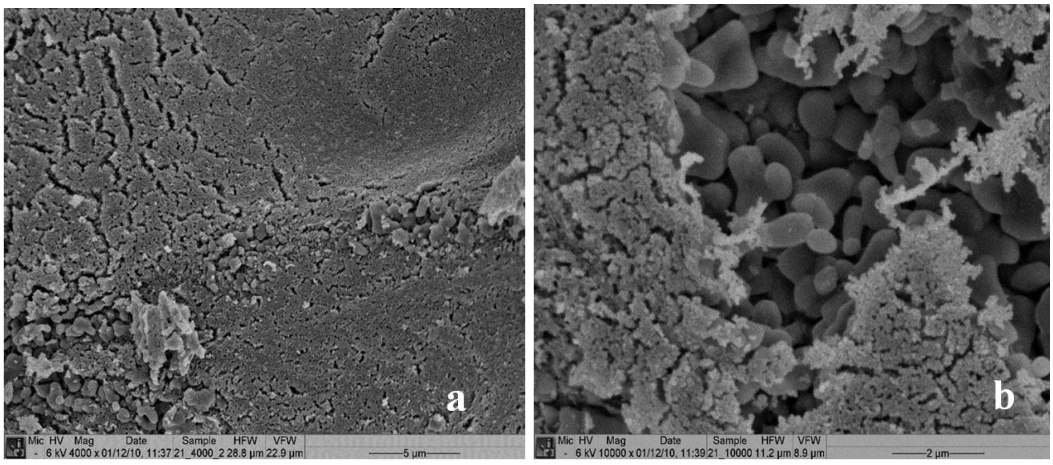

Figure 2-17: SEM images of isolated NGP-ACP prepared by the modified method as outlined in section 2.2.5.2: a-4000x and b-10000x.

Figure 2-18 and Figure 2-19 show the SEM images of unpurified and isolated HC-ACP, respectively. During the isolation step, an obvious removal of crystals occurred from the prepared ACP. There was no clear evidence of complexes in samples although they might be embedded in the shell structure of the products.

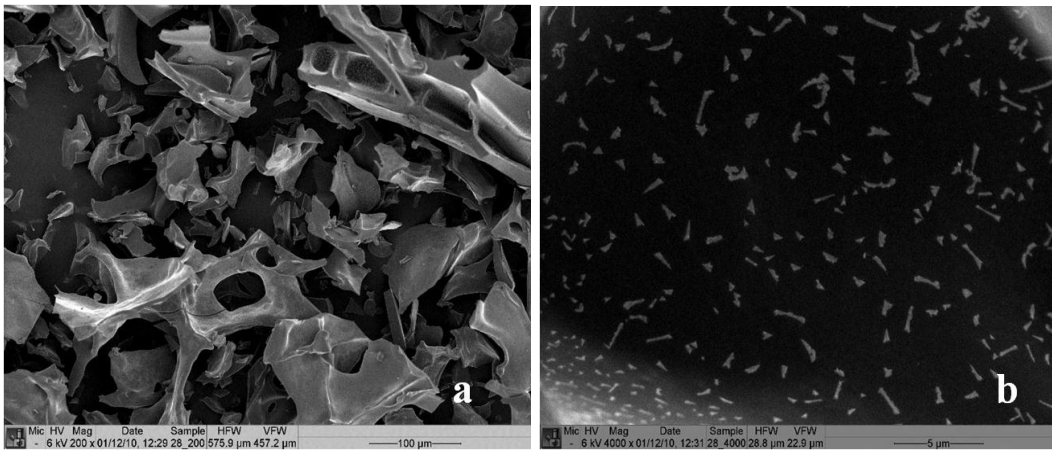

Figure 2-18: SEM images of unpurified HC-ACP by the modified method: a-200x and b-4000x.

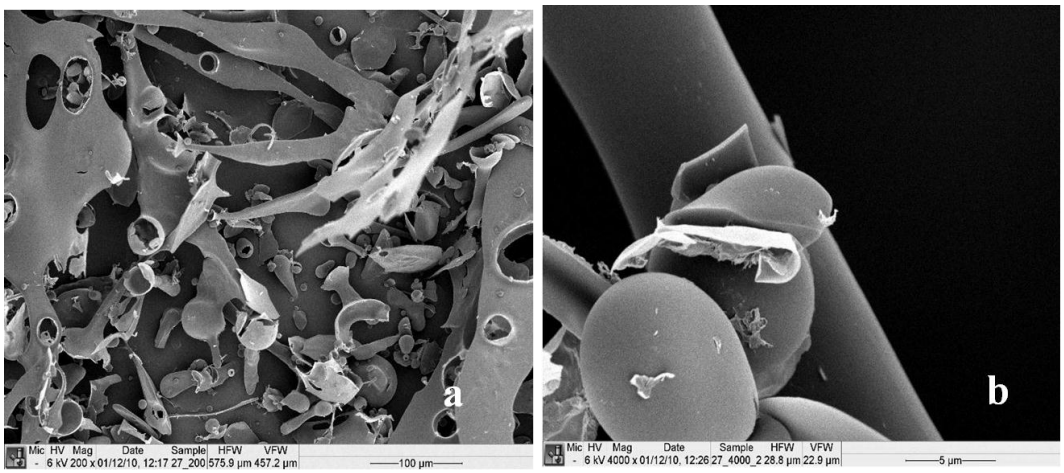

Figure 2-19: SEM images of isolated HC-ACP by the modified method: a-200x and b-4000x.

The TEM images of NGP-ACP and HC-ACP colloids (figure 2-20) revealing the particle size at nano-scale and the spherical shape of these complexes.

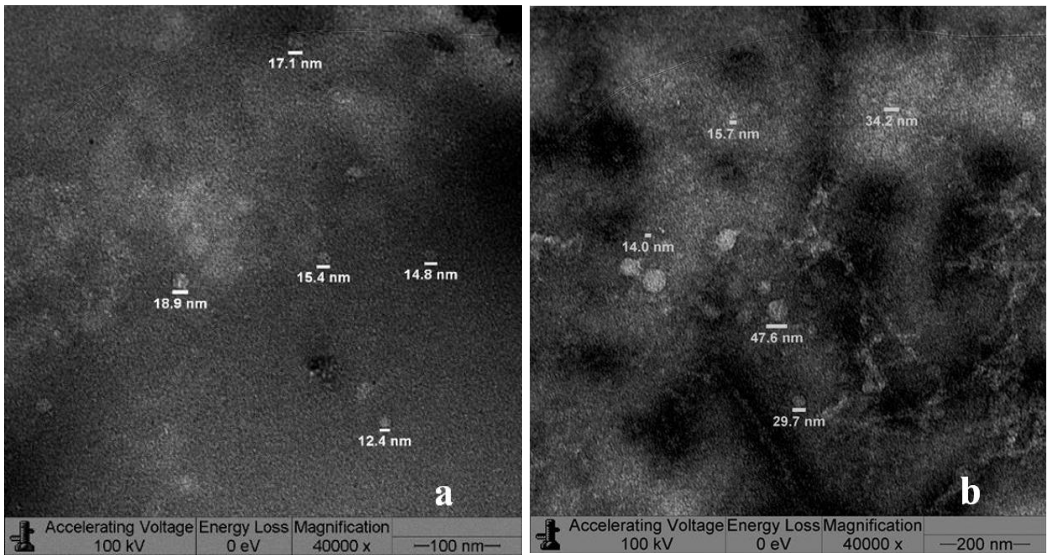

Figure 2-20: TEM images of colloids prepared by the modified method: a- NGP-ACP and b-HC-ACP.

2.3.3.4 Thermal stability study

2.3.3.4.1 Thermal gravimetric analysis

TGA profiles of the isolated NGP-ACP and HC-ACP prepared by the modified methods described in sections 2.2.5.2 and 2.2.5.3 shows the weight loss in percentage and mass throughout water evaporation and decomposition phases (figure 2-21). The weight loss was higher in the isolated HC-ACP than that in the isolated NGP-ACP.

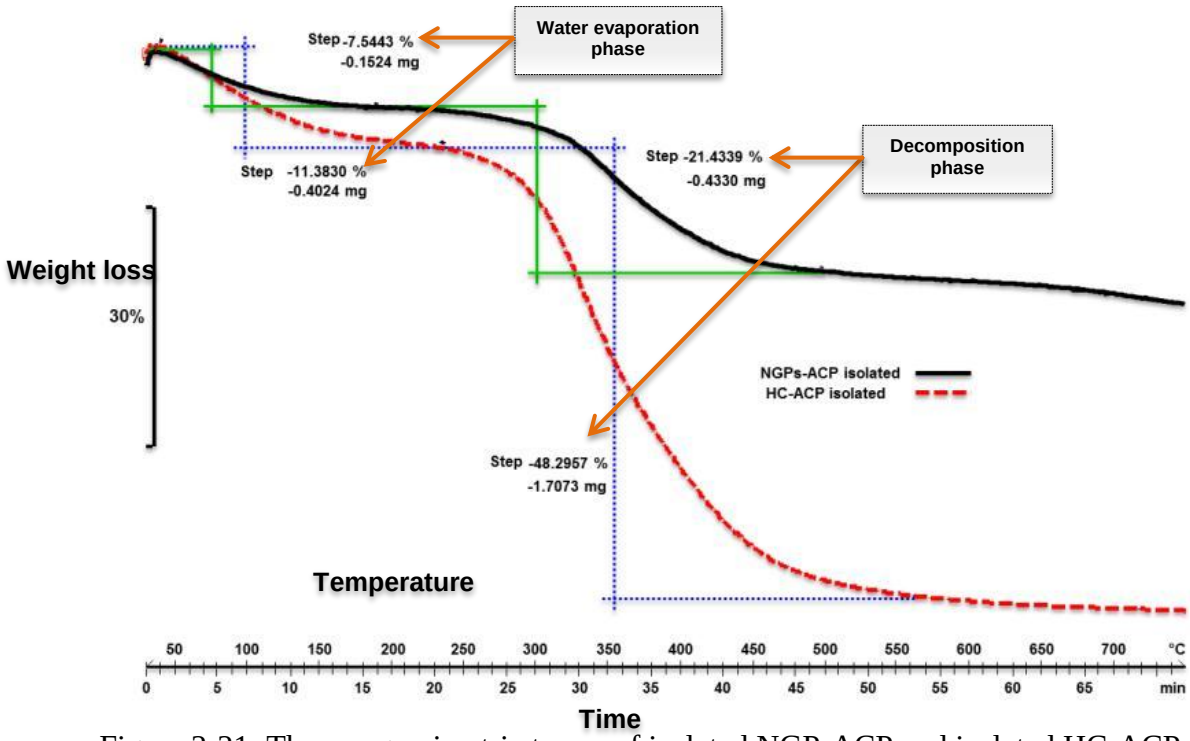

Figure 2-21: Thermo gravimetric traces of isolated NGP-ACP and isolated HC-ACP

2.3.3.4.2 Differential scanning calorimetry

DSC profiles of isolated and unpurified NGP-ACP powder were relatively similar as shown in figure 2-22. However, the crystals in the unpurified NGP-ACP as observed in the SEM image may not be present in sufficient quantity to show a melting endotherm in the DSC curve. The DSC trace of isolated and the unpurified HC-ACP as shown in figure 2-23 illustrated a variance in the intensity of water evaporation endotherm. In addition, the unpurified sample showed a broad melting endotherm, which might be attributed to the remaining peptides.

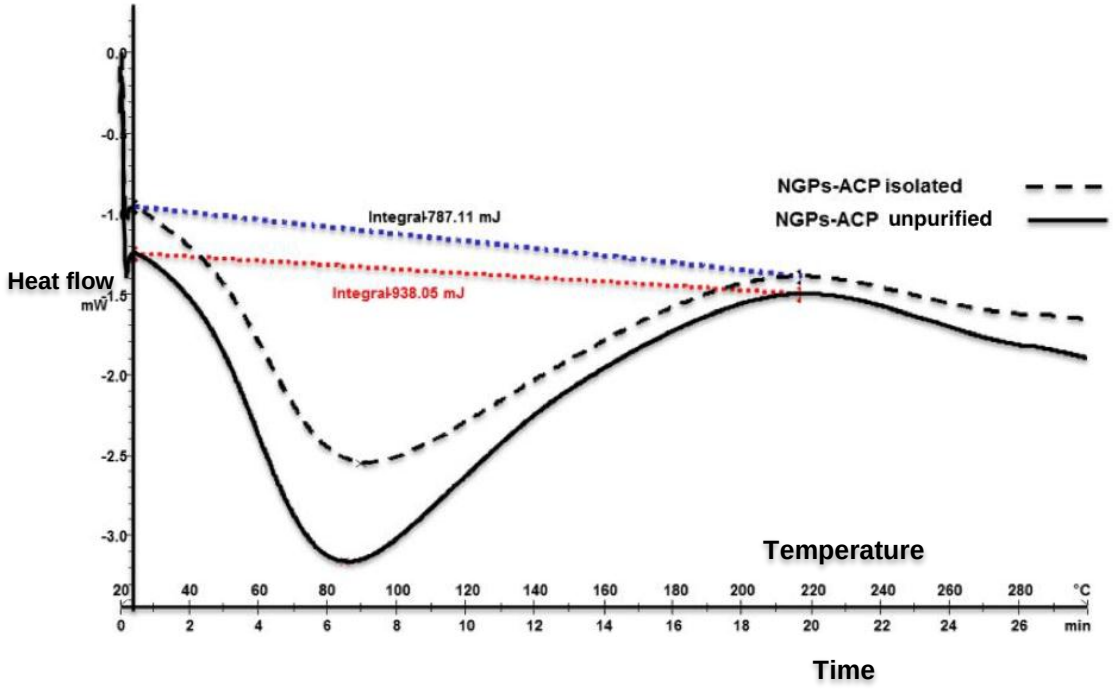

Figure 2-22: Differential scanning calorimetry of isolated and unpurified NGP-ACP freeze dried powder.

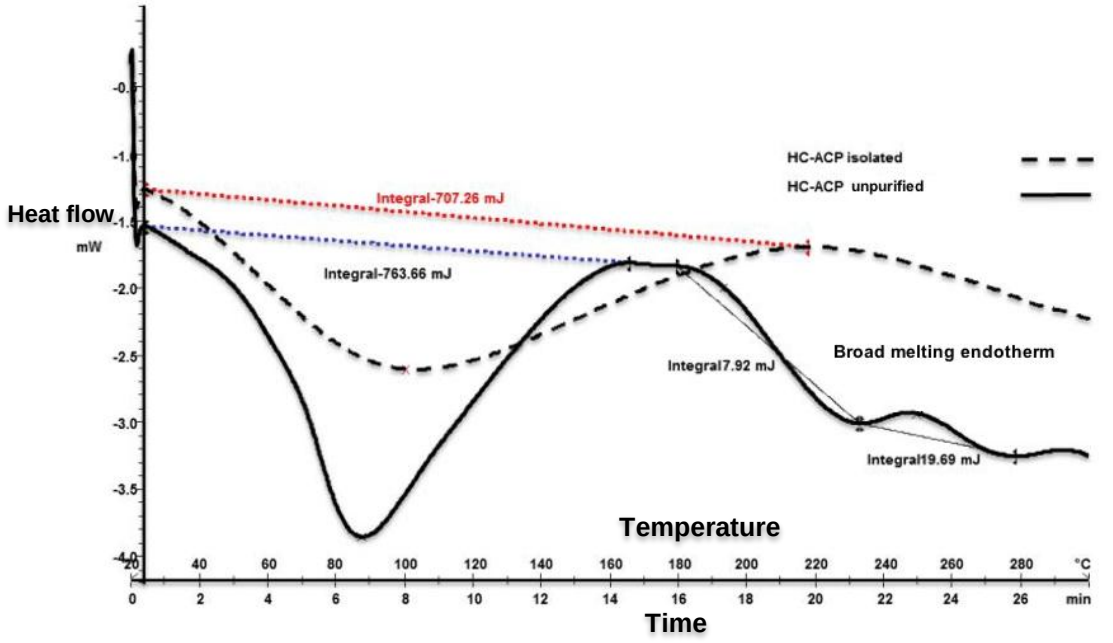

Figure 2-23: Differential scanning calorimetry of isolated and unpurified HC-ACP freeze dried powder.

2.3.3.5 Dynamic vapour sorption (DVS) analysis

The water vapour sorption effect on mass of isolated NGP-ACP and HC-ACP powders was studied by subjecting the samples to an increase in relative humidity at constant temperature as shown in figure 2-24 and figure 2-25.

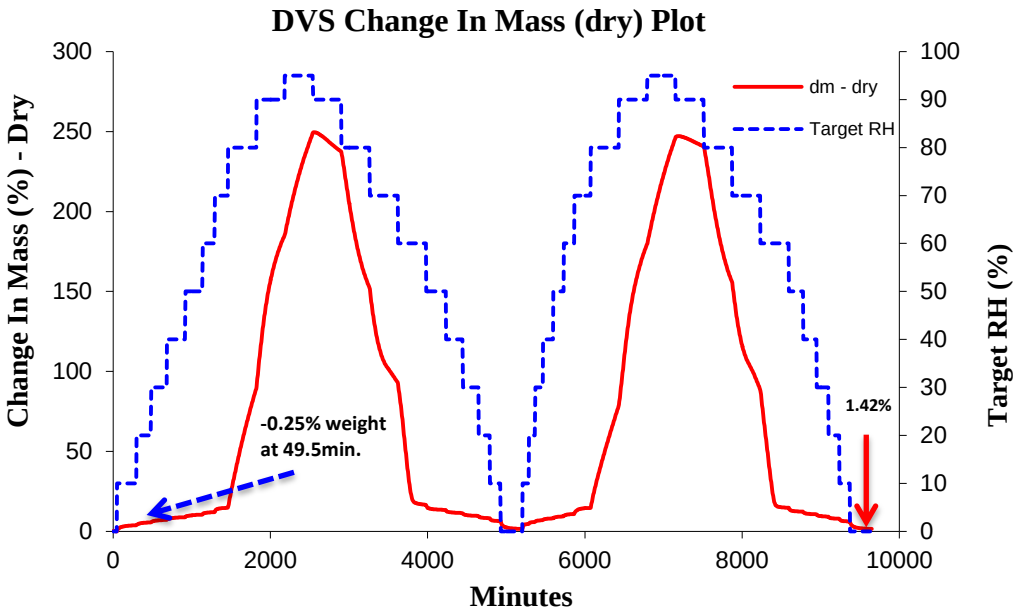

Figure 2-24: DVS kinetic of isolated NGP-ACP powder showing the weight increment upon cycling the relative humidity.

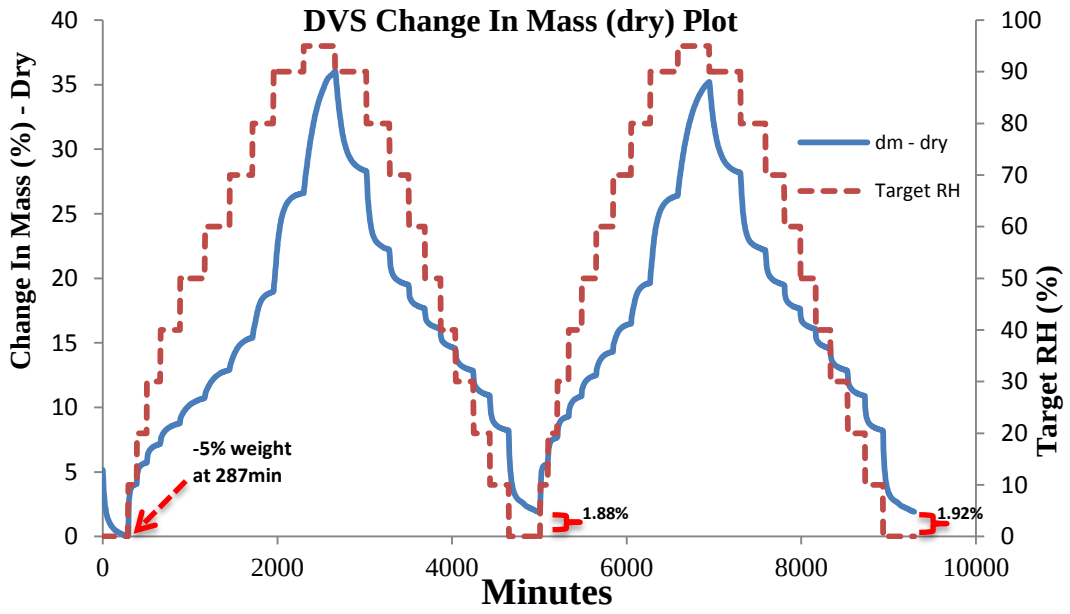

Figure 2-25: DVS kinetic of isolated HC-ACP powder showing the weight increment upon cycling in relative humidity.

Figure 2-26 and figure 2-27 show the DVS isotherms of the isolated NGP-ACP and HC-ACP powders respectively. These isotherms show the water vapour desorption and sorption effect on the % mass change of powders.

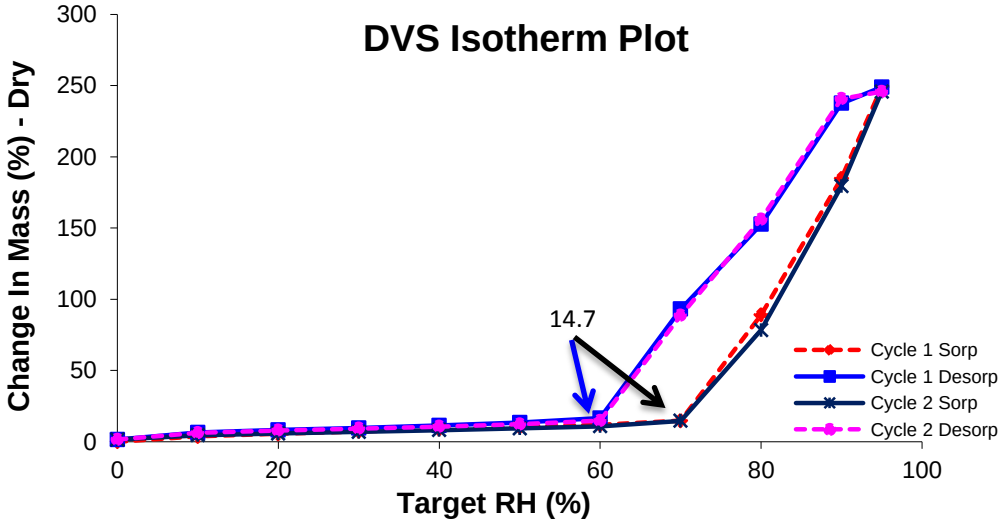

Figure 2-26: DVS isotherm plots of isolated NGP-ACP powder showing two cycles of water sorption and desorption effects on mass change.

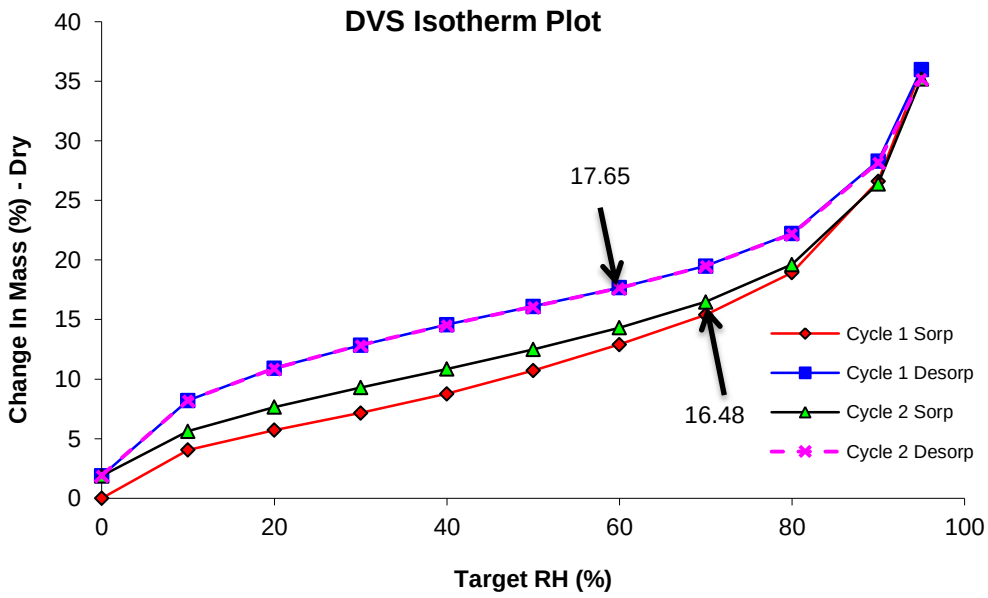

Figure 2-27: DVS isotherm of isolated HC-ACP powder following one and two cycles of water sorption and desorption effects on mass change

2.4 Discussion

2.4.1 Preparation of CPP and NGP

CPP was prepared as a control for the purpose of comparing the peptide contents of NGP and the stabilizing efficiency on the amorphous calcium phosphate nanocomplexes. The modification in the method of preparation of CPP from sodium caseinate showed a significant increase in the percentages recovery of CPP. The grade of used trypsin was about a one tenth less potent than that an alternative costly one (13,000-20,000 BAEE units/mg protein) (Sigma, 2011). Therefore, 20 times amount of enzyme was suggested to be used in the method of preparation. In addition, the duration of digestion was extended to 36h and amount of $CaCl_2.2H_2O$ was increased up to 0.47g. These changes showed increased efficiency sufficient to produce a 10-fold increase in the recovery of CPP. The final modification was carried out using acetone instead of ethanol and combining precipitation and washing processes in order to minimize the total duration of the preparation. This modification exhibited a 4-times increase in the final weight of CPP.

2.4.2 LC-MS Analysis of CPP and NGP

LC-MS analysis of isolated peptides was performed according to the bottom –up strategy of digested protein analysis (Manuilov *et al.*, 2011; Miquel *et al.*, 2005), which determines the molecular weight of peptides generated from proteolysis. The column has zwitterionic functional groups that enhanced the capability for separation of peptides by hydrophilic partitioning is shown in figure 2-28.

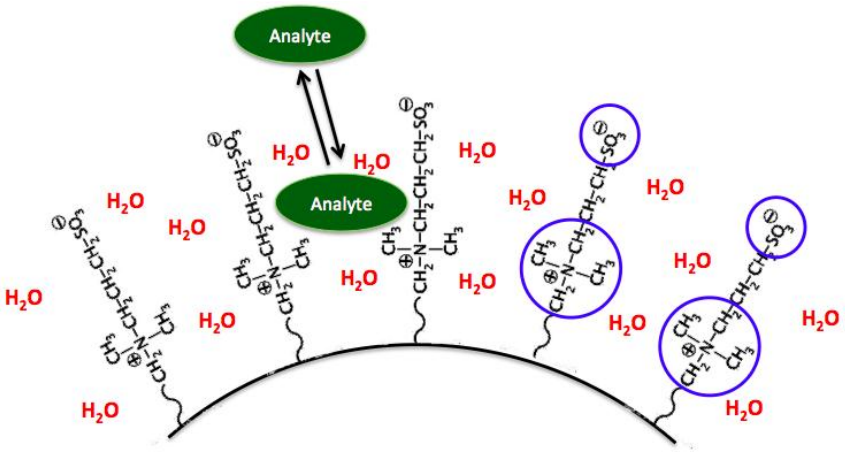

Figure 2-28: HILIC column stationary phase: shows the functional groups of the column which include positively charged ammonium and negatively charged sulphate groups. The zwitterionic characteristic of these functional groups facilitate the partitioning of the hydrophilic peptides. Modified from (Merck SeQuant AB, 2009)

The LC-MS analysis revealed the peaks corresponding to the main fractions of CPP in agreement to that stated by Cross and colleagues (Cross *et al.*, 2005b) with the exception of αS2-casein(46–70). The m/z peaks of αS1-casein (33-52), b β-casein (1-24) and β-casein (1-25) were close to (1177.44, 1484.1 and 1562.14) those identified as casein phosphopeptides after simulated gastrointestinal digestion by porcine pepsin, pancreatin and bile extract of whole casein (Miquel *et al.*, 2006).

Dephosphorylation β-casein (1-24), αS2 casein (2-22) and αS1 casein (2-22) peaks were observed in isolated CPP and NGP, which resemble those reported by Kjeldsen and colleagues in a phosphorylate peptide analysis of extracted human αs1-casein from fresh milk of a healthy Caucasian woman in the eighth month of lactation (Kjeldsen *et al.*, 2007).

2.4.3 Characterisation of the prepared ACP

The molar ratio of calcium to phosphate that was used in these preparations was 1.67, which was higher than that used by (Reynolds, 1991). Furthermore this ratio, and a ratio of 1.5 were used to prepare hydroxyapatite and amorphous calcium phosphate respectively by other groups (Sun *et al.*, 2010), while the preparations of ACP described here contain a third component: a stabilising agent (negatively charged ionizable peptides containing phosphate and carboxylate) that is needed to build the complex by ionic binding to calcium and in turn to phosphate. This required that a higher molar ratio be used. The weight of the prepared ACP was significantly ($p < 0.05$) influenced by the isolation step of the preparation following the removal of the non-complexed mixture of electrolytes and peptides.

2.4.3.1 Particle size analysis

The Zetasizer nano ZS uses the dynamic light scattering technique to measure particle diffusion under Brownian motion. This diffusion is converted into particle size and size distribution curves using the Stokes-Einstein relation (equation 2.3). The Stokes-Einstein relation in its classical form is given by:

$$D = \frac{K_B T}{\alpha \pi \eta R} \qquad \text{----------} \qquad \text{Equation 2.3}$$

Where D is the diffusion coefficient, K_B is the Boltzmann constant, T is the absolute temperature α is a constant, η is the viscosity of the solvent, and R is the hydrodynamic radius of the particle diffusing in a solvent (Cappelezzo *et al.*, 2007). Size distribution curves by volume and number were calculated mathematically using the Mie theory (Nobbmann *et al.*, 2009).

Average particle size diameter of the prepared CPP-ACP was significantly different from NGP-ACP and HC-ACP ($p \leq 0.05$) as shown in Figure 2-13. A low content of αS2 casein (1-23) and αS1 casein (59-79) in NGP might be responsible for this effect. Freeze dried ACP did not show consistent measurements as a result of large aggregates which formed upon drying.

2.4.3.2 Solid state form analysis of NGP-ACP and HC-ACP

An unstable ACP preparation is characterised by direct conversion to crystalline apatite in a few hours (Eanes *et al.*, 1973) and shows X- ray patterns characterised by the presence of sharp 2θ peaks typical of apatite crystals at 26 and 32 angles (Boskey, 1997). The X-ray patterns of the prepared ACP did not show these peaks and the diffraction patterns were similar to that prepared by Cross and colleagues (Cross *et al.*, 2005b). Accordingly, this suggests that the agents used were efficient enough to hold the calcium phosphate in stable, amorphous form.

2.4.3.3 Scanning and transmission electron microscopy imaging

Scanning electron microscopy images of the prepared NGP-ACP display the shape and size of complexes. There was evidence of aggregation into a core containing larger complexes shielded by smaller aggregates. In addition, nanocomplexes of NGP-ACP adhered to each other upon freeze-drying. This might be responsible for lowering solubility and dissolution of calcium and phosphate as a result of decreasing surface area. The isolation step of NGP-ACP was found to remove the non-complexed electrolytes. However, isolation promoted the formation of a packed complex of the prepared NGP-ACP, possibly showing a decrease in solubility.

Transmission electron microscopy images were employed by Cross and colleagues as evidence that an amorphous form of CPP-ACP had been isolated (Cross *et al.*, 2005b). In our experiment, it was applied to show that the prepared ACP complexes had diameters less than 25nm and revealed the lack of crystallinity.

2.4.3.4 Thermal stability study

TGA was used to study the effect of programmed increase in temperature on the sample weight changes. The measurements indicate the solvent content and degradation temperature (Cheremisinoff, 1996). The TGA trace of isolated NGP-ACP and HC-ACP revealed a difference in moisture content and decomposition weight loss, which might be caused by a low content of amorphous calcium

phosphate in HC-ACP (i.e. the presence of a higher percentage of non complexed peptides).

DSC analysis showed higher moisture content in the unpurified ACP that might be caused by the presence of unbounded peptides, in addition to sodium chloride and calcium phosphate precipitate that arose during the pH stabilisation process and chemical reaction of non-complexed calcium chloride and disodium hydrogen phosphate, respectively. Additionally, the unpurified HC-ACP showed a fluctuating rapid decline in the decomposition phase within broad melting curves that might be attributable to other protein in the complexes.

TGA and DSC analysis indicate that the isolated NGP-ACP and HC-ACP were stable enough to be used in future studies of drug delivery dosage forms.

2.4.3.5 Dynamic vapour sorption (DVS) analysis

Dynamic vapour sorption analysis is widely used to study water uptake into amorphous and crystalline material (Hunter *et al.*, 2010). The results obtained established that the HC-ACP needed 285 minutes for a steady state of mass change while NGP-ACP needed 49.5 minutes. This suggests that HC-ACP had a higher ability to hold moisture. In addition, the remaining moisture content after 2 cycles did not show significant changes (1.42 and 1.92% of NGP-ACP and HC-ACP respectively).

The isotherm plots were consistent and there was no appreciable mass per cent variance at 60% RH. However, a massive difference was present above 70% RH. NGP-ACP showed a high rate of water uptake with a maximum weight percentage of 247% at 95%RH, while HC-ACP showed only 35.2%.

2.4.4 Stabilisation efficiency theory

The prepared ACP that were stabilised by NGP and HC reinforced the finding of the capability of peptides containing free phosphate and carboxyl groups reported by Termine and colleagues (Termine *et al*., 1970), mentioned in (section 2.1).

2.5 Conclusions

ACP complexes were successfully prepared from NGP and HC by a rapid and simpler modified method of mixing all the components at pH 5 and complexing by pH adjustment to pH 7. The isolation step successfully removed electrolyte, although it was responsible for aggregate formation of prepared complex particles, especially in NGP-ACP that might have a subsequent effect on the solubility and calcium release.

The prepared complexes displayed nanoscale particle size as measured by the Zetasizer NanoZS and TEM. In addition, SEM images demonstrated the shape and particle size of NGP-ACP, although it did not yield good data for HC-ACP. The non-crystalline form of the prepared isolated ACP was suggested by the X-ray powder diffraction. TGA and DSC revealed that the isolated ACP had lower moisture content than that in unpurified ACP. Furthermore, these complexes showed a less than 20% weight of water uptake at relative humidity of 60% and below.

In conclusion, these studies suggest that stabilized complexes can be produced by isolation of enriched casein fractions using methods adapted from the literature. The technique remains lengthy and alternative templates might offer advantages in the production of stable nanocomplexes. The work on this initiative is described in the next chapter.

Chapter 3. Stabilisation of amorphous calcium phosphate by acidic hydrolysed carboxymethyl cellulose (ahCMC).

3.1 Introduction

3.1.1 The stabilising activity of casein phosphopeptides on amorphous calcium phosphate

As mentioned in Chapter 2, isolated casein phosphopeptides are mainly composed of β-casein (1→24) and αS1-casein (59→79), which are characterised by a unique content of the Pse-Pse-Pse-Glu-Glu cluster motif. This residue has a key action for stabilising of amorphous calcium phosphate at the nucleation stage of the nanocomplex formation (Reynolds, 1999). Casein phosphopeptide-based amorphous calcium phosphate (CPP-ACP) nanocomplexes have been shown to have a potential effect on enamel remineralisation and CPP has been demonstrated to stabilize amorphous calcium phosphate under alkaline conditions (pH 9) (Cross *et al.*, 2005b).

With regard to the structural content of CPP it has been shown that there are additional groups that might play a role in the stabilising activity as shown in Figure 3.1. These are negatively charged groups that are ionisable in an alkaline medium at pH 9. Linear polymers with carboxylic acid groups, for example pectin, sodium alginate and sodium carboxymethyl cellulose are ionisable at this pH and therefore might also contribute a stabilising action to Pse-Pse-Pse-Glu-Glu cluster motif associated with the amorphous calcium phosphate nanocomplex.

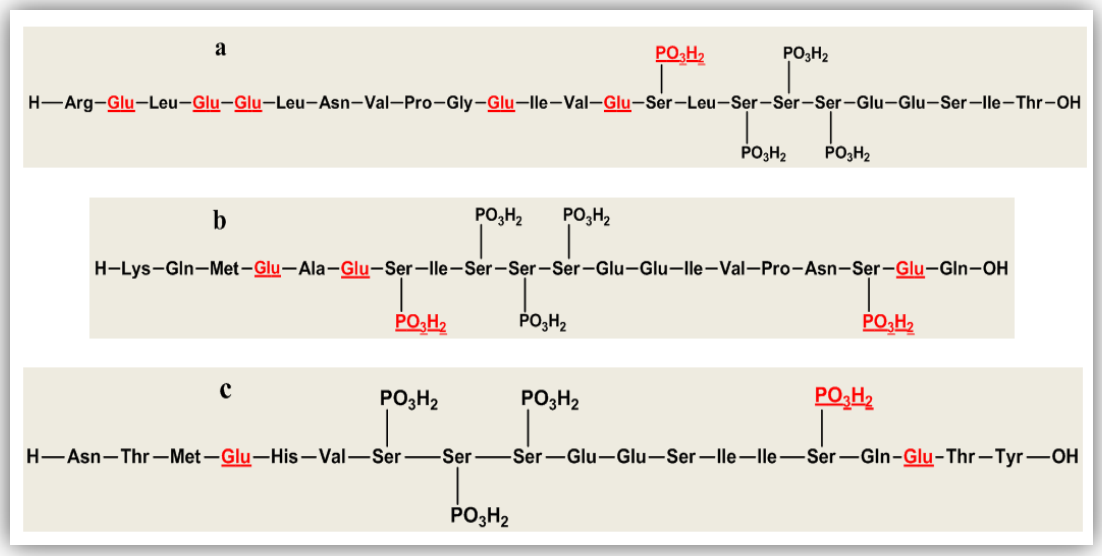

Figure 3.1: Chemical structure of CPP showing the carboxyl and phosphate groups in Glu and Ser-PO_3H_2 that might also have an additional stabilising action to the Pse-Pse-Pse-Glu-Glu cluster motif on ACP: a- β-casein (1→24) and b-αS1- casein (59→79) c- αS2-casein (1→23)

3.1.2 Examples of linear polymers containing carboxyl groups and their degree of substitution

At the outset, it was proposed that the solubility of stabilizing agent might play a crucial role in the dissociation of the ACP complex and release of calcium and phosphate ions in a manner or under conditions that prevented the precipitation of calcium phosphate. Following this proposal, sodium alginate, pectin and sodium carboxymethyl cellulose were selected to evaluate their stabilising efficiency on amorphous calcium phosphate.

Polymer solubility is generally affected by the degree of methoxy substitution with a lower degree of substitution yielding a cellulose polymer with a low water solubility (Dow, 2002). The degree of substitution is the average of a specific group on the polymer chain. The range of values is determined by number of possible sites of substitution for example, from 0 to 3 in cellulose polymers because the modification is usually generated through hydroxyl group reaction at positions 2, 3 and 6 of the

saccharide unit as shown in Figure 3.2. A carboxymethyl cellulose with a maximum DS (1.24) of carboxymethylation is obtained by 15% (w/v) NaOH for 5h reaction period (Heinze *et al.*, 1999). A non-uniform substitution is usually obtained in the preparation of carboxymethyl cellulose (Merle *et al.*, 1999).

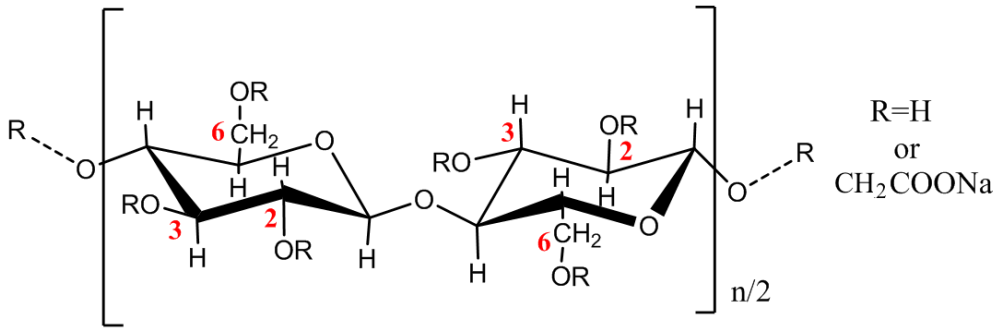

Figure 3.2: Substitution sites on the carboxymethyl cellulose unit.

3.1.2.1 Sodium alginate

Sodium alginate is a natural polymer with chemical structure of two basic units, β-(1→4)-D-mannosyluronic and α- (1→4)-L-gulosyluronic (Figure **3.3**) and has a molecular weight range of 20,000 to 240,000 daltons. It is slowly soluble in water and has been therapeutically used as an anti-reflux agent, as it reacts in the stomach to form a strong alginic acid raft (Washington *et al.*, 1985). The compound is widely employed in oral solid dosage forms as binder and disintegrant as well as thickening agent in suspension and cream, furthermore it is used in the aqueous microencapsulation of drugs (Rowe *et al.*, 2009). It has been employed as a component of plaque inhibitory mixture in mouthwash and dentifrice dental dosage forms and was discovered to show excellent dentinal tubule occluding action. It meets the requirements for a good tooth desensitising agent (Smetana *et al.*, 1999).

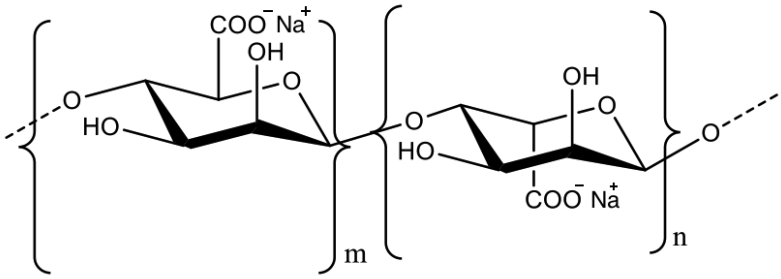

Figure 3.3: Structural units of sodium alginate

3.1.2.2 Pectin

Pectin is a complex polysaccharide polymer, which is soluble in water and mainly composed of α- (1→4)-D-galacturonic acid as shown in figure 3.4. There are two different types of pectin, which are classified according to their aqueous solubility. The solubility in water is dependent on the molecular weight and the degree of methoxy ester substitution of the carboxyl groups. The solubility is enhanced by preventing the molecular association as a result of the steric effect of the methoxy substituent (Thakur *et al.*, 1997). Pectin has been used for the direct management of diarrhoea, as well as a pharmaceutical excipient to assist gel formulation in modified release oral dosage forms (Murata *et al.*, 2004) and as the basis of a pH-dependent colonic drug delivery system (Liu *et al.*, 2003).

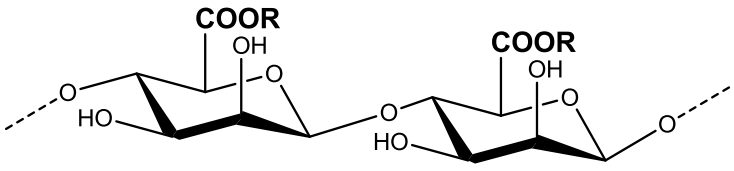

Figure 3.4: Structural unit of pectin. R= H or CH_3

3.1.2.3 Sodium carboxymethyl cellulose

Sodium carboxymethyl cellulose is a cellulose polymer presented as sodium carboxy methyl ether, as shown in figure 3.5. It is white to off-white in colour, odourless and biodegradable, powder. It is soluble in hot and cold water. At low concentrations, solutions are characterised by high viscosity that makes them useful in pharmaceutical applications, such as thickening, binding and as a stabilising agent (Vais *et al.*, 2002). The aqueous solubility depends on the degree of the substitution (DS). It is dispersible in water forming clear colloids. In pharmaceutical applications, it is employed in tablet coating, as a tablet binder, viscosity enhancing agent, wound dressing (water absorbing agent) and disintegrant in capsule oral dosage forms (Rowe *et al.*, 2009). Commercially available grades of Walocel C™ have a DS range of 0.7 - 0.9 (DowWolff, 2009).

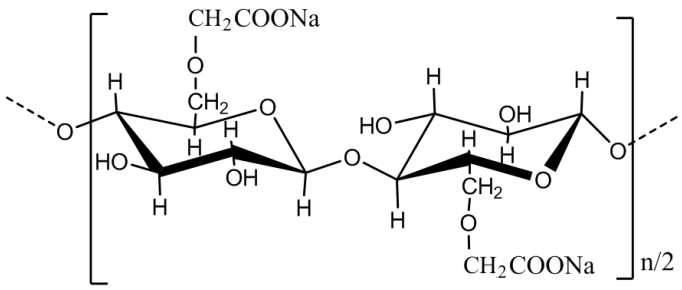

Figure 3.5: Structural unit of sodium carboxymethyl cellulose with a DS equal to1.0.

3.1.3 Objectives:

The objective of this study was to identify a polymer containing suitable negatively charged ionizable groups (carboxyl) that are able to stabilise amorphous calcium phosphate in the amorphous form at colloidal dimensions. The polymer that showed this stabilizing efficiency was then to be characterised for molecular weight and degree of substitution. In addition, the prepared colloidal and freeze dried isolated ACP was then to be characterised with regard to particle analysis and the physical properties.

3.2 Materials and methods

3.2.1 Materials

Sodium alginate [2% (w/w) solution of 250cps at 25° C], sodium carboxymethyl cellulose (MW~90,000), calcium chloride dihydrate, disodium hydrogen phosphate, NaOH, HCl 37% (v/v) and deuterium oxide were purchased from Sigma–Aldrich (UK). Pectin GENU® (citrus) USP/100 was used as supplied from CP-Kelco (USA), sodium carboxymethyl cellulose grades (Walocel®) were provided by Dow Wolff Cellulosic (Germany).

3.2.2 Preparation of ACP stabilized by carboxyl containing polymers

Sodium alginate, pectin and sodium CMC (grade CRT 10,000 PA) (where CRT refers to the viscosity grade of sodium carboxymethyl cellulose; P, refers to powder granulometry and A as an indication of a purity better than 99.5%) were selected and investigated for their ability to stabilise the ACP at a concentration of 10mg. mL^{-1} in Milli-Q water. The ACP colloids were prepared using the preparation method described in section 2.2.5.1. The prepared products were subjected to particle size characterisation.

3.2.3 Preparation of ACP stabilized by different grades of sodium CMC

Sodium CMC of different grades (molecular weight) as shown in Table 3-1 were used in order to examine the effect of molecular weight or chain length on the particle size of the prepared ACP.

No.	Grade
1	CRT 100 PA
2	CRT 1,000 PA
3	CRT 10,000 PA
4	CRT 20,000 PA 7
5	CRT 30,000 PA

Table 3-1: The grades of sodium CMC used in the preparation of CMC-ACP. The number refers to the value of viscosity that relates to the molecular weight of the CMC.

3.2.4 Preparation of ACP stabilized by ahCMC

3.2.4.1 Preparation of acidic hydrolysed CMC.

Acid- hydrolysed CMC with a low molecular weight was prepared using the method described by Burns (Burns, 1977). A 2%w/v sodium CMC (CRT 100 PA) was hydrolysed in 3N HCl solution at 40° C for 7h, with sampling at one hour intervals. The collected samples were rapidly alkalinized using 3N NaOH solution to pH 9 followed by a gradual addition of chilled acetone to precipitate the sodium CMC. Excess addition of acetone was avoided to prevent precipitation of sodium chloride. The supernatant was then removed followed by filtration on an acetone pre-wetted filter paper. The final products were left to dry in a fume hood overnight and subsequently lyophilized.

3.2.4.2 Determination of the molecular weight of ahCMC

3.2.4.2.1 Zetasizer nanoZS method

Sodium CMC (CRT 100 PA) of concentrations 2, 3, 4 and 5 % (w/v) were prepared in 0.5N NaOH solution. The Mark–Houwink equation (equation 3-1) previously used by Eremeeva and colleagues (Eremeeva *et al.*, 1998) was employed in the calculation of the molecular weight of the CMC.

$[\eta] = KM^a$ ---------- Equation 3-1

Where:

[η]= The intrinsic viscosity (100mL.gm^{-1}).

M= Average molecular weight of polymer.

K=5.37 x $10^{-4.}$

a= which is equal to 0.73 at 0.5N NaOH solvent system.

3.2.4.2.2 Viscosity method

A technique based on viscosity measurement was utilized to estimate the average molecular weight of the supplied CRT 100 PA. The relative viscosity, inherent viscosity and reduced viscosity were calculated according to the following equations (Martin, 1993):

$$Relative\ Viscosity\ \ (\eta\ rel.) = \frac{t}{t_o}$$ ----------Equation3-2

Where: t = Efflux time (seconds) of polymer solution.

t_o = Efflux time (seconds) of solvent.

$$Inherent\ Viscosity\ \ (\eta\ inh.) = \frac{ln\ \eta\ rel.}{C} = [\eta] - k_2[\eta]^2 C$$ ----------Equation 3-3

Where: C = Concentration of polymer solution (% w/v).

$$Reduced\ Viscosity\ \ (\eta\ red.) = \frac{\eta\ rel. - 1}{C} = [\eta] + k_1[\eta]^2 C$$ … Equation 3-4

The relative viscosity of CRT 100PA concentrations at 0.05, 0.075, 0.1, 0.125 and 0.15% (w/v) in 0.5N NaOH were measured using U-tube capillary viscometers (Schott-Germany) size M2 as shown in Figure 3.6. Sodium CMC MW~90,000 (CMC-90kDa) was used as a control. Once the viscosity values determined, the average molecular weight was calculated using Mark-Houwink equation.

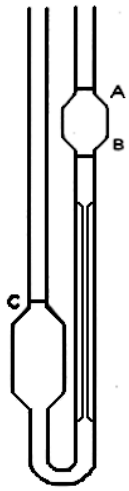

Figure 3.6: U-tube capillary viscometer showing: (A) is the starting efflux level of sodium CMC solution, (B) is the end efflux level of sodium CMC solution and (C) is the volume level required in the experiment.

3.2.5 Determination of degree of substitution (DS)

Proton magnetic resonance was used in the measurement of the degree of substitution (DS) of sodium CMC as described by Ho and colleagues (Ho *et al.*, 1980). DS is calculated by measuring the integrated carboxymethyl signals at the region of 4 - 4.5 (parameter 'A') and comparing this to the measured integration of non-substituted protons of the glucose unit at the region of 3 - 4 (parameter 'B'). The DS is then calculated as 0.5A/0.133 B.

Three samples were prepared for DS measurement using ^{1}H NMR on Bruker AV500. 30 mg mL^{-1} of sodium CMC (CRT 100 PA) and 4h acidic hydrolysed CMC and 60 mg mL^{-1} of 7h acidic hydrolysed CMC. Deuterium oxide was used as the solvent system. Sodium CMC of (90kDa) at 0.7 DS was used as a control.

3.2.6 Preparation of ACP stabilized by acidic hydrolysed CMC

The same method as described under section 2.2.5.1 was used in the preparation of ahCMC-ACP. Samples of acid-hydrolysed CMC at a concentration of 10 mg mL^{-1} in Milli-Q water separated at 1, 2, 3, 4, 5, 6 and 7h were selected for particle size measurement to identify the chain length of polymer that could be used to stabilize the nanoparticle sized ACP.

3.2.7 Preparation of ACP stabilized by selected acidic hydrolysed CMC

Following the results obtained from the section 3.2.6, ACP colloid was prepared by a modified method (section 2.2.5.2) using selectively acid- hydrolysed CMC.

3.2.8 Characterisation of prepared ahCMC-ACP

The prepared colloids and isolated ahCMC-ACP were characterised by particle size analysis, solid-state analysis, scanning and transmission electro microscopy, thermal stability and dynamic vapour sorption analysis using methods as described in sections 2.2.6.1, 2.2.6.2, 2.2.6.3, 2.2.6.4 and 2.2.6.5.

3.3 Results

3.3.1 ACP stabilized by carboxyl containing polymers

When calcium dichloride and disodium phosphate were added to sodium alginate, gel masses were observed as shown in Figure 3.7. This suggested that sodium alginate was unable to stabilise calcium phosphate. In comparison, when pectin was used, a homogenous colloidal system was produced suggesting a potential stabilisation ability of the ACP complex. Particle size analysis as shown in Figure 3.8 revealed a size distribution of around 670nm for the prepared pectin-ACP colloid.

Figure 3.7: Gelled masses of sodium alginate on addition of calcium dichloride and disodium hydrogen phosphate

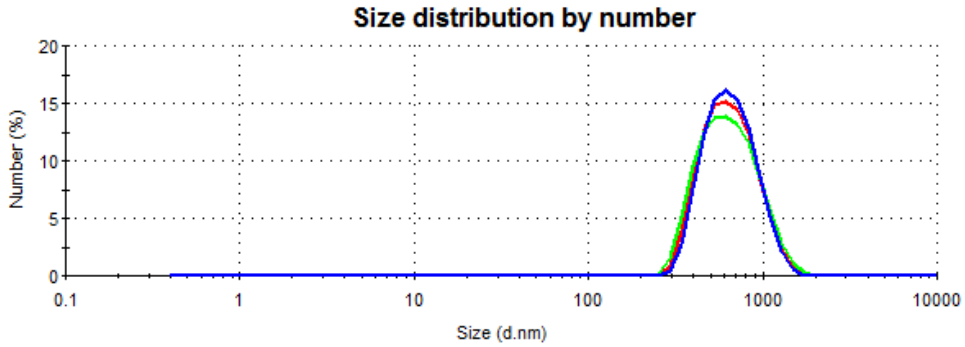

Figure 3.8: Particle size distribution of ACP stabilised by pectin L/100 showing a mono dispersed system of around 670nm particle size.

The particle size analysis of the prepared CRT (10,000 PA)-ACP colloid revealed a poly-dispersed system with peak particle sizes of about 50, 160 and 1160nm diameter (size distribution by number) while distribution by intensity showed peak distributions with medians of 50, 192, 1809, and 4752nm as shown in Figure 3.9.

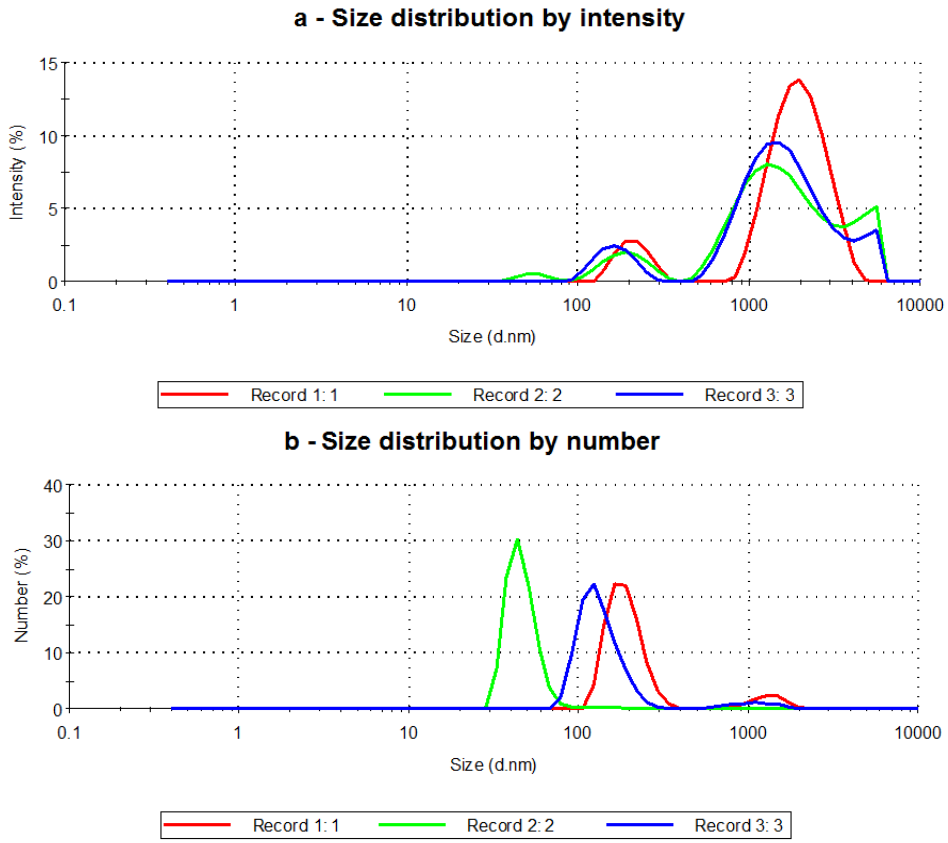

Figure 3.9: Particle size distribution curves of ACP stabilised by CMC CRT (10,000 PA): a-Size distribution by intensity % and b-Size distribution by number %.

3.3.2 ACP stabilized by sodium CMC grades

Figure 3.10 presents the data obtained relating the polymer chain length of sodium CMC to the particle size of the prepared CMC-ACP. Since the grade with lowest chain length did not approximate the 10nm diameter particle size, shorter chain length sodium CMC prepared by acidic hydrolysis was used to reduce the size of ACP nanocomplexes.

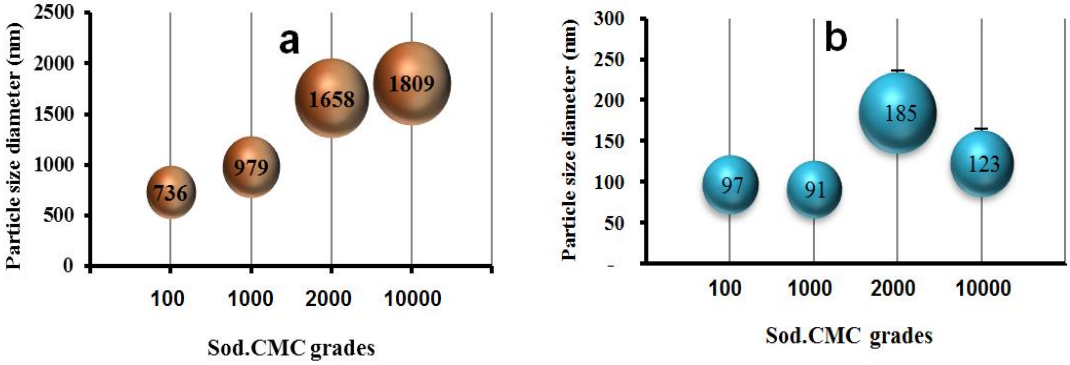

Figure 3.10: Mean CMC-ACP particle size diameter (±SEM, n=3) of different grades (molecular weight): a-Size distribution by intensity % and b-Size distribution by number %. Numbers inside symbol are particles size diameters in nm.

3.3.3 Preparation of ACP stabilized by ahCMC

3.3.3.1 Preparation of ahCMC.

Seven acidic hydrolysed sodium CMC products were obtained which were subjected to molecular weight determination and measurement of the degree of substitution.

3.3.3.2 Molecular weight determination

The accurate molecular weight of CRT 10,000 PA is not usually specified (Lavdas, 2010). Therefore, there was a need to identify the starting molecular weight of the product to standardize the experiment. The molecular weight was measured using the methods described in the sections that follow.

3.3.3.2.1 Zetasizer Nanos method

Two studies were carried out to determine the molecular weight of sodium CMC (CRT 100 PA) and the results obtained are tabulated in Table 3-2. The average calculated molecular weights were 9.1±4.9 and 21.3±11.6 kDa. However, Debye plots show a huge fluctuation in data as shown in Figure 3.11. These results indicate that this method was not suitable to measure the molecular weight of the sodium CMC (CRT 100 PA) polymer.

	1st attempt			2nd attempt		
Conc. g/L	Intensity kcps	KC/RoP 1/kDa	Calculated MW, (kDa)	Intensity kcps	KC/RoP 1/kDa	Calculated MW, (kDa)
2	61.2	0.118	8.47	61.2	0.0503	19.88
3	93.9	0.0779	12.84	93.9	0.0333	30.03
4	112.8	0.0785	12.74	112.8	0.0336	29.76
5	53.2	0.427	2.34	53.2	0.183	5.46
Average			9.1±4.9			21.3±11.6

Table 3-2: Calculated molecular weight of sodium CMC (CRT 100 PA) by Zetasizer nanoZS

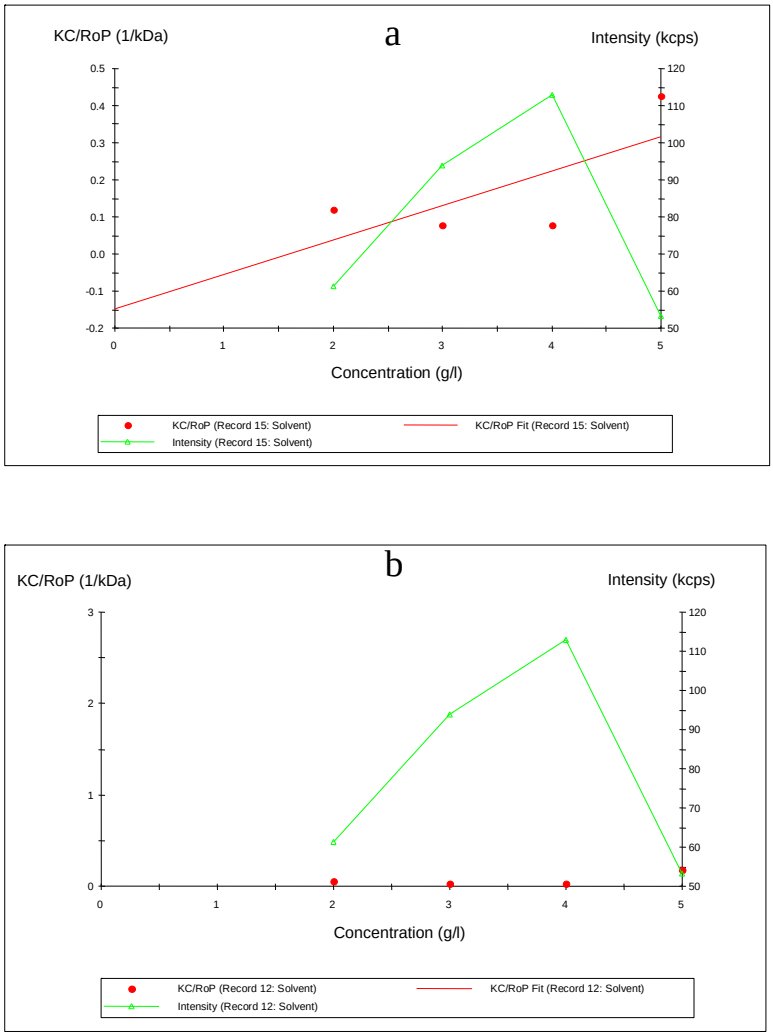

Figure 3.11: Debye Plots of CRT 100 PA produced by Zetasizer nanoZS. a-1st measurement and b-2nd measurement. Inconsistent data were observed, suggesting that the method was inappropriate for this type of sample.

3.3.3.2.2 Viscosity method

The regression correlation of inherent viscosity and reduced viscosity versus concentrations for CMC-90kDa are as shown in Figure 3.12. The linear regression coefficients were found to be 0.99 and 0.90 respectively, with intercepts of 2.01 and 2.1, which represent the respective intrinsic viscosities. From this relationship, the calculated average molecular weight was estimated to be in range of 78.4 to 82.8 kDa. Thus, this method showed a measured molecular weight with 8 to 13 % lower than that mentioned by the supplier. In addition, the regression correlation for the

rheological data of CRT 100 PA provided linear regression coefficients of 0.97 and 0.93 respectively, with intercepts of 4.25 and 4.48 that estimated that the average molecular weight was between 218.64 to 235.46 kDa. From this, it was calculated that the true median molecular weight of CRT 100PA was in the range between 251.04 and 255.93 kDa.

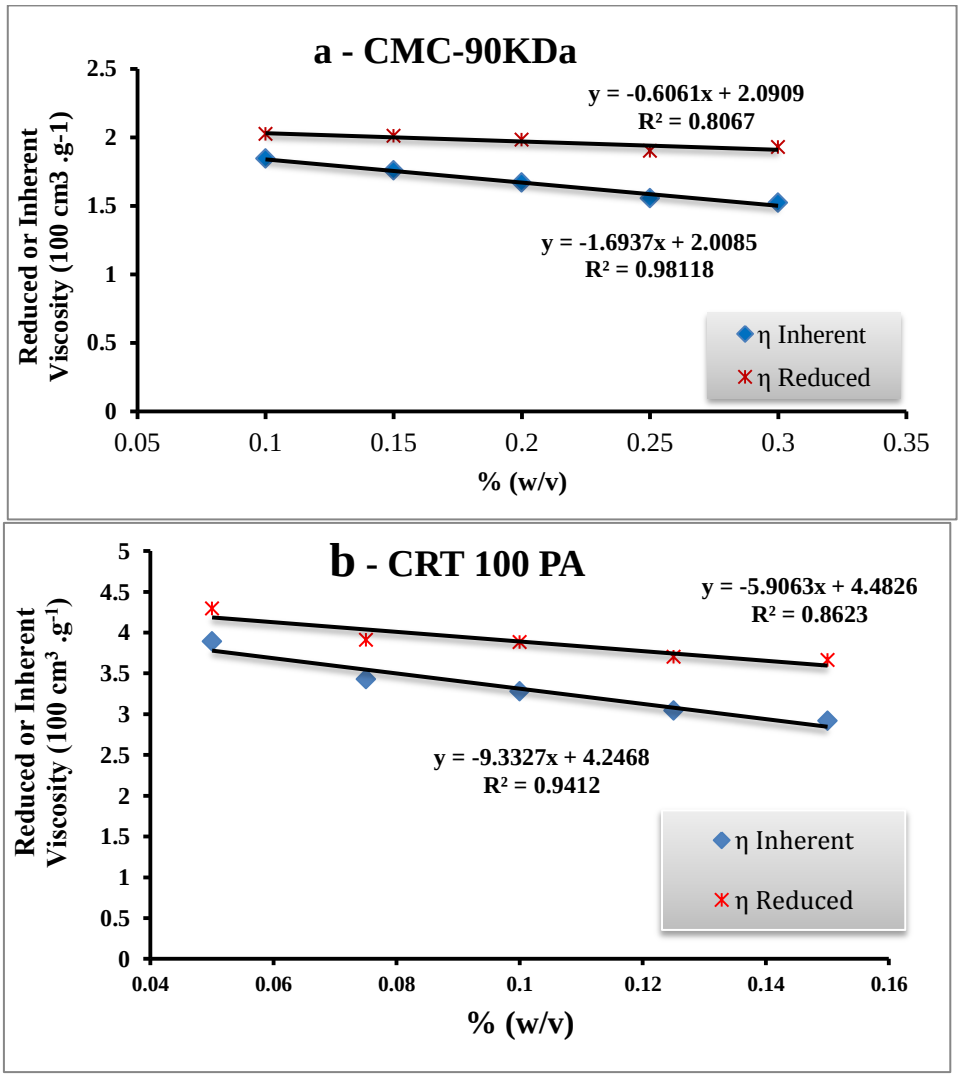

Figure 3.12: Reduced or inherent viscosity versus concentration for CMC polymers in 0.5N NaOH: a- CMC-90kDa and b - CRT 100 PA.

3.3.3.3 DS determination

^{1}H NMR spectrum of CRT 100 PA, 4h acidic hydrolysed CMC, 7h acidic hydrolysed CMC and CMC-90kDa samples were integrated at regions 3.1-4.05 and 4.05-4.45 that represent the substituted and unsubstituted protons at C1, C3 and C6 respectively, as shown in Figure 3.13. The calculated DS was 0.84 for CMC-90kDa, which is a 0.14 higher than that mentioned by the supplier (0.7). In addition CRT 100 PA, 4h acidic hydrolysed CMC, 7h acidic hydrolysed CMC showed calculated DS of 0.86, 0.74 and 0.72 respectively. Therefore, 4h and 7h acidic hydrolysis reaction caused a reduction in DS of 0.12 and 0.14 respectively.

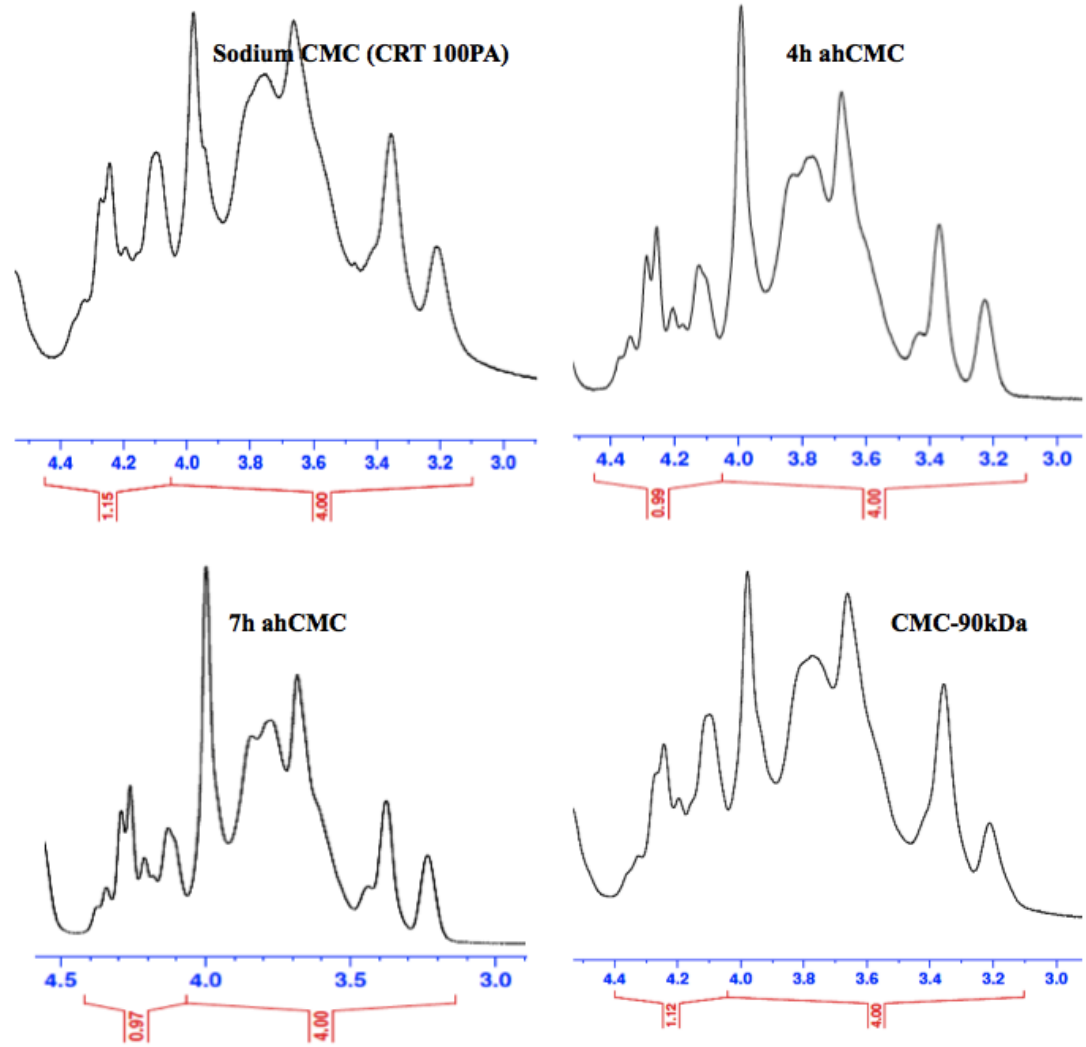

Figure 3.13: 1H-NMR spectra of sodium CMC (CRT 100 PA), 4h ahCMC, 7h ahCMC and CMC-90kDa.

3.3.3.4 Preparation of ACP stabilized by ahCMC

Figure 3.14 shows the particle size analysis of the prepared CMC-ACP produced from acidic hydrolysed CMC after 1, 2, 3, 4, 5, 6 and 7h treatment. With an increased treatment, hydrolysis reached a maximum at 4h with precipitation in the 6 and 7h incubations.

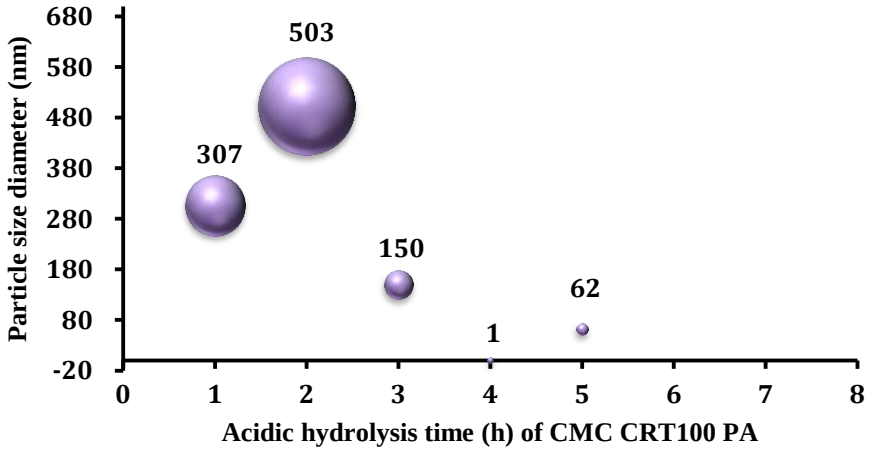

Figure 3.14: Means ACP particle size (n=3) stabilized by acidic hydrolysed CMC. Samples prepared at 6 and 7h were precipitated.

3.3.3.5 Preparation of ACP stabilized by selected hydrolysed CMC

The 4h acidic hydrolysed CMC (4h ahCMC) with measured molecular weight of 21,991 and 23,137g/mol (Figure 3.15) was selected for use to prepare ahCMC-ACP using modified method of preparation (section 2.2.5.2).

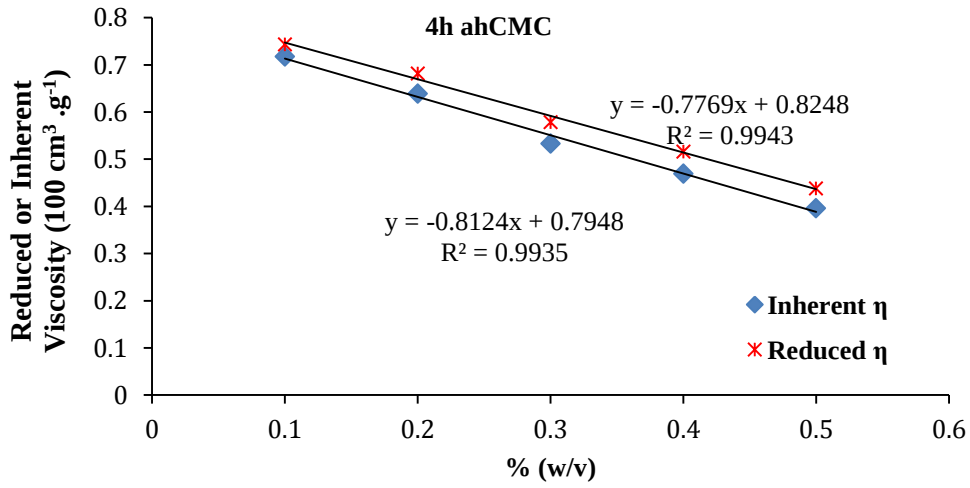

Figure 3.15: Reduced and inherent viscosity versus concentration for 4h hydrolysed CMC polymers in 0.5N NaOH.

3.3.4 Characterisation of prepared ACP stabilised by 4h ahCMC

The freeze dried isolated ACP stabilised by 4h ahCMC was white in colour with light fluffy friable needle structure (Figure 3.16-a). Unpurified freeze-dried ahCMC-ACP showed similar structure with a crumply network texture, as shown in Figure 3.16-b. The isolation process at 4h, showed that for each 1g CMC, 3.42 g of unpurified and 1.28 g of isolated 4h ahCMC-ACP were produced.

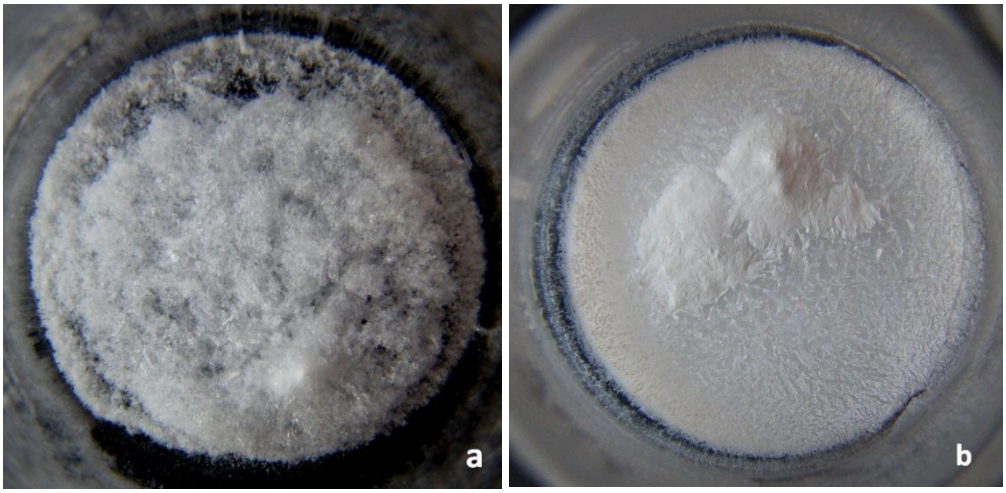

Figure 3.16: Freeze-dried ACP stabilised by 4h ahCMC: a-Isolated ahCMC-ACP and b- unpurified ahCMC-ACP.

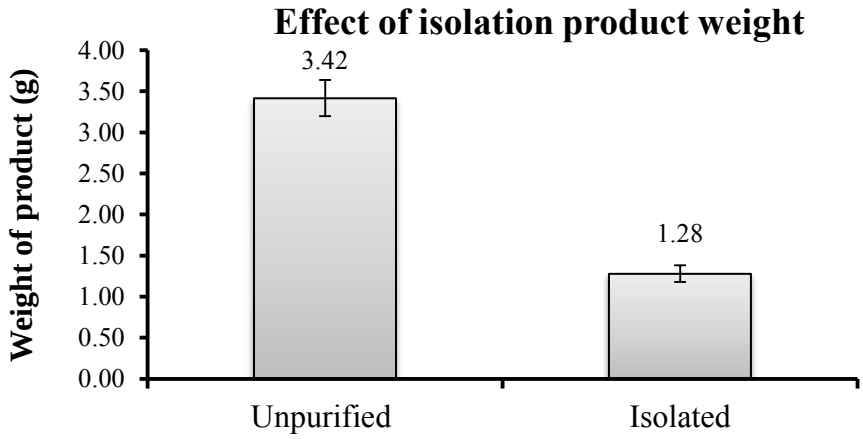

Figure 3.17: The total product weight of 4h ahCMC-ACP, shows the effect of isolation process on the product weight, (n=3, ±SEM).

3.3.4.1 Particle size analysis

The prepared ACP colloid stabilised by 4h acidic hydrolysed ahCMC showed particle size of about 10nm diameter (particle size distribution by number) as shown in Figure 3.18. However during the isolation step, the particles sizing did not show a constant reading. The water removal from ACP during freeze-drying process leads to agglomeration of nanoparticles into large sediments.

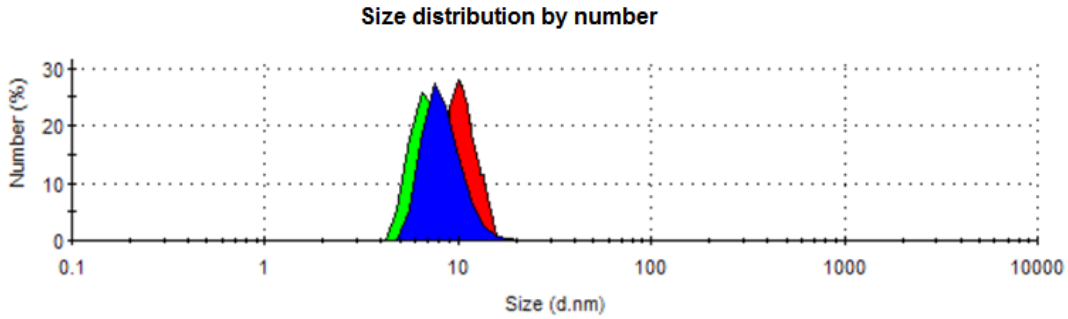

Figure 3.18: The Zetasizer NanoZS particle size distribution curves (by number %) of prepared 4h ahCMC-ACP colloid, shows the prepared ACP of particle size around 10nm diameter.

3.3.4.2 Solid state form analysis

The X-ray diffraction analysis of the isolated 4h ahCMC-ACP confirmed the absence of crystalline structure in the isolated ACP as shown in Figure 3.19.

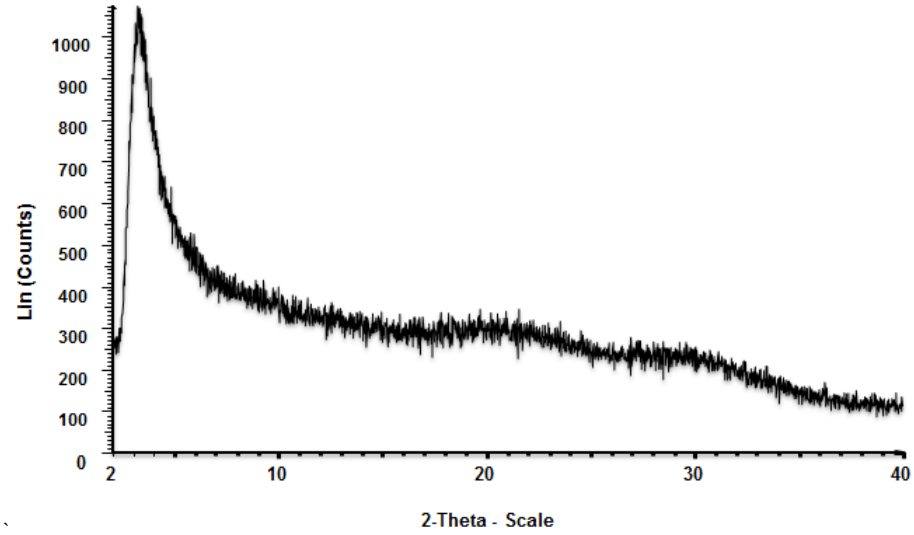

Figure 3.19: X-ray diffraction chromatogram of the prepared 4hr.ahCMC-ACP. No crystalline structure was observed.

3.3.4.3 SEM and TEM imaging

Figure 3.20 shows the obtained SEM images of freeze dried 4h ahCMC-ACP. The unpurified and isolated products had flake-like structure of light and hard dense shells respectively. In addition, the higher magnification image (Figure 3.21) shows that the inner structures of the nanocomplexes were packed to form aggregates. Figure 3.22 shows the TEM images of the nanocomplexes in colloidal preparation of 4h ahCMC-ACP.

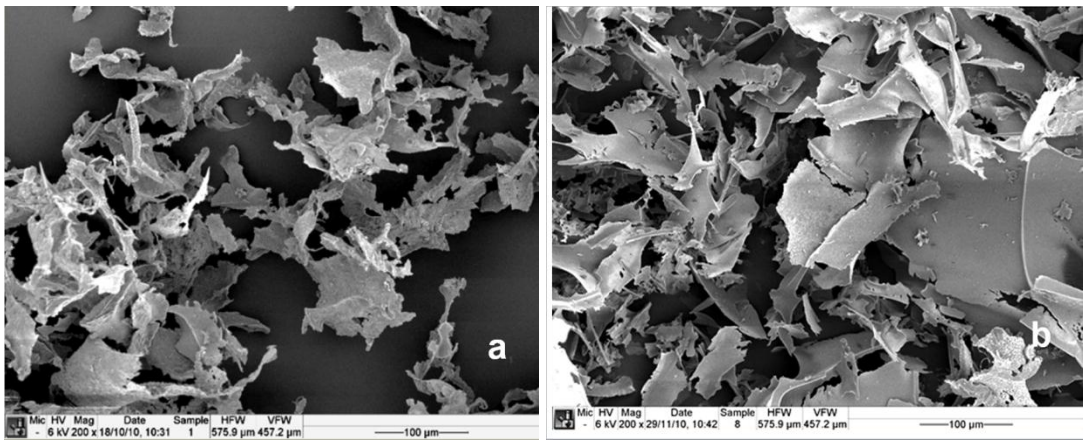

Figure 3.20: SEM images (200X) of 4h ahCMC-ACP showing the effect of isolation (centrifugation) on particles aggregation: a- isolated ACP and b- unpurified ACP

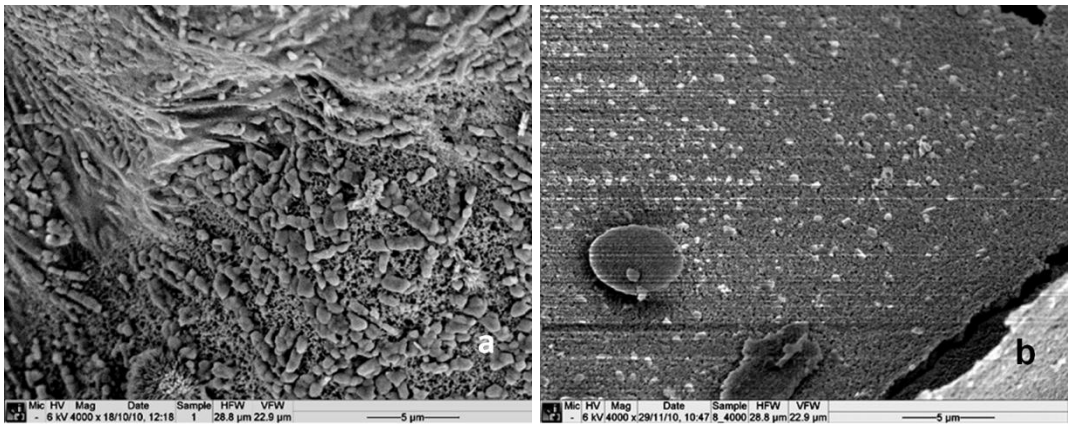

Figure 3.21: SEM images (4000X) of 4h ahCMC-ACP showing the effect of isolation (centrifugation) on the inner structure of the nanocomplexes, which were packed to form aggregates: a- isolated ACP and b- unpurified ACP

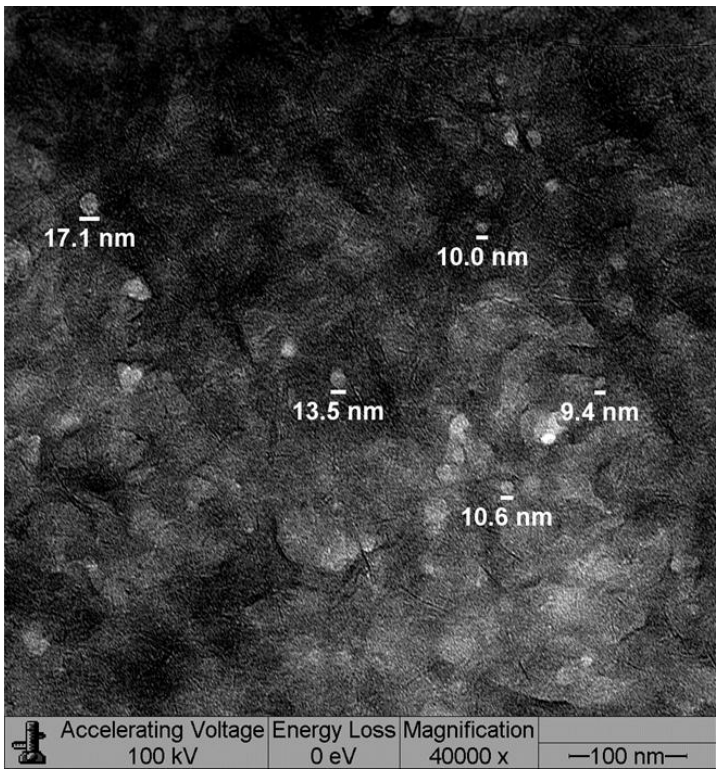

Figure 3.22: TEM image of 4h ahCMC-ACP colloid prepared by the modified method. Unlike SEM, this imaging technique allows the visualisation of the individual nanocomplexes.

3.3.4.4 Thermal stability study

Figure 3.23 represents plot of the isolated 4h ahCMC-ACP, which showed the water evaporation and decomposition phases. The moisture content was found to be 7.79% and weight loss of 21.46% on decomposition. The DSC thermogram showed that the isolated 4h ahCMC-ACP had higher endothermic band of water evaporation phase (Figure 3.24).

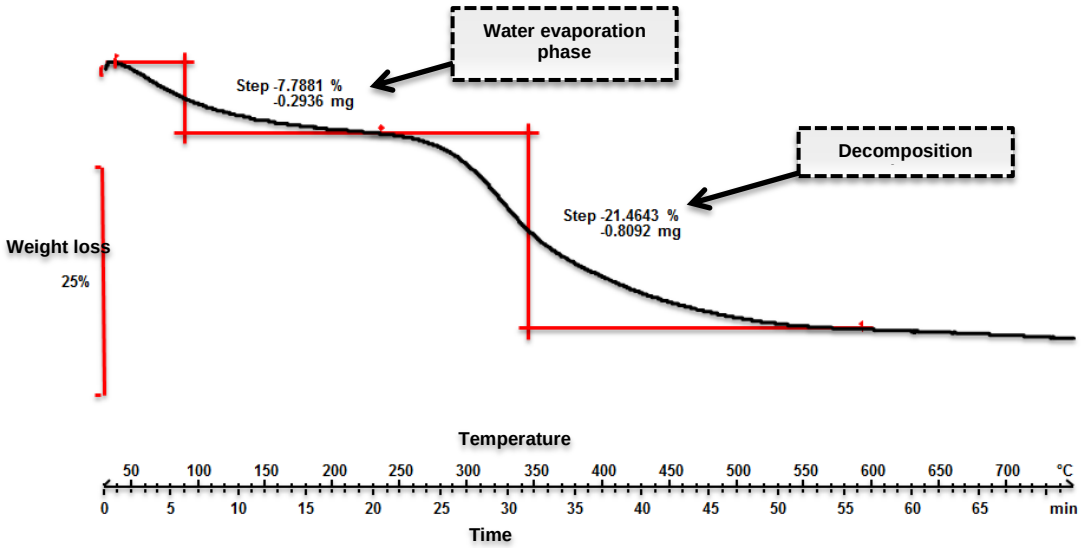

Figure 3.23: TGA of the isolated 4h ahCMC-ACP, showing the water evaporation and decomposition phases.

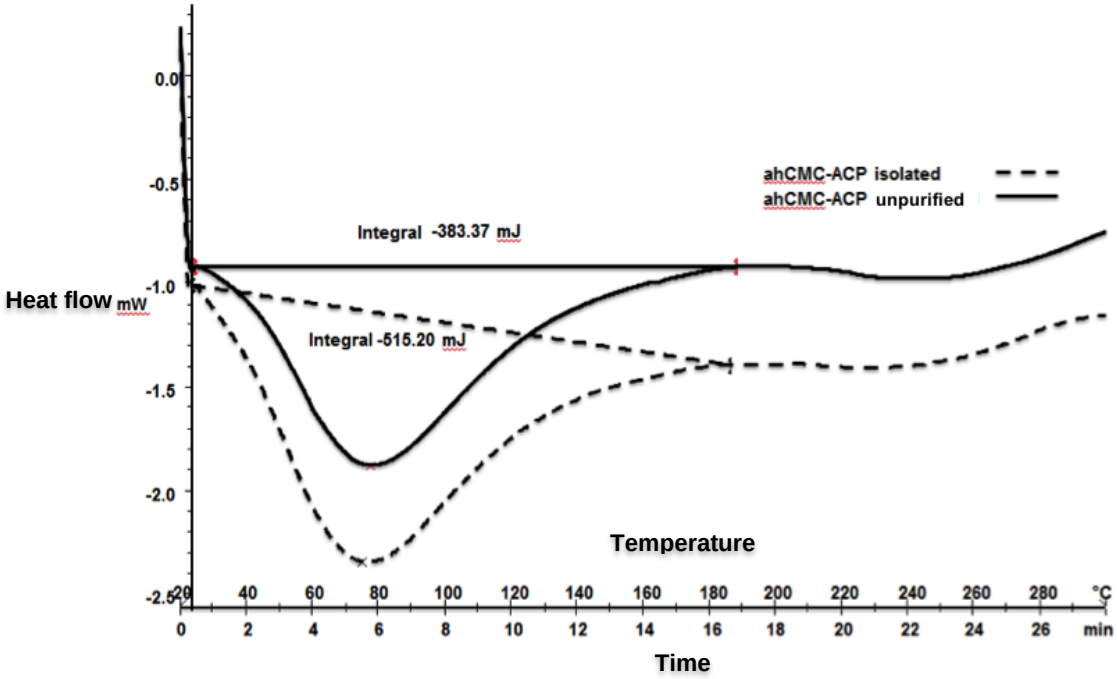

Figure 3.24: DSC thermogram traces of unpurified and isolated 4h ahCMC-ACP showed a difference in endotherm bands during the evaporation of water.

3.3.4.5 Dynamic vapour sorption (DVS) analysis

The dynamic vapour sorption chart (DVS) shown in Figure 3.25 illustrates the weight change in the isolated 4h ahCMC-ACP sample as function of water sorption and was analysed over two cycles of increment followed by decrement in the

percentage relative humidity at constant temperature. Figure 3.26 shows the DVS isotherm plot of freeze-dried isolated 4h ahCMC-ACP, illustrating the percentage weight gain in the sample as a function of water sorption and desorption.

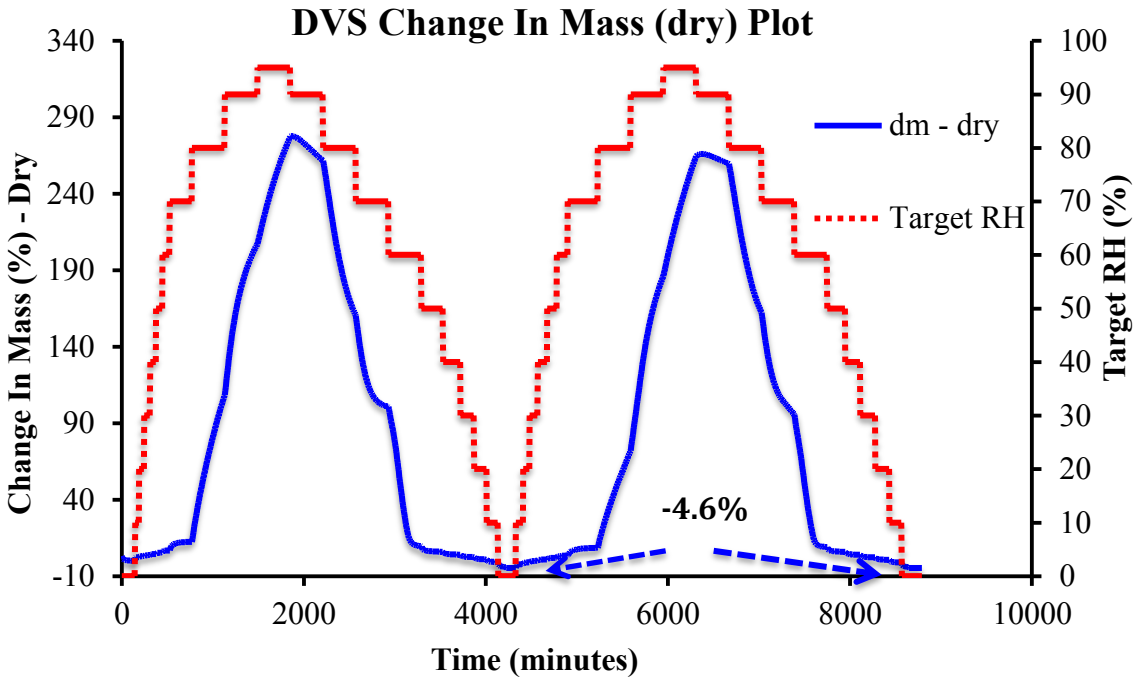

Figure 3.25: DVS kinetic of isolated 4h ahCMC-ACP powder showing the weight gain following two cycle of relative humidity.

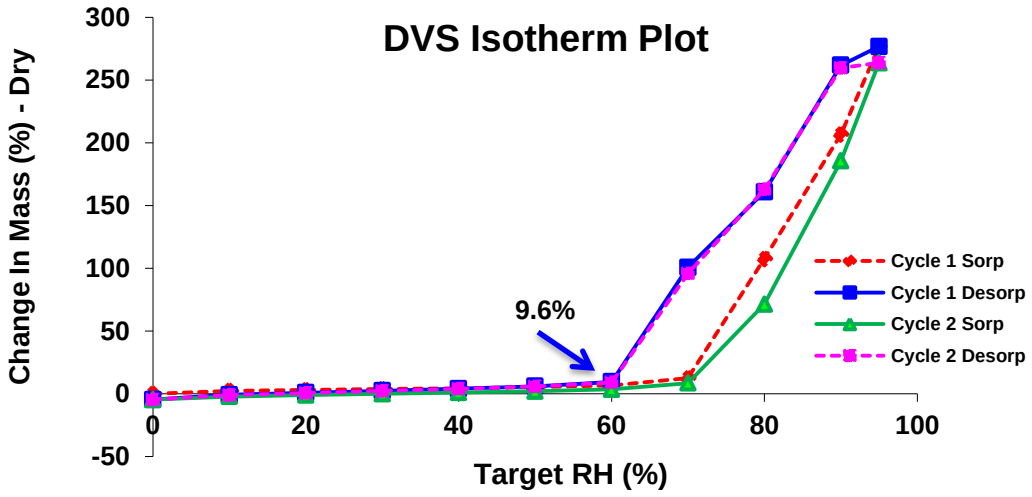

Figure 3.26: DVS isotherm of isolated 4hahCMC-ACP powder showing the effect of one and two cycles of water sorption and desorption on the sample weight.

3.4 Discussion

3.4.1 ACP stabilized by carboxyl containing polymers

Sodium alginate gelled upon the addition of calcium dichloride and disodium hydrogen phosphate. This might be caused by the crosslinking interaction between the carboxyl group, which is directly attached to the rigid cyclohexose unit and the calcium ions. The result agreed with that seen in sodium alginate formulation of ofloxacin nanospheres described by (Sangeetha *et al.*, 2010). Since the pectin-ACP was complexed successfully, the chemical structure of pectin seems capable of stabilising ACP. However, a large particle size was observed. On this basis, pectin with a shorter chain length might be useful to minimise the particle size of ACP.

In addition CRT 10,000 PA-ACP complex of the poly-dispersed colloid was produced and this appeared similar to that attained by NGP-ACP. The sodium CMC has structural specificity that is valuable to stabilize a colloidal ACP. Furthermore, sodium CMC with a lower molecular weight would be useful to minimize the particle size to a nanometer dimensions, analogous to that achieved by the groups of Zhao and by Luo in producing stabilising Fe-Pd nanoparticles, mean diameter 17.2 nm using sodium CMC with a molecular weight of 90kDa (Zhao et al., 2007; Luo et al., 2011).

3.4.2 ACP stabilized by sodium CMC grades

All grades of sodium CMC investigated showed a capability in stabilising calcium phosphate. This indicates sodium CMC is able to form a complex by bonding to a divalent, positively charged ions in agreement with data obtained by (Keith, 1990). In these studies, the sodium CMC was used as complexing agent with chlorhexidine (divalent cationic) to change the liquid state into solid-state complex to minimise the unpalatable properties of orally used chlorhexidine. In addition, sodium CMC was used to selectively precipitate whey protein as demonstrated by Hidalgo and colleagues (Hidalgo *et al.*, 1971).

The solubility of sodium CMC might enhance the solubility of the complex and affect calcium ion release. In addition, the sodium CMC-ACP complexes will be in a dispersed form, which enhances the rate of dissolution and calcium release according to that reported by the Lopez group who employed sodium CMC as a fluidised polymer suspension rather than as a dry state powder in toothpaste formulation, to prevent formation of lumps and enhancing the rate of polymer dissolution (Lopez *et al.*, 1999).

The particle size of the prepared ACP was found to decrease with the reduction of the sodium CMC chain length; however the materials commercially available were of too long a chain length to allow us to reach the requisite size of about 10 nm. Therefore acidic hydrolysed sodium CMC with shorter chain length might enable the generation of structures of a particle size necessary for this application of dental enamel remineralisation.

3.4.3 Preparation of ACP stabilized by ahCMC

It was found that the accessibility of acid into cellulose during the course of acid treatment was enhanced to a great degree by carboxy methyl substitution than that of swelling. In addition, carboxymethylation improved the swelling property of cellulose. As a result, this chemical modification exhibited a dual effect to increase the performance of the acid- hydrolysis reaction (Borsa *et al.*, 1990).

The prepared ahCMC showed a further decrease in the particle size of the prepared ACP with decrease in the polymer chain length; however the 5, 6 and 7h ahCMC did not generate colloids. However, 4h ahCMC produced a colloid stable for a few hours transferring to gel containing lumps of aggregates. Therefore 4h ahCMC was selected for trial preparation by a modified method of preparation. The 4h ahCMC with measured molecular weight range of 21,991 to 23,137g/mol and 0.7415 degree of substitution showed a stable poly dispersed colloid of about 10nm diameter (size distribution by number). The calculated production yields were found to be 342% and 128% w/w for unpurified and isolated 4h ahCMC-ACP respectively.

3.4.4 Characterisation of prepared ACP stabilised by 4h ahCMC

3.4.4.1 Solid state form analysis

Raynaud and colleagues reported that the X-ray diffraction analysis of calcium phosphate apatites prepared with variable Ca/P ratio was showed the appearance of 2θ peaks at 26, 31 and 32 angles (Raynaud *et al.*, 2002) and the absence of the peaks in the obtained X-ray diffraction chromatogram of freeze dried isolated 4h ahCMC-ACP confirmed that the prepared ACP was stable amorphous form and free from apatite. In addition, the trace served as evidence for the absence of unbound CMC, characterised by the crystallinity band of 2θ peak at 20 angle, as shown by Moosavi-Nasab and workers (Moosavi-Nasab *et al.*, 2010).

3.4.4.2 SEM and TEM imaging

The isolation step of 4h ahCMC-ACP preparation showed a similar effect that occurred in NGP-ACP preparation (section 2.3.3.3) that led to the formation of large aggregates of nanocomplexes.

The obtained TEM image of 4h ahCMC-ACP colloid provided evidence of ACP nanocomplexes of about 10nm particle size. In addition, 4h ahCMC-ACP particles had a spherical shape that agreed with that reported by (Abbona *et al.*, 1996). The authors describe TEM imaging of ACP prepared by mixing of equimolar concentrations of calcium and phosphate, which shows a presence of the hydroxyapatite flake-like structures within short blades. In contrast, the prepared 4h ahCMC-ACP showed little evidence of a hydroxyapatite like structure.

3.4.4.3 Thermal stability study

TGA analysis of the 4h ahCMC-ACP showed percentages of weight loss during water evaporation and decomposition similar to that recorded for NGP-ACP analysis in section 2.3.3.4.2. This indicates there was a similarity in the amorphous form of these complexes. This data is in contrast to the data obtained from the DSC analysis. The isolated 4h ahCMC-ACP showed a higher endothermic band than that in the

unpurified fraction. This indicates the amorphous form of isolated 4h ahCMC-ACP is more stable that that of unpurified 4h ahCMC-ACP. This was the reverse of the situation that was obtained in the NGP-ACP experiments.

3.4.4.4 Dynamic vapour sorption (DVS) analysis

The data from the DVS analysis of the isolated 4h ahCMC-ACP showed a percentage of mass change with relative humidity. This is in agreement with that observed in NGP-ACP which indicates a similarity in the amorphous 4h ahCMC-ACP and NGP-ACP. The 4h ahCMC-ACP required 140minutes to reach a steady state mass change at 0%RH, which indicates the CMC polymer can retain more moisture in the prepared ACP. In addition, the DVS change in mass showed a negative percentage of moisture was remained at the beginning and at the end of the second cycle which indicates the 4h ahCMC-ACP was not completely dry at the start of the first cycle. The DVS isotherm plot demonstrated a similarity in the profile to that obtained for NGP-ACP, in which acceleration in mass gain was evident above 60%RH. This implies the behaviour of water uptake of 4h ahCMC-ACP and NGP-ACP was similar.

3.4.5 Stabilisation efficiency theory

The efficiency of 4h ahCMC as well as sodium CMC grades and pectin to stabilise ACP strengthen the Termine and co-workers, finding (section 2.1) of the capability of the polymer containing free carboxyl group to enhance the stability of the ACP (Termine *et al*., 1970).

3.5 Conclusions

Pectin and sodium CMC polymers showed a potential to stabilize ACP, while sodium alginate did not. The particle size of the prepared ACP, stabilized by sodium CMC, decreased with a reduction in molecular weight or chain length of the sodium CMC polymer. CRT 100 PA showed a stabilizing efficiency on the particle size of

the prepared ACP. The ahCMC stabilise the prepared ACP at lower particle size, especially 4h ahCMC. The prepared ACP stabilized by 4h ahCMC had a nano particle size of about 10nm diameter. The X-ray powder diffraction and TEM imaging suggested the non-crystalline form of the prepared isolated 4h ahCMC-ACP.

Further studies have to be directed to the formulation of the isolated 4h ahCMC-ACP into dental film dosage forms with the evaluation of calcium release using a specially designed dissolution cell and dental enamel remineralisation efficiency on a human enamel blocks.

Chapter 4. Formulation and characterisation of a dental film containing ACP.

4.1 Introduction

The local release of therapeutic agents such as antibacterial, antifungal and anesthetics are required to treat periodontal and dental diseases (Rathbone *et al.*, 2003). This includes preventive therapy, for example fluoride salts (Tayle, 1988). A diverse range of dosage forms have been produced, including lozenges, mouthwashes, aerosols, gels (Collins *et al.*, 1989), chewing gum (Schirrmeister *et al.*, 2007), mucoadhesive tablets (Ishida *et al.*, 1982), the Periochip® (Heasman *et al.*, 2001), microparticles (Rathbone *et al.*, 2003) , a hollow fiber device (Tayle, 1988) and gingival anesthetic patches such as DentiPatch® (Mantelle, 2008). This indicates market interest in improving patient compliance (palatability) and a range of therapeutic possibilities for the dental dosage forms.

Although most dental formulations are self-administered, more specific forms of treatment employing oral local sustained release delivery, for example the Periochip®, need a health care professional to administer and remove the exhausted device. Other self-administered formulations, for example based on microparticulates in a matrix, can be left *in situ* and do not need to be removed at the end of the treatment. For the patient with poor dental hygiene, it is useful to treat gum disease with a single device giving a sustained level of drug. Esposito and colleagues described a formulation based on tetracycline microparticulates prepared by a double emulsion technique employing different grades of poly-lactide and poly-lactide-co-glycolide polymers. The systems gave a prolonged release profile *in vitro* (Esposito *et al.*, 1997).

In order to increase the residence time of the fluoride in the treatment of dental caries, viscous bases such as polyurethane and other resins applied as a lacquer in solvents have been used as a sustained release carrier for fluoride. Fluoride varnish, Duraphat®, was firstly introduced in 1964 containing 5% sodium fluoride in a viscous resin base. This was followed by the introduction of Fluo Protector® in 1975

which contained 0.9% fluorsilane (0.1%fluoride), in a polyurethane base, as the active ingredients. Fluoride varnish has been considered as a standard preventivedental care in most of Europe, Scandinavia, and Canada for more than 25 years (Hazelrigg *et al.*, 2003).

To achieve localized anesthesia, a transmucosal gingival anesthetic patch (DentiPatch®) first developed in 1990, was launched in 1996 by Noven Pharmaceuticals. This was designed to deliver local anesthetics including lidocaine or benzocaine, for pre-injection dental anesthesia (Mantelle, 2008). The DentiPatch® systems, loaded with 20% lidocaine, gave a measured reduction of the pain of dental injection and was superior to 20% benzocaine topical gel (Kreider *et al.*, 2001; Shafiei *et al.*, 2008).

Tissue association of the dosage forms on the oral mucosa is a function of bioadhesiveness or stickiness on mucosal or dental surfaces. Other factors, such as erodability of the hydrocolloidal carrier, may be important. Jain and colleagues have described the periodontal pocket as an administration and storage site to allow sustained-release of drugs (Figure 4.1). These drug delivery systems were manufactured as fibers, strip, film, gels, microparticles, nanoparticles and vesicles (Jain *et al.*, 2008).

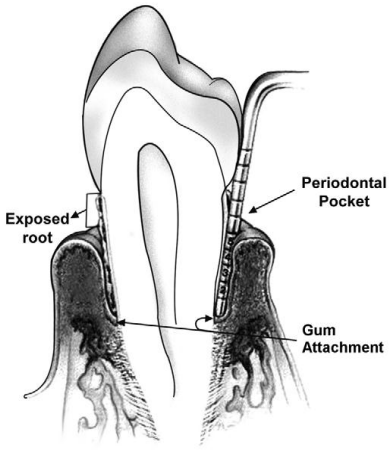

Figure 4.1: Administration of a drug delivery system into a periodontal pocket
From (Jain *et al.*, 2008).

Cilurzo and colleagues showed that the dissolution of polymeric matrix *in vivo* controlled the residence time of a mucoadhesive patch provided that it was sufficiently adhesive. In addition, they prepared compacts from polymeric raw materials (10 tons compression force). Texture analysis was used to determine the adhesion of the formulation against a hydrated mucin surface mounted to the bottom of the analyser. The compacts were fixed on the probe surface by cyanoacrylate glue. A pressing force (1.3N) was applied by the texture analyser for 6 minutes to establish a contact between mucin and the compact. The probe was then pulled free to measure the stickiness and work of adhesion (Cilurzo *et al.*, 2003).

4.1.1 Adhesion theory

Adhesion is defined as "the establishment of interfacial bonds and the mechanical load required in breaking an assembly". The study of adhesion mechanisms is complicated because understanding adhesion process includes many different scientific fields. In the varied disciplines, the approaches of mechanical interlocking, electronic, weak boundary layers and the interface, adsorption (thermodynamic), diffusion and chemical bonding theories have been proposed. A single general mechanism is unable to unite all the experimental findings, suggesting that several mechanisms will be involved concurrently. Overall, it is supposed that the adsorption (thermodynamic) theory has the broadest applicability. Adsorption is essential to initiate other mechanisms and the subsequent increase in adhesion strength (Pizzi and Mittal, 2003) .

4.1.2 Film dosage form

Buccal adhesive films are preferable to the mucoadhesive tablets because of the flexibility, comfort and contact time of these forms compared to oral gels (Perioli et al., 2004). So far the film dosage form has been prepared for local and systemic drug delivery. Localized delivery of active ingredients has been applied to tissues such as buccal (Okamoto et al., 2002; Okamoto et al., 2001), vaginal (Liu and Kresevic, 2009) , skin (Padula *et al.*, 2003) and the periodontium diseases (El-Kamel *et al.*, 2007) (Shifrovitch *et al.*, 2009). Systemic delivery has been widely used as a carrier

for different drugs such as glipizide (Semalty et al., 2008), caffeine (Semalty et al., 2008), nicotine (Cilurzo *et al.*, 2010) and oxybutynin (Nicoli *et al.*, 2006)

The casting method of solvent drying had been extensively used in the fabrication of film dosage form for fast and sustained release delivery of drugs. Murata and colleagues used a casting method in the preparation of film dosage form from natural polysaccharides and found that the model drugs were released rapidly by erosion in 10mL dissolution medium (Murata et al., 2004). The orally bioabsorbable sustained release film containing metronidazole had been prepared by Shifrovitch and co-workers, using casting method to overcome the disadvantage of the non-bioabsorbable sustained release film devices containing chlorhexidine, metronidazole and minocycline that it must be removed from the periodontal pocket (Shifrovitch et al., 2009).

4.1.3 Calcium analysis.

Calcium is one of the basic elements of the ACP and there are different methods of the quantitative analysis of the calcium ion concentration, for example, the titrimetric method, flame photometry and atomic absorption. In the titrimetric method sodium edetate (EDTA) was used as a complexing agent in alkaline conditions (Jeffery *et al.*, 1989), this method was reported to be the official method for quantitative analysis of calcium in most containing salts (Pharmacopoeia, 2012). It is reported that flame photometry method was applied using wavelength of 422.7 nm and blue filter for calcium analysis (Luh and Niketic, 1959) . However, a preliminary purification was required by extraction as calcium oxalate followed by dissolution in perchloric acid (BWB-Technologies, 2011). In atomic absorption spectrophotometry, two different techniques were required to minimize the encountered interferences use of releasing agents (such as strontium chloride, lanthanum chloride, or EDTA) or on ionisation buffer such as potassium chloride (Jeffery *et al.*, 1989). Inductively coupled plasma MS is the up-to-date method for quantitative analysis of calcium, which involves acidification by nitric acid (Borkowska-Burnecka *et al.*, 2010) and (Ardini *et al.*, 2011).

A calcium ion selective electrode (Figure 4.2) is composed of two main units an inner stem and a sensing module, that represent the reference and sensing electrodes combined in one electrode. This electrode has to be filled with accompanianed reference solution before use. Its work is based on the principle of measurement of the difference in the electrical potentials between the reference and sensing module. The electrode potential is generated by the separation of charge at the surface of the electrode and the accumulation of the counter ion in the bulk of the solution phase (Pungor, 1998).

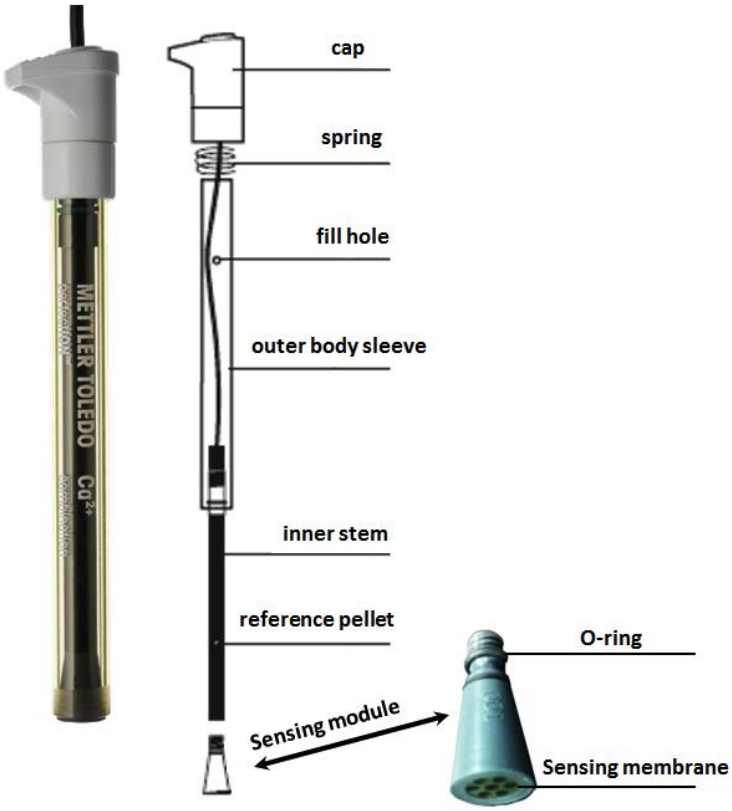

Figure 4.2: The components of a calcium ion selective electrode. Modified from (Mettler-Tolledo, 2010).

4.1.4 Objectives

The objectives of this study were to complete the pre-formulation analysis and formulate the prepared ACP into a dental film dosage form. The polymer used in the formulation was selected by preparing hydrogels from different types and grades of polymers. The polymer showing the highest adhesion parameters was selected for use in the dental film formulation. The prepared dental films were characterised for physical observation, flexibility, degree of swelling, adhesion, calcium content and calcium release using a specially designed dissolution cell.

4.2 Materials and methods

4.2.1 Chemicals

All the polymers used were pharmaceutical grade. Different grades of hydroxypropyl methylcellulose (Methocel®) and methylcellulose (Methocel®) were supplied from Dow (USA). Hydroxy ethyl cellulose (Natrosol®) was provided from Hercules-Aqualon (USA), sodium carboxymethyl cellulose was purchased from BDH-GPR (UK), different grades of sodium carboxymethyl cellulose (Walocel®) were supplied from Dow Wolff Cellulosics – Germany. Gum Arabic, gum tragacanth, sodium alginate, erythrosin extra bluish (lot#BCBC5076V), 0.1 M calcium ion standard solution (lot#0001428523), sodium bicarbonate, lactic acid and amorphous calcium phosphate – lot#04122MH (ACP-standard) were purchased from Sigma-Aldrich UK and xanthan gum from CPKelco (USA). Calcium standard metal solution 1000 ppm in 2% (v/v) nitric acid (lot#CL5-48CA) ICP-MS Spex CertiPrep was purchased from Fisher-Scientific (UK). Degassed water was freshly prepared by vacuum for 1 hour.

4.2.2 Toothpastes

Tooth mousse® (TM) was used as supplied from GC Corporation (Japan). Aquafresh Multi-Action + Whitening® (AF) GlaxoSmithKline (UK), Colgate Smile Age 2-6® (CS) and Colgate Cavity Protection® (CC) Colgate (UK) were purchased from a

pharmacy as the control preparation to which the prepared hydrogels could be compared.

4.2.3 Teeth samples and enamel blocks

Human incisors mounted in solid Perspex cubes were kindly provided by the Dental School at the University of Dundee. The teeth were mounted in an acrylic block so that the labial surface of tooth was exposed to facilitate the measurement of adhesive parameters of the hydrocolloids. Teeth samples and the enamel blocks were kept moist with an artificial saliva formulation, Xialine II™ (Preetha and Banerjee, 2005).

4.2.4 Calcium analysis and method validation

Calcium compounds form the main active pharmaceutical ingredients (API) in the prepared complexes, therefore a selective and specific method of calcium analysis using ion selective electrodes (ISE) was suggested. The PerfectIon™ combination calcium electrode Mettler-Toledo (Switzerland) was used for quantitative measurement of calcium. All the calcium measurements were carried out at a measured laboratory temperature of 17° C.

The HCl solution (pH 5), the prepared Xialine II™ artificial saliva and sodium bicarbonate – lactic acid buffers (pH of 5, 5.5, 6, 6.5 and 7) were used to construct the calibration curves to quantify the calcium content in the prepared ACP samples. Stock solutions of calcium of 1000ppm were prepared by dissolving 3.668g $CaCl_2.2H_2O$ in 1000mL solvent media and then serial dilutions were prepared from these stock solutions.

The calcium measurement using a calcium electrode was validated for linearity, precision and reproducibility. A comparative assessment of measurements for selected standards and samples from the release studies was completed in the Department of Chemistry, Strathclyde University using inductively coupled plasma mass spectrophotometry (ICP-MS).

4.2.4.1 Linearity

Standard calibration curves were assembled from three replicates of measurement for theseries of calcium concentrations. A plot of calcium content concentration versus recorded millivolt (mV) signal was constructed and the best fit estimated from linear regression. The obtained equation of best fit was used to calculate calcium concentration within the minimum and maximum standards.

4.2.4.2 Precision and reproducibility

The determination of precision was carried out by measurement of three calcium standard concentrations within the linear range. Three successive reading were taken to test the within-day repeatability. The inter-day reproducibility was performed on three days since the manufacturer advised that the electrode should not be stored in storage solution for more than three days. In view of this, the electrode was recalibrated at each setup. In addition, the sensitivity was verified every 2h with the least concentrated standard.

4.2.4.3 Validation of the calcium electrode in the calcium quantification

Validation of the selective electrode in calcium quantification was confirmed by re-analysis of selected samples and standards using a second method inductively-coupled plasma mass spectrometer (ICP-MS Agilent 7700 (Japan)). Samples, standards and blanks were diluted by 10 fold in 2% Nitric Acid Solution. This gave a concentration range that was appropriate to the analysis technique. A paired t-test was used to statistically differentiate between measurements obtained from both methods of calcium analysis.

4.2.5 Analysis of calcium content in the prepared ACP

The analysis of calcium content of the prepared ACP was carried out in triplicate by preparing 0.1% (w/v) ACP solutions at pH-5 (HCl-solution). The calcium content was measured using the calcium electrode. The signal voltages were noted and used to establish the calibration curve at pH 5.

4.2.6 Analysis of the effect of pH on the solubility of the isolated ACP

The pH-metric solubility method (Avdeef *et al.*, 2000) was used for the determination of the solubility profiles of the prepared isolated ACP. The pH-solubility analysis was carried out in triplicate in a pH cycle in the series 7, 6.5, 6, 5.5, 5, 5.5, 6, 6.5, and 7. The solubility of the ACP samples was determined by measuring calcium ion concentrations in the supersaturated solutions of the prepared ACP and ACP standard (Sigma Aldrich) in sodium bicarbonate – lactic acid buffers. The super saturation state of the prepared solutions was confirmed by leaving excess insoluble ACP and ACP-standard in the prepared solutions with stirring for 5 minutes. The pH descending and ascending series were performed by addition of 1M of lactic acid and 1M of $NaHCO_3$ respectively.

4.2.7 Preparation of hydrogels

4.2.7.1 Hydroxy propyl methyl cellulose (HPMC):

A 10% (w/v) HPMC (grade K15M) gel was prepared according to Dow technical handbook (Dow, 2002) by dispersing HPMC particles in 1/3 of volume of (90º C) distilled water. However, a very thick dough was produced upon addition of water. This produced mass was difficult to solubilise without bubble formation. The method was modified by gradual addition of HPMC powder with continuous non-vortex stirring (to prevent air trapping) into 90% of the final volume of distilled water at a constant temperature of 90º C using a hotplate. A uniform dispersion system was obtained and removed from the heating source with stirring until the temperature dropped to around 70º C. The final volume was made up by addition of distilled

water with stirring and the product was transferred to a 20º C water bath with continuous stirring. The viscosity of product increased and once capable of supporting the dispersion, the stirrer was removed and the product transferred into the container that was refrigerated at 3º C for 24hr to complete hydration. The samples of HPMC gel shown in Table 4-1 were prepared by the modified method.

No.	Grade	Concentration % w/v	No.	Grade	Concentration % w/v
1	K15M	20	18	E10M	15
2		15	19		10
3		10	20		5
4		5	21	F50 LV	15
5	K100M	10	22		10
6		5	23		5
7		3.5	24	E50 LV	15
8		2.5	25		10
9	F4M	15	26		5
10		10	27	E15 LV	15
11		5	28		10
12	K4M	10	29		5
13		7.5	30	A15LV prem.	15
14		5	31		12
15	E10M	15			
16		10			
17		5			

Table 4-1: HPMC grades and concentrations used in gel samples

4.2.7.2 Methyl cellulose (MC)

Gel samples of methylcellulose polymer (Table 4-2) were prepared by the modified method that was used for preparation of HPMC samples.

No.	Grade	Concentration % w/v
32	A4M	15
33		10
34		5
35	A15C	15
36		10
37		5
38	A4C	15
39		10
40		5

Table 4-2: MC grades and concentrations used in gel samples

4.2.7.3 Hydroxyethyl cellulose (HEC):

Initial attempts to prepare hydrogels containing 2, 4 and 6% (w/v) of HEC by using hot water with gradual addition of powder with stirring resulted in the formation of lumps that needed a long time to dissolve, in addition to the bubble formation. As an alternative, a suspension of HEC in absolute ethanol was prepared which was added to hot water with stirring. Stringy lumps were formed during addition and the preparation needed stirring for a long time to dissolve. At the end of the procedure, the formulation produced contained bubbles. Finally, a protocol was developed which involved wetting of HEC powder using small amount of absolute ethanol. Hot water was then added with stirring to produce a homogenous system. The products remained clear and free from bubbles (Samples 42-44).

4.2.7.4 Sodium carboxymethyl cellulose (CMC) of BDH-GPR

Sodium carboxymethyl cellulose of BDH-GPR was used to prepare samples 45-47, at 6, 8 and 10% (w/v). The polymer is presented as granules and the viscosity of 1% is 30-70cp at 20º C. The polymer was wetted by small amount of absolute ethanol followed by the addition of hot water with continuous stirring. However, the product contained bubbles. When cold degassed water was used instead of hot water, the obtained gels were clear and free from bubbles.

4.2.7.5 Sodium carboxymethyl cellulose (Walocel®):

Seven grades of sodium CMC were used to prepare samples listed in Table 4-3. These were supplied in powder form. A first attempt to prepare 10% (w/v) of CRT 40,000 PA by wetting the polymer with absolute ethanol followed by the addition of degassed water with stirring was unsatisfactory. Addition of sodium CMC-ethanolic suspension to degassed water with stirring again resulted in aslurry that contained non-dissolved material. The sample was left for 48h but the product still contained lumps and bubbles with a very thick texture. Therefore, preparation of a sample from this grade at 10% (w/v) concentration was not attempted.

A preparation at 5% (w/v) was attempted using the wetting method, however, a clear hydrogel was not produced. Finally, an ethanolic suspension of sodium CMC was added quickly (within two seconds) into hot degassed water (90º C) with stirring continued for two minutes. The product was clear and free from bubbles. Samples were placed in fume hood for 2h and then the containers were closed and refrigerated.

No.	Grade	Concentration % w/v	No.	Grade	Concentration % w/v
48	CRT 40,000 PA	5	59	CRT 2,000 PA	8
49		2.5	60		6
50	CRT 20,000 PA	5	61		4
51		4	62	CRT 1,000 PA	10
52		2.5	63		8
53	CRT 10,000 PA	6	64		6
54		4	65	CRT 100 PA	12
55		2			
56	CRT 30,000 PA	6			
57		4			
58		2			

Table 4-3: Sodium CMC (Walocel®) grades and concentration used in gel samples

4.2.7.6 The effect of linear and/or branched water-soluble polymers mixed with a selected hydrogel product on the adhesion parameters

The polymer hydrogel with highest adhesion parameters was mixed with a series of linear and/or branched water-soluble polymers. These mixtures were prepared by mixing of these polymers into the selected hydrogel using slab and spatula (Table 4-4). Samples were left 24h to complete the hydration of the polymer and to allow the interaction between them.

No.	Polymer	Concentration % (w/v)	No.	Polymer	Concentration % (w/v)
66	Gum Arabic	10	75	Tragacanth	7.5
67		15	76		15
68		20	77		30
69	Xanthan gum	7.5	78	Gum Arabic: Xanthan gum	15:15
70		15	79		15:7.5
71		30	80		7.5:15
72	Sodium alginate	7.5	81	Xanthan gum: Sodium alginate	7.5:15
73		15	82		15:7.5
74		30	83		7.5:7.5

Table 4-4: Concentrations of polymers mixed into the selected hydrogel

4.2.7.7 Mixtures of polymers with high adhesive properties

In order to determine the best mixture of polymers for investigation, the prepared hydrogels were arranged from lower to higher adhesion properties. The polymers that showed hydrogels with higher adhesion parameters in sections 4.2.8.1 - 4.2.8.5 were used to prepare hydrogels of mixed polymers with concentration ratios as shown in Table 4-5. The prepared hydrogels of mixed polymers were characterised to study the effect of mixing polymers on the adhesion properties of the prepared hydrogels.

	Polymers	Concentration % w/v
87	E10M: E4M	7.5:7.5
88		10:5
89		5:10
90	A4C: E10M	7.5:7.5
91		10:5
92		5:10
93	F4M: E10M	7.5:7.5
94		10:5
95		5:10

Table 4-5: Formulations of hydrogels using mixture of polymers

4.2.7.8 Analysis of mixing short and long chain polymer on the adhesion of hydrogels

The effect of polymer mobility on the adhesion properties was investigated by mixing of low molecular weight polymer into formulas 18 and 38 (Table 4-6) to enhance the mobility of polymer chains.

No.	Polymer	Concentration % w/v
96	E10M: E15LV	7.5:7.5
97		5:10
98		10:5
99	A4C: A15LV	7.5:7.5
100		5:10
101		10:5

Table 4-6: Formulations of low and high molecular weight mixed polymers

4.2.8 Analysis of the adhesion properties

The adhesion test was used to measure the adhesion parameters (stickiness, stringiness and adhesion work) of the prepared hydrogels on the tooth surface at room temperature using a TA-XT2™ texture analyser running Texture Exponent 32 ver. 4.0.13 software. Table 4-7 shows the setting used in the adhesion test. The cylindrical probes of 3mm and 6mm diameter were evaluated to find the most effective formulation.

Caption	Value	Units
Pre-Test Speed	0.50	mm/s
Test Speed	0.50	mm/s
Post-Test Speed	0.50	mm/s
Applied Force	250.0	g
Return Distance	5	mm
Contact Time	10	s
Trigger Type	Auto	-
Trigger Force	5.0	g

Table 4-7: The adhesion test setting used in the analysis of the adhesion properties of the prepared hydrogels.

4.2.8.1 Analysis of the adhesion properties of commercial tooth pastes

The adhesion properties of the toothpastes were measured using the tooth samples T5, T8 and T9 and the data obtained were compared with a selected formula parameters.

4.2.9 Formulations of dental film dosage form containing isolated ACP

The dental films containing 1 and 2% (w/v) ACP were prepared using the casting method. The two formulations were prepared using 3% (w/v) of HPMC grade E10M and a mixture of HPMC grades F4M (1% w/v) and E10M (2% w/v). The ACP was dispersed in three quarters of the final volume of distilled water, HPMC was then added gradually with stirring at constant temperature at 40° C using a stirrer hotplate. The hot plate was removed and the container was wrapped with a cold wetted tissue to dissolve the HPMC. A sample of the prepared hydrogel (12.5 mL) was drawn and poured into a plastic Petri dish (diameter, 10 cm) using 20 mL plastic syringe and refrigerated at 3º C for 2h. The films were formed after 24h at 37° C constant room temperature.

4.2.10 Characterisation of the prepared dental films

4.2.10.1 Physical observations

The prepared films were subjected to physical examination for appearance and thickness. The Sony H50™ camera was used to record the difference in the appearance of the prepared dental films and the film thickness at three different positions using a microscope. The examination of the prepared film was carried out using Polyvar-Reichert-Jung™ instrument equipped with Luminera-1™ digital camera and Infinity Analyse™ software ver. 5.0.3 used to capture the images. In addition, the thickness of the prepared films was measured in triplicate by cutting of 1mm width strip from the film and affixing onto a glass slide with acetate tape. The film strip was flipped upside down at a midpoint between terminals of that strip as

shown in Figure 4.3. The Image J™ ver. 1.44 software was used for determination of the film thickness at that flip point.

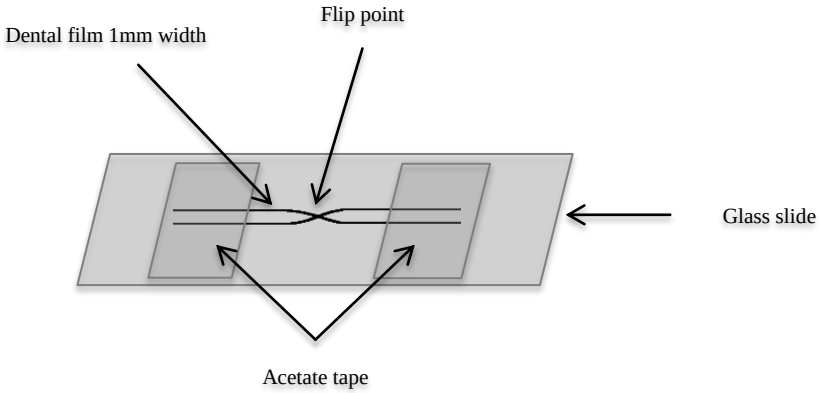

Figure 4.3: A plot demonstrates the dental film strip preparation for the measurement of dental film thickness.

4.2.10.2 Analysis of flexibility

The flexibility of the prepared dental films was analysed using the cycle until reset test on TA-XT2 texture analyser. The analysis was performed using 30% (laboratory) relative humidity. The dental filmstrip size of 16mm x 8mm was used in this test. Both sides of the strip were mounted on the probe and the bottom using a double-sided tape-leaving 8mm length of strip free for the analysis as shown in Figure 4.4. The attained relative humidity was confirmed using hygrometer. Table 4-8 shows the setting used for the cycle until reset test. The test was carried out for 15 minutes. This analysis was performed in triplicate for each dental film.

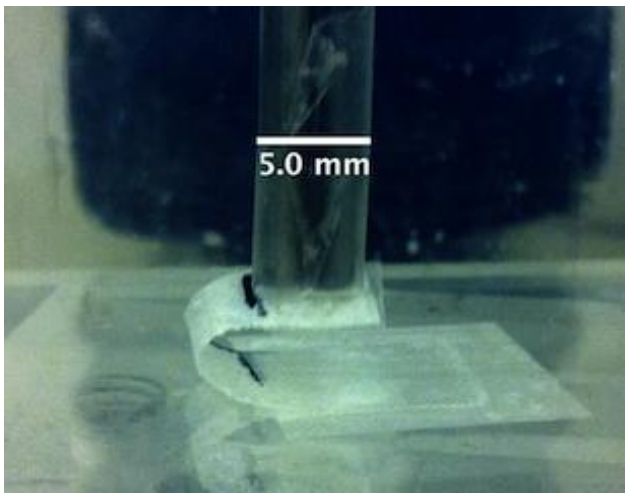

Figure 4.4: The setting of dental film for flexibility analysis. A strip, 16mm x 8mm, was mounted at both sides on the bottom and probe surface by double-sided tape and a 8mm x 8mm of the strip was left free for the analysis.

Caption	Value	Units
Pre-Test Speed	5	mm/s
Test Speed	5	mm/s
Post-Test Speed	10	mm/s
Target Mode	0	-
Distance	5	mm
Trigger Type	2= Pre Travel	-
Trigger distance	1	mm

Table 4-8: The setting of the cycle until reset test used in the analysis of dental film flexibility.

4.2.10.3 Analysis of degree of swelling

The dental film swelling analysis was performed using Xialine II™ artificial saliva. A sample of dental film of about 0.8 cm^2 was weighed and placed into pre-weighed stainless steel basket [basket of tablet dissolution apparatus (Pharmacopoeia, 2012)]. The basket containing the dental film sample was submerged into a Petri dish (diameter, 10cm) containing 35mL of artificial saliva as shown in Figure 4.5. The increase in weight of the dental film sample was measured at five minutes intervals until a constant weight was detected. This test was carried out in triplicate. The degree of swelling was calculated using the equation 4-1.

$$\boldsymbol{The\ degree\ of\ swelling} = (\boldsymbol{Wt} - \boldsymbol{Wo})/\boldsymbol{Wo} \qquad \text{Equation 4-1}$$

Where Wt and Wo are the weight of dental film sample at time t and time zero respectively.

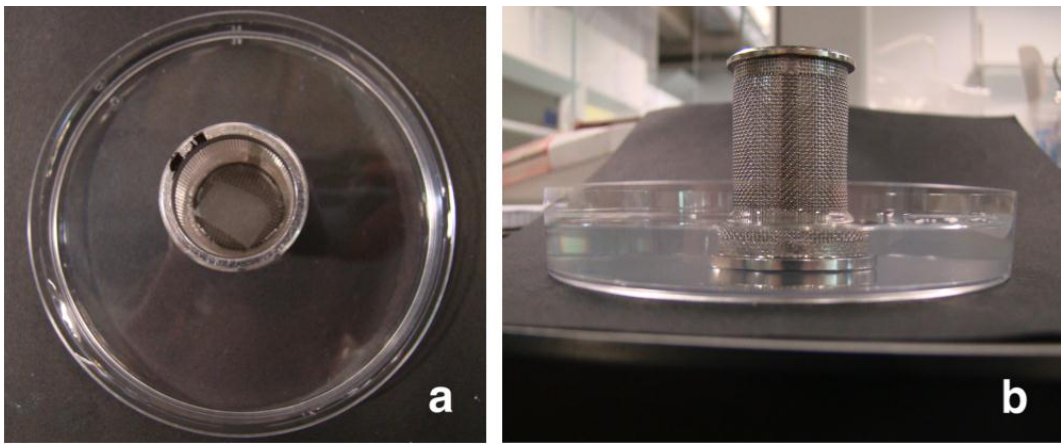

Figure 4.5: The measurement of degree of swelling of dental film by placing the dental film sample into pre-weighed stainless steel basket submerged into artificial saliva containing Petri dish: a- Top view and b- Side view.

4.2.10.4 Analysis of adhesion

The adhesion properties of the prepared dental films were characterised using a TA-XT2 texture analyser. Samples of the dental film, as 6mm diameter circles, were mounted on a microscope glass slide using double sided tape (Figure 4.6) and the 5mm cylindrical probe was used to perform the adhesion test. The mounted sample of the dental film was pre-wetted with one-drop of Xialine™ artificial saliva for 30 seconds. This test was performed six times for each dental film and the TA-XT2 texture analyser setting used as shown in Table 4-9.

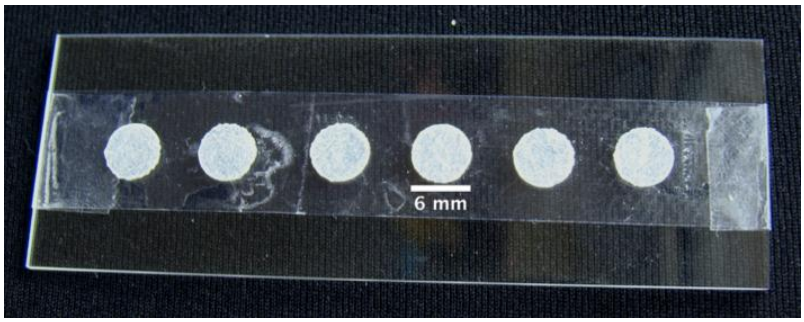

Figure 4.6: The dental film samples for adhesion test analysis. Sample of 6mm diameter circles mounted on the glass slide with double-sided tape.

Caption	Value	Units
Pre-Test Speed	0.50	mm/s
Test Speed	0.50	mm/s
Post-Test Speed	0.50	mm/s
Applied Force	250.0	g
Return Distance	5	mm
Contact Time	10	s
Trigger Type	Auto	-
Trigger Force	5.0	g

Table 4-9: The setting of the TA TX2 texture analyser used in the adhesion test of dental film samples.

4.2.10.5 Analysis of calcium content

The sample solution of dental film was prepared by dissolving a 5mg piece of dental film in pH-5 HCl solvent medium. The calcium concentrations in the prepared samples were determined using the calcium electrode method with the corresponding linear calibration curves equations. Three samples were taken for each film at different positions and an average was used as a reference to differentiate between formulations as well as a calculation of the calcium percentage released in the calcium dissolution-release study.

4.2.10.6 Calcium release study of the prepared dental films

The calcium release study was performed using specially designed dissolution cell as shown Figure 4.7 at 37° C constant room temperature. The best position of the dissolution cell was studied prior to conducting the calcium release study. The flow pattern of the dissolution medium was tested inside the dissolution cell using four different positions, as shown in Figure 4.8. Erythrosin extra bluish was used as a colouring agent and was infused into the dissolution chamber by a cannula inserted into the inlet tube of the dissolution cell. The diffusion of colouring agent was monitored at each position, the best diffusion position was selected for the calcium release study.

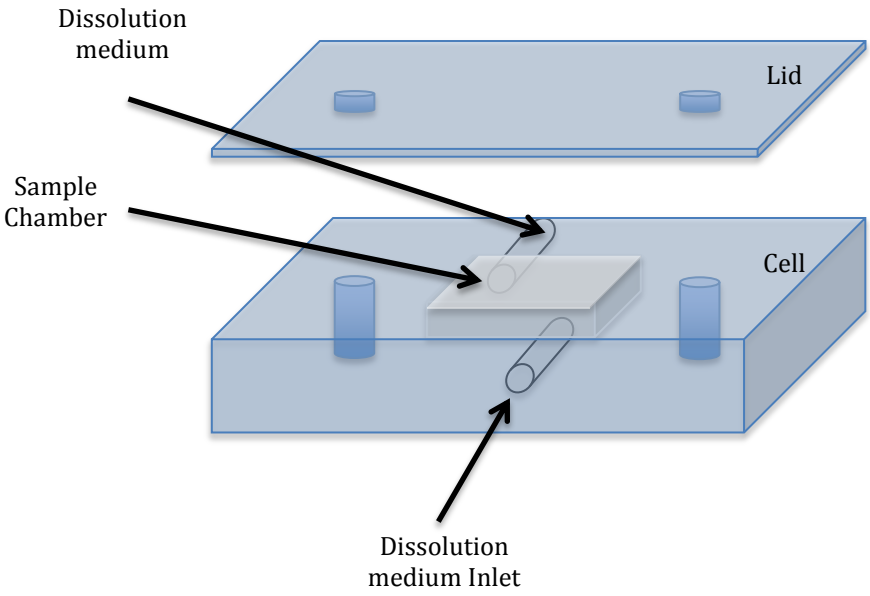

Figure 4.7: A plot demonstrates the design of dissolution cell for measurement of the calcium release from the dental film dosage form.

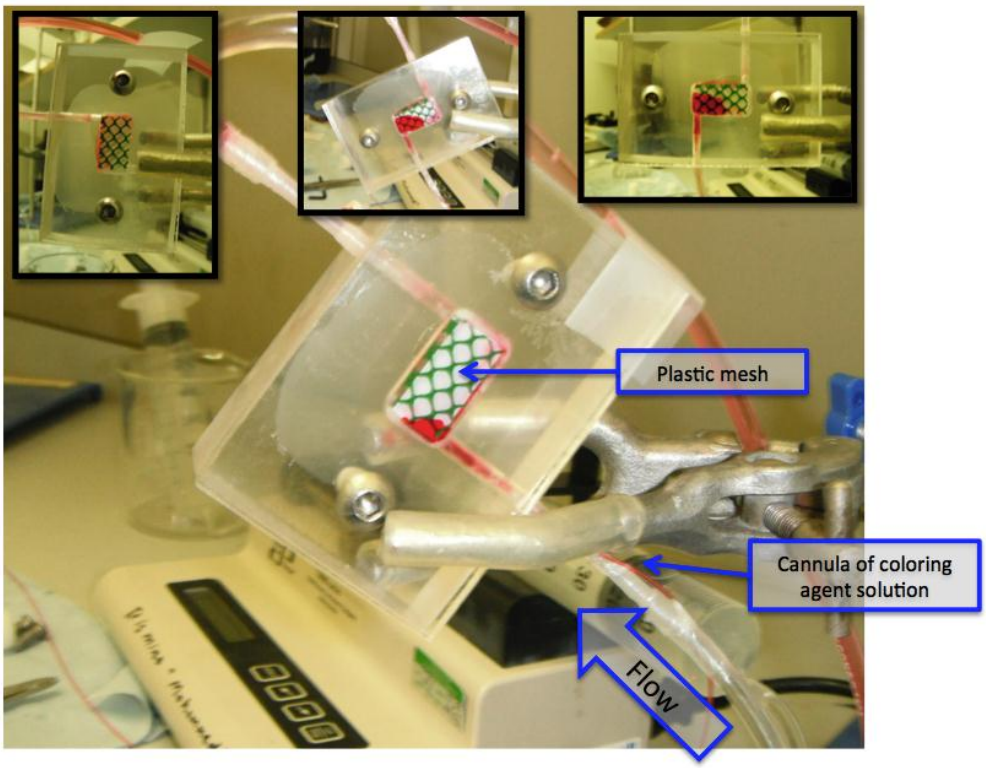

Figure 4.8: A photograph of the dissolution cell, shows the position used in the flow pattern study of dissolution medium.

The sample of pre-weighed film with an approximate size of 0.8cm x 1.8cm was held in the dissolution chamber by plastic mesh. The lid of the cell was sealed using silicone vacuum grease to prevent leakage of dissolution medium. Three samples from each film were tested using Xialine II™ artificial saliva as a dissolution medium. A 7.5 mL dissolution medium was pumped at a constant flow rate 0.125 mL. min^{-1} for 60 minutes into the dissolution chamber using a Cole-Parmer syringe pump. The dissolution samples were collected in 10 minute time interval. The time zero was recorded when the dissolution chamber had completely filled with the dissolution medium. The dissolution cell was washed and dried using distilled water prior to each use. The collected samples were stored in a refrigerator until calcium measurement. The calcium electrode measurements were performed after allowing the samples to warm up to laboratory temperature (≈ 17° C).

4.2.11 Analysis of calcium release kinetics

The calcium release data were subjected to mathematical models in order to study the kinetics or behaviour of the calcium release from the samples of the films. Zero order (equation 4-2) first order (equation 4-3) (Costa and Sousa Lobo, 2001) , Higuchi (equation 4-4) and Korsmeyer and Peppas (equation 4-5) models were applied in this study.

$$Q_t = k_0 t \qquad \textbf{Equation 4-2}$$

$$\ln(100 - Q_t) = lnQ_0 - kt \qquad \textbf{Equation 4-3}$$

$$Q_t = k_H t^{1/2} \qquad \textbf{Equation 4-4}$$

$$Q_t = k_{KP} t^n \qquad \textbf{Equation 4-5}$$

Where Q_t is the percentage of calcium release at time equal to t, k_0 is the zero order release rate constant, Q_0 is the percentage of calcium release at time equal to 0, k is the first order release rate constant, k_H is the Higuchi release rate constant, k_{KP} is the Korsmeyer-Peppas release rate constant and n is the diffusional exponent (Costa and

Sousa Lobo, 2001; Cilurzo *et al.*, 2008; Costa *et al.*, 2001; Desai *et al.*, 1965; Korsmeyer *et al.*, 1983; Peppas, 1985).

4.2.12 Data analysis

The linearity of the calibration curves was tested using regression correlation analysis. The validation of the calcium electrode method was tested using a paired t-test to differentiate between records obtained from both calcium electrode and ICP methods of calcium ion quantification in selected samples. An unpaired t-test was used to differentiate between the solubilities of the prepared ACP. The effect of the formulation on the degree of swelling was tested using one-way ANOVA with Tukey's post-hoc test (Minitab V.16).

4.3 Results

4.3.1 Calcium analysis and method validation

4.3.1.1 Calibration curves

Figure 4.9 and Figure 4.10 show calibration curves for calcium concentrations in HCl solution (pH 5) and Xialine II™ artificial saliva respectively. Table 4-10 illustrates the straight-line equations of calcium calibration curves in sodium bicarbonate – lactic acid buffer (pH : 5, 5.5, 6, 6.5 and 7). Linear relationships were obtained as a result of plotting millivolt (mV) versus log (ppm) concentration.

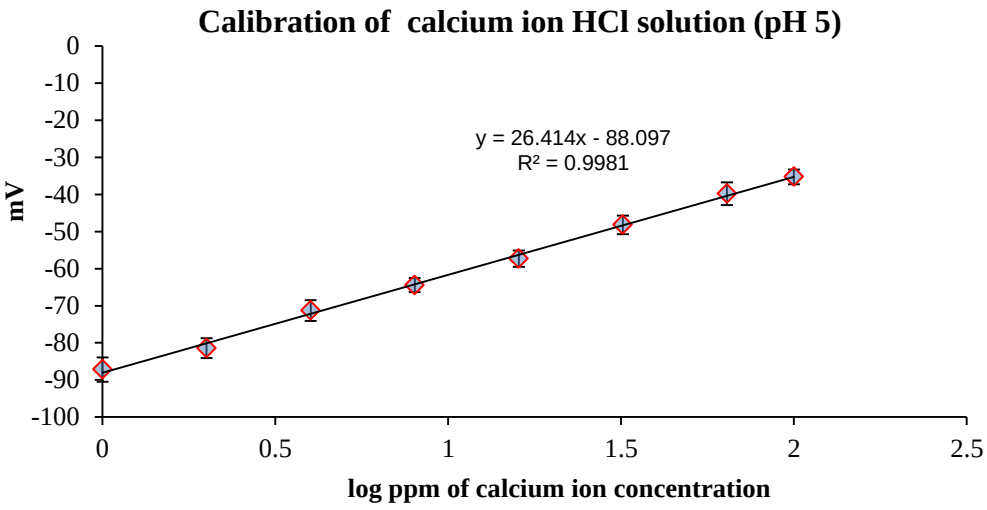

Figure 4.9: Calibration curve of calcium in HCl solution (pH 5).

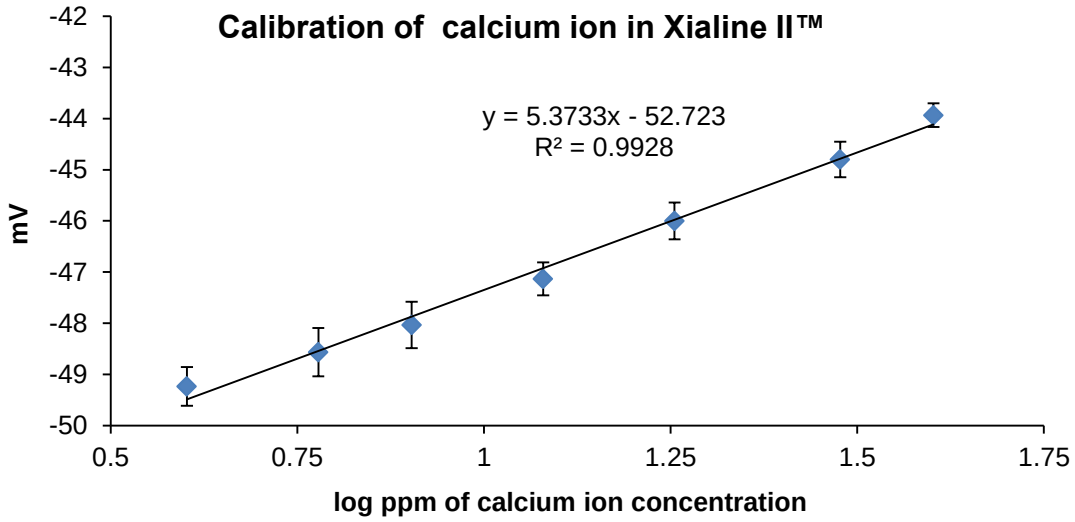

Figure 4.10: Calibration curve of calcium in Xialine II™ artificial saliva.

pH	Equation	r^2
5	y = 26.55x - 98.701	0.99472
5.5	y = 25.85x - 96.347	0.99375
6	y = 27.1x - 100.08	0.99129
6.5	y = 27.2x - 99.243	0.99762
7	y = 26.5x - 97.288	0.99953

Table 4-10: the straight-line equations of calcium calibration curves in sodium bicarbonate – lactic acid buffer (pH of 5, 5.5, 6, 6.5 and 7)

4.3.1.2 Calcium ion analysis validation

The calcium ion measurements of selected samples using calcium electrode method were compared with ICP method as shown in Figure 4.11. The profiles demonstrate a general equivalence for the measurement of calcium ion in the selected samples by calcium electrode and the ICP method, although there is some deviation.

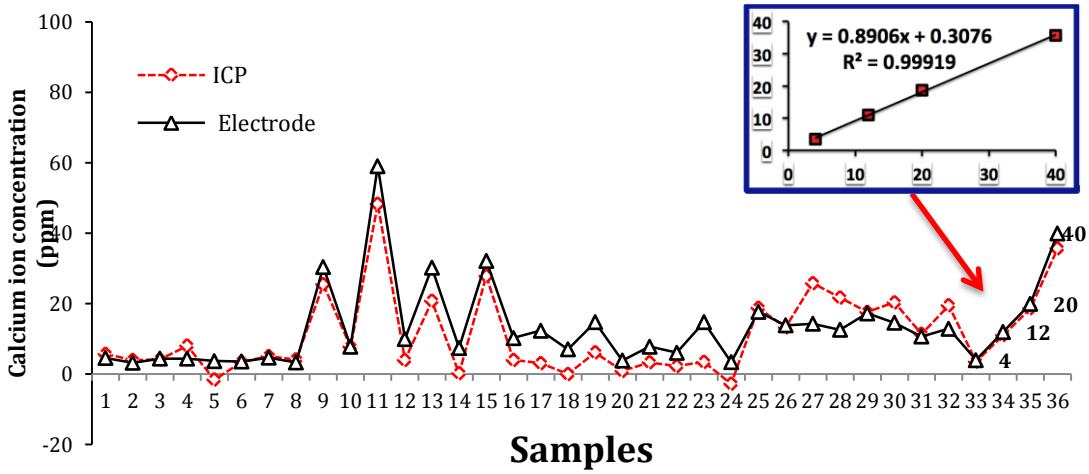

Figure 4.11: Profiles of calcium electrode and ICP measurements in co-analysed samples. Data labelled 4,12, 20 and 40 were given a calibration curve in ICP method. The slope of 0.89 indicates that ICP had a lower reading of 89% of the actual values.

4.3.2 Analysis of calcium content in prepared ACP

The calcium content in the prepared ACP is shown in Figure 4.12. The isolation process showed an effect on the calcium content of the prepared ACP. The data indicated the calcium contents in the isolated NGP-ACP and isolated HC-ACP were higher than that in the unpurified, whereas the isolated 4h ahCMC-ACP showed a lower calcium content than that in the unpurified sample.

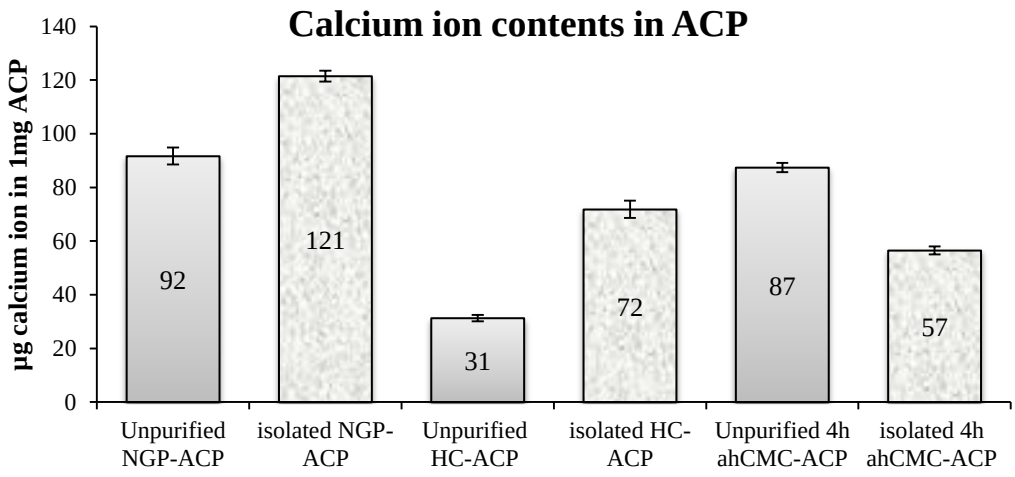

Figure 4.12: Mean calcium content in the prepared ACP (±SEM, n=3) showing the effect of the isolation process on calcium content.

4.3.3 Analysis of the effect of pH on the solubility of the isolated ACP

Figure 4.13 shows the effect of pH change on the solubility of the isolated ACP and amorphous calcium phosphate standard in sodium bicarbonate - lactic acid buffers. The higher concentrations of calcium ion were found in the saturated solutions of 4h ahCMC-ACP. Lower concentrations of calcium ions were detected in the saturated solutions containing ACP-standard

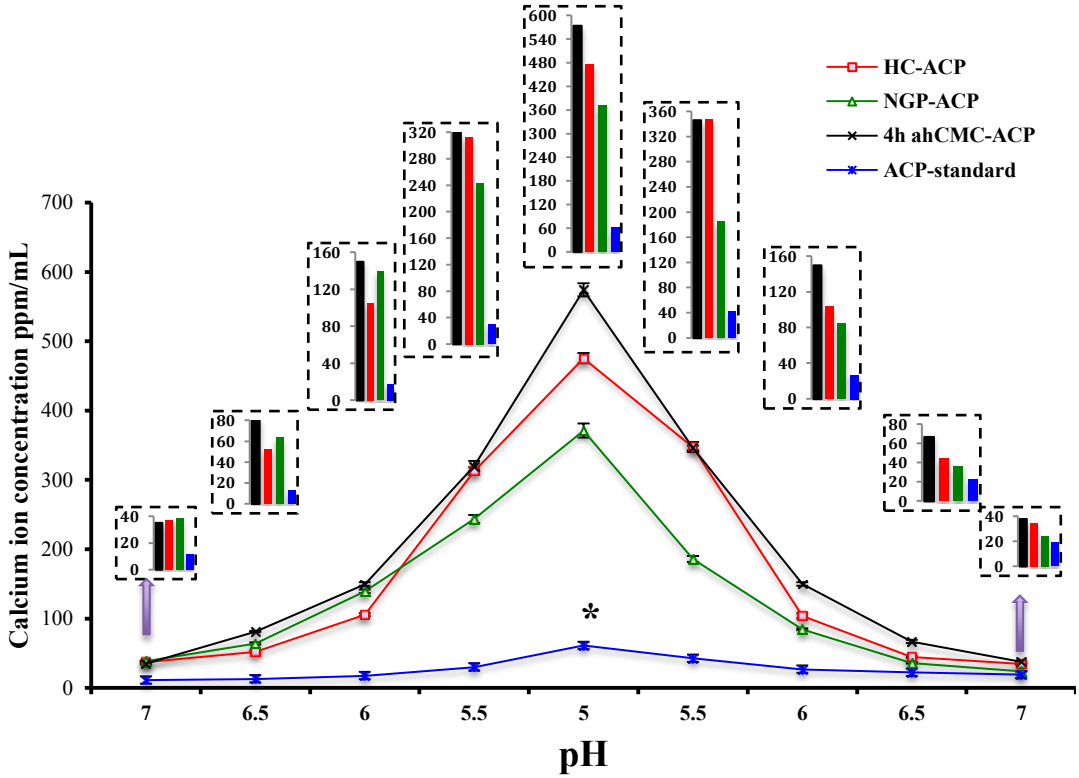

***** A significant difference ($p<0.05$).

Figure 4.13: Mean calcium ion concentrations (n=3,±SEM) in saturated solutions of the prepared isolated ACP and ACP-standard in lactic acid - sodium bicarbonate buffers.

4.3.4 Adhesion analysis of the prepared hydrogels

The adhesive test was completed using a cylindrical probe. The adhesive test is a protocol that measures the compression or extrusion force, stickiness, work of adhesion and stringiness as shown in Figure 4.14.

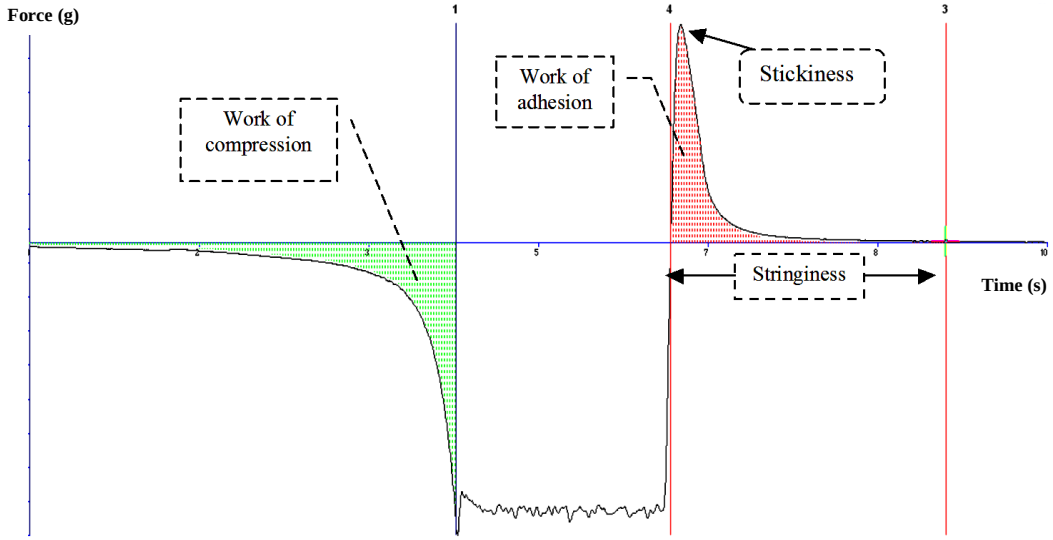

Figure 4.14: Profile of the adhesive test parameters of compression force, stickiness, work of adhesion and stringiness.

4.3.4.1 The probe and size of sample:

Two cylindrical probes were used with diameters of 3 and 6mm. Two Perspex discs (3mm thickness) were used for the sampling of the hydrogel. These discs contain holes of 3.4mm and 6.4mm diameter for measurement with the 3mm and 6mm cylindrical probes respectively (Figure 4.15). When the 3mm diameter probe was used, the profile obtained did not show differences between samples. The 6mm probe was therefore selected for use in further adhesion tests.

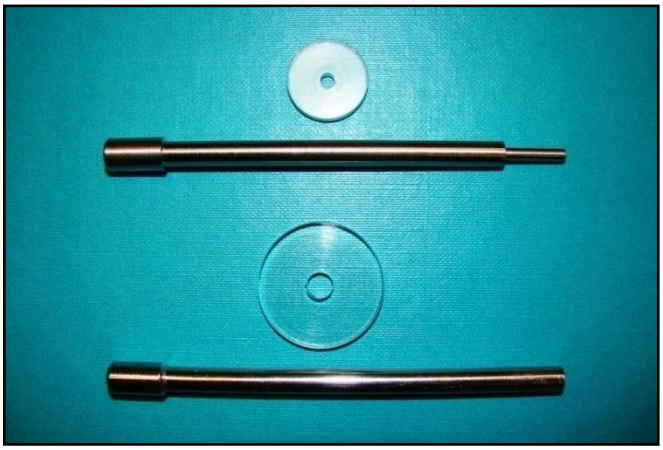

Figure 4.15: 3mm and 6mm diameter cylindrical probes and Perspex discs

4.3.4.2 Polymer effect

Forty-three runs for the adhesive test were completed to allow measurement for each formulation using the three tooth samples at room temperature. Samples that had a watery texture were excluded from the adhesive test analysis. The effect of polymer types on the adhesion properties of the prepared hydrogels using HPMC, MC, EC and sodium CMC showed adhesion parameters of stickiness, stringiness and work of adhesion as shown in Figure 4.16.

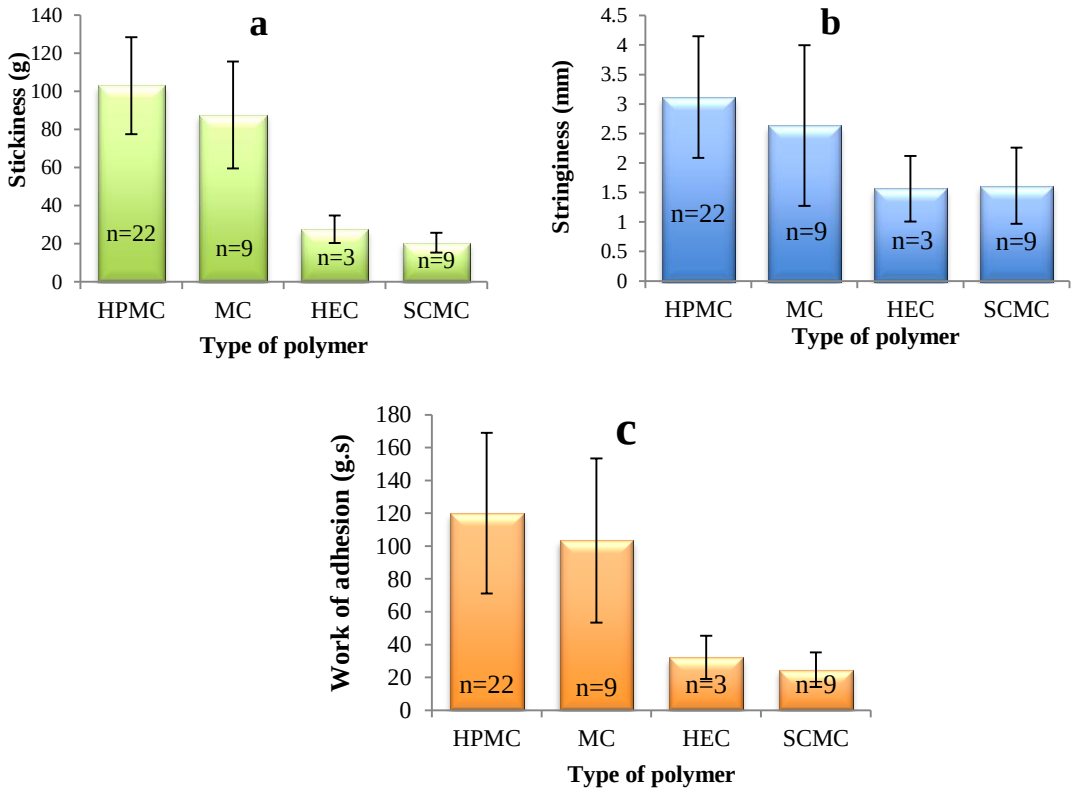

Figure 4.16: Mean (±SE) adhesion parameters of stickiness (a), stringiness (b) and work of adhesion (c), show the effect of polymer type on the measured adhesion parameteres of the prepared hydrogels.

The results of the stickiness, stringiness and work of adhesion measurements for the prepared hydrogels are shown in Figure 4.17, Figure 4.17 and Figure 4.19. In order to correlate the data, stickiness was plotted separately against stringiness and work of adhesion as shown in Figure 4.20. It was suggested that simultaneous plotting of the three variables using a three dimensional plot might assist in discrimination. This is shown in Figure 4.21.

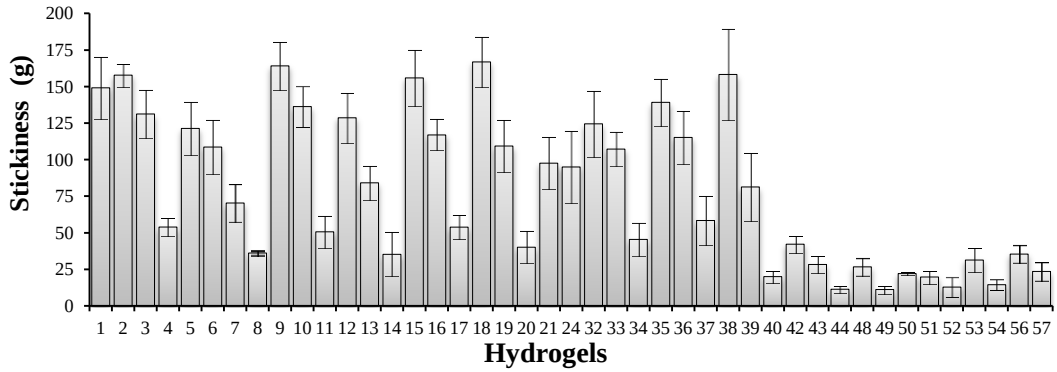

Figure 4.17: Mean stickiness of the prepared hydrogels, (±SEM, n=3)

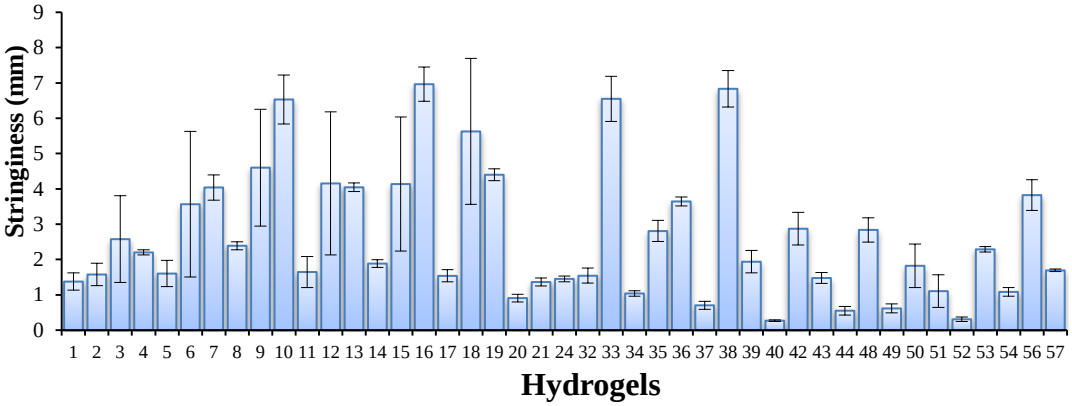

Figure 4.18: Mean stringiness of the prepared hydrogels, (±SEM, n=3).

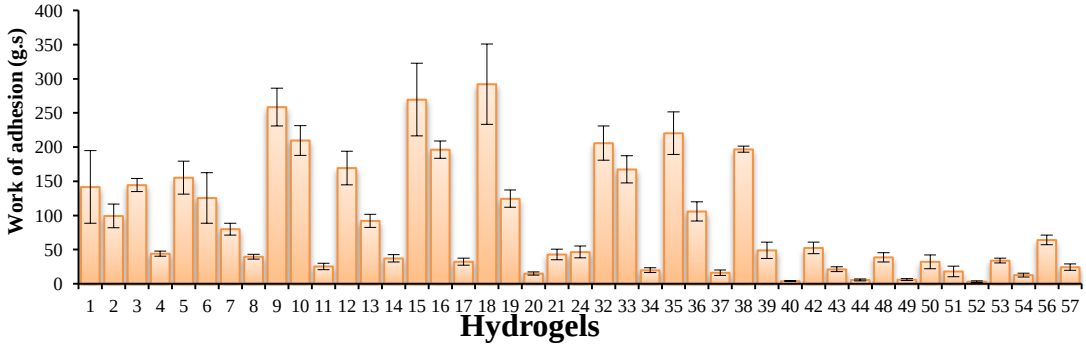

Figure 4.19: Mean work of adhesion of the prepared hydrogels, (±SEM, n=3).

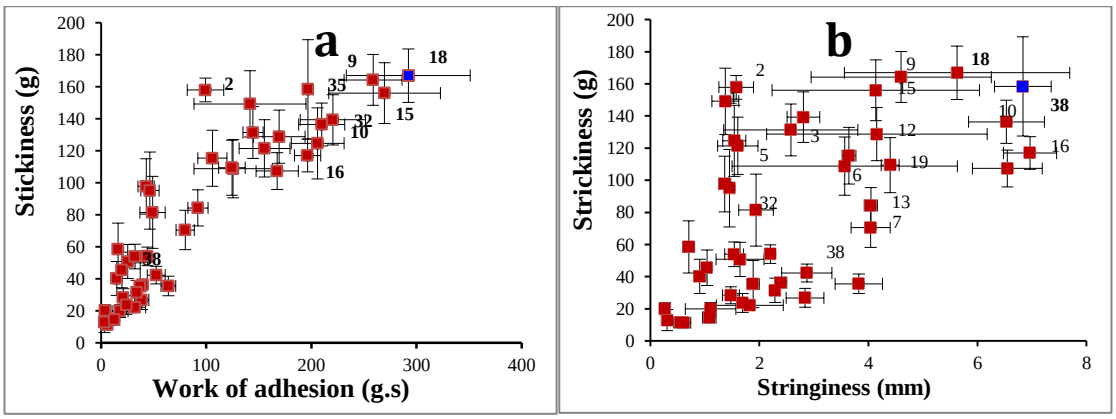

Figure 4.20: a- Mean stickiness versus stringiness. b-Mean stickiness versus work of adhesion, (±SEM, n=3).

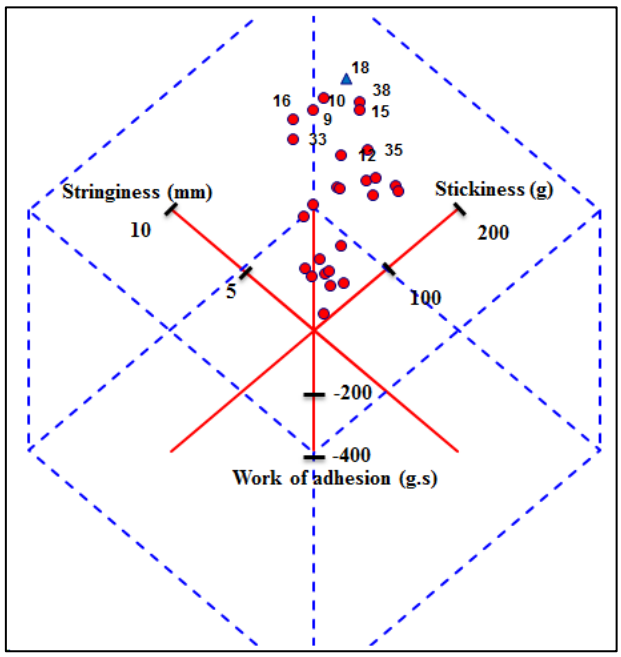

Figure 4.21: A three dimensional scatter plot of means of stickiness, stringiness and work of adhesion. Note that sample 18 occupies the furthest space from the origin of the three axis.

4.3.4.3 The effect of linear and/or branched water-soluble polymers mixed with a selected hydrogel product on the adhesion parameters

The addition of linear and/or branched water-soluble polymers to sample 18 was attempted in order to increase the adhesion parameters. The texture analysis (Figure 4.22 and Figure 4.23) of the prepared hydrogels illustrates that the effect of the additional excipients on the adhesion properties of the prepared hydrogels.

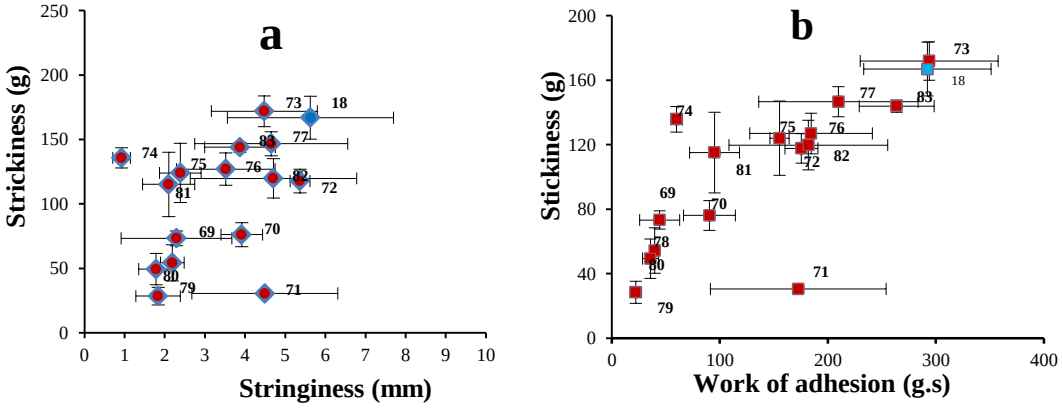

Figure 4.22: Effect of addition of linear and/or branched polymer on adhesion parameters of sample 18. a-Mean stickiness versus stringiness, b-Mean stickiness versus work of adhesion, (±SEM, n=3).

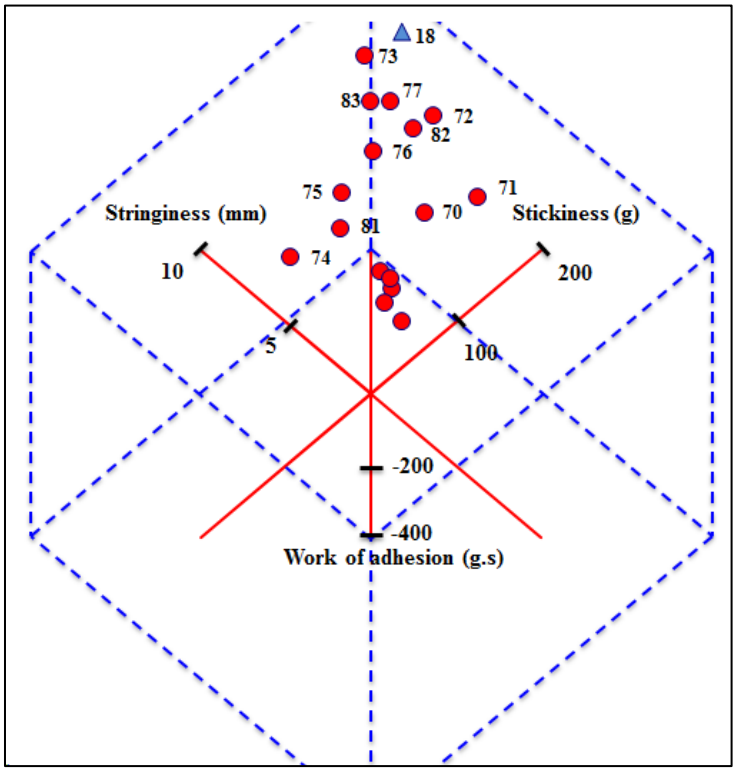

Figure 4.23: A three dimensional scatter plot of mean of stickiness, stringiness and work of adhesion. Note that sample 18 occupies the furthest space from the origin of the three axis.

4.3.4.4 Mixtures of polymers with high adhesive properties

Polymer grades of E10M, E4M, F4M and A4C showed hydrogels with higher adhesion parameters as shown in Figure 4.24. Therefore, these selected grades were used to prepare hydrogels of mixed polymers. Formulas of mixed polymers showed that the maximum increase in the measured adhesion parameters was obtained in formula 95, shown in Figure 4.25.

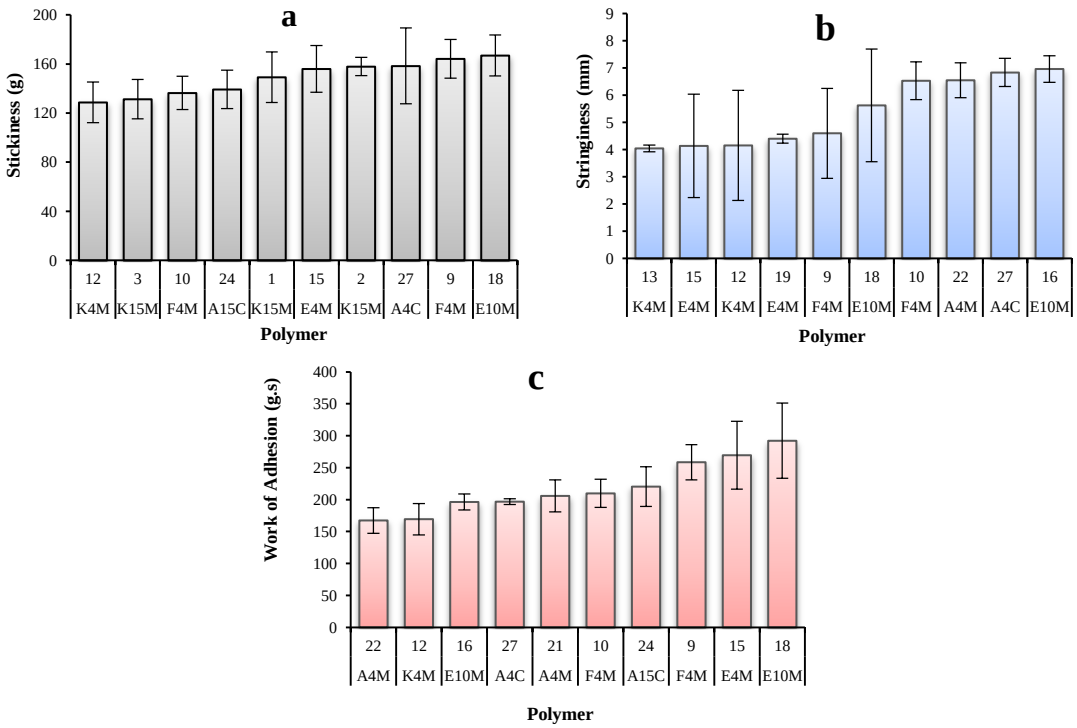

Figure 4.24: Polymers arranged from higher to lower adhesion parameters

(a) Stickiness, (b) Stringiness and (c) Work of adhesion

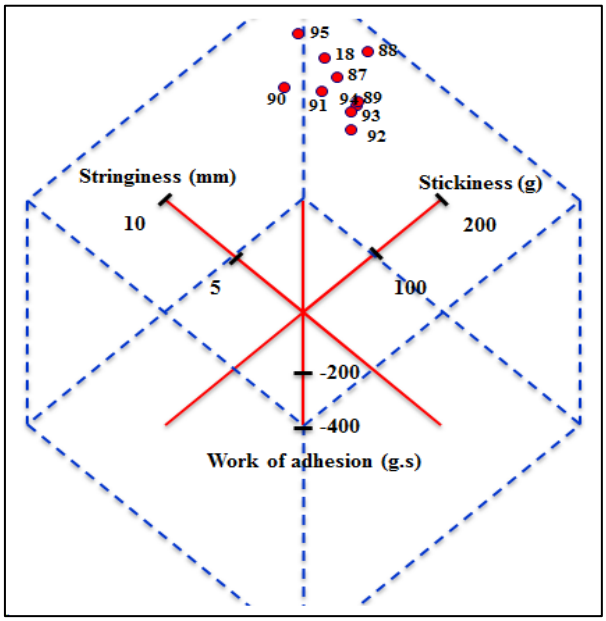

Figure 4.25: A three dimensional scatter plot of means of stickiness, stringiness and work of adhesion, showing the effect of the mixed polymers on adhesion properties of the prepared hydrogels. Note that sample 95 occupies the furthest space from the origin of the three axis.

4.3.4.5 Analysis of the effect of mixing short and long chain polymer on the adhesion of the prepared hydrogels

The incorporation of short with long chain polymers into the formulation was attempted in order to enhance the mobility as well as the adhesiveness of polymer in the prepared hydrogel. The effect of mixing short and long chains of the selected polymer on the adhesion properties of the prepared formulas is shown in Figure 4.26. The prepared formulas showed less adhesion than that in control formula (18).

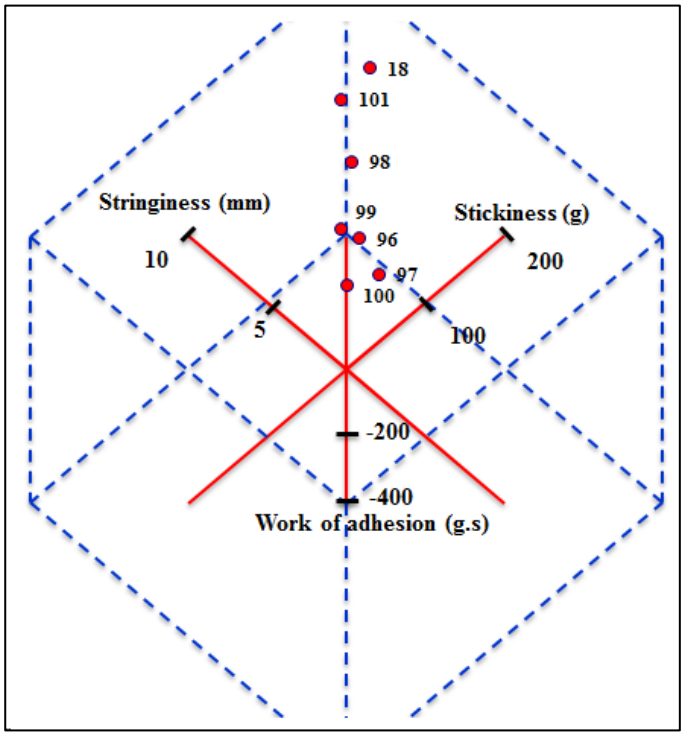

Figure 4.26: A three dimensional scatter plot of means of stickiness, stringiness and work of adhesion, showing the effect of mixing short and long chain polymers on the adhesion of hydrogels.

4.3.4.6 Analysis of the adhesion properties of official tooth pastes

Figure **4.27** shows the difference in the adhesion properties between formula 18 and selected brands of toothpastes. This analysis was performed in order to identify the attained degree of adhesiveness in the formula 18 in comparison to a control of different brands of toothpastes.

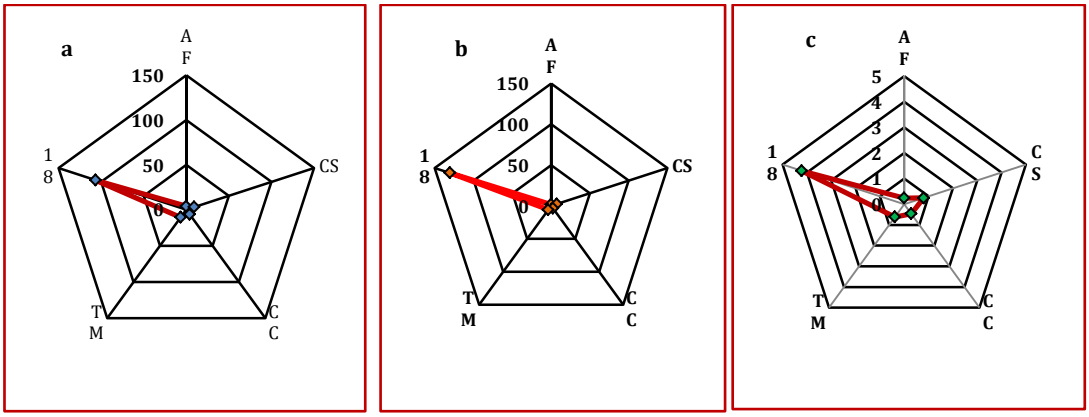

Figure 4.27: Adhesion parameters of formula 18 versus branded toothpastes, (a) Stickiness, (b) work of adhesion and (c) stringiness.

4.3.5 Characterisation of the prepared dental films

4.3.5.1 Physical observations

The isolated ACP and ACP-standard were used in the dental film fabrication and 16 dental films were produced. The 1% (w/v) 4h ahCMC-ACP and 3% E10M-HPMC film was dry, slightly rough, white (translucent), flexible and non-elastic. 2% (w/v) 4h ahCMC-ACP and 3% E10M-HPMC film was dry, rough, white (opaque), flexible and non-elastic, as shown in Figure 4.28. Similar observations were recorded for 4h ahCMC-ACP containing films that were prepared by a mixture of 2% (w/v) E10M-HPMC and 1% (w/v) F4M-HPMC.

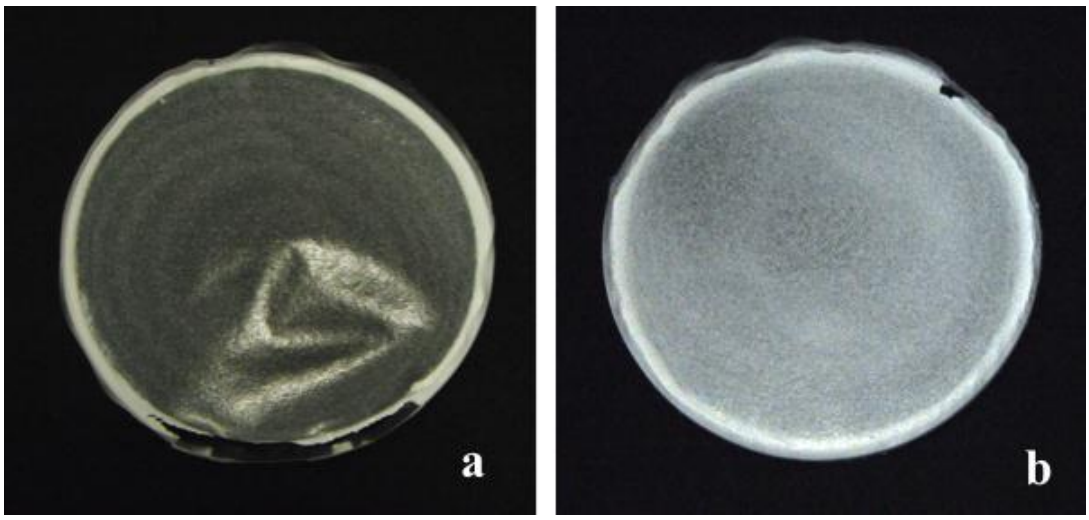

Figure 4.28: The photographs show the difference in the visual observations between (a)- 1% (w/v) 4h ahCMC-ACP and (b)- 2% (w/v) 4h ahCMC-ACP loaded dental films prepared from 3% E10M-HPMC.

The dental film prepared by 1% (w/v) NGP-ACP and 3% E10M-HPMC was dry, rough, white, flexible and non-elastic. 2% (w/v) NGP-ACP and 3% E10M-HPMC film was dry, rough, white (cloudy), flexible and non-elastic, as shown in Figure 4.29. A similar appearance was observed in the films prepared from mixture of 2% (w/v) E10M-HPMC and 1% (w/v) F4M-HPMC.

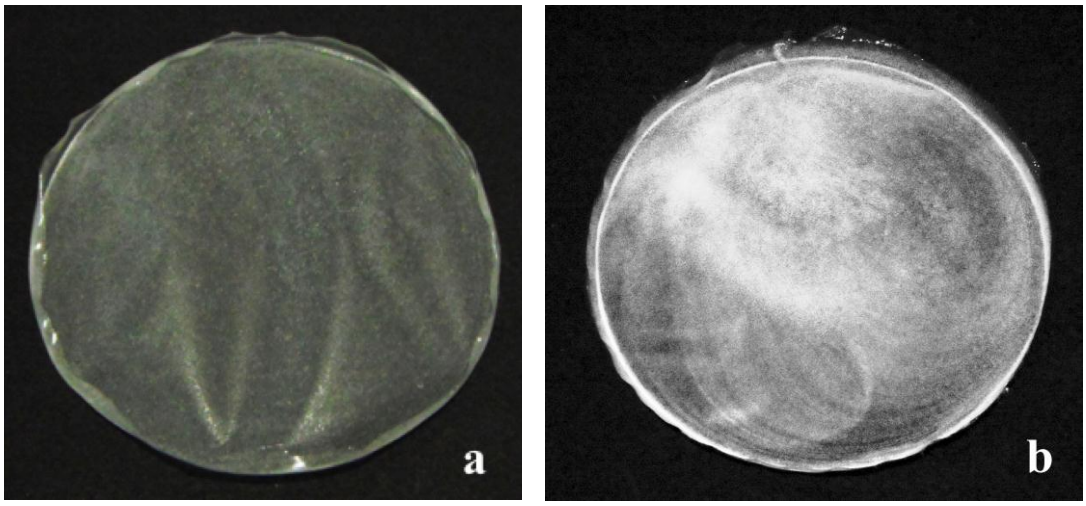

Figure 4.29: The photographs show the difference in the visual observations between (a)- 1% (w/v) NGP-ACP and (b)- 2% (w/v) NGP-ACP loaded dental films prepared from 3% E10M-HPMC.

The dental film prepared by 1% (w/v) HC-ACP and 3% E10M-HPMC was dry, glossy, transparent, flexible and non-elastic. 2% (w/v) HC-ACP and 3% E10M-HPMC was dry, slight glossy, dumped transparent, flexible and non-elastic, as shown in Figure 4.30. A similar observation was recorded for the films prepared by a mixture of 2% (w/v) E10M-HPMC and 1% (w/v) F4M-HPMC.

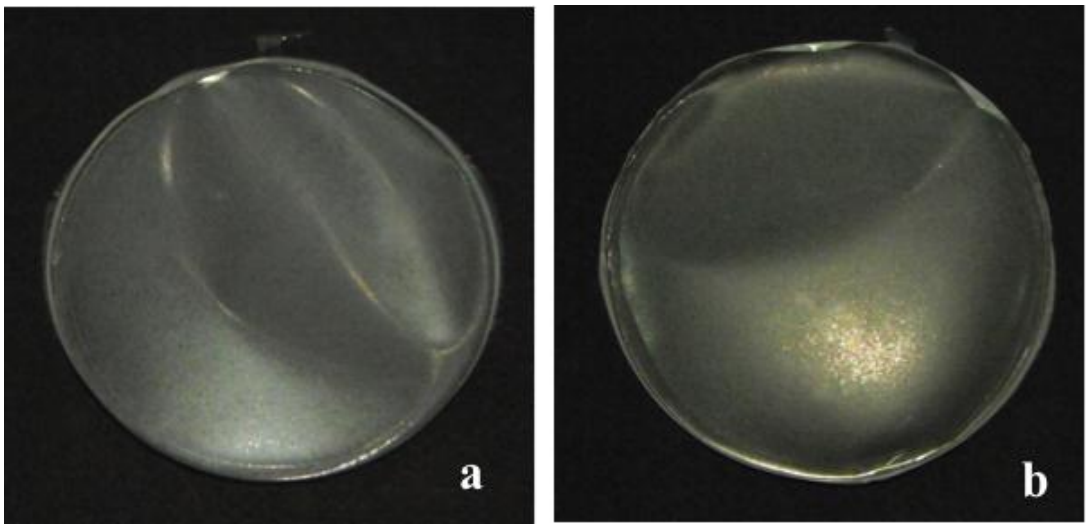

Figure 4.30: The photographs show the difference in the visual observations between (a)- 1% (w/v) HC-ACP and (b)- 2% (w/v) HC-ACP loaded dental films prepared from 3% E10M-HPMC.

The dental film prepared by 1% (w/v) ACP-standard and 3% E10M-HPMC was dry, rough, dotted, white, flexible and non-elastic. 2% (w/v) ACP-standard and 3% E10M-HPMC film had a dry, rough, heavily dotted, white, flexible and non-elastic, as shown in Figure 4.31. Similar observations were obtained in the films prepared by a mixture of 2% (w/v) E10M-HPMC and 1% (w/v) F4M-HPMC.

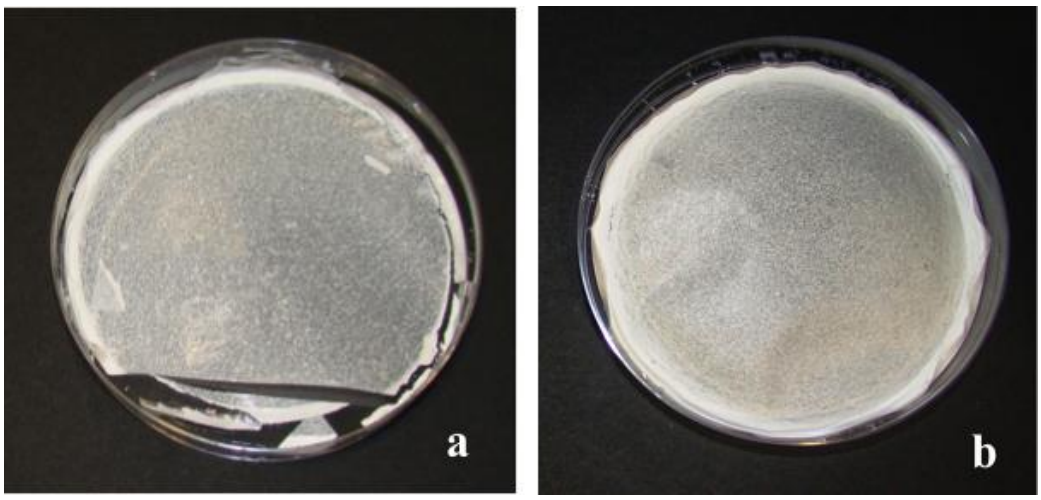

Figure 4.31: The photographs show the difference in the visual observations between (a)- 1% (w/v) ACP-standard and (b)- 2% (w/v) ACP-standard loaded dental films prepared from 3% E10M-HPMC.

The prepared dental films were subjected to thickness analysis using the previously described method. Figure 4.32 shows an example for the measurement of dental film thickness. The data obtained showed the effect of the type of loaded ACP as well as the used polymer on the film thickness, as shown in Figure 4.33.

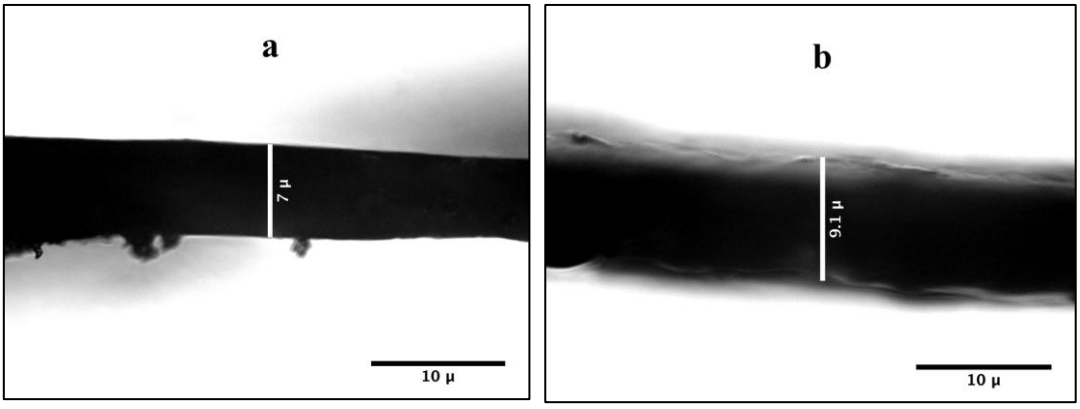

Figure 4.32: Images (25X) of 1% (a) and 2% (b) 4h ahCMC-ACP containing dental films;, images show the effect of ACP loading on the film thicknesses.

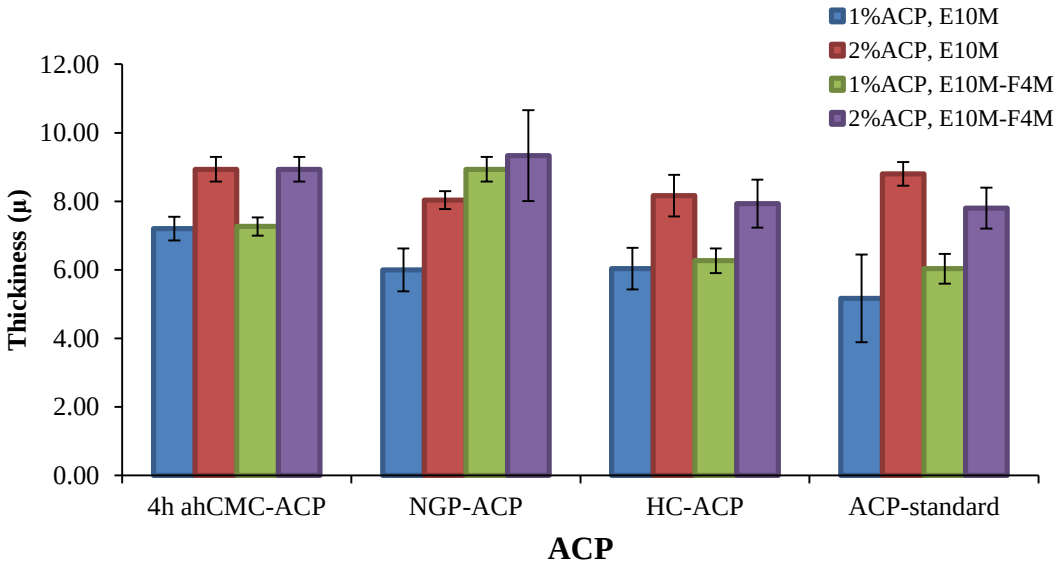

Figure 4.33: Mean thickness for the prepared dental films (±SEM, n=3).

4.3.5.2 Analysis of flexibility

The measurement of flexibility of the prepared dental films was shown by the resistance of the film to the applied force on bending and relaxation of the film, that was generated by the descendant and ascendant movement of the probe. The average of the resistance forces was used as a parameter of the film flexibility and is shown in Figure 4.34. In addition, it shows positive and negative kick-off peaks at the change of direction of the probe movement.

.

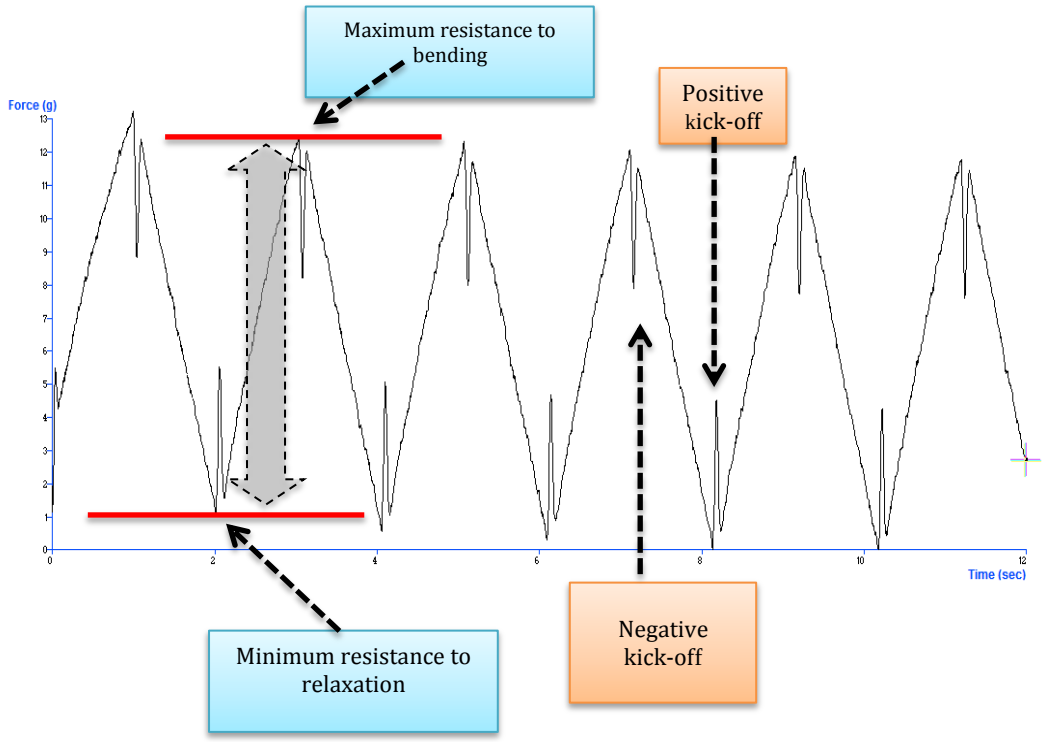

Figure 4.34: The texture analysis chromatogram of the flexibility test of the prepared dental films shows the difference between the resistance forces to bending and relaxation of the film strip upon the probe movement.

The flexibility analysis of the prepared dental films showed the effect of the percentage concentration and the type of ACP as well as the type of polymer used in formulations, as shown in Figure 4.35, Figure 4.36, Figure 4.37, and Figure 4.38.

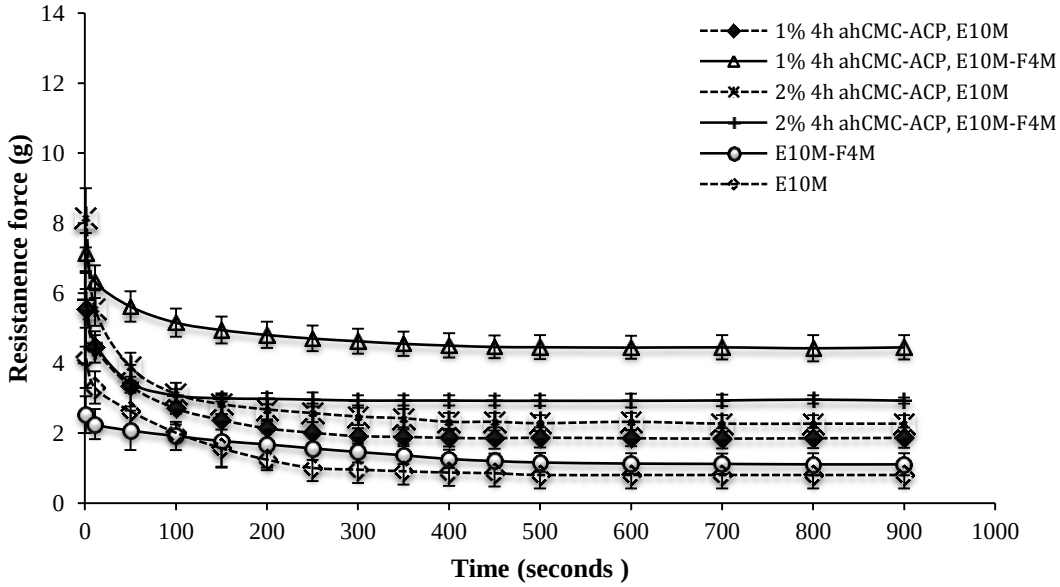

Figure 4.35: The flexibility profiles of the dental films containing 4h ahCMC-ACP show the effect of ACP loading and type of polymer on the average resistance forces of the film strip on bending and relaxation of the film, generated by the descending and ascending movement of the probe**.**

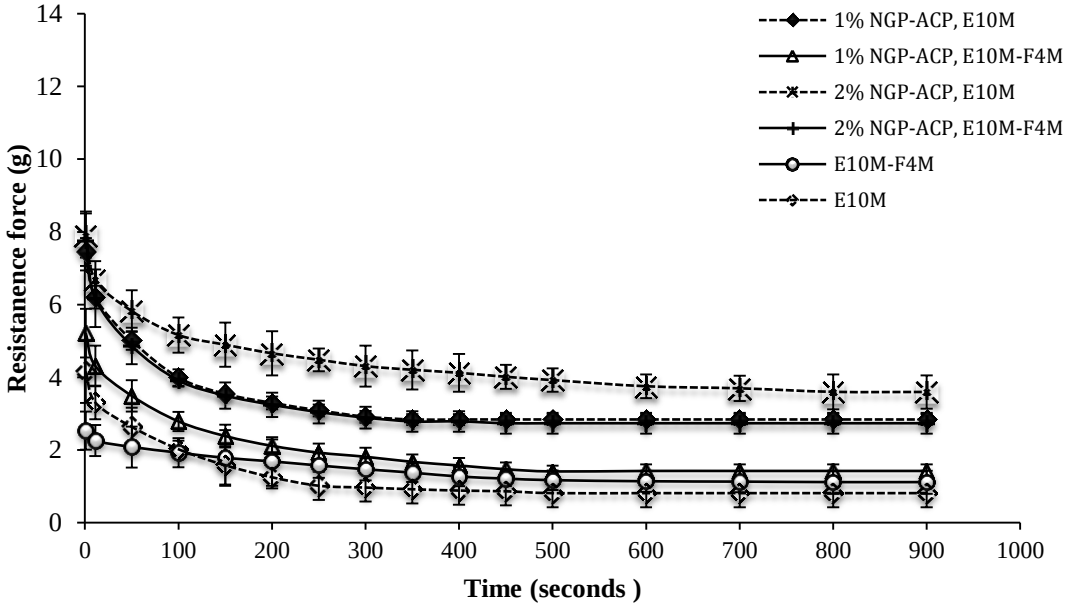

Figure 4.36: The flexibility profiles of the dental films containing NGP-ACP showing the effect of ACP loading and type of polymer on the average resistance forces of the film strip on bending and relaxation of the film, generated by the descending and ascending movement of the probe**.**

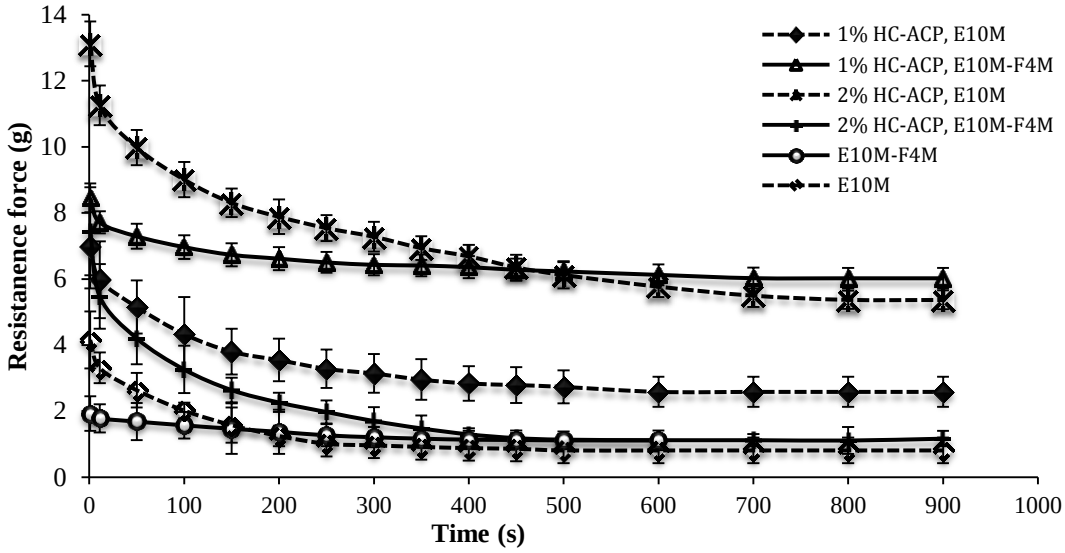

Figure 4.37: The flexibility profiles of the dental films containing HC-ACP show the effect of ACP loading and type of polymer on the average resistance forces of the film strip on bending and relaxation of the film, generated by the descending and ascending movement of the probe**.**

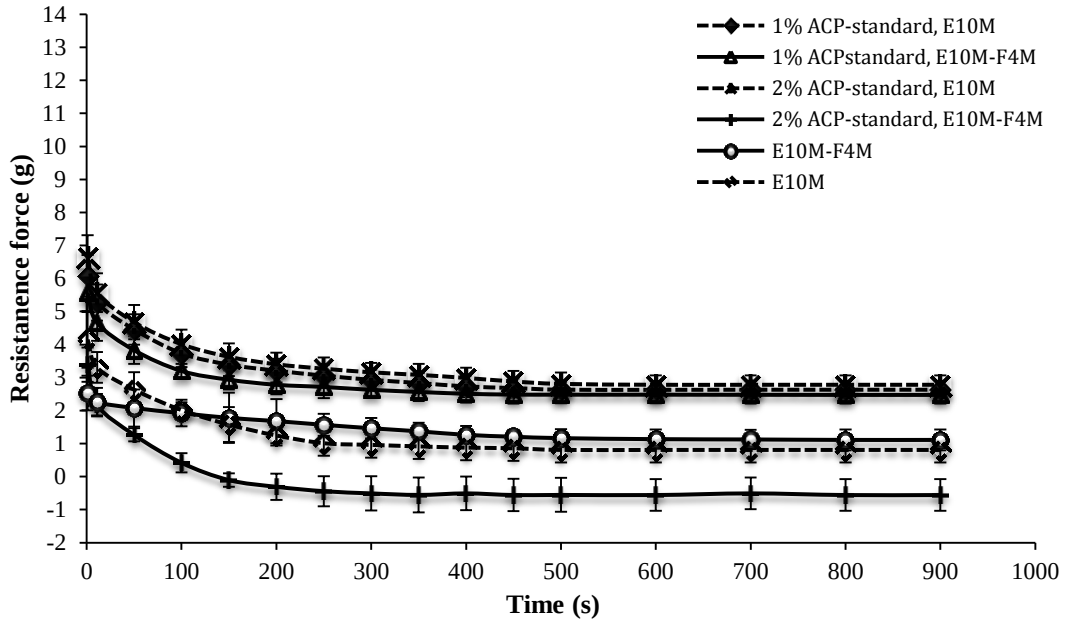

Figure 4.38: The flexibility profiles of the dental films containing ACP-standard showing the effect of ACP loading and type of polymer on the average resistance forces of the film strip on bending and relaxation of the film, generated by the descending and ascending movement of the probe**.**

4.3.5.3 Analysis of degree of swelling

Based on the water uptake and swelling of the used HPMC polymer (E10M and F4M) in the dental film formulations, the effect of the type and percentage of loaded ACP on the degree of swelling of the prepared dental films were measured. The degree of swelling of the prepared dental films showed an effect by the grade of the HPMC polymer, type and percentage of loaded ACP as shown in Figure 4.39. The behaviour of the swelling of the prepared dental films showed a fast swelling within first 5 minutes and a near constant estate after 10 minutes, as shown in Figure 4.40.

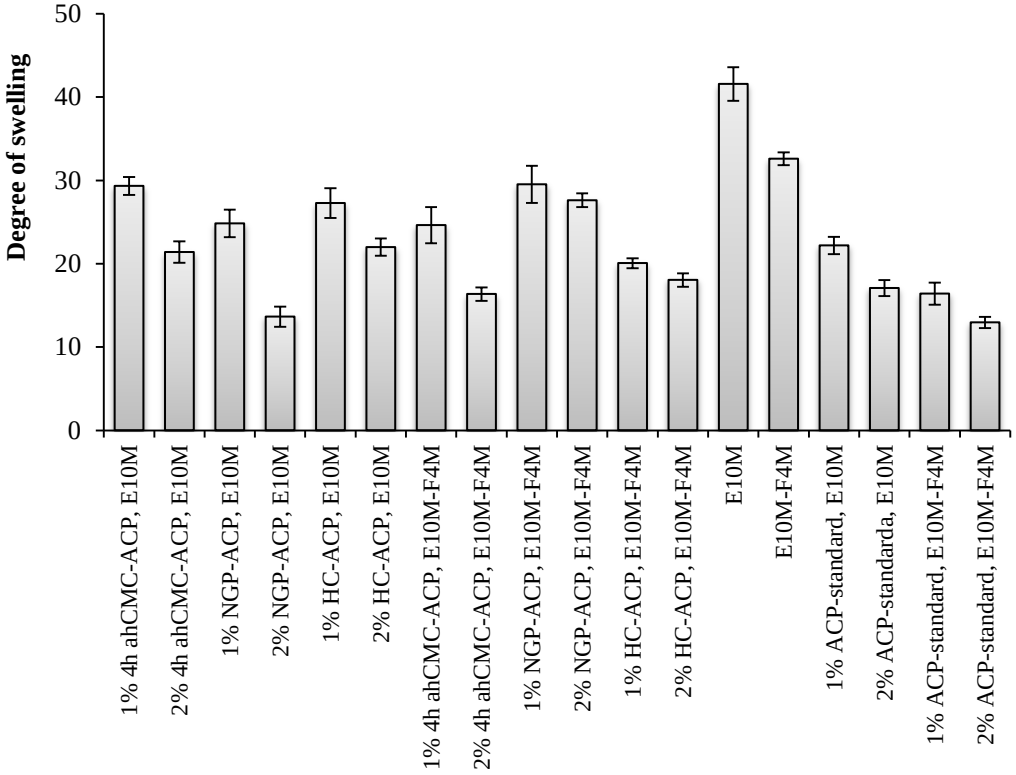

Figure 4.39: The degree of swelling of the prepared dental films in Xialine II™ artificial saliva showing the effect of the grade of polymer, type and percentage loaded of ACP on the water uptake of the prepared dental films.

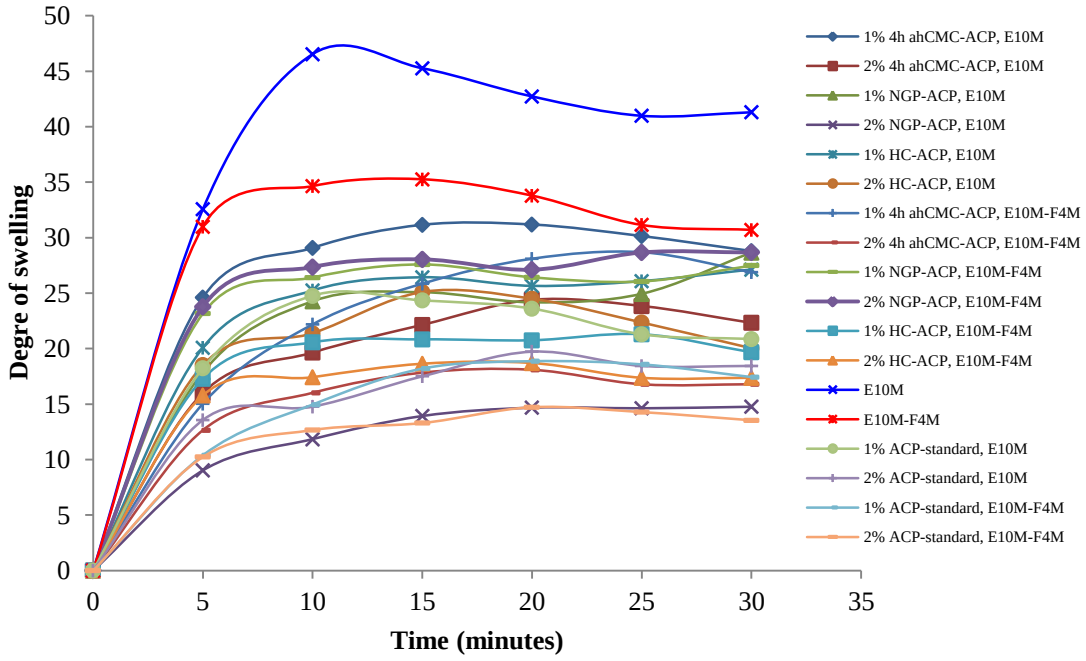

Figure 4.40: The swelling behaviour of the prepared dental films in Xialine II™ artificial saliva. The swelling appears to be fast for the first five minutes, reaching equilibrium swelling after 10 minutes hydration.

4.3.5.4 Analysis of adhesion

The Adhesion parameters of stickiness, work of adhesion and stringiness were measured in the prepared dental films. The percentages of ACP, type of ACP and type of polymer showed effects on the measured adhesion parameters, as shown in Figure 4.41, Figure 4.42 and Figure 4.43.

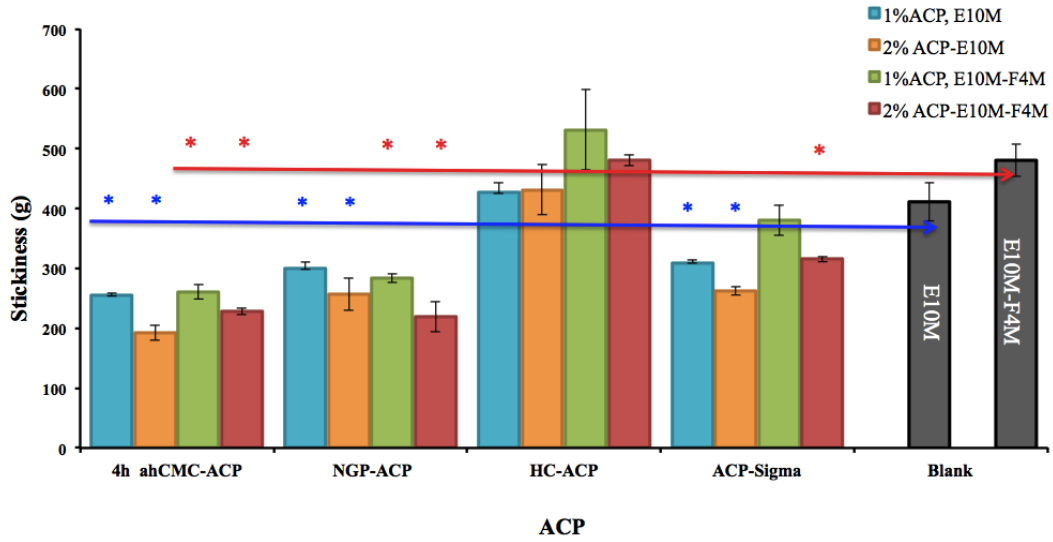

* Significant difference ($p<0.05$)

Figure 4.41: Mean stickiness of the dental films, showing the effect of the polymer and the ACP loading (±SEM, n=6).

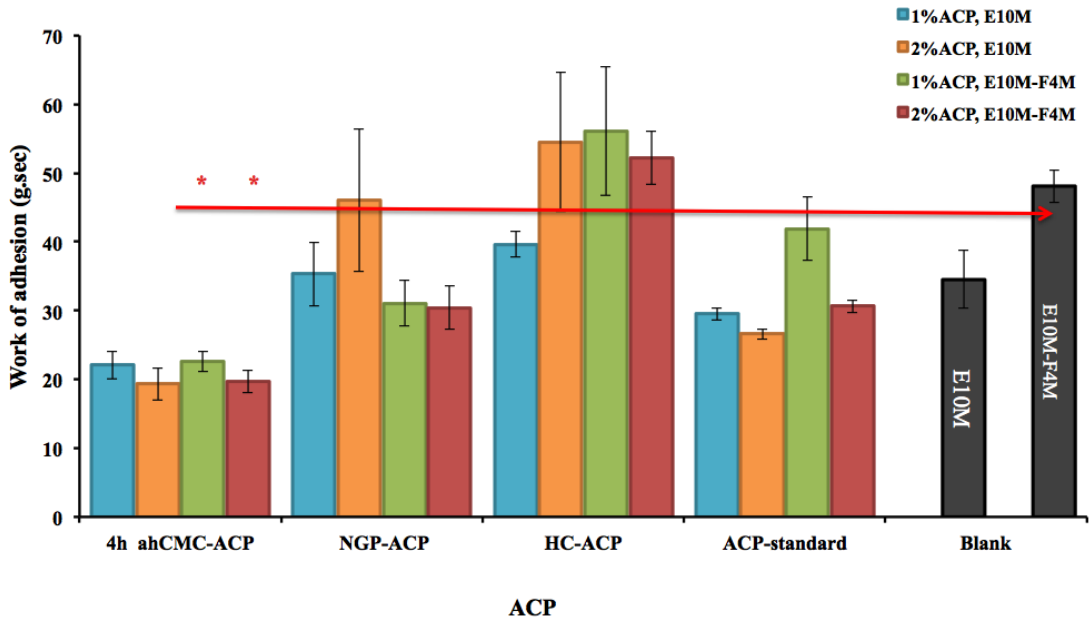

* Significant difference ($p<0.05$)

Figure 4.42: Mean work of adhesion of the dental films, showing the effect of the polymer and the ACP loading (±SEM, n=6).

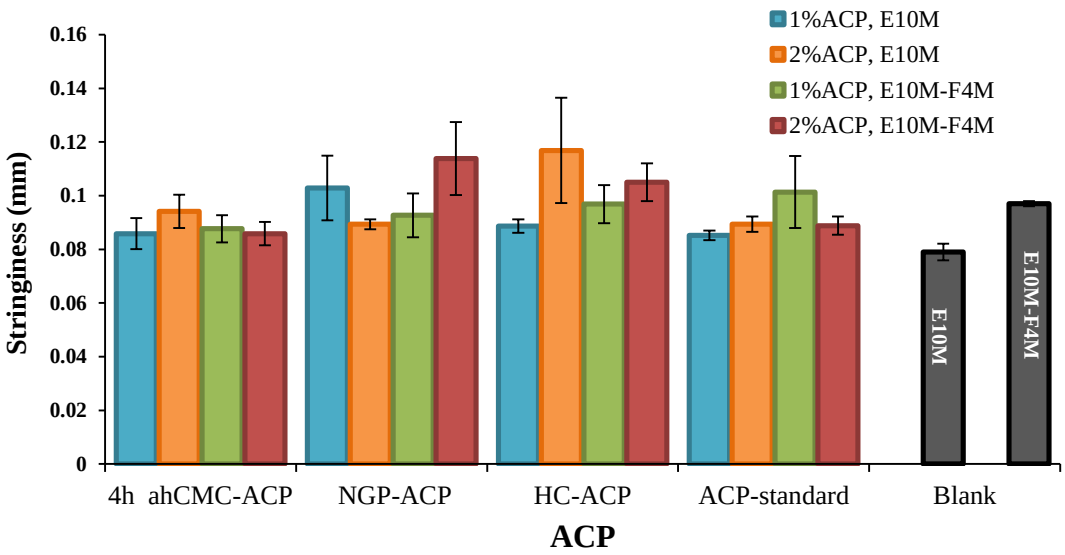

Figure 4.43: Mean stringiness of the dental films, shows the effect of the polymer and the ACP loading (±SEM, n=6).

4.3.5.5 Analysis of calcium content

The effect of the formulation constituents of the prepared dental films on the calcium content was analysed. Figure 4.44 shows the calcium contents uniformity of the prepared dental films.

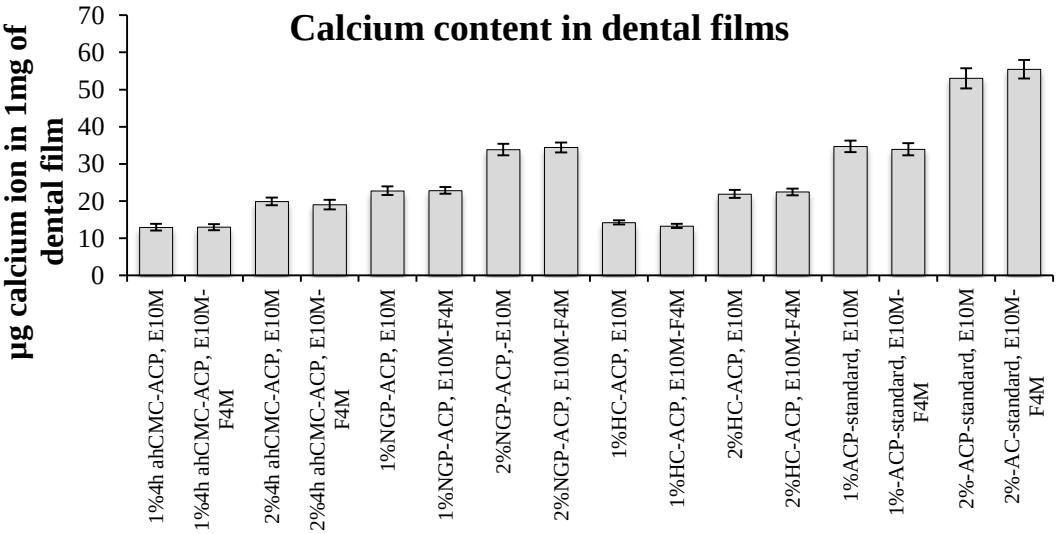

Figure 4.44: Calcium content (mean µg ± SEM) in dental film samples (1mg , n=3).

4.3.5.6 Calcium release study of the prepared dental films

The calcium release study was used for further evaluation of the prepared dental films. To obtain a smooth flow through the device, and avoid stagnancy, the orientation of the cell was examined. The best position of the diffusion cell was found to be the angular-vertical position at which a complete diffusion of the colouring agent throughout the dissolution chamber was observed as shown in Figure 4.45.

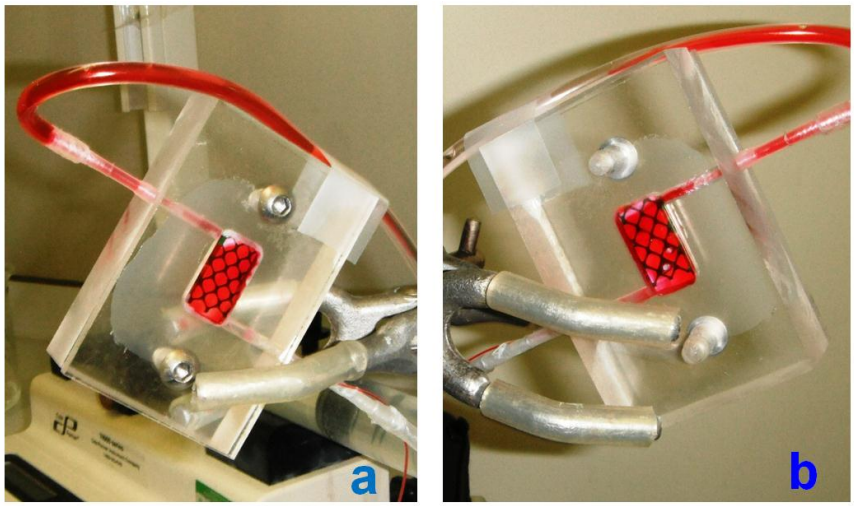

Figure 4.45: The angular-vertical position of the dissolution cell. The frontal (a) and posterior (b) images of the dissolution cell show the complete diffusion of the red colouring agent in dissolution chamber.

The prepared dental films showed variable calcium release profiles dependent on the effect of the grade of polymer used in the formulation of dental films, as well as the effect of type and percentages of loaded ACP, as shown in Figure 4.46, Figure 4.47, Figure 4.48 and Figure 4.49.

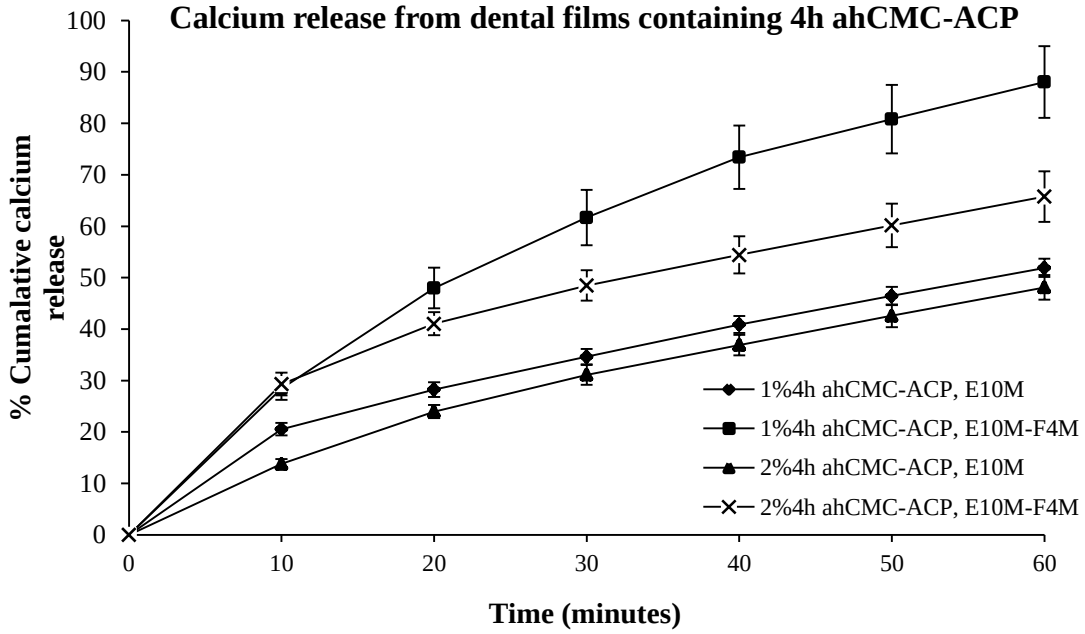

Figure 4.46: Calcium release profiles of the prepared dental films containing 4h ahCMC-ACP. (Mean ±SEM, n=3). Profiles demonstrate effect of the loading with ACP and formulation on the calcium release.

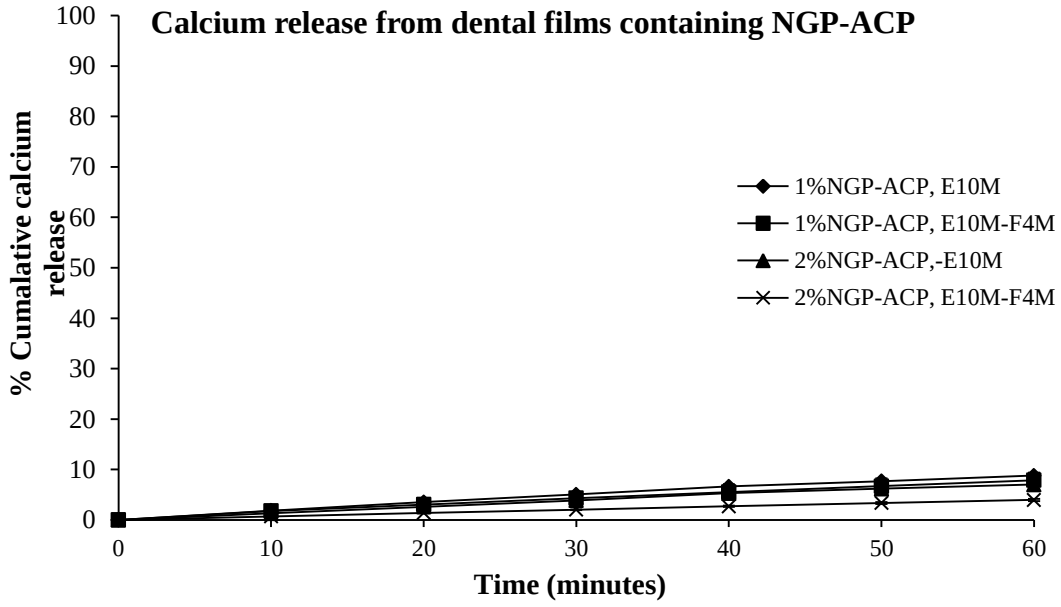

Figure 4.47: Calcium release profiles of the prepared dental films containing NGP-ACP. (Mean ±SEM, n=3). Profiles demonstrate the effect of the loading with ACP and formulation on the calcium release.

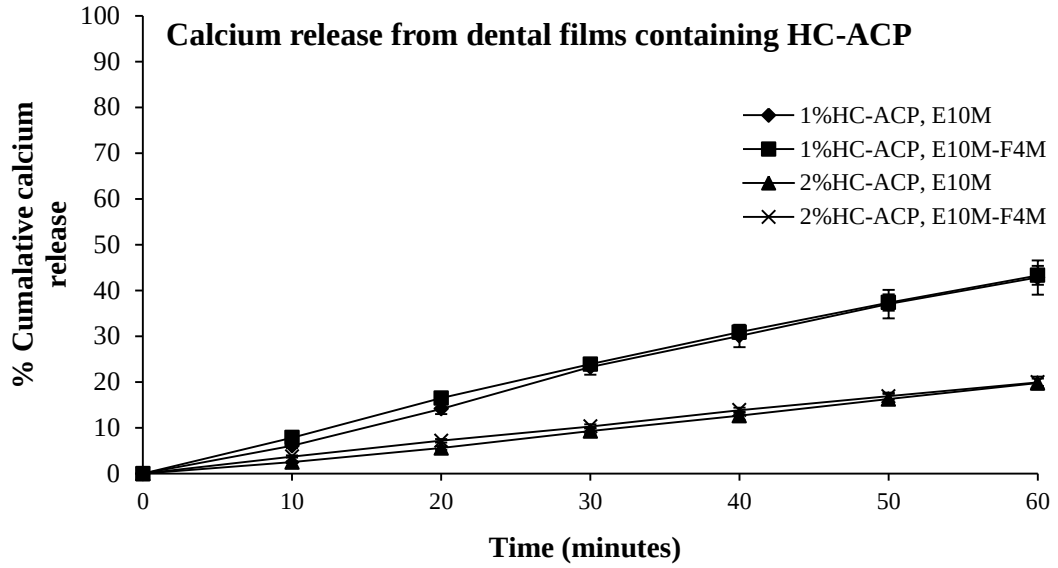

Figure 4.48: Calcium release profiles of the prepared dental films containing HC-ACP. (Mean ±SEM, n=3). Profiles demonstrate effect of the loading with ACP and formulation on the calcium release.

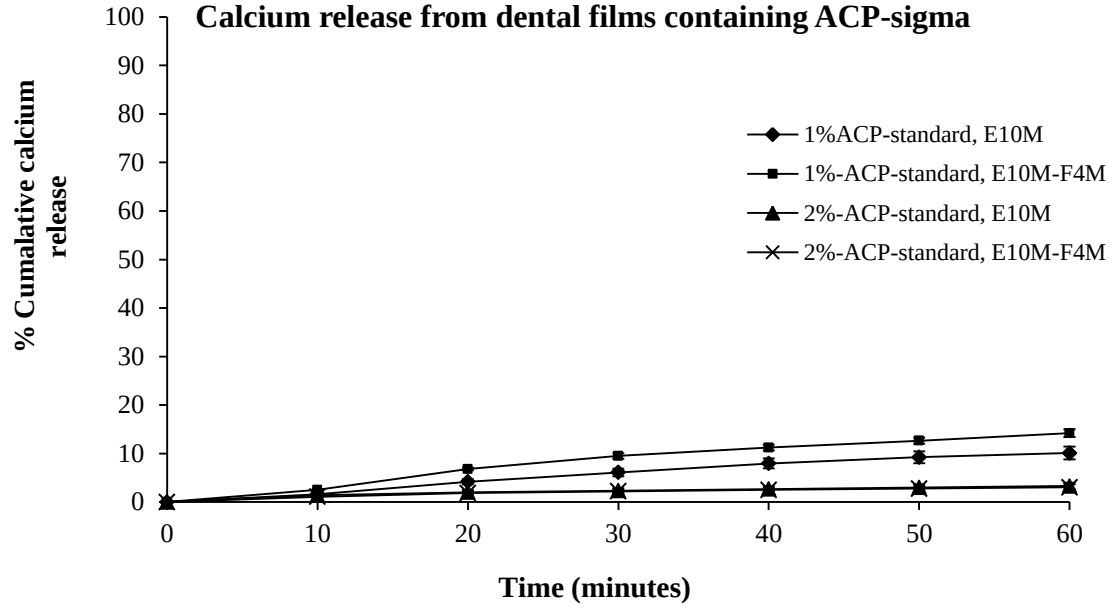

Figure 4.49: Calcium release profiles of the prepared dental films containing ACP-standard. (Mean ±SEM, n=3). Profiles demonstrate effect of the loading with ACP and formulation on the calcium release

4.3.5.7 Analysis of calcium release kinetics

The application of the mathematical models on the data of calcium release of the prepared dental films revealed regression coefficients (r^2) illustrated in **Table 4-11** The highest regression coefficients (r^2) indicate the most applicable kinetic mode of calcium release from the prepared dental films.

Kinetics / Dental films	1st		Zero		Higuchi		Korsmeyer & Peppas		
	r^2	k	r^2	K_0	r^2	k_H	r^2	k_{KP}	n
1%4h ahCMC-ACP, E10M	0.9608	-0.0078	0.9960	0.6222	0.9962	6.8471	0.9968	2.1935	0.632
1%4h ahCMC-ACP, E10M-F4M	0.8823	-0.0092	0.9625	1.1668	0.9947	13.052	0.9908	2.3196	0.517
2%4h ahCMC-ACP, E10M	0.9072	-0.0101	0.9847	0.6666	0.9994	7.3892	0.9987	1.5920	0.444
2%4h ahCMC-ACP, E10M-F4M	0.926	-0.0066	0.9769	0.7017	0.9983	7.8054	0.9961	2.7935	0.689
1%HC-ACP, E10M	0.8943	-0.016	0.9083	0.7408	0.9954	8.156	0.9939	0.7469	1.098
1%HC-ACP, E10M-F4M	0.9083	-0.014	0.8943	0.705	0.9964	7.76	0.9971	0.9627	0.950
2%HC-ACP, E10M	0.9281	-0.0172	0.9281	0.3479	0.9805	3.7917	0.9995	0.4676	1.160
2%HC-ACP, E10M-F4M	0.937	-0.0139	0.937	0.3254	0.9880	3.5598	0.9366	0.6948	0.9366
1%NGP-ACP, E10M	0.9131	-0.0129	0.991	0.1392	0.9968	1.5367	0.9976	0.5511	0.8749
1%NGP-ACP, E10M-F4M	0.9469	-0.0125	0.9996	0.1221	0.9891	1.3361	0.9994	0.5537	0.8337
2%NGP-ACP,-E10M	0.9089	-0.014	0.98991	0.1166	0.9945	1.2858	0.9965	0.4360	0.9563
2%NGP-ACP, E10M-F4M	0.9364	-0.0142	0.9997	0.0653	0.9872	0.7138	0.9999	0.3356	0.952
1%ACP-standard, E10M	0.8454	-0.0146	0.9714	0.1695	0.9965	1.8888	0.9775	0.4706	1.0178
1%-ACP-standard, E10M-F4M	0.7996	-0.0132	0.94709	0.2217	0.9877	2.491	0.9538	0.6277	0.9384
2%-ACP-standard, E10M	0.9239	-0.007	0.89249	0.055	0.9971	0.4087	0.9968	0.7207	0.4753
2%-ACP-standard, E10M-F4M	0.8726	-0.008	0.95531	0.0367	0.9902	0.4114	0.9847	0.6170	0.5511

Table 4-11: Fitting of calcium release data from dental films. The coloured cells present the highest regression coefficients (r^2).

4.4 Discussion

4.4.1 Calcium analysis and method validation

The analysis of the calcium ion concentration from the *in vitro* release samples proved a challenge using the conventional methods described in section 4.1.4. The *in vitro* release samples contained the calcium ions, phosphate ions and stabilising agents. In addition, it was suspected that the supernatant contained non-dissociated ACP nanocomplexes. The acidification or alkalization of samples might therefore influence the measured calcium content. To overcome this problem, a calcium ion selective electrode (ISE) method was selected in the analysis as the electrode has versatility over a wide range of pH (2.5-11) (Mettler-Tolledo, 2010).

4.4.1.1 Calibration curves

The calcium ion content and release profiles from the prepared dental films were determined quantitatively using the calcium ion selective electrode. Calibration curves of millivolt (mV) versus log (ppm) calcium ion concentration were constructed in order to generate quantitative measurements for the calcium containing samples. The produced calibration curves showed linearity described by r^2 values using a regression correlation statistical analysis. The equation to the regression line was used to determine the calcium ion concentration in the collected samples.

4.4.1.2 Calcium ion analysis validation

The calcium ion measurements in the samples showed a significant difference ($p<0.05$) between ICP and electrode methods. However, ICP method resulted in lower readings for most of the selected samples. This suggests a systematic difference between the methods of analysis. This is confirmed by the slope of 0.89 derived from standards of 4, 12, 20 and 40 ppm as shown in Figure 4.11. Reconciliation of the data obtained from calcium electrode by multiplying by 0.89 correlated the two methods of analysis. These findings are in agreement with

descriptions reported by Granholm and colleagues in determination of calcium in black liquor (Granholm *et al.*, 2009)

4.4.2 Analysis of calcium content in prepared ACP

The purification process for the preparation of the ACP showed an effect on the calcium content. In addition, the washing caused a significant ($p<0.05$) increase of the calcium content in isolated NGP-ACP and isolated HC-ACP. For the 4h ahCMC-ACP, the unpurified product showed a significantly ($p<0.05$) higher content of calcium than that in the isolated product. The dissolution and removal of free (non-complexed) peptides by washing might explain the higher content of calcium in the isolated NGP-ACP and isolated HC-ACP. This process of microfiltration had been used in separation and determination of the free calcium and phosphate in solutions of CPP-ACP (Reynolds, 1997). Therefore, it might be responsible for removal of free (non-complexed) calcium and phosphate in the isolated 4h ahCMC-ACP.

4.4.3 Analysis of the effect of pH on the solubility of the isolated ACP

The ACP-standard was used as control to standardize the solubility of the isolated ACP in sodium bicarbonate and lactic acid buffers at different pH. Sodium bicarbonate is the major component of salivary buffer in stimulated saliva (Thylstrup and Fejerskov,1994). The buffer of sodium bicarbonate and lactic acid was used to simulate the conditions around tooth enamel.

To obtain equilibrium conditions, researchers have used extended stirring or shaking times, for example the literature reports values between 17 hours to 4 days for the solubility study of compounds (Bergstrom *et al.*, 2004; Seadeek *et al.*, 2007; Sugano *et al.*, 2006). In our studies much shorter contact times, 5 minutes was used, in order measure the initial dissolution rates of ACP to screen the intended final dissolution study time. In our case, this maximum was set to sixty minutes, Issues regarding the stability of ACP in the aqueous solution were not considered.

The lowering of pH showed an increase in the ionisation and solubility of calcium element in all used samples of ACP. However ACP-standard was least affected ($p<0.05$). In addition, the 4h ahCMC-ACP preparation showed appreciably higher solubility in comparison to the NGP-ACP and HC-ACP samples. The pH cycle revealed a reversible solubility in all samples that might indicate that the calcium was re-complexed into ACP in the presence of the stabilising agent. Furthermore, the ACP-standard showed a low solubility and supersaturated solutions are unlikely to be formed under these conditions.

4.4.4 Adhesion analysis of the prepared hydrogels

The most appropriate probe was selected according to the results obtained from using both 3mm and 6mm diameter cylindrical probes. The profile obtained from 3mm diameter probe did not show a valuable difference between three samples. This might be as a result of a small surface area of contact. Therefore a 6mm probe was used in the analysis of adhesion tests of the prepared hydrogels.

HPMC and MC samples showed a higher stickiness and were clearly distinguishable ($p<0.05$) from sodium CMC samples (Figure 4.16-a). In addition, the HPMC samples showed a higher stringiness than sodium CMC ($p<0.05$) and there was no significant difference from the MC samples (Figure 4.16-b). Furthermore, the HPMC and MC samples showed a higher work of adhesion than the other formulations ($p<0.05$) samples, as shown in Figure 4.16-c.

The results of the stickiness measurement indicate that higher values were obtained in samples 2, 9, 15, 18, and 38. Higher stringiness values were obtained in samples 10, 16, 33 and 38. Samples 9, 15 and 18 showed highest work of adhesion. In order to correlate the data, stickiness was plotted separately against stringiness and work of adhesion and samples 38 and 18 showed the highest values (Figure 4.20) and there was no significant difference between them. It was suggested that simultaneous plotting of the three variables using a three dimensional plot might assist in discrimination. This is shown in Figure 4.21. From this, it was seen that sample 18

had the highest values of parameters measured and was selected as the base material for the addition of linear and/or branched water-soluble polymers.

4.4.4.1 Tooth effect

The microstructure of the surface of the teeth (section 1.1.2) contributed toward variance in the measurement, as the interfacial area of contact between the hydrogel and tooth surface affects the adhesion. Thus stickiness varied consistently between samples ($p<0.05$), whereas work of adhesion and stringiness were not significantly different. This result indicates that the stickiness was a tooth surface dependent variable while work of adhesion and stringiness were formulation dependent.

4.4.4.2 The effect of linear and/or branched water-soluble polymers mixed with a selected hydrogel product on the adhesion parameters

HPMC is a linear polymer, while gum Arabic (acacia) is a natural branched polymer of galactose, rhamnose, arabinose and glucouronic acid (EL-Khier *et al.*, 2009). During preparation of samples 66-68, an interaction between HPMC and acacia was noticed, specifically release of water of hydration. These samples were not included in adhesion analysis. A possible mechanism suggested is that the fixed water in HPMC is lost by attachment of the HPMC hydroxyl groups with hydrogen bonds on the acacia polymer. Samples 78-79, however, did not show the same behaviour perhaps because the presence of xanthan gum accommodated the extra water. Xanthan gum is composed of a β-D-(1,4)- glucose backbone which is a branched trisaccharide of two β-D-(1,2)-mannose molecules separated by β-D-(1,4)-glucouronic acid (Pongjanyakul and Puttipipatkhachorn, 2007). Sodium alginate is salt of alginic acid which is a linear polymer composed of β-D-(1,4)-mannosyluronic acid and α-L-(1,4)-glucosyluronic acid. Tragacanth gum consists of a mixture of 30-40% (w/v) of water soluble tragacanthin and 60-70% (w/v) of water insoluble bassorin (Kibbe, 2000).

Gum Arabic, xanthan gum, sodium alginate and tragacanth gum were added to examine whether linear and/or branched polymers can increase the adhesion parameters of the linear polymer gel formed by HPMC-E10M.

The adhesion analysis of the prepared hydrogels, illustrates that there is no increase in the adhesion parameters with additional excipients. The results clearly highlighted a decrease in the adhesion parameters as a result of polymer addition. This reduction was significant ($p<0.05$) for xanthan-containing samples. Conversely there was no significant change in sodium alginate containing samples.

4.4.4.3 Mixtures of polymers

The prepared formula 95 containing a mixture of HPMC grades F4M 5% w/v and E10M 10% w/v showed relatively higher adhesion properties than that of formula 18. The mixing of short and long chain of selected HPMC polymers did not show an increase in adhesion properties that is in agreement with the Russell finding that the long chain showed a better capability over the short chain to anchor to the surface of the substrate (Russell, 2002). On the contrary, a decrease in the measured adhesion was found. In addition, results indicate that the adhesion was directly proportional to the concentration of long chain polymer rather than short chain polymer. Therefore both formula 18 and 95 were selected to prepare dental film containing the prepared isolated ACP.

4.4.4.4 Analysis of the adhesion properties of commercial tooth pastes

There was a highly significant difference between formula 18 and commercial toothpaste preparations. This might be as a result of their content of anionic surfactant (Gloxhuber *et al.*, 1992). With regard to the tooth mousse, surfactants concentrations are not disclosed. The toothpaste preparations used in these studies had low adhesion properties in comparison to formula18.

4.4.5 Characterisation of the prepared dental films

The increase in the thickness of the prepared film with increase in the ACP loading indicates that there was an increase in the volume of the dried film. This might be due to low interaction and interpenetration between the polymer and the ACP.

4.4.5.1 Analysis of flexibility

One of the main mechanical properties that characterised in film dosage is film elasticity or flexibility. Film elasticity has been widely described in terms of tensile strength, percentage of elongation and Young's modulus (Azeredo *et al.*, 2010; Cilurzo *et al.*, 2010; Khunawattanakul *et al.*, 2010; Lin *et al.*, 1995) in addition to the puncture strength (Bodmeier and Paeratakul, 1994). Also, the flexibility of the film dosage form has been tested in term of number of times film folding causes cracking in the film under strong light (Cilurzo *et al.*, 2008; Liew *et al.*, 2011).

The positive and negative kick-off peaks of about 4g, as shown in Figure 4.34 indicates the sensitivity of the texture analyser upon changing the direction of the movement of the probe.

The prepared dental films were flexible and the presence of ACP significantly ($p<0.05$) modified the flexibility of the prepared film causing an increase in the firmness. The obtained flexibility profiles showed a significant ($p<0.05$) difference between samples of the prepared dental films. In addition, dental films showed a steady phase of resistance forces in the initial stages of the time scale. The formulation of dental film, type and percentage of ACP showed a significant effect on the duration of this phase that indicates there was a partial separation between the dispersed particles of ACP and the polymer. In addition, the resistance forces were affected by the HPMC grade, as is in agreement with results reported by (Fahs *et al.*, 2010).

4.4.5.2 Analysis of degree of swelling

The prepared dental films with the mixture of HPMC grades E10M and F4M exhibited a significantly ($p<0.05$) lower degree of swelling in comparison with those containing only E10M. This indicates that the HPMC polymer with the shorter chain length (grade F4M) was responsible for reducing the degree of swelling in the prepared dental films, which is in agreement with Khan and Maheshwari (2011). In addition, the percentages and types of the ACP showed a significant effect on the degree of swelling. This might be due to different solubilities of ACP preparations, as described in section 4.3.3. Sai Cheong Wan and co-workers have shown that the poorly soluble drug decreased the swelling of the HPMC containing matrices, which is agreement with our findings. Unloaded films showed a significantly higher degree of swelling than that of ACP containing dental films (Sai Cheong Wan *et al.*, 1995).

4.4.5.3 Adhesion analysis of the prepared dental films

Generally, ACP showed an effect on the adhesion properties of the prepared dental films. The NGP-ACP and 4h ahCMC-ACP showed a significant ($p<0.05$) lowering effect on the stickiness of the prepared dental films in comparison with blank dental films. However, HC-ACP containing films did not show a stickiness lowering effect. This difference may be attributed to the difference in the surface roughness property of the dental films, as mentioned in section 4.3.5.1. The rough surfaces in dental film formulations containing NGP-ACP and 4h ahCMC-ACP resulted in a decrease of contact area between the probe surface and HPMC in the dental film resulting in a reduction of the detachment area and consequently the adhesion. This finding agrees with that reported by Persson and Tosatt (2001).

A significant lowering effect of ACP on the work of adhesion was obtained in dental films containing 4h ahCMC-ACP. This effect might be due to the low physical bonding between the ACP particles and HPMC. In addition, the inclusion of ACP dental films produce no significant effect on the stringiness in comparison with unloaded dental films.

4.4.5.4 Calcium release study of the prepared dental films

The calcium release data showed the influence of the type and percentages of the loaded ACP on calcium release from samples of the prepared dental films, as well as, the influence of the dental film formulations. A higher percentage of calcium release was obtained in the dental film containing a 1% w/w loading of ACP. This indicates that the 2% w/w ACP had a higher interaction with HPMC polymer that might be interfere with the dissolution of the dental film.

Dental films containing 4h ahCMC-ACP showed the highest percentage of calcium release which correlated with the result obtained from the pH-solubility study of the prepared ACP (section 4.3.3). Dental films containing ACP-standard showed the lowest release of calcium, suggesting a strong direct relationship between the solubility of ACP and the total amount of the released calcium from HPMC-based film, in agreement with data reported by Chakraborty and co-workers (Chakraborty *et al.*, 2009).

The calcium release study from the prepared dental films showed the effect of the formulation on the calcium release. The prepared dental films containing mixture of HPMC grades of E10M and F4M exhibited a higher calcium release in comparison with those containing only E10M. This indicates the presence of low molecular weight HPMC grade (F4M) enhanced the dissolution of ACP and calcium release, which may be as a result of the lower viscosity, as reported by (Akbari *et al.*, 2011) and Campos-Aldret and Villafuerte-Robles (1997).

The kinetics of the calcium release from the prepared dental films were studied using four different models in order to understand the behaviour and the factors that control the calcium release. The highest obtained r^2 from the data analysis of calcium release kinetics proved the diffusion release behaviour of calcium from all the prepared dental films except 1%NGP-ACP, E10M-F4M and 2%NGP-ACP, E10M-F4M dental films which showed a zero order release of calcium. However, 1%NGP-ACP, E10M-F4M and 2%NGP-ACP, E10M-F4M dental films showed r^2 of 0.9891 and 0.9872 respectively, suggesting a fit the Higuchi model.

The application of the Korsmeyer-Peppas model suggested Fickian diffusional of calcium release in 1% 4h ahCMC-ACP_E10M-F4M, 2% 4h ahCMC-ACP_E10M, 2% ACP-standard_E10M and 2% ACP-standard_E10M-F4M dental films. However the rest of the dental films exhibited a non Fickian and super case-II transport. The super case II is the case in which the diffusion of calcium ion might be associated with polymer relaxation and erosion throughout the formation of hydrated gel layer, as reported by Sriamornsak and Sungthongjeen (2007) and Cox *et al.* (1999).

These findings support the proposal that the effect of thepolymer on the release of calcium from dental films depends on the solubility of ACP and the polymer behavior in the dissolution media, whether swollen, eroded and/or diffused. If erosion is slower than the diffusion process, the release from polymer will be controlled by diffusion. If the diffusion of dissolution media into the polymer is faster than erosion but slower than polymer relaxation, swelling potentially controls the calcium release. If the erosion is the fastest process, drug release is dominated by this effect.

Finally, the calcium release kinetics indicated that the prepared dental films showed complex behaviour of swelling, diffusion and erosion to release calcium. These inter-relationships of polymer swelling, erosion and diffusion depend on polymer and ACP solvation effects, loading and type of ACP, as shown in Figure 4.50.

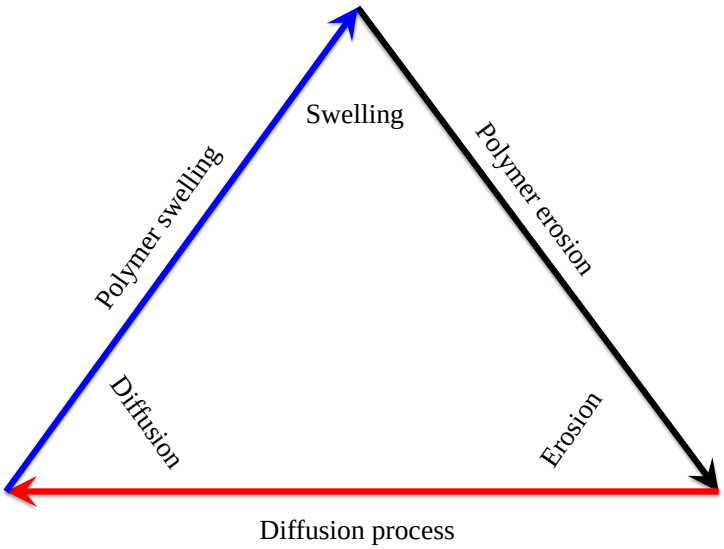

Figure 4.50: The mechanisms of calcium release from dental film containing ACP. Calcium released by diffusion, polymer swelling and polymer erosion.

4.5 Conclusions

The isolation process was successful in increasing the calcium content in NGP-ACP and HC-ACP. However, there was a decrease observed for the 4h ahCMC-ACP preparation. A reversible solubility of the prepared ACP was obtained upon a cycle of pH change and 4h ahCMC-ACP showing solubility higher than NGP-ACP and HC-ACP at all pH conditions investigated. The hydrogel formulations of 3% w/v HPMC (E10M grade) and a mixture of 2% w/v E10M and 1% w/v F4M HPMC grades appear to be suitable for the formulation of a flexible dental film containing ACP and can be produced by a casting method. The physical properties of the prepared film are affected by the type and percentage loading of ACP.

The solubility of ACP has a direct effect on the calcium release from ACP-containing dental films. The kinetics of calcium release followed a Higuchi mode, with different diffusional models of Fickian, non-Fickian and super case II transport, depending on the type and percentage loading of ACP, as well as the grade of HPMC. Dental films containing 2% w/v 4h ahCMC-ACP and 2% w/v HC-AC

formulated with a mixture of 2%w/v E10M and 1% w/v F4M are the most appropriate to deliver calcium ions for dental enamel remineralisation.

Further study was directed to the *in vitro* retaining effect of the prepared ACP on an orally relevant biofilm in the next chapter. Then dental enamel remineralisation efficiency on a human enamel blocks using 2% w/w 4h ahCMC-ACP and 2% w/w HC-ACP dental films prepared from a mixture of 2% w/v E10M and 1% w/v F4M HPMC grades is investigated in the subsequent chapter.

Chapter 5. Dental biofilm

5.1 Introduction:

The pellicle is a film of non-cellular bacteria-free salivary proteins formed on the enamel surface of teeth exposed to the oral environment. This layer affords a suitable surface for bacterial adherence at the first stage of plaque formation (Yao *et al.*, 2001). This film, known as the acquired pellicle, is composed of glycoproteins, mucins, proline-containing proteins, histidine-containing proteins and enzymes such as α-amylose. Bacterial attachment and colonization on this pellicle will form a dental plaque. Thus, the term dental biofilm refers to acquired pellicle and dental plaque (Quirynen *et al.*, 2005).

5.1.1 Biofilm formation

The majority of microorganisms within mature dental biofilm are attached to each other for colonization (Costerton *et al.*, 1995). The primary survival mechanism of microorganisms is attachment and retention to the surface (Marsh, 2005). The surface roughness has been shown to have a potentl effect on the adherence of bacteria to the tooth surface, probably as a result of providing protected sites and a larger surface area for colonization subsequent to biofilm formation (Gurgan *et al.*, 1997). It is reported that up to 500 species have the capability of colonising the tooth as a biofilm (Page *et al.*, 2000).

Hannig and colleagues developed an *in situ* biofilm model by mounting of appliances containing enamel specimens in the intraoral space of human subjects for periods of 2, 6, 12 and 24 hours (Hannig *et al.*, 2003). The bacteria *Streptococcus mutans* has the ability to form glucans from sucrose by glucosyl transferases, which is important for adhesion and biofilm formation. On this basis, it has been considered the principal causative factor for dental caries (Li *et al.*, 2009).

5.1.2 Biofilm microstructure:

The biofilm thickness is affected by the presence of some substrates. For example, it is greatly increased when sucrose is added to the culture media. In contrast, a mucin-limited media produced a thin porous film (

Figure **5-1**).

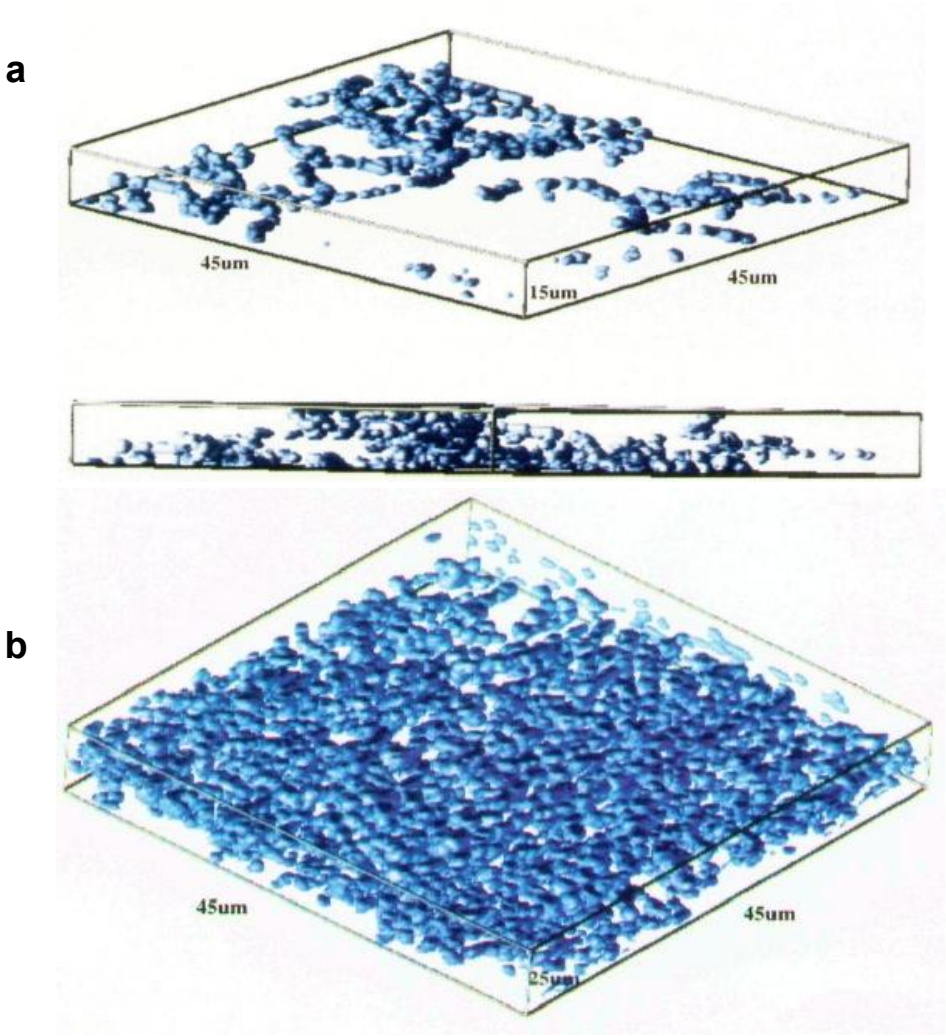

Figure 5-1: Biofilm microstructures grown in a continuous culture biofilm system under either: (a) mucin-limited or (b) sucrose-supplemented conditions. Images stained with ethidium bromide. From (Singleton *et al.*, 1997)

The microstructure and molecular modeling of the cultured biofilm has been characterized by confocal imaging, as shown in Figure 5-2. The confocal images of were simulated in to two and three-dimensional models to analyse the diffusivity of the oral biofilm.

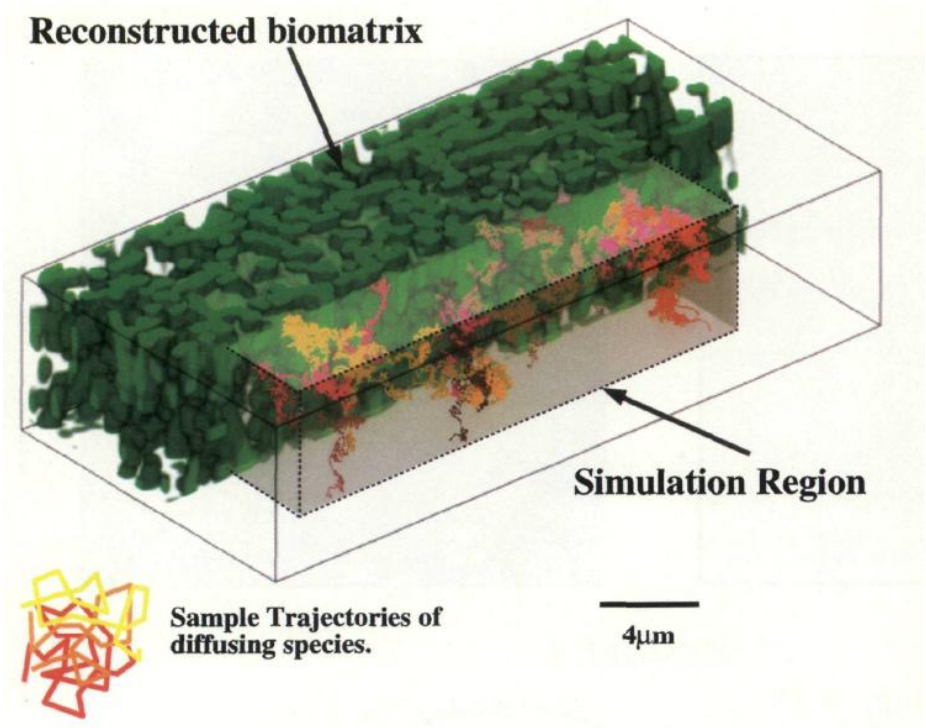

Figure 5-2: Three-dimensional diffusion simulation in an extracted biofilm microstructure. From (Singleton *et al.*, 1997)

5.1.3 Biofilm compositions

Yao and colleagues described protein components of the pellicle produced under *in vitro* and *in vivo* conditions. The components were analysed by gel electrophoresis and mass spectrophotometry. Eleven main proteins were identified from *in vitro* pellicle and *in vivo* pellicle which showed an existence of albumin, amylase, lysozyme and statherin, in addition to several fragmented precursor proteins. The pellicle proteins produced *in vivo* differed from those produced *in vitro,* with a low content of proline-rich proteins, which might have arisen from exclusively oral

contents (Yao *et al.*, 2001). Siqueira and Oppenheim subjected similar specimens to centrifugal and gel filtrations followed by LC-MS analysis. Seventy eight natural peptides, originating from 29 different proteins, were identified in the enamel pellicle acquired *in vivo* (Siqueira *et al.*, 2009).

5.1.4 Objectives

The objectives of this short investigation were to culture an orally relevant biofilm on a limited number of human tooth samples to assess whether adhesion of the preparation might be an issue. The films were characterised using an upright fluorescence microscope. The effect of cultured biofilm on the tooth surface hydrophobicity and adhesion properties were analysed by contact angle measurement and adhesion tests on a selected formula. In addition, the effect of the concentration of isolated ACP produced by methods described in Chapters 2 and 3 and added to the media on the cultured oral biofilm was studied. Confocal scanning microscopy was used to determine the effect, measuring thickness of biofilm as a marker.

5.2 Materials and methods

5.2.1 Materials

Brain-heart broth (BHI) and sodium fluorescein were purchased from Sigma-Aldrich UK.

5.2.2 Oral relevant biofilm growth on teeth samples

An orally relevant biofilm was cultured followingcollection of 5 mL saliva from each three adult volunteers in the morning before brushing. The collected saliva was pooled and 2 of 3 mL were inoculated into 2 conical flasks containing 250 mL of brain heart infusion broth and incubated for 5h at 37° C. One batch was incubated anaerobically while the other was incubated aerobically with shaking. The aerobic incubated flask was then added to the other with gentle mixing and 5mL of the prepared inoculum was added to 45 mL of freshly prepared and sterile BHI. Three tooth samples were immersed in the prepared mixture and incubated for 24h at 37°C. Following incubation, samples were removed and immediately used in the experiments.

5.2.3 Examination of cultured biofilm

The imaging of the cultured biofilm was carried out using an upright microscope with 40x objective lens and a fluorescent light to illuminate the tooth surfaces. The selected tooth samples were T5, T8 and T9.

5.2.4 Effect of biofilm on the adhesion properties of 15% (w/v) HPMC- E10M

The tooth samples (T1, T2 and T3) were selected to study the effect of biofilm on the adhesion parameters of 15% (w/v) HPMC-E10M using a 6 mm diameter cylindrical probe. The adhesion test setting used was the same as that applied in a previously described protocol (see section 4.2.4).

5.2.5 Effect of biofilm on the hydrophobicity of teeth surfaces

Contact angle measurements were used to estimate the change in the degree of hydrophobicity of tooth surface using the teeth samples with the flattest surfaces (T5, T8 and T9). 5µL distilled water was dropped onto the tooth surface and the contact angles were estimated using an average of measurements derived from approaching and retiring sides using Infinity Analyse™ software ver. 5.0.3, as illustrated in Figure 5-3. The controls used were the contact angles for the teeth free from biofilms.

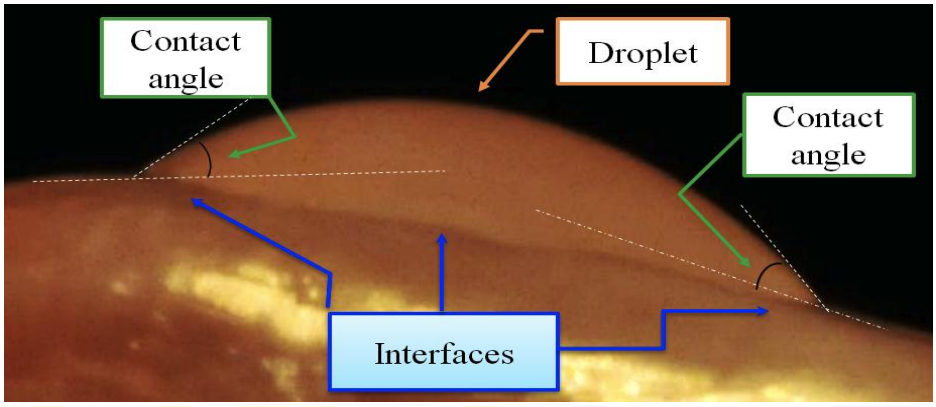

Figure 5-3: Image showing the contact angle measurement method: The angles of tangents to the baselines (drop-tooth surface contact interface). Tangents were drawn by setting two circles fitting to the drop surface at the edges.

5.2.6 Effect of ACP on biofilm

The effect of prepared isolated ACP on thebiofilm was studied by incubation of the culture media (section 4.2.1) with additions of 0, 2, 4 and 8% (w/v) of isolated NGP-ACP, HC-ACP and 4h ahCMC-ACP for 72 hours at 37º C on a rough glass surface. The rough surfaces were generated by scratches made on a glass cover slide, as shown in Figure 5-4. At the end of the experiment, the glass cover slides containing cultured biofilm were rinsed with normal saline (0.9% w/v NaCl) for a minute then immersed in 0.2% (w/v) sodium fluorescein for a second minute for staining. The samples were then rinsed with normal saline for a minute and then left in hood for an hour to dry. The prepared samples were then transferred onto glass slides and covered with cover slips sealed with grease, as shown in Figure 5-5.

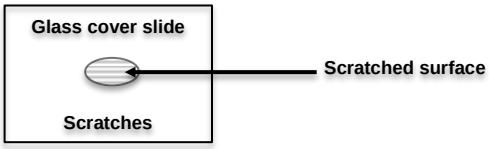

Figure 5-4: Drawing of the rough surface for biofilm culture, generated by scratching on the glass cover slide.

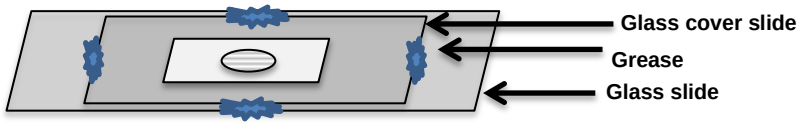

Figure 5-5: Diagram illustrates slide preparation of cultured biofilm for confocal microscopy.

Two and three dimensional images were taken with Leica-SP5 confocal laser scanning microscope based on Dr600B upright Leica (objective 40x (NA1.25 HEXPL. APO) oil immersion lens; Velocity ver. 5.5 (Improvision, Perkin-Elmer). Three-dimensional images were created by taking stacks of 2 microns thickness images moving from the bottom to the top of biofilm. The thickness of biofilm was calculated as mean depth of sixteen pre-set positions on the image field, as shown in Figure 5-6.

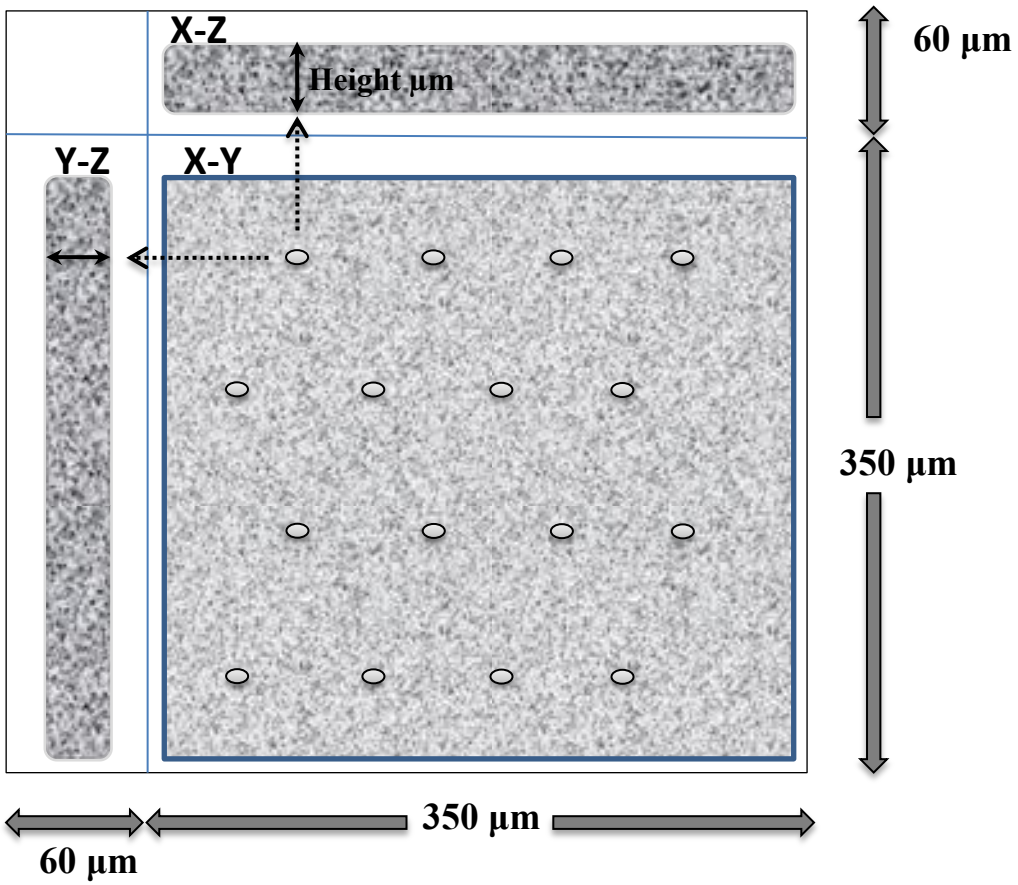

Figure 5-6: Diagram showing the sixteen pre-set positions of thickness measurement using 3-dimensional confocal image technique.

5.2.7 Statistical analysis

One-way ANOVA with Tukey's post-hoc test (Minitab V.16) was used to analyse the effect of biofilm on the tooth surface hydrophobicity and the adhesion properties. In addition, this test was used to analyse the effect of the type and concentration of isolated ACP on the thickness of the cultured biofilm.

5.3 Results

5.3.1 Examination of cultured biofilm

Microphotography of the cultured biofilm on tooth samples showed a considerable difference between individual tooth samples. For example, T5 showed extensive coverage of the tooth surface with biofilm spots, as shown in Figure 5-7, while T8 and T9 showed few spots (Figure 5-8 and Figure 5-9).

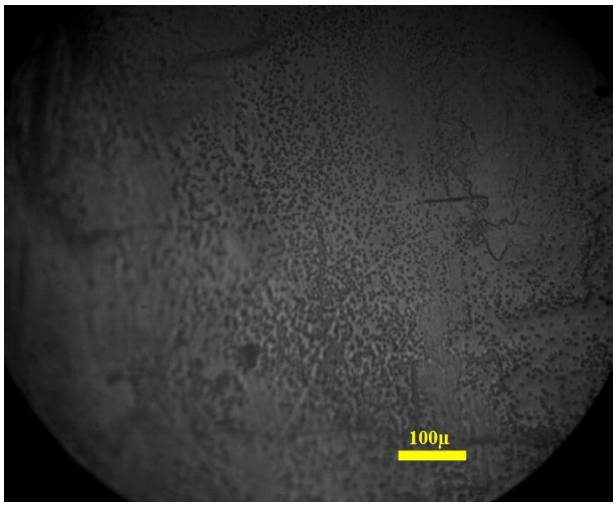

Figure 5-7: Microphotography of the cultured biofilm on the surface of T5 shows large number of biofilm spots.

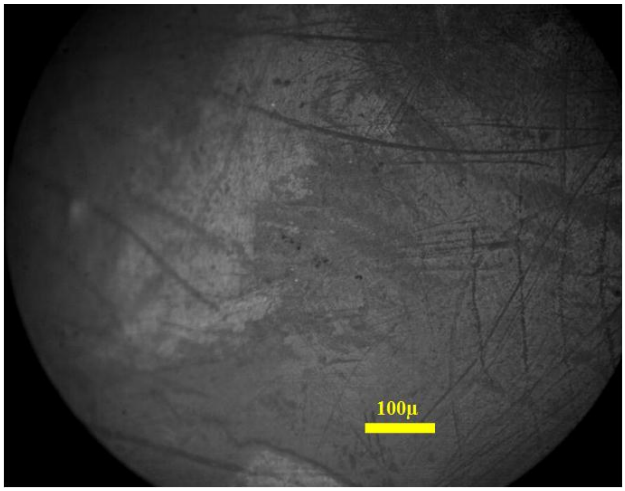

Figure 5-8: Microphotography of the cultured biofilm on the surface of T8 shows fewer biofilm spots than for T5.

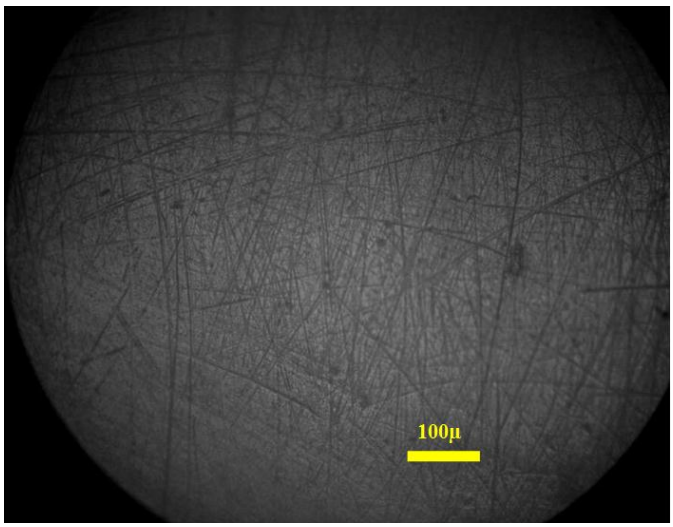

Figure 5-9: Microphotography of the cultured biofilm on the surface of T9 shows low number of biofilm spots.

5.3.2 Effect of biofilm on the adhesion properties of 15% (w/v) HPMC- E10M

The adhesion parameters of 15% (w/v) HPMC- E10M on teeth surfaces having a cultured biofilm were measured. There was no significant effect of the biofilm on these measurements of adhesion of 15% (w/v) HPMC- E10M as shown in Figure 5-10.

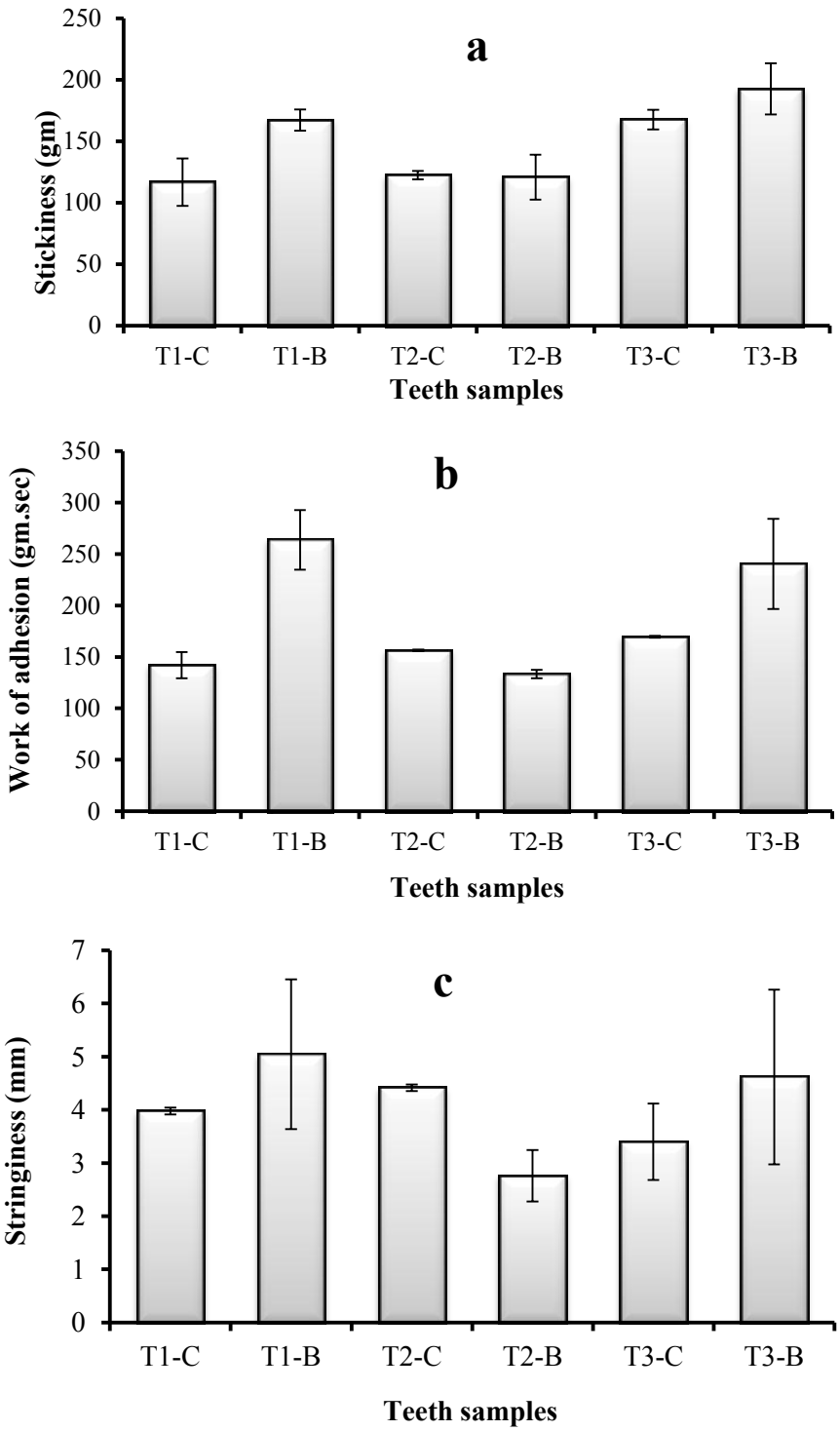

Figure 5-10: a) Mean Stickiness, b)-work of adhesion and c)-Stringiness for T1, T2 and T3 control and cultured biofilm (n=3). C = control and B = biofilm (Mean ±SEM, n=3).

5.3.3 Effect of biofilm on the hydrophobicity of teeth surfaces

The contact angle was used to estimate the hydrophobicity of the flat surfaces. The angles were measured on the tooth surfaces by taking the average of both side angles of the drop as well as of the bubble (Lelah *et al.*, 1985). Teeth surfaces mostly are characterised by irregular to concave planes. To compensate for this disparity, average contact angles of both sides were measured and used for the analysis of effect of the biofilm on hydrophobicity. Figure 5-11 shows the effect of cultured biofilm on the measured contact angle of teeth samples.

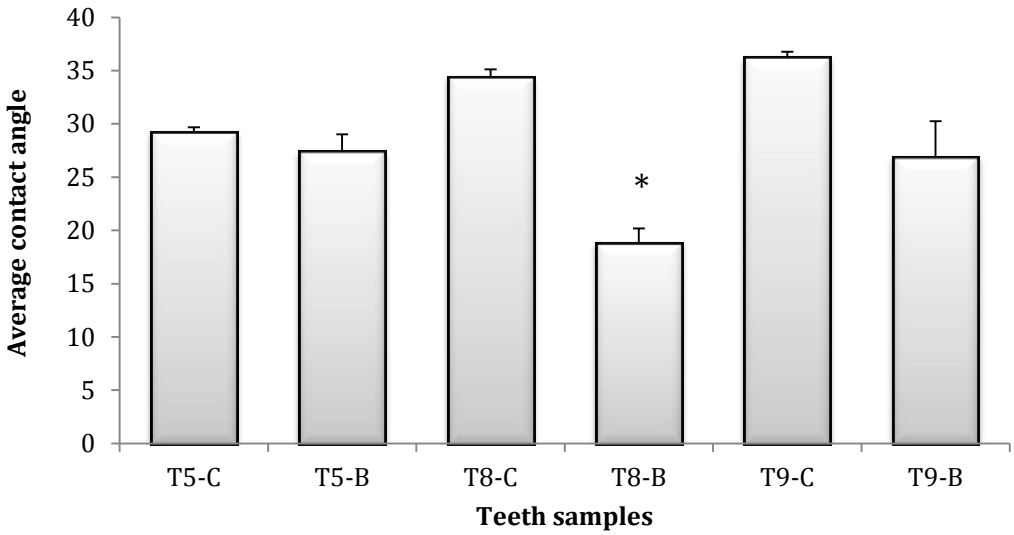

* Significant difference ($p<0.05$)

C=Control

B= biofilm.

Figure 5-11: Contact angles of control and cultured biofilm on surfaces of teeth samples (Mean ±SEM, n=3).

5.3.4 Effect of ACP on biofilm thickness

Confocal images with measured biofilm thickness were obtained as shown in Figure 5-12. The measured thickness of the produced biofilms indicates that the isolated ACP had an effect on thickness of the biofilm produced. This effect varied

depending on type and percentage of ACP. However, 2% (w/v) percentage produce a difference from the controls for all types ACP, with higher percentages generally showing a decrease in biofilm thickness, as shown in Figure 5-13.

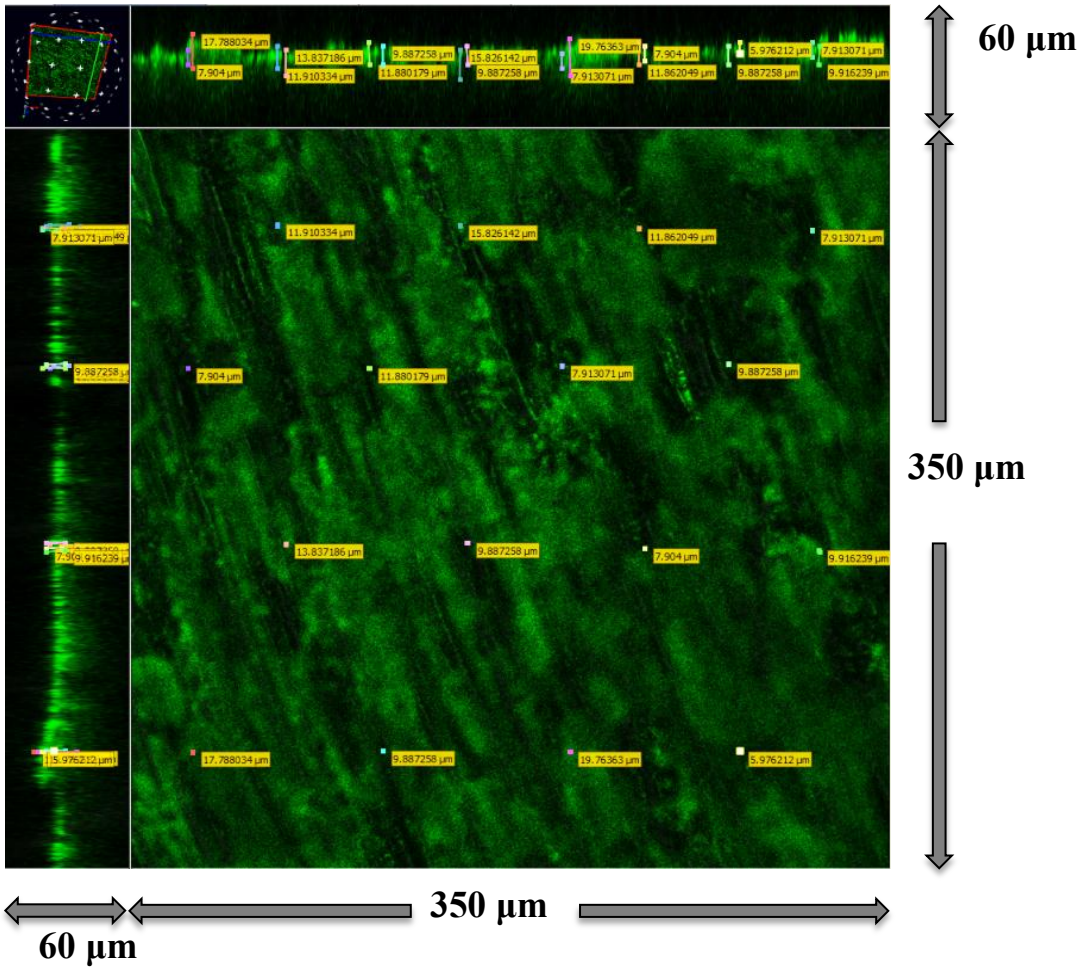

Figure 5-12: A three dimensional confocal image shows measured thickness of biofilm at sixteen pre-set positions.

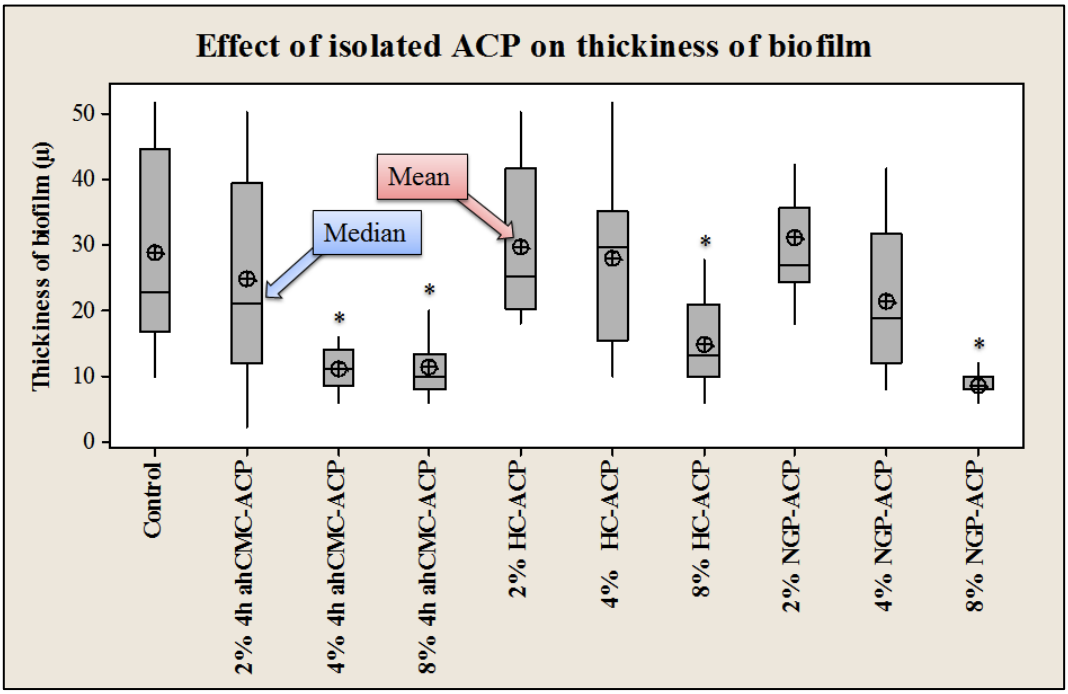

* Significant difference ($p<0.05$)

Figure 5-13: Effect of ACP concentrations on biofilm thickness grown on a scratched glass cover slide.

5.4 Discussion

5.4.1 Examination of cultured biofilm

The obtained images showed a large difference in the density of biofilm spots on the teeth surfaces. This observation might result from differences in the storage conditions and undisclosed pre-treatment might cause inhibitory effects in the culture. In addition, the enamel surface roughness might have played an important role in the culture of the biofilm between teeth samples, as suggested by the findings of Gurgan and colleagues (Gurgan *et al.*, 1997).

5.4.2 Effect of biofilm on the adhesion properties of 15% (w/v) HPMC- E10M

The similarity in the adhesion properties between control and test indicates that the cultured biofilms were not sufficient to cover teeth surfaces and cause a change in the adhesion parameters. This result might be caused by the short incubation period or a deficiency in the media used, an observation in agreement with Li and colleagues (Li *et al.*, 2009), who used sucrose solution 1% (w/v) to fortify the culture of the oral biofilm.

5.4.3 Effect of biofilm on the hydrophobicity of teeth surfaces

The hydrophobicity of thetooth surface was analysed as a function of dental biofilm formation in this experiment. *Bacillus subtilis* biofilm was analysed for wetting resistance against different water/ethanol volume ratios using contact angle goniometer (Epstein *et al.*, 2011). The biofilm effect on the hydrophobicity of the tooth surface was found to have a significant effect ($p<0.05$) observed for T8, but this was not observed in the other tooth samples.

5.4.4 Effect of ACP on biofilm

Glass cover slides were scratched to support the biofilm culture instead of dental enamel because of transparency and lack of sufficient quantity of dental enamel blocks. Hydroxyapatite discs were used by Hope *et al.* (2003) to support the cultured biofilm and this is apotential alternative to glass.

An equal thickness of cultured biofilm was observed in controls and 2% (w/v) ACP, whereas 4% (w/v) of NGP-ACP and HC-ACP showed a non-significant decrease in the thickiness. Higher percentage incorporation led to a significant reduction in thickness of biofilms ($p<0.05$). In addition, 4% and 8% (w/v) of the 4h ahCMC-ACP preparations showed a comparable effect. Thus 4h ahCMC-ACP exhibited a higher efficiency in reducing biofilm in culture. This finding is in agreement with recent work in which the presence of CPP-ACP caused a delay in the formation of biofilm (Rahiotis *et al.*, 2008).

5.5 Conclusions

This short series of studies indicate that the cultured biofilm on a tooth surface had little effect on the adhesion properties of 15% (w/v) HPMC-E10M. However, the effect of the biofilm was not conclusive since the measured hydrophobicity of teeth surfaces varied within and between the tooth samples. This suggested that a larger number of teeth would be required and there was insufficient time at the end of the study period to embark on a fresh study. Nevertheless, some promising data was obtained which justified the inclusion of this piece of research in the thesis. All the prepared isolated ACP showed a promising inhibitory action on cultured orally relevant biofilm at 8% (w/v), in addition 4% (w/v) 4h ahCMC-ACP exhibited a similar inhibitory to the 8% (w/v) preparation.

Chapter 6. Enamel remineralisation potential of 2% w/v 4h ahCMC-ACP and 2% w/v HC-ACP containing dental films prepared from a mixture of 2% w/v E10M and 1% w/v F4M HPMC grades

6.1 Introduction

6.1.1 Demineralisation and remineralisation

After meals or sugar-containing drinks, the bacterial population of the oral cavity ferments the carbohydrate leading to the formation of cariogenic metabolites supporting plaque, particularly in susceptible areas of the tooth surface, such as crevices and gaps that are not readily cleane. The cariogenic metabolites demineralise the tooth enamel and establish a lesion, usually visible as white spot on illumination. The plaque works as a barrier that prevents the pH neutralisation and tooth remineralisation by the secreted saliva, which is saturated with calcium and phosphate. Under neutral pH conditions, the demineralisation is stopped or reversed (remineralisation) by the presence of the calcium and phosphate ions, which form a saturated solution in the saliva (Lata *et al.*, 2010). The pH cycle of plaque acidification and neutralisation is therefore parallel with cycle of demineralisation and remineralisation of the enamel (Lippert *et al.*, 2004). Increasing demineralisation produces a greater dissolution of enamel and dentine, ending with lesion cavitation (Featherstone, 2008). To treat demineralised enamel, calcium and phosphate ions are required, in addition to the establishment of a neutral pH. However, at a neutral pH the ions combine to form a sparingly soluble calcium hydrogen phosphate. The amorphous material (ACP) provides supersaturation in the casein fraction (CPP-ACP) and has shown potential remineralising efficiency on tooth enamel (Reynolds, 2008; Reynolds, 2009).

6.1.2 Determination of the degree of enamel demineralisation or remineralisation

The early stage of the caries lesion is manifested as a slight increase in the porosity of the enamel sub-surface region (Kidd *et al.*, 2004) and the more dense hard enamel reflects a higher content of minerals (Bonar *et al.*, 1991). Following this observation, scientists have extensively used the enamel porosity as a parameter to measure the degree of demineralisation or remineralisation of enamel. In addition, the porosity has been utilized for detection of carious lesions using techniques such as quantitative light-induced fluorescence, electrical resistance and radiography (Kidd et al., 2004). Microradiography produces a photographic image obtained by the X-ray absorbance of an enamel slice. Proprietary software is then used to quantify the mineral content in term of volume percentage, as shown in Figure 6.1. The use of microradiography in dental research is mentioned in an early report by Angmar and co-workers in 1963 (cited by Damen *et al.*, 1997) and used in enamel remineralisation analysis (Amaechi *et al.*, 2001).

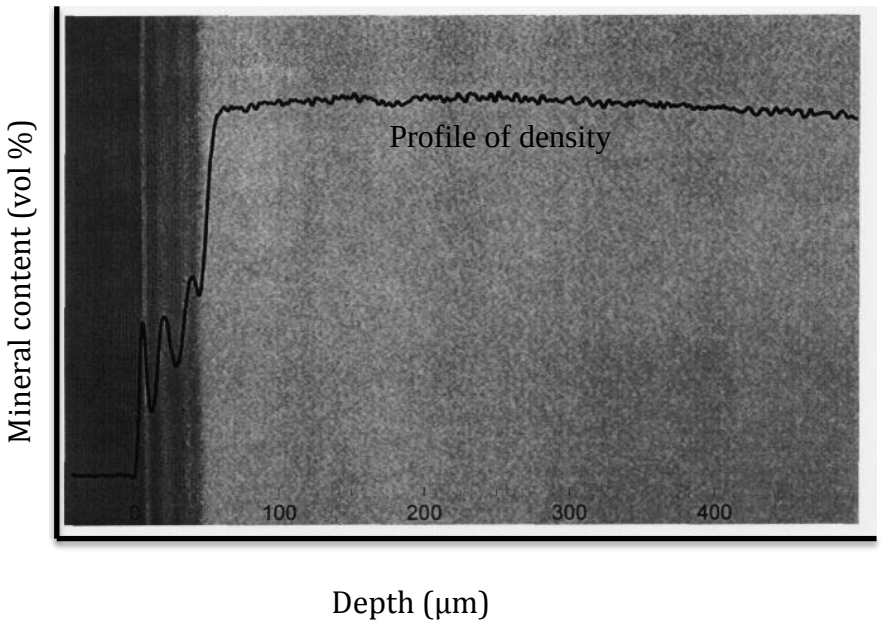

Figure 6.1: A TMR image of bovine enamel with subsurface artificial lesion. From Damen et al. (1997).

The analysis of the relationship between the mechanical characteristics of dental enamel and its microstructure and chemistry facilitates a means to evaluate a range of dental treatments (Cuy et al., 2002). The micro hardness test has been used to analyse the mechanical properties of the tooth enamel by nano-indentation and micro-indentation techniques. The technique of indentation uses a Vicker's indenter (Figure 6.2). Kinney and co-workers have used the nano-indentation technique previously to measure the hardness of human peri-tubular and inter-tubular dentine (Kinney et al., 1996). In addition, nano-indentation has been utilized to investigate the effect of in vitro demineralisation and remineralisation on human tooth enamel (Lippert *et al.*, 2004).

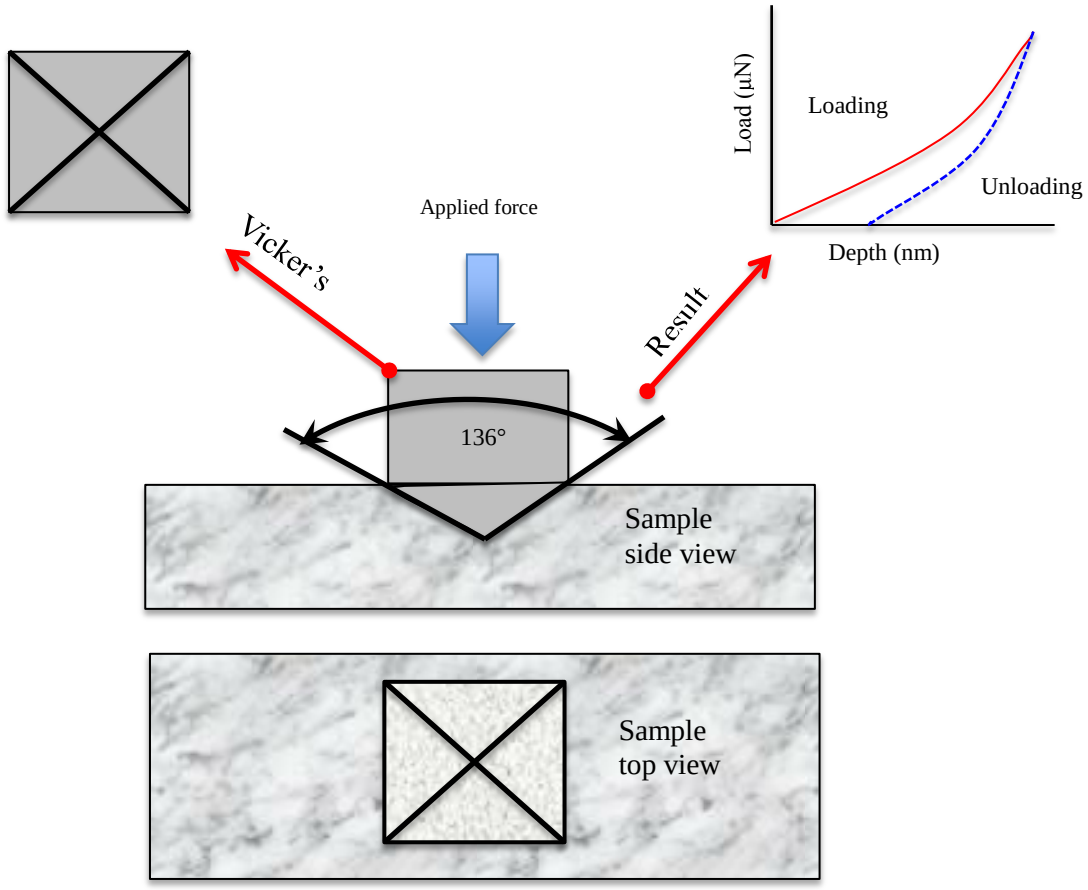

Figure 6.2: Diagram of nanoindentation testing and the profiles result.

Electron probe microanalysis (EPMA) was firstly introduced in dental applications in 1961 by Boyde and colleagues (Boyde *et al.*, 1961) and generally was used in the quantitative determination of the major elements in tooth caries lesions (Ngo *et al.*, 1997). It is a non-destructive elemental analysis at a micron-sized surface. Basically, it provides the quantitative and qualitative determination of the ionization of elements at the focus of the beam by measuring the specific X-ray signature from the surface, as shown in Figure 6.3 (Cameca, 2010).

The use of EPMA has been developed from a qualitative (Besic *et al.*, 1969) to a quantitative analysis of the calcium and phosphorus content in the human teeth (Wirsing *et al.*, 1974); (Sanchez-Quevedo *et al.*, 1998); (Arnold *et al.*, 2007).

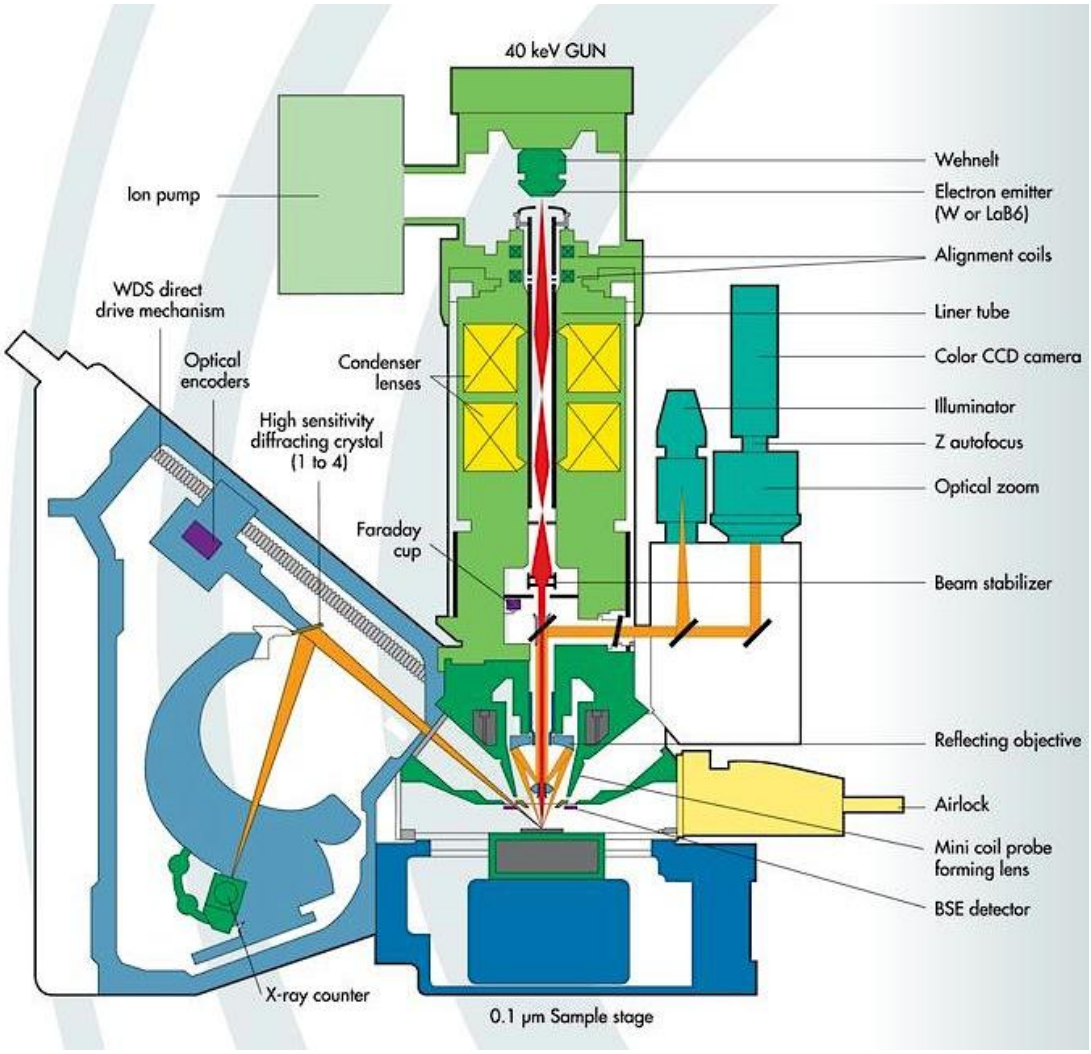

Figure 6.3: Cameca SX100 electron probe microanalysis. From Industry (2011).

6.1.3 Objectives

The objective of the work descried in this chapter was to explore the enamel remineralisation efficiency of 2% (w/v) 4h ahCMC-ACP and HC-ACP containing dental films prepared with a mixture of 2% w/v E10M and 1%w/v F4M using the EPMA technique to quantify the depth of enamel remineralisation. The quantification has to be carried out in depth of the enamel blocks by counts mapping of calcium and phosphorus deposition on the surface of cross-section of enamel blocks.

6.2 Materials and methods

6.2.1 Chemicals

Lactic acid, sodium fluoride, calcium chloride dihydrate and sodium dihydrogen phosphate were purchased from Sigma-Aldrich UK. Artificial saliva Xialine II™ was prepared as mentioned in section 4.2.3.

6.2.2 Teeth samples and enamel blocks

Human incisors were obtained from the University of Dundee / Dental School,

Teeth samples and enamel blocks were kept moist with prepared artificial saliva Xialine II™.

6.2.3 Methods

The demineralisation solution was prepared from calcium chloride dihydrate (2.2mM), sodium dihydrogen phosphate (2.2mM), lactic acid (0.05M), fluoride (0.2ppm as sodium fluoride) and pH was adjusted to 4.5 using 50% w/v sodium hydroxide (Lata *et al.*, 2010). The enamel blocks were prepared by cutting off a plane parallel labial slice of the tooth surface using a high-speed diamond saw as shown in Figure 6.4. The labial surface of the enamel block was flattened by a

diamond disc in order to standardise the surface for remineralisation analysis. Each block had been coated with nail varnish leaving the flattened labial surface exposed for experimentation. The preliminary stage of enamel subsurface carious lesion was generated by immersion of the enamel block into demineralising solution for three days at 37º C. The enamel block with an induced carious lesion was then cross-sectioned into two parts, control and test. The outsides of the samples were also coated with nail varnish. The control was treated by a regimen of daily pH cycling of demineralisation for 3h followed by 21h in prepared artificial saliva of Xialine II™, for five successive days at 37º C. The test samples were treated by application of a pre-wetted piece of the dental film containing ACP, with prepared artificial saliva of Xialine II™, for one hour. The residue of the applied dental film was removed from the sample using tissue and artificial saliva of Xialine II™. Test enamel was then demineralized for 3h followed by 20h in the prepared artificial saliva of Xialine II™. The same regimen was used for five days at 37º C. The treated enamel blocks were then cross sectioned by diamond saw and positioned in acrylic block using cyanoacrylate glue, so that the surface of enamel in depth was exposed to elements mapping for the calcium and phosphorus content. A thin carbon coat was applied under vacuum in order to prevent surface charging by the electron bombardment. A Cameca-SX100 (France) electron probe microanalysis with three wavelength dispersive X-ray detectors (WDX) were used for elements mapping of the calcium and phosphorus deposition on the surface of the enamel block. The measurements were performed using a 10 keV acceleration voltage and 40 nA beam current. X-ray intensities were measured for calcium Kα=3.690 and phosphorus Kα=2.010 (Bruker-Elemental, 2011) simultaneously by three spectrometers, one for calcium and two for phosphorus.

6.2.4 Statistical analysis

The remineralisation effect was measured in term of counts mapping of the calcium and phosphorus atoms deposition at the surface of cross-sectioned enamel blocks. The efficiencies of 2% (w/v) 4h ahCMC-ACP and of 2% (w/v) HC-ACP containing dental films were compared to the control enamels using t-test analysis.

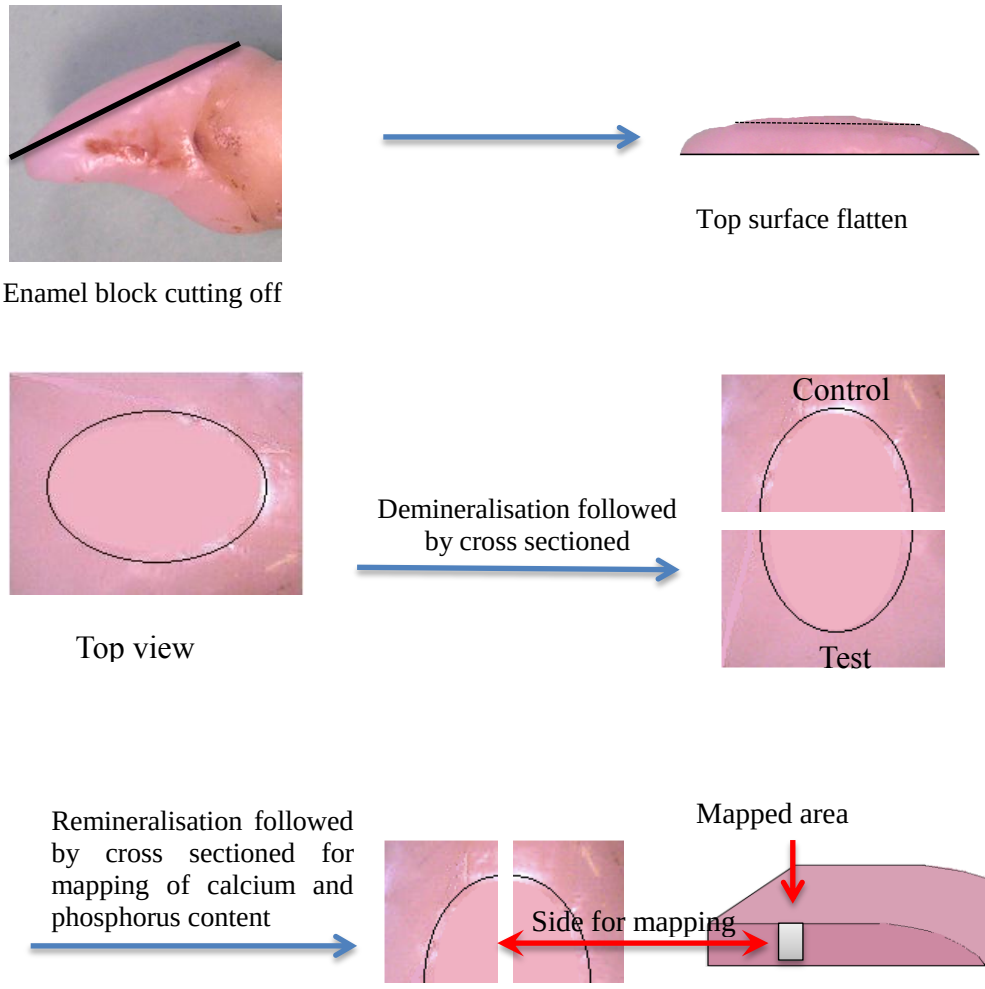

Figure 6.4: Flow diagram illustrating the steps in the remineralisation study on an enamel block and sample preparation for electron probe microanalysis.

6.3 Results

The maps of calcium and phosphorus counts of the control and test enamel blocks were obtained, as shown in Figure 6.5 and Figure 6.6. The test enamel treated by 2% (w/v) 4h ahCMC-ACP containing dental film, showed a higher density of calcium and phosphorus than that in control enamel. The test enamel treated by of 2% (w/v) HC-ACP containing dental film showed a relatively similar elemental density to the control enamel.

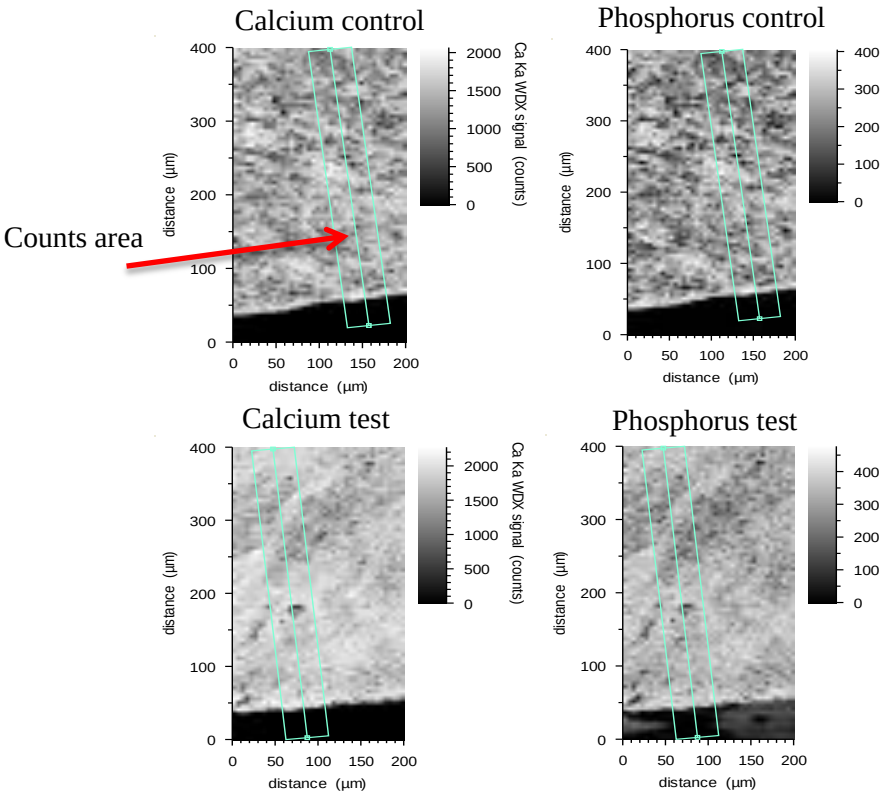

Figure 6.5: The electron probe microanalysis maps of calcium and phosphorus counts of the control and test remineralised enamels with 2% (w/v) 4h ahCMC-ACP containing dental film. The test enamel shows a higher elemental density in comparison to the control enamel using a regimen of remineralisation for 5 days on artificial carious lesion prepared by 3days of demineralisation.

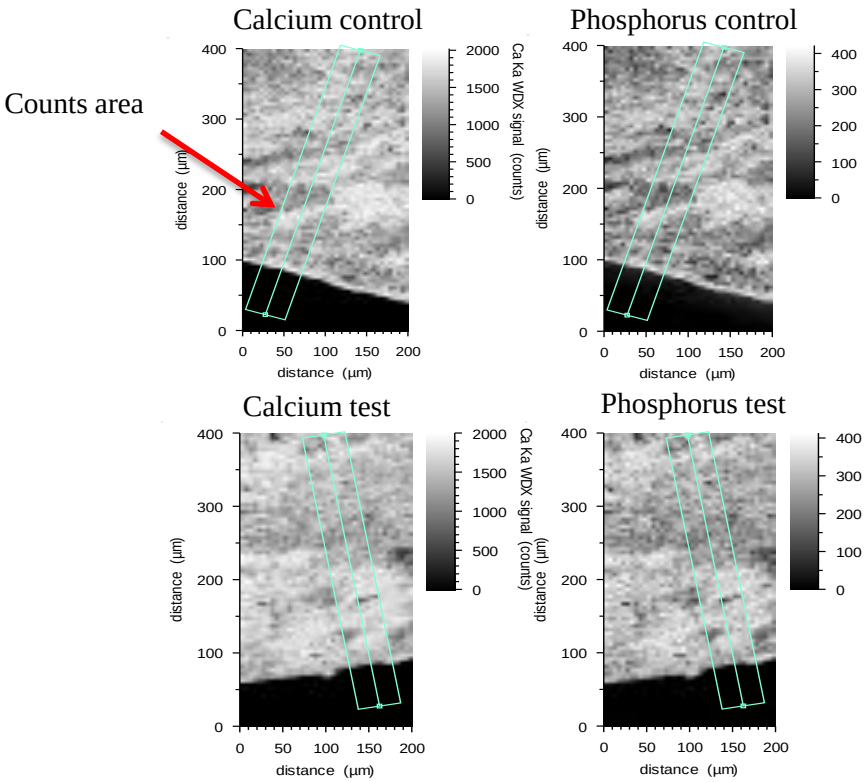

Figure 6.6: The electron probe microanalysis maps of calcium and phosphorus in counts of the control and test remineralised enamels with 2% (w/v) HC-ACP containing dental film. Test enamel shows a relatively similar elemental density in comparison to the control enamel using a regimen of remineralisation for 5 days on artificial carious lesion prepared by 3days of demineralisation.

The maps were scanned into count calcium and phosphorus and the obtained data were transferred into profiles of smooth lined scatter as shown in Figure 6.7 and Figure 6.8 using Microsoft Excel 2011(Mac).

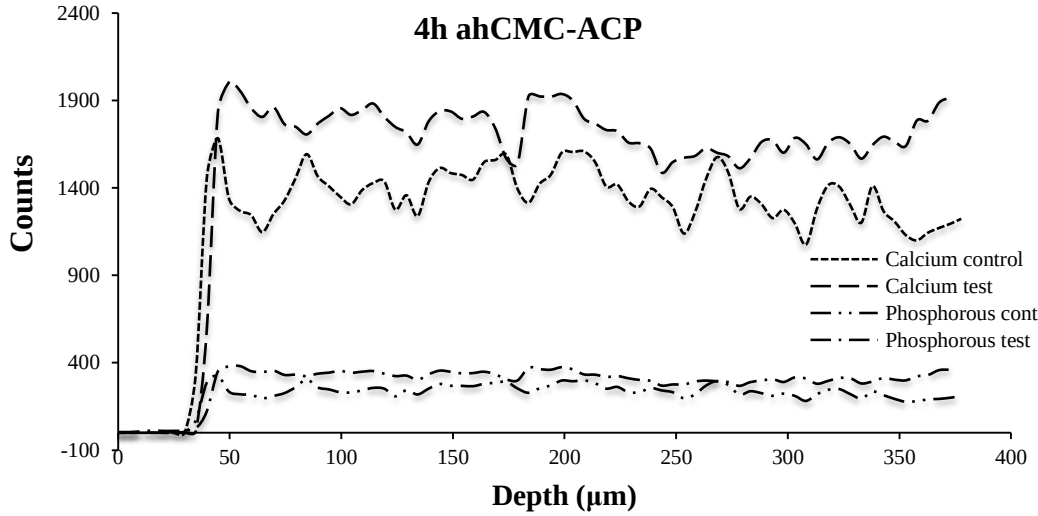

Figure 6.7: Profiles of the calcium and phosphorus counts for control and test enamel treated by of 2% (w/v) 4h ahCMC-ACP containing dental film. Test enamel shows a higher level of elemental counts than that in control enamel using a regimen of remineralisation for 5 days on artificial carious lesion prepared by 3days of demineralisation.

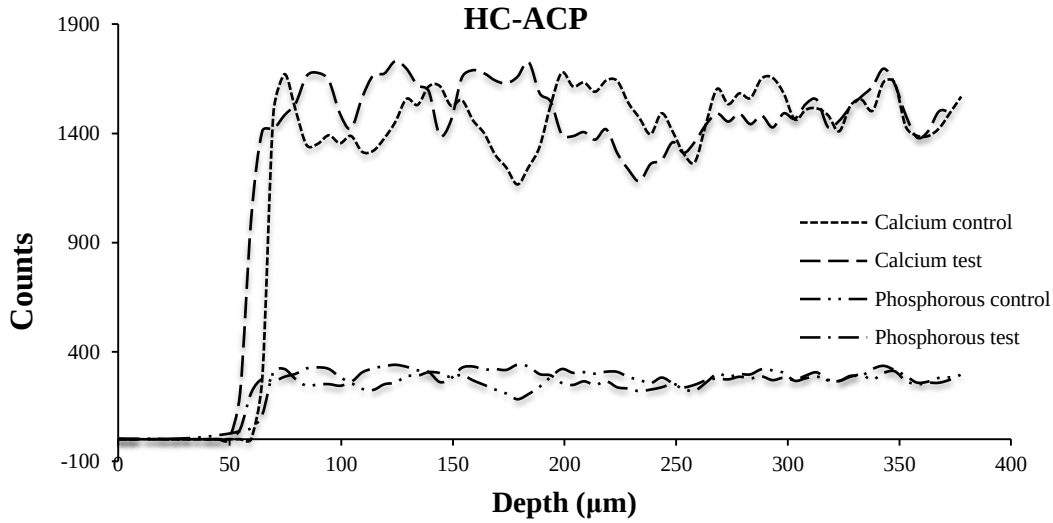

Figure 6.8: Profiles of the calcium and phosphorus counts for control and test enamel treated by of 2% (w/v) HC-ACP containing dental film. Both enamels show relatively similar levels of elemental counts using a regimen of remineralisation for 5 days on artificial carious lesion prepared by 3days of demineralisation.

In order to intensify the differences between the control and test, increasing the period of the preliminary subsurface carious lesion to 6 days was carried out. In addition, the remineralisation regimen on the test enamel was changed to ten successive days of a daily application of dental film for an hour followed by a 3h period of demineralisation and 8h in artificial saliva, another dental film was then applied for an hour, followed by 11h in artificial saliva.

The maps of calcium and phosphorus counts obtained from the modified regimen of remineralisation are shown in Figure 6.9 and Figure 6.10 for 4h ahCMC-ACP and HC-ACP containing dental films respectively. Figure 6.11 and Figure 6.12 show the smoothed profiles transferred from the maps of calcium and phosphorus counts of the enamel blocks.

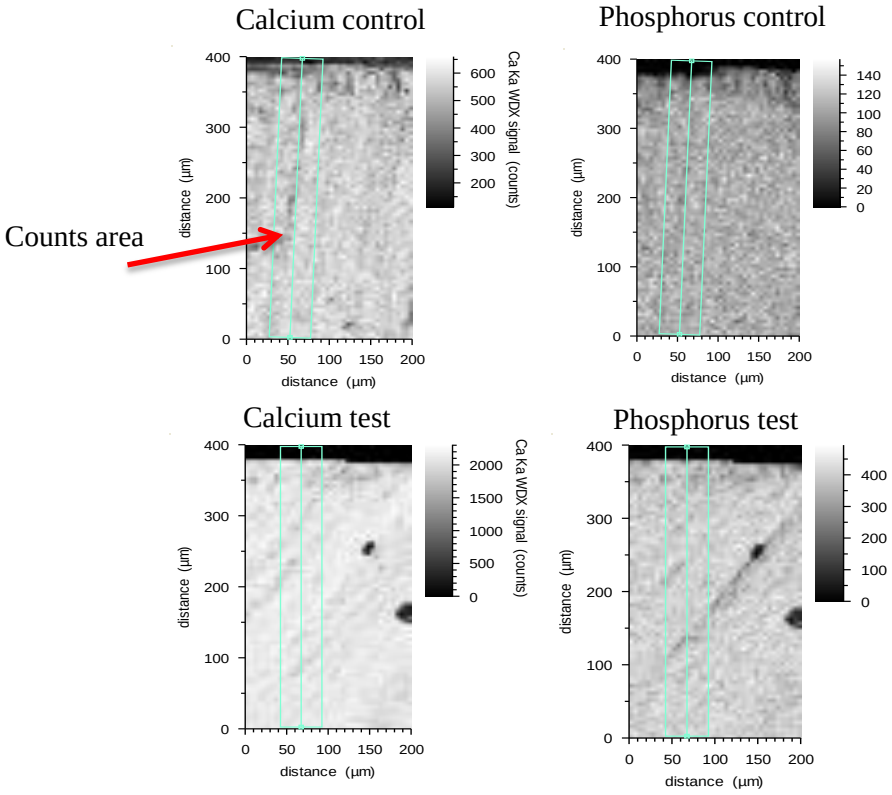

Figure 6.9: The electron probe microanalysis maps of calcium and phosphorus counts in control and test remineralised enamels with 2% (w/v) 4h ahCMC-ACP containing dental film. The test enamel shows a higher elemental density in comparison to the control enamel using a regimen of remineralisation for 10 days on artificial carious lesion prepared by 6 days of demineralisation.

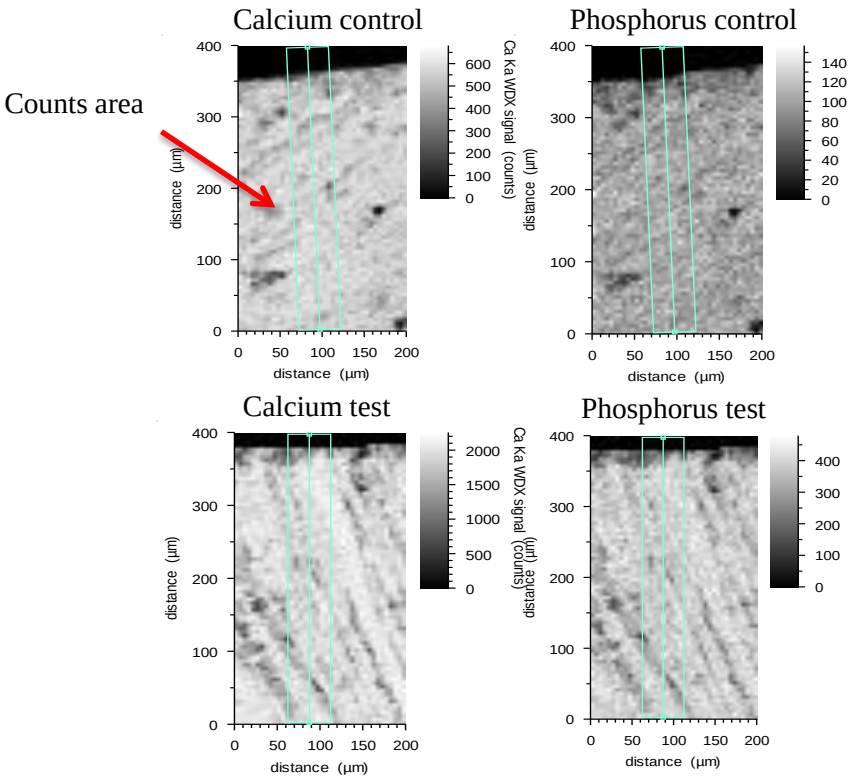

Figure 6.10: The electron probe microanalysis maps of calcium and phosphorus counts in control and test remineralised enamels with 2% (w/v) HC-ACP containing dental film. The test enamel shows a higher elemental density in comparison to the control enamel using a regimen of remineralisation for 10 days on artificial carious lesion prepared by 6 days of demineralisation.

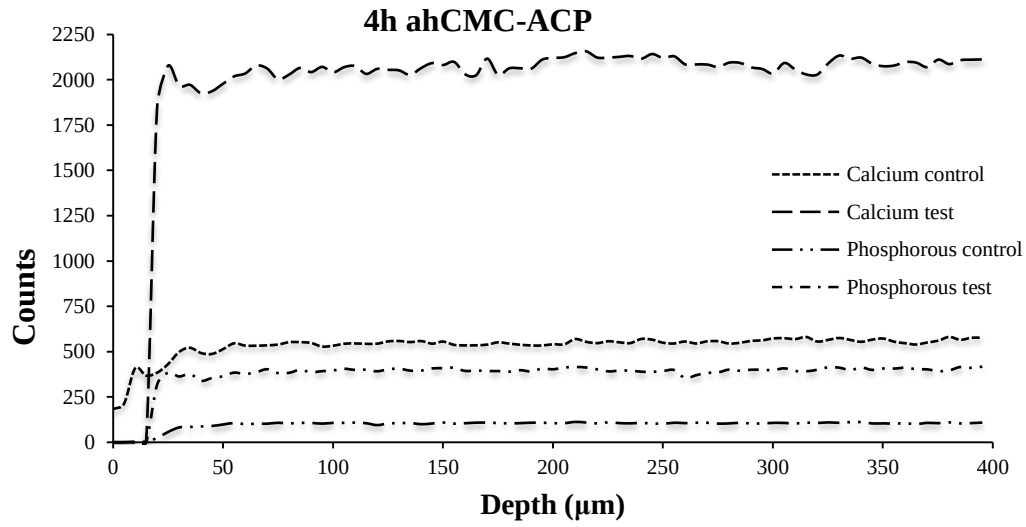

Figure 6.11: Profiles of the calcium and phosphorus counts for control and test enamel remineralised by the modified regimen using of 2% (w/v) 4h ahCMC-ACP containing dental film. The test enamel shows a higher level of elemental counts than that in control enamel using a regimen of remineralisation for 10 days on artificial carious lesion prepared by 6 days of demineralisation.

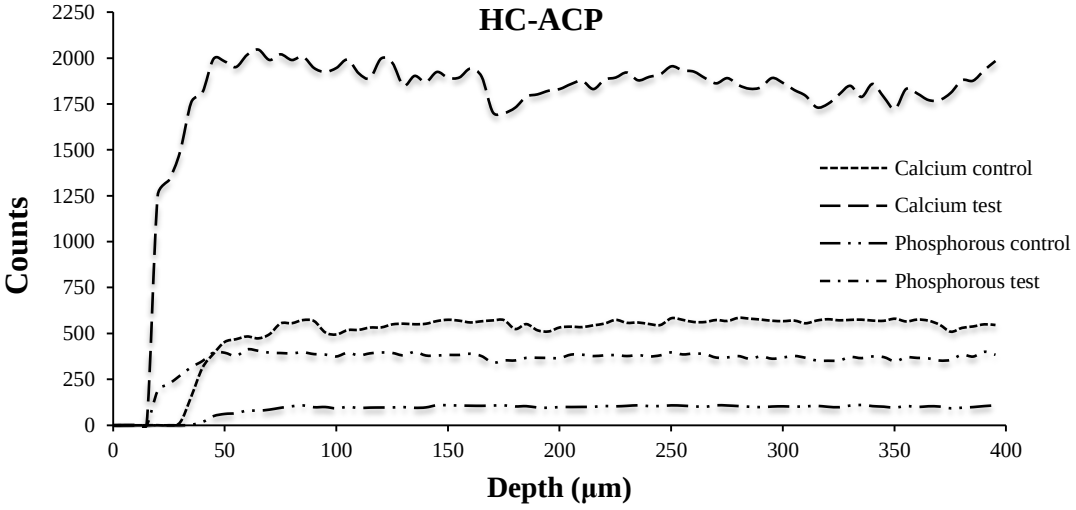

Figure 6.12: Profiles of the calcium and phosphorus counts for control and test enamel remineralised by the modified regimen using 2% (w/v) HC-ACP containing dental film. The test enamel shows a higher level of elemental counts than that in control enamel using a regimen of remineralisation for 10 days on artificial carious lesion prepared by 6 days of demineralisation.

6.1 Discussion

The quantitative evaluation of the change in the calcium and phosphorus density that occurred in the test and control remineralised enamels demonstrated that the EPMA technique was appropriate for this assessment. The first regimen of remineralisation showed a significant ($p<0.05$) remineralisation effect of the 2% (w/v) 4h ahCMC-ACP containing dental film on the enamel samples, While 2% (w/v) HC-ACP containing dental film showed a non-significant remineralisation effect. The difference between the remineralisation effects of the 2% (w/v) 4h ahCMC-ACP and 2% (w/v) HC-ACP containing dental films might be related to the released amount of calcium and phosphorus from the dental films, which correlated to the previously obtained significant higher release of calcium from 2% (w/v) 4h ahCMC-ACP containing dental films in section 4.3.5.6.

The modified regimen of remineralisation showed a significant ($p<0.05$) remineralisation effect of both 2% (w/v) 4h ahCMC-ACP and 2% (w/v) HC-ACP containing dental films. The twice daily applications of dental film significantly intensify the remineralisation efficiency of the prepared dental films that indicates the importance of dosing regimen on the remineralisation, which is might be the cause of the non-benefit of hardening of the previously softened enamel reported by Wegehaupt and colleagues (Wegehaupt *et al.*, 2011)

Finally, the remineralisation effect of the prepared dental films was observed to occur in these experiments up to a depth of 400µm which is much deeper than that obtained by Yamazaki and Margolis of about 150µ (2008). In addition, it did not superficially remineralise the test enamel leaving demineralised areas underneath as was observed using a sugar-free chewing gum containing CPP-ACP (Shen et al., 2001); (Iijima et al., 2004). It is accepted that the type of ACP and regimen used in these experiments were probably closes to optimisation than those previously reported.

6.2 Conclusions

In summary, this study has demonstrate that the EPMA technique showed the capability to quantify the depth of enamel remineralisation throughout the counting of elemental deposition of calcium and phosphorus on the surface of cross-sectioned enamel blocks and a regimen of 6 days preliminary subsurface carious lesion generation and ten days of twice a day application of dental is suitable to obtain an intensified remineralisation effect. Both 2% w/v 4h ahCMC-ACP and 2% w/v HC-ACP containing dental films prepared with a mixture of 2% w/v E10M and 1%w/v F4M had a substantial remineralisation efficiency on human enamel blocks with constant and even deposition of calcium and phosphorus in depth of 400µm.

Chapter 7. Summary and future work.

Dental caries continues to be a major public health problem affecting 60-90 % of school aged children and most adults, although it is mostly an avoidable disease It is a reversible disorder initiated with enamel dissolution by acidic metabolite of the oral flora and, within a certain limit, reversed by remineralisation with saliva enriched with the essential elements at neutral pH. Therefore, the reinforcement of the remineralisation plays an important role in the prevention strategies for dental caries. Based on the chemical microstructure of the human enamel, the dynamic movement from demineralisation to remineralisation involves dissolution and deposition of hydroxyl (in demineralisation), fluoride (in remineralisation), calcium and phosphate. Thus, most prevention strategies depend on the bioavailability of these elements. Fluoridation to decrease dental decay employs fluoridated water, salt and toothpastes. The fluoridation of water has been considered to be the most successful strategy in the developed countries, with each US $ spent saving $8 to $49 in the cost of future dental treatment. This is equivalent to a $4.6 billion annual cost saving in the United States. However, this mass treatment is not without itscritics arguing about effectiveness and warning of the intoxication signs for dental and skeletal fluorosis associated with over dosage. This is a special concern for ingested fluoride supplements.

An alternative proposed the use of toothpaste enriched with fluoride, calcium and phosphate. This concept had been explored, with a realization that there would be a limitation in remineralisation efficiency due to the low solubility of the calcium phosphate salt that forms at neutral pH. For this reason, milk casein in a calcium, citrate and phosphate micellar complex has been suggested as a more suitable ingredient for a remineralisation formulation. Reynolds led investigations using the tryptic digestion of casein, which showed a promising result that led to preparation of CPP-ACP. Following this lead, numerous studies have been conducted on the remineralisation effect of the CPP-ACP loaded into different application forms including solution, chewing gum and toothpaste. Commercially, two brands of MI Tooth mousse GC® and Trident Xtra Care® containing CPP-ACP are available in the market.

The argument developed in this thesis is that, regarding CPP, additional groups might play a role beside the Pse-Pse-Pse-Glu-Glu peptide cluster in the amorphous calcium phosphate complexation. To develop this idea, in the first part of this study, food grade alternatives of HC and NGP extracts were examined. In order to identify the principle and method of the preparation of CPP-ACP, the prepared CPP and NGP were analysed for peptide content using LC-MS. Thereafter, Reynolds's method was adapted to prepare CPP-ACP and NGP-ACP nanocomplexes which were then characterised for particle size analysis. Following this, the preparation of NGP-ACP and HC-ACP nanocomplexes were simplified into a rapid and simpler method by mixing all the components at pH 5 and complexing by pH adjustment to 7. The characterisation of the prepared NGP-ACP and HC-ACP nanocomplexes using conventional nanoparticle size analyzer suggested the developed method was at least equivalent.

A simpler system should be able to bind the phosphate and calcium separately and an important breakthrough was the use of polymers as nanocomplex initiators. It was hypothesised that polymer containing carboxyl groups should be able to stabilise ACP nanocomplexes in the amorphous form. Sodium alginate, pectin and sodium CMC polymers were inspected using the modified method of ACP preparation. ACP was potentially stabilised by pectin and sodium CMC polymers, while sodium alginate produced a gel rather than a complex. Thereafter, the studies focused on the use of sodium CMC as a more promising candidate and an examination of the effect of polymer chain on the particle size of the prepared ACP was carried out. Polymer grades with different molecular weight were used in the preparation of the ACP and produced a decrease in particle size of the prepared ACP that correlated with a decrease in the chain length of the used polymer. In order to prepare ACP with nano sized particles, acid hydrolysis of sodium CMC grade CRT 100 PA of 1 to 7h of hydrolysis time was suggested to produce a polymer with shorter chain length and a nano particle size of about 10nm diameter ACP was efficiently stabilised by a preparation optimally hydrolysed for four hours.

The physical properties of the prepared ACP preparations were studied using conventional analysis techniques. The Zetasizer NanoZS was used for the analysis of the particle size of the prepared colloidal ACP. The SEM imaging to demonstrate the shape and size of prepared NGP-ACP; in spite of this the 4h ahCMC-ACP samples did not clearly reveal the nanocomplexes expected. X-ray powder diffraction analysis and TEM imaging suggested the non-crystalline form in the isolated NGP-ACP, HC-ACP and 4h ahCMC-ACP samples. TGA and DSC analysis showed the lower moisture content of isolated ACP in comparison to the unpurified ACP. DVS analysis of prepared NGP-ACP, HC-ACP and 4h ahCMC-ACP exhibited a less than 20% weight of water uptake at relative humidity of 60% and less.

Future work is required to study the age stability of the amorphous form of the prepared ACP. There was not time in this work to use accelerated stability testing but this should be a relatively simple exercise in future studies. Investigating the holding of the material under different pH conditions will also be important, as the matrix for the complex may vary.

The next step in this series of studies was the formulation of the prepared ACP into a dental film dosage form. Two important physicochemical measurements were required for preformulation study the ACP. These were the determination of calcium content and the pH solubility of the prepared ACP. For both analyses, there was a requirement to measure the calcium ion contents in solutions of ACP. The most conventional methods of calcium determination require complete solution of the calcium, and it was appreciated that ACP preparations might contain non dissolved calcium in ACP complexes. The use of an ion selective electrode was suggested for calcium content and the pH solubility studies. This method had been validated for linearity, precision and reproducibility in addition to the re-measuring of selected samples and standards measured using a second method of inductively coupled plasma mass spectrometry.

The isolation process of ACP demonstrated an increase the calcium content in NGP-ACP and HC-ACP and a decrease in 4h ahCMC-ACP. A higher solubility was

obtained with the 4h ahCMC-ACP sample and the cycle of the pH change showed a reversible solubility of the prepared ACP. The adhesion parameters of prepared polymers hydrogels were used to evaluate the appropriate polymer(s) for dental film formulations. The hydrogel formulations of E10M HPMC grade and a mixture of E10M and F4M (2:1 ratio) HPMC grades were selected for the formulation of dental films containing ACP.

The casting method was suitable for use in the preparation of dental films containing 1 and 2% (w/v) ACP. The two formulations were prepared using 3% (w/v) of HPMC grade E10M and mixture of 1% (w/v) F4M and 2% (w/v) E10M HPMC grades. A series of studies were carried out to characterise the prepared dental films, such as films flexibility, degree of swelling, adhesion, calcium content and calcium release, using a specially designed dissolution cell. The formulation, type and percentage loaded of ACP showed an effect on the flexibility and degree of swelling of the prepared dental films. The rough surface of prepared dental films in NGP-ACP and 4h ahCMC-ACP containing dental film led to a decrease in dental film stickiness.

The calcium release study of the dental films had been projected to use a specially designed dissolution cell that held the sample of the dental film in between of two plastic meshes. The appropriate position of the dissolution cell was investigated by testing four different positions and the dissolution medium flow pattern was inspected by inclusion of colouring agent by cannula into the tube of dissolution medium flow. The solubility of the loaded ACP showed an effect on the calcium release from the dental films and consequently, 4h ahCMC-ACP and HC-ACP containing dental films demonstrated higher calcium release especially from the dental films prepared from a mixture of E10M and F4M.

The kinetic of calcium release from dental films was calculated in order to understand the behaviour and the factors affecting the release. Four kinetics models of zero order, first order, Higuchi and Korsmeyer-Peppas were applied tothe obtained release data. The acquired findings indicated that the calcium release was

controlled by the solubility of the loaded ACP and the polymer behaviour in contact with dissolution media that is mostly occurring in the HPMC based dosage form. In addition, the suggested behaviour of the calcium release was a compromised system of swelling, erosion and diffusion behaviours that shifted toward the predominant one depending on formulations and ACP contents.

The enamel subsurface carious lesion begins after the biofilm formation on the tooth surface and leads to dental caries. In addition, biofilm has been shown to act as a barrier under which demineralisation occurrs. Therefore, a short study targeted the analysis of the tooth surface hydrophobicity and adhesion effect of a biofilm using contact angle measurement and adhesion testing on a selected formula of hydrogel. The biofilm was characterized using an upright fluorescence microscope. In addition, the investigation of the effective inhibitory concentrations of isolated ACP on the biofilm formation was proposed by the addition of the produced isolated ACP into the biofilm culture media. Confocal scanning laser microscope was used to determine the thickness of the *in vitro* orally relevant cultured biofilms as a marker.

The cultured biofilm was found to have little effect on the adhesion properties of prepared hydrogel (15% w/v E10M HPMC grade) on the tooth surface. Besides, the measured hydrophobicity of the tooth surfaces was incomplete. However, it exhibited inter individual variability between tooth samples. Furthermore, optimistic inhibitory effective concentrations on the cultured biofilm were found to be 8% (w/v) from NGP-ACP and HC-ACP and 4% (w/v) from 4h ahCMC-ACP. However, 4% (w/v) 4h ahCMC-ACP showed a similar inhibitition to 8% (w/v).

Further work should be conducted on a higher number of replicates especially on the inhibitory effective concentrations of the ACP on the cultured biofilm. In addition, a quantitative elemental analysis of the calcium and phosphorus in the biofilm should be conducted in order to explore the remineralisation effect of the prepared ACP on tooth surface through the biofilm layer.

The near view end point in this work was projected on the quantification of the enamel remineralisation proficiency of the produced ACP using the dental films that showed the higher calcium release. Therefore, 2% (w/v) 4h ahCMC-ACP and HC-ACP containing dental films with a mixture of 2% (w/v) E10M and 1% (w/v) F4M were selected to conduct this study on human enamel blocks. However, the main challenge was the methodology of quantitative determination of calcium and phosphorus deposition into the depth of the enamel blocks. The microradiography and nano-indentation technologies have been extensively used in the measurement of the enamel change in remineralisation studies. As an alternative, the EPMA method is recommended as better option in the quantification of the calcium and phosphorus into the enamel samples.

Cross sections taken through the remineralised enamel block were used to facilitate estimation of deposition of the minerals using EPMA technology. A recently reported study examined the effects of a regimen of 3 days of preliminary enamel subsurface carious lesion, followed by a 5 day remineralisation period. Our regimen mimicked this as closely as possible in an *in vitro* setting employing dental films containing ACP. The data obtained demonstrated substantial remineralisation efficiency for the 4h ahCMC-ACP containing dental film. This suggests that a modified regimen of 6 days of enamel subsurface carious lesions and ten days of daily twice applications of dental film might amplify the observable effects. Promising significant remineralisation efficiencies were found for both dental films with steadily constant levels of calcium and phosphorus deposition up to a depth of 400μm in the enamel blocks.

Further work is indicated regarding the measurement of the remineralising efficiency of dental film containing ACP using an *in situ* appliance study. Formulation studies might explore additives that enhance the calcium release or increase the loading of ACP with minimum effect on the adhesion properties of the dental film. In addition, in order to find out the most appropriate dosage, alternative dosage forms such as tooth varnish and Denticap loaded with the prepared ACP could be studied and compared with the dental film.

References

Abbona F, Baronnet A (1996). A XRD and TEM study on the transformation of amorphous calcium phosphate in the presence of magnesium. *Journal of Crystal Growth* **165**(1-2)**:** 98-105.

Akbari J, Enayatifard R, Saeedi M, Saghafi M (2011). Influence of Hydroxypropyl Methylcellulose Molecular Weight Grade on Water Uptake, Erosion and Drug Release Properties of Diclofenac Sodium Matrix Tablets. *Tropical Journal of Pharmaceutical Research* **10**(5)**:** 535-541.

Amaechi BT, Higham SM (2001). In vitro remineralisation of eroded enamel lesions by saliva. *J Dent* **29**(5)**:** 371-376.

Ardini F, Magi E, Grotti M (2011). Determination of ultratrace levels of dissolved metals in seawater by reaction cell inductively coupled plasma mass spectrometry after ammonia induced magnesium hydroxide coprecipitation. *Analytica Chimica Acta* **706**(1)**:** 84-88.

Arnold WH, Gaengler P (2007). Quantitative analysis of the calcium and phosphorus content of developing and permanent human teeth. *Annals of anatomy = Anatomischer Anzeiger : official organ of the Anatomische Gesellschaft* **189**(2)**:** 183-190.

Avdeef A, Berger CM, Brownell C (2000). pH-metric solubility. 2: correlation between the acid-base titration and the saturation shake-flask solubility-pH methods. *Pharm Res* **17**(1)**:** 85-89.

Azeredo HM, Mattoso LH, Avena-Bustillos RJ, Filho GC, Munford ML, Wood D, *et al.* (2010). Nanocellulose reinforced chitosan composite films as affected by nanofiller loading and plasticizer content. *J Food Sci* **75**(1)**:** N1-7.

Barbour ME, Shellis RP (2007). An investigation using atomic force microscopy nanoindentation of dental enamel demineralization as a function of undissociated acid concentration and differential buffer capacity. *Physics in Medicine and Biology* **52**(4)**:** 899-910.

Bergstrom CA, Luthman K, Artursson P (2004). Accuracy of calculated pH-dependent aqueous drug solubility. *Eur J Pharm Sci* **22**(5)**:** 387-398.

Besic FC, Knowles CR, Wiemann MR, Keller O (1969). Electron Probe Microanalysis of Noncarious Enamel and Dentin and Calcified Tissues in Mottled Teeth. *Journal of dental research* **48**(1)**:** 131-139.

Bodmeier R, Paeratakul O (1994). Mechanical Properties of Dry and Wet Cellulosic and Acrylic Films Prepared from Aqueous Colloidal Polymer Dispersions Used in the Coating of Solid Dosage Forms. *Pharmaceutical Research* **11**(6)**:** 882-888.

Bonar LC, Shimizu M, Roberts JE, Griffin RG, Glimcher MJ (1991). Structural and composition studies on the mineral of newly formed dental enamel: a chemical, x-ray diffraction, and 31P and proton nuclear magnetic resonance study. *J Bone Miner Res* **6**(11)**:** 1167-1176.

Bonizzi I, Buffoni JN, Feligini M (2009). Quantification of bovine casein fractions by direct chromatographic analysis of milk. Approaching the application to a real production context. *J Chromatogr A* **1216**(1)**:** 165-168.

Borkowska-Burnecka J, Szymczycha-Madeja A, Zyrnicki W (2010). Determination of toxic and other trace elements in calcium-rich materials using cloud point extraction and inductively coupled plasma emission spectrometry. *Journal of hazardous materials* **182**(1-3)**:** 477-483.

Borsa J, Tanczos I, Rusznak I (1990). Acid-Hydrolysis of Carboxymethylcellulose of Low Degree of Substitution. *Colloid Polym Sci* **268**(7)**:** 649-657.

Boskey AL (1997). Amorphous calcium phosphate: The contention of bone. *Journal of dental research* **76**(8)**:** 1433-1436.

Boyde A, Switsur VR, Fearnhead RW (1961). Application of the scanning electron-probe x-ray microanalyser to dental tissues. *J Ultrastruct Res* **5:** 201-207.

Bruker-Elemental (2011). Periodic Table of Elements and X-ray Energies, Energies.pdf PTaX-r (ed). Bruker Nano GmbH

Berlin-Germany: Bruker Elemental

Burns MEP, H. J. (1977). Cellulose ether having low molecular weight and a high degree of methyl substitution. USA: The Procter & Gamble company.

BWB-Technologies (2011). A guide to Flame photometer Ananlysis. In: *BWB Technologies* Vol. 2011. Essex: BWB Technologies UK Ltd.

Cai F, Manton DJ, Shen P, Walker GD, Cross KJ, Yuan Y, *et al.* (2007). Effect of addition of citric acid and casein phosphopeptide-amorphous calcium phosphate to a sugar-free chewing gum on enamel remineralization in situ. *Caries Res* **41**(5)**:** 377-383.

Cai F, Shen P, Morgan MV, Reynolds EC (2003). Remineralization of enamel subsurface lesions in situ by sugar-free lozenges containing casein phosphopeptide-amorphous calcium phosphate. *Aust Dent J* **48**(4)**:** 240-243.

Cameca (2010). Electron Probe Micro-Analysis Vol. 2011: Ametek.

Campos-Aldrete ME, Villafuerte-Robles L (1997). Influence of the viscosity grade and the particle size of HPMC on metronidazole release from matrix tablets. *European Journal of Pharmaceutics and Biopharmaceutics* **43**(2)**:** 173-178.

Cappelezzo M, Capellari CA, Pezzin SH, Coelho LA (2007). Stokes-Einstein relation for pure simple fluids. *The Journal of chemical physics* **126**(22)**:** 224516.

Chakraborty S, Khandai M, Sharma A, Patra Ch N, Patro VJ, Sen KK (2009). Effects of drug solubility on the release kinetics of water soluble and insoluble drugs from HPMC based matrix formulations. *Acta Pharm* **59**(3)**:** 313-323.

Chen F, Wang D (2010). Novel technologies for the prevention and treatment of dental caries: a patent survey. *Expert Opin Ther Pat* **20**(5)**:** 681-694.

Cheremisinoff NP (ed) (1996). *Polymer Characterization Laboratory Techniques and Analysis*. NOYES PUBLICATIONS: New Jersey, U.S.A.

Cilurzo F, Cupone IE, Minghetti P, Buratti S, Selmin F, Gennari CG, *et al.* (2010). Nicotine fast dissolving films made of maltodextrins: a feasibility study. *AAPS PharmSciTech* **11**(4)**:** 1511-1517.

Cilurzo F, Cupone IE, Minghetti P, Selmin F, Montanari L (2008). Fast dissolving films made of maltodextrins. *European Journal of Pharmaceutics and Biopharmaceutics* **70**(3)**:** 895-900.

Cilurzo F, Minghetti P, Selmin F, Casiraghi A, Montanari L (2003). Polymethacrylate salts as new low-swellable mucoadhesive materials. *J Control Release* **88**(1)**:** 43-53.

Cochrane NJ, Saranathan S, Cai F, Cross KJ, Reynolds EC (2008). Enamel subsurface lesion remineralisation with casein phosphopeptide stabilised solutions of calcium, phosphate and fluoride. *Caries Res* **42**(2)**:** 88-97.

Collins A, Deasy P, MacCarthy D, Shanely D (1989). Evaluation of a controlled-release compact containing tetracycline hydrochloride bonded to tooth for the treatment of periodontal disease. *International Journal of Pharmaceutics* **51:** 103.

Costa P, Sousa Lobo JM (2001). Modeling and comparison of dissolution profiles. *Eur J Pharm Sci* **13**(2)**:** 123-133.

Costerton JW, Lewandowski Z, Caldwell DE, Korber DR, Lappin-Scott HM (1995). Microbial biofilms. *Annual review of microbiology* **49:** 711-745.

Cox PJ, Khan KA, Munday DL, Sujja-areevath J (1999). Development and evaluation of a multiple-unit oral sustained release dosage form for S(+)-ibuprofen: preparation and release kinetics. *International Journal of Pharmaceutics* **193**(1)**:** 73-84.

Cross K, Huq N, Reynolds E (2005a). Investigation of the anticariogenic casein phosphopeptide α-S1-casein(59-79) interacting with the mineral ions in amorphous

calcium phosphate, using NMR spectroscopy. *Australian Dental Journal ADRF Special Research Supplement* **50**(4)**:** S10-S11.

Cross KJ, Huq NL, Palamara JE, Perich JW, Reynolds EC (2005b). Physicochemical characterization of casein phosphopeptide-amorphous calcium phosphate nanocomplexes. *Journal of Biological Chemistry* **280**(15)**:** 15362-15369.

Cuy JL, Mann AB, Livi KJ, Teaford MF, Weihs TP (2002). Nanoindentation mapping of the mechanical properties of human molar tooth enamel. *Archives of Oral Biology* **47**(4)**:** 281-291.

Damen JJ, Exterkate RA, ten Cate JM (1997). Reproducibility of TMR for the determination of longitudinal mineral changes in dental hard tissues. *Adv Dent Res* **11**(4)**:** 415-419.

Deakins M (1942). Changes in the Ash, Water, and Organic Content of Pig Enamel During Calcification. *Journal of dental research* **21**(5)**:** 429-435.

Dentaire S (2011). Dentin. In: *Dental information and photography of the world*: Studio Dentaire

Desai SJ, Simonelli AP, Higuchi WI (1965). Investigation of factors influencing release of solid drug dispersed in inert matrices. *J Pharm Sci* **54**(10)**:** 1459-1464.

Dow (2002). Methocel cellulose ethers technical handbook, Company D (ed): Dow Campany.

DowWolff (2009). The ideal hydrocolloid for dairy applications. In: *Food & Nutrition*, Cellulosics DW (ed). Walsrode: Dow Wolff Cellulosics

Eanes ED, Termine JD, Nylen MU (1973). Electron-Microscopic Study of Formation of Amorphous Calcium Phosphate and Its Transformation to Crystalline Apatite. *Calc Tiss Res* **12**(2)**:** 143-158.

Eastoe JE (1979). Enamel protein chemistry--past, present and future. *J Dent Res* **58**(Spec Issue B)**:** 753-764.

Eggert FM, Allen GA, Burgess RC (1973). Amelogenins. Purification and partial characterization of proteins from developing bovine dental enamel. *Biochem J* **131**(3)**:** 471-484.

El-Kamel AH, Ashri LY, Alsarra IA (2007). Micromatricial metronidazole benzoate film as a local mucoadhesive delivery system for treatment of periodontal diseases. *AAPS PharmSciTech* **8**(3)**:** E75.

EL-Khier MKS, Ishag KEA, Yagoub AEGA, and Abu Baker AA (2009). Supplementing Laying Hen Diet with Gum Arabic (*Acacia senegal*): Effect on Egg Production, Shell Thickness and Yolk Content of Cholesterol, Calcium and Phosphorus. *Asian Journal of Poultry Science* **3**(1).

Epstein AK, Pokroy B, Seminara A, Aizenberg J (2011). Bacterial biofilm shows persistent resistance to liquid wetting and gas penetration. *Proceedings of the National Academy of Sciences* **108**(3)**:** 995-1000.

Eremeeva TE, Bykova TO (1998). SEC of mono-carboxymethyl cellulose (CMC) an a wide range of pH; Mark-Houwink constants. *Carbohydrate Polymers* **36**(4)**:** 319-326.

Esposito E, Cortesi R, Cervellati F, Menegatti E, Nastruzzi C (1997). Biodegradable microparticles for sustained delivery of tetracycline to the periodontal pocket: formulatory and drug release studies. *J Microencapsul* **14**(2)**:** 175-187.

Fahs A, Brogly M, Bistac S, Schmitt M (2010). Hydroxypropyl methylcellulose (HPMC) formulated films: Relevance to adhesion and friction surface properties. *Carbohydrate Polymers* **80**(1)**:** 105-114.

Featherstone JD (2008). Dental caries: a dynamic disease process. *Aust Dent J* **53**(3)**:** 286-291.

Fejerskov O, Kidd E, Nyvad B (2008). *Dental caries : the disease and its clinical management*. 2nd edn. Blackwell Munksgaard: Oxford ; Ames, Iowa.

Fosse G (2002). Enamel prisms in multituberculates. How to calculate their numerical density in enamel micrographs. A review. In: *Paleontologisk Museum,* . Oslo, Norway: Universitetet i Oslo.

Garcia-Godoy F, Hicks MJ (2008). Maintaining the integrity of the enamel surface: the role of dental biofilm, saliva and preventive agents in enamel demineralization and remineralization. *J Am Dent Assoc* **139 Suppl:** 25S-34S.

Gloxhuber C, Kunstler K (eds) (1992). *Anionic surfactants Biochemstry, Toxicology, Dermatology*. Marcel Dekker inc.: New York.

Goforth S (2004). Test tube teeth Vol. 2008: University of Wisconsin, Board of Regents.

Granholm K, Ek P, Sokalski T, Harju L, Bobacka J, Ivaska A (2009). Determination of Calcium with Ion-Selective Electrode in Black Liquor from a Kraft Pulping Process. *Electroanalysis* **21**(17-18)**:** 2014-2021.

Gray H, Standring S (2005). *Gray's anatomy : the anatomical basis of clinical practice*. 39th ed. edn. Elsevier Churchill Livingstone: Edinburgh.

Guatelli-Steinberg D, Reid DJ, Bishop TA (2007). Did the lateral enamel of Neandertal anterior teeth grow differently from that of modern humans? *Journal of Human Evolution* **52**(1)**:** 72-84.

Gurgan S, Bolay S, Alacam R (1997). In vitro adherence of bacteria to bleached or unbleached enamel surfaces. *Journal of oral rehabilitation* **24**(8)**:** 624-627.

Hannig M, Hess NJ, Hoth-Hannig W, De Vrese M (2003). Influence of salivary pellicle formation time on enamel demineralization--an in situ pilot study. *Clin Oral Investig* **7**(3)**:** 158-161.

Hazelrigg CO, Dean JA, Fontana M (2003). Fluoride varnish concentration gradient and its effect on enamel demineralization. *Pediatr Dent* **25**(2)**:** 119-126.

Heasman PA, Heasman L, Stacey F, McCracken GI (2001). Local delivery of chlorhexidine gluconate (PerioChip) in periodontal maintenance patients. *J Clin Periodontol* **28**(1)**:** 90-95.

Heinze T, Pfeiffer K (1999). Studies on the synthesis and characterization of carboxymethylcellulose. *Angewandte Makromolekulare Chemie* **266:** 37-45.

Hendricks S, Hill W (1942). The inorganic constitution of bone. *Science* **96:** 255-257.

Hidalgo J, Hansen PMT (1971). Selective Precipitation of Whey Proteins with Carboxymethylcellulose. *Journal of Dairy Science* **54**(9)**:** 1270-1274.

Ho FFL, Klosiewicz DW (1980). Proton Nuclear Magnetic-Resonance Spectrometry for Determination of Substituents and Their Distribution in Carboxymethylcellulose. *Analytical Chemistry* **52**(6)**:** 913-916.

Holt C, Timmins PA, Errington N, Leaver J (1998). A core-shell model of calcium phosphate nanoclusters stabilized by beta-casein phosphopeptides, derived from sedimentation equilibrium and small-angle X-ray and neutron-scattering measurements. *European Journal of Biochemistry* **252**(1)**:** 73-78.

Holt C, Wahlgren NM, Drakenberg T (1996). Ability of a beta-casein phosphopeptide to modulate the precipitation of calcium phosphate by forming amorphous dicalcium phosphate nanoclusters. *Biochemical Journal* **314:** 1035-1039.

Hope CK, Wilson M (2003). Measuring the thickness of an outer layer of viable bacteria in an oral biofilm by viability mapping. *J Microbiol Methods* **54**(3)**:** 403-410.

Hunter NE, Frampton CS, Craig DQM, Belton PS (2010). The use of dynamic vapour sorption methods for the characterisation of water uptake in amorphous trehalose. *Carbohydrate Research* **345**(13)**:** 1938-1944.

Iijima Y, Cai F, Shen P, Walker G, Reynolds C, Reynolds EC (2004). Acid resistance of enamel subsurface lesions remineralized by a sugar-free chewing gum containing casein phosphopeptide-amorphous calcium phosphate. *Caries Res* **38**(6)**:** 551-556.

Industry D (2011). CAMECA SX 100. In: *Cameca* Vol. 2011.

Ishida M, Nambu N, Nagai T (1982). Mucosal dosage form of lidocaine for toothache using hydroxypropyl cellulose and carbopol. *Chem Pharm Bull (Tokyo)* **30**(3)**:** 980-984.

Jain N, Jain GK, Javed S, Iqbal Z, Talegaonkar S, Ahmad FJ, *et al.* (2008). Recent approaches for the treatment of periodontitis. *Drug Discov Today* **13**(21-22)**:** 932-943.

Jeffery GH, Bassett J, Mendham J, Denney R (eds) (1989). *Vogel's Textbook of quantitative chemical analysis*. Longman Group UK Limited: Essex.

Kanekanian AD, Williams RJH, Brownsell VL, Andrews AT (2008). Caseinophosphopeptides and dental protection: Concentration and pH studies. *food chemistry* **107**(3)**:** 1015-1021.

Keith AD (1990). Chlorhexidine complex. In: *United States Patent*, Patent US (ed), p 4. USA: Zetachron, Inc.

Keyes PH (1958). Dental caries in the molar teeth of rats. II. A method for diagnosing and scoring several types of lesions simultaneously. *J Dent Res* **37**(6)**:** 1088-1099.

Khan AM, Maheshwari RK (2011). Studies of relationship between swelling and drug release in the sustained release hydrophilic matrices containing different grades of hydroxypropylmethylcellulose. *Research Journal of Pharmaceutical, Biological and Chemical Sciences* **2**(4)**:** 970-975.

Khunawattanakul W, Puttipipatkhachorn S, Rades T, Pongjanyakul T (2010). Chitosan-magnesium aluminum silicate nanocomposite films: physicochemical characterization and drug permeability. *Int J Pharm* **393**(1-2)**:** 219-229.

Kibbe AH (2000). Handbook of pharmaceutical excipients, Rowe RC, Quinn ME, Sheskey PJ (eds): American pharmaceutical association and pharmaceutical press.

Kidd EAM, Fejerskov O (2004). What Constitutes Dental Caries? Histopathology of Carious Enamel and Dentin Related to the Action of Cariogenic Biofilms. *Journal of dental research* **83**(suppl 1)**:** C35-C38.

Kinney JH, Balooch M, Marshall SJ, Marshall Jr GW, Weihs TP (1996). Hardness and young's modulus of human peritubular and intertubular dentine. *Archives of Oral Biology* **41**(1)**:** 9-13.

Kjeldsen F, Savitski MM, Nielsen ML, Shi L, Zubarev RA (2007). On studying protein phosphorylation patterns using bottom-up LC-MS/MS: the case of human alpha-casein. *The Analyst* **132**(8)**:** 768-776.

König KG MTMH (1958). Methodik der Kurzfristig Erzeugten Rattenkaries. *Dt Zahn-, Mund- u Kieferheilk* **29:** 99-127.

Korsmeyer RW, Gurny R, Doelker E, Buri P, Peppas NA (1983). Mechanisms of solute release from porous hydrophilic polymers. *International Journal of Pharmaceutics* **15**(1)**:** 25-35.

Kreider KA, Stratmann RG, Milano M, Agostini FG, Munsell M (2001). Reducing children's injection pain: lidocaine patches versus topical benzocaine gel. *Pediatr Dent* **23**(1)**:** 19-23.

Kumar VL, Itthagarun A, King NM (2008). The effect of casein phosphopeptide-amorphous calcium phosphate on remineralization of artificial caries-like lesions: an in vitro study. *Aust Dent J* **53**(1)**:** 34-40.

Kumosinski TF, Brown EM, Farrell HM, Jr. (1991). Three-dimensional molecular modeling of bovine caseins: alpha s1-casein. *J Dairy Sci* **74**(9)**:** 2889-2895.

Kumosinski TF, Brown EM, Farrell HM, Jr. (1993). Three-dimensional molecular modeling of bovine caseins: an energy-minimized beta-casein structure. *J Dairy Sci* **76**(4)**:** 931-945.

Larsen MJ (1975). Degrees of Saturation with Respect to Apatites in Parotid Saliva at Various Ph Values. *Scandinavian Journal of Dental Research* **83**(1)**:** 7-12.

Lata S, Varghese NO, Varughese JM (2010). Remineralization potential of fluoride and amorphous calcium phosphate-casein phospho peptide on enamel lesions: An in vitro comparative evaluation. *J Conserv Dent* **13**(1)**:** 42-46.

Lavdas M (2010). Your request at Dow: WALOCEL CRT Molecular Weight, p 1. Dow Europe GmbH Customer Technical Support Center - Performance Chemicals.

Lelah MD, Grasel TG, Pierce JA, Cooper SL (1985). The Measurement of Contact Angles on Circular Tubing Surfaces Using the Captive Bubble Technique. *Journal of Biomedical Materials Research* **19**(9)**:** 1011-1015.

Li F, Chai ZG, Sun MN, Wang F, Ma S, Zhang L, *et al.* (2009). Anti-biofilm effect of dental adhesive with cationic monomer. *J Dent Res* **88**(4)**:** 372-376.

Li YB, Weng WJ, Cheng K, Du PY, Shen G, Wang JX, *et al.* (2003). Preparation of amorphous calcium phosphate in the presence of poly(ethylene glycol). *Journal of Materials Science Letters* **22**(14)**:** 1015-1016.

Liew KB, Tan YT, Peh KK (2011). Characterization of Oral Disintegrating Film Containing Donepezil for Alzheimer Disease. *AAPS PharmSciTech*.

Lin S-Y, Lee C-J, Lin Y-Y (1995). Drug-polymer interaction affecting the mechanical properties, adhesion strength and release kinetics of piroxicam-loaded Eudragit E films plasticized with different plasticizers. *Journal of Controlled Release* **33**(3)**:** 375-381.

Lippert F, Parker DM, Jandt KD (2004). In vitro demineralization/remineralization cycles at human tooth enamel surfaces investigated by AFM and nanoindentation. *J Colloid Interface Sci* **280**(2)**:** 442-448.

Liu L, Fishman ML, Kost J, Hicks KB (2003). Pectin-based systems for colon-specific drug delivery via oral route. *Biomaterials* **24**(19)**:** 3333-3343.

Liu X, Kresevic J (2009). Bioadhesive film Vol. AA61K31565FI, AA61K31565FI edn, pp 1-19. USA: Wyeth Madison, NJ, US.

Lopez J-P, Melbouci M, Dewald G (1999). Toothpaste compositions containing fluidized polymer suspensions of carboxymethyl cellulose. In: *United States Patent*, Patent US (ed). USA.

Losee FL, Van Reen R, Peckham SC, Hess WC, Henderson N, Gerende LJ (1957). Dietary casein-sucrose ratios and their effects on mineralized tissues. *J Dent Res* **36**(6)**:** 904-910.

Luh BS, Niketic G (1959). Flame photometric determination of calcium, magnesium, and potassium in canned tomatoes *Journal of Food Science* **24**(3)**:** 305-309.

Mantelle JA (2008). *DentiPatch Development*. Second edn, vol. 1. MARCEL DEKKER AG: USA.

Manuilov AV, Radziejewski CH, Lee DH (2011). Comparability analysis of protein therapeutics by bottom-up LC-MS with stable isotope-tagged reference standards. *MAbs* **3**(4)**:** 387-395.

Margolis HC (1990). An assessment of recent advances in the study of the chemistry and biochemistry of dental plaque fluid. *J Dent Res* **69**(6)**:** 1337-1342.

Marsh PD (2005). Dental plaque: biological significance of a biofilm and community life-style. *J Clin Periodontol* **32 Suppl 6:** 7-15.

Martin A (ed) (1993). *Physical Pharmacy*. Wiliams &Wilkins: Baltimore, Maryland.

Merck SeQuant AB (2009). ZIC-HILIC: Merk.

Merle L, Charpentier D, Mocanu G, Chapelle S (1999). Comparison of the distribution pattern of associative carboxymethylcellulose derivatives. *European Polymer Journal* **35**(1)**:** 1-7.

Mettler-Tolledo (2010). perfectION™ Combination calcium Electrode Succeful Ion Measurement. In: *perfectION™ Guide Book,* AG MT (ed): Mettler-Toledo AG.

Miquel E, Gomez JA, Alegria A, Barbera R, Farre R, Recio I (2006). Identification of casein phosphopeptides after simulated gastrointestinal digestion by tandem mass spectrometry. *Eur Food Res Technol* **222**(1-2)**:** 48-53.

Miquel E, Gomez JA, Alegria A, Barbera R, Farre R, Recio I (2005). Identification of casein phosphopeptides released after simulated digestion of milk-based infant formulas. *J Agric Food Chem* **53**(9)**:** 3426-3433.

Moosavi-Nasab M, Yousefi AR, Askari H, Bakhtiyari M (2010). Fermentative Production and Characterization of Carboxymethyl Bacterial Cellulose Using Date Syrup. *World Academy of Science, Engineering and Technology* **68:** 1467-1971.

Morgan MV, Adams GG, Bailey DL, Tsao CE, Fischman SL, Reynolds EC (2008). The anticariogenic effect of sugar-free gum containing CPP-ACP nanocomplexes on approximal caries determined using digital bitewing radiography. *Caries Res* **42**(3)**:** 171-184.

Murata Y, Miyashita M, Kofuji K, Miyamoto E, Kawashima S (2004). Drug release properties of a gel bead prepared with pectin and hydrolysate. *Journal of Controlled Release* **95**(1)**:** 61-66.

Ngo H, Ruben J, Arends J, White D, Mount GJ, Peters MCRB, *et al.* (1997). Electron Probe Microanalysis and Transverse Microradiography Studies of Artificial Lesions in Enamel and Dentin: A Comparative Study. *Advances in Dental Research* **11**(4)**:** 426-432.

Nicoli S, Penna E, Padula C, Colombo P, Santi P (2006). New transdermal bioadhesive film containing oxybutynin: In vitro permeation across rabbit ear skin. *International Journal of Pharmaceutics* **325**(1–2)**:** 2-7.

Nobbmann U, Morfesis A (2009). Light scattering and nanoparticles. *Materials Today* **12**(5)**:** 52-54.

Okamoto H, Nakamori T, Arakawa Y, Iida K, Danjo K (2002). Development of polymer film dosage forms of lidocaine for buccal administration: II. Comparison of preparation methods. *J Pharm Sci* **91**(11)**:** 2424-2432.

Okamoto H, Taguchi H, Iida K, Danjo K (2001). Development of polymer film dosage forms of lidocaine for buccal administration. I. Penetration rate and release rate. *J Control Release* **77**(3)**:** 253-260.

Oliveira DMMA, Torres CP, Gomes-Silva JM, Chinelatti MA, De Menezes FC, Palma-Dibb RG, *et al.* (2010). Microstructure and mineral composition of dental enamel of permanent and deciduous teeth. *Microsc Res Techniq* **73**(5)**:** 572-577.

Padula C, Colombo G, Nicoli S, Catellani PL, Massimo G, Santi P (2003). Bioadhesive film for the transdermal delivery of lidocaine: in vitro and in vivo behavior. *J Control Release* **88**(2)**:** 277-285.

Page RC, Offenbacher S, Schroeder HE, Seymour GJ, Kornman KS (2000). Advances in the pathogenesis of periodontitis: summary of developments, clinical implications and future directions. *Periodontol 2000* **14:** 216-248.

Peppas NA (1985). Analysis of Fickian and non-Fickian drug release from polymers. *Pharm Acta Helv* **60**(4)**:** 110-111.

Perioli L, Ambrogi V, Angelici F, Ricci M, Giovagnoli S, Capuccella M, *et al.* (2004). Development of mucoadhesive patches for buccal administration of ibuprofen. *J Control Release* **99**(1)**:** 73-82.

Persson BNJ, Tosatti E (2001). The effect of surface roughness on the adhesion of elastic solids. *The Journal of Chemical Physics* **115**(12)**:** 5597-2610.

Pharmacopoeia B (2012). The British Pharmacopoeia. In: *Calcium*, Office S (ed) Vol. 1&2, p v. London Great Britain: London : Published for the General Medical Council by Constable & Co.

Pizzi A, Mittal KL (eds) (2003). *Handbook of adhesive technology* Marcel Dekker: New York.

Pongjanyakul T, Puttipipatkhachorn S (2007). Xanthan-alginate composite gel beads: molecular interaction and in vitro characterization. *Int J Pharm* **331**(1)**:** 61-71.

Preetha A, Banerjee R (2005). Comparison of Artificial Saliva Substitutes. *Trends Biomater. Artif. Organs* **18**(2)**:** 178-187.

Pungor E (1998). The Theory of Ion-Selective Electrodes. *Anal Sci* **14**(2)**:** 249-256.

Quirynen M, Brecx M, Steenberghe D (2005). Biofilms: Recent Advances In Their Study And Control. In: *Biofilms in the Oral Cavity: Impact of Surface Characteristics*, Evans LV (ed). Amsterdam: Taylor & Francis.

Rahiotis C, Vougiouklakis G, Eliades G (2008). Characterization of oral films formed in the presence of a CPP-ACP agent: an in situ study. *J Dent* **36**(4)**:** 272-280.

Ramalingam L, Messer LB, Reynolds EC (2005). Adding casein phosphopeptide-amorphous calcium phosphate to sports drinks to eliminate in vitro erosion. *Pediatr Dent* **27**(1)**:** 61-67.

Rathbone MJ, Hadgraft J, Roberts MS (eds) (2003). *Modified-realease drug delivery technology*. Marcel Dekker inc.: New York.

Raynaud S, Champion E, Bernache-Assollant D, Thomas P (2002). Calcium phosphate apatites with variable Ca/P atomic ratio I. Synthesis, characterisation and thermal stability of powders. *Biomaterials* **23**(4)**:** 1065-1072.

Reynolds E (1991). Anticariogenic Phosphopepotides, Patents US (ed) Vol. 5015628, p 8. USA.

Reynolds EC (1999). Anticariogenic casein phosphopeptides. *Protein and Peptide Letters* **6**(5)**:** 295-303.

Reynolds EC (2008). Calcium phosphate-based remineralization systems: scientific evidence? *Aust Dent J* **53**(3)**:** 268-273.

Reynolds EC (2009). Casein Phosphopeptide-Amorphous Calcium Phosphate: The Scientific Evidence. *Advances in Dental Research* **21**(1)**:** 25-29.

Reynolds EC (1987). The prevention of sub-surface demineralization of bovine enamel and change in plaque composition by casein in an intra-oral model. *J Dent Res* **66**(6)**:** 1120-1127.

Reynolds EC (1997). Remineralization of enamel subsurface lesions by casein phosphopeptide-stabilized calcium phosphate solutions. *Journal of dental research* **76**(9)**:** 1587-1595.

Reynolds EC, Black CL (1987). Reduction of cholate's cariogenicity by supplementation with sodium caseinate. *Caries Res* **21**(5)**:** 445-451.

Reynolds EC, Cai F, Shen P, Walker GD (2003). Retention in plaque and remineralization of enamel lesions by various forms of calcium in a mouthrinse or sugar-free chewing gum. *J Dent Res* **82**(3)**:** 206-211.

Reynolds EC, Cain CJ, Webber FL, Black CL, Riley PF, Johnson IH, *et al.* (1995). Anticariogenicity of calcium phosphate complexes of tryptic casein phosphopeptides in the rat. *J Dent Res* **74**(6)**:** 1272-1279.

Reynolds EC, del Rio A (1984). Effect of casein and whey-protein solutions on caries experience and feeding patterns of the rat. *Arch Oral Biol* **29**(11)**:** 927-933.

Reynolds EC, Riley PF, Adamson NJ (1994). A selective precipitation purification procedure for multiple phosphoseryl-containing peptides and methods for their identification. *Anal Biochem* **217**(2)**:** 277-284.

Robinson C, Shore RC, Brookes SJ, Strafford S, Wood SR, Kirkham J (2000). The Chemistry of Enamel Caries. *Critical Reviews in Oral Biology & Medicine* **11:** 481-495.

Rowe RC, Quinn ME, Sheskey PJ (eds) (2009). *Handbook of Pharmaceutical Excipients*. Pharmaceutical Press London, UK.

Russell TP (2002). Surface-Responsive Materials. *Science* **297**(5583)**:** 964-967.

Sai Cheong Wan L, Wan Sia Heng P, Fun Wong L (1995). Matrix swelling: A simple model describing extent of swelling of HPMC matrices. *International Journal of Pharmaceutics* **116**(2)**:** 159-168.

Sanchez-Quevedo MC, Nieto-Albano OH, Garcia JM, Gomez de Ferraris ME, Campos A (1998). Electron probe microanalysis of permanent human enamel and dentine. A methodological and quantitative study. *Histology and histopathology* **13**(1)**:** 109-113.

Sangeetha S, Deepika K, Thrishala B, Ch.Chaitanya, Damodharan.N HGA (2010). Formulation and in vitro evaluation of sodium alginate nanospheres containing ofloxacin. *Internation Journal of Applied Pharmaceutics* **2**(4)**:** 1-3.

Schirrmeister JF, Seger RK, Altenburger MJ, Lussi A, Hellwig E (2007). Effects of various forms of calcium added to chewing gum on initial enamel carious lesions in situ. *Caries Res* **41**(2)**:** 108-114.

Seadeek C, Ando H, Bhattachar SN, Heimbach T, Sonnenberg JL, Blackburn AC (2007). Automated approach to couple solubility with final pH and crystallinity for pharmaceutical discovery compounds. *J Pharm Biomed Anal* **43**(5)**:** 1660-1666.

Selwitz RH, Ismail AI, Pitts NB (2007). Dental caries. *Lancet* **369**(9555)**:** 51-59.

Semalty M, Semalty A, Kumar G (2008). Formulation and characterization of mucoadhesive buccal films of glipizide. *Indian J Pharm Sci* **70**(1)**:** 43-48.

Shafiei L, Mortazavi M, Ghanizadeh A (2008). Comparison of the Efficacy of Lidocaine Patch and Benzocaine Gel

in Reducing Injection Pain in Children. *Journal of Dentistry of Shiraz University of Medical Sciences* **9**(2)**:** 190-198.

Shen P, Cai F, Nowicki A, Vincent J, Reynolds EC (2001). Remineralization of enamel subsurface lesions by sugar-free chewing gum containing casein phosphopeptide-amorphous calcium phosphate. *J Dent Res* **80**(12)**:** 2066-2070.

Shifrovitch Y, Binderman I, Bahar H, Berdicevsky I, Zilberman M (2009). Metronidazole-Loaded Bioabsorbable Films as Local Antibacterial Treatment of Infected Periodontal Pockets. *Journal of Periodontology* **80**(2)**:** 330-337.

Sigma (2011). Trypsin from porcine pancreas Vol. 2011, p Product properties: Sigma-Aldrich Co. LLC.

Silcock P, Bridger L, Keer A, Ferguson M (2009). Phosphoprotein preparations for bioactive metal ion delivary and teeth remineralisation Patent U (ed). USA.

Singleton S, Treloar R, Warren P, Watson GK, Hodgson R, Allison C (1997). Methods for microscopic characterization of oral biofilms: analysis of colonization, microstructure, and molecular transport phenomena. *Adv Dent Res* **11**(1)**:** 133-149.

Siqueira WL, Oppenheim FG (2009). Small molecular weight proteins/peptides present in the in vivo formed human acquired enamel pellicle. *Arch Oral Biol* **54**(5)**:** 437-444.

Smetana AJ, Hayes J, Yeh K-C, McCulloch L (1999). Treatment of Dental Hypersensitivity. In: *United States Patent*, Patent US (ed), p 5. USA.

Smith CE (1998). Cellular and chemical events during enamel maturation. *Crit Rev Oral Biol Med* **9**(2)**:** 128-161.

Southward CR (2008). Casein Products, pp 1-13: Consumer and Applications Science Section, New Zealand Dairy Research Institute.

Sriamornsak P, Sungthongjeen S (2007). Modification of theophylline release with alginate gel formed in hard capsules. *AAPS PharmSciTech* **8**(3)**:** E1-E8.

Sugano K, Kato T, Suzuki K, Keiko K, Sujaku T, Mano T (2006). High throughput solubility measurement with automated polarized light microscopy analysis. *J Pharm Sci* **95**(10)**:** 2115-2122.

Sun LM, Chow LC, Frukhtbeyn SA, Bonevich JE (2010). Preparation and Properties of Nanoparticles of Calcium Phosphates With Various Ca/P Ratios. *Journal of Research of the National Institute of Standards and Technology* **115**(4)**:** 243-255.

Tayle P (ed) (1988). *Drug delivery devices*. Marcel Dekker: New York and Basel.

Termine JD, Belcourt AB, Christner PJ, Conn KM, Nylen MU (1980). Properties of dissociatively extracted fetal tooth matrix proteins. I. Principal molecular species in developing bovine enamel. *J Biol Chem* **255**(20)**:** 9760-9768.

Termine JD, Peckauskas RA, Posner AS (1970). Calcium phosphate formation in vitro. II. Effects of environment on amorphous-crystalline transformation. *Arch Biochem Biophys* **140**(2)**:** 318-325.

Termine JD, Posner AS (1970). Calcium phosphate formation in vitro. I. Factors affecting initial phase separation. *Arch Biochem Biophys* **140**(2)**:** 307-317.

Thakur BR, Singh RK, Handa AK (1997). Chemistry and uses of pectin--a review. *Crit Rev Food Sci Nutr* **37**(1)**:** 47-73.

Thylstrup A, Fejerskov O (eds) (1994). *Textbook of Clinical Cariology*. Munksgaard: Copenhagen.

Vais AE, Palazoglu TK, Sandeep KP, Daubert CR (2002). Rheological Characterization Of Carboxymethylcellulose Solution Under Aseptic Processing Conditions. *Journal of Food Process Engineering* **25**(1)**:** 41-61.

Warshawsky H (1989). Oraganization of Crystals in Enamel. *The Anatomy Record* **224:** 242-262.

Washington N, Wilson CG, Davis SS (1985). Evaluation of ' raft-forming' antacid neutralizing capacity: in vitro and in vivo correlations. *International Journal of Pharmaceutics* **27:** 279-286.

Wegehaupt FJ, Taubock TT, Stillhard A, Schmidlin PR, Attin T (2011). Influence of extra- and intra-oral application of CPP-ACP and fluoride on re-hardening of eroded enamel. *Acta Odontol Scand***:** 1-7.

Whitaker EJ (2006). Primary, secondary and tertiary treatment of dental caries: a 20-year case report. *Journal of the American Dental Association* **137**(3)**:** 348-352.

White DJ (1987). Use of Synthetic Polymer Gels for Artificial Carious Lesion Preparation. *Caries Research* **21**(3)**:** 228-242.

Wirsing A, Judd G, Ansell GS (1974). Electron probe microanalysis of human enamel microstructure. *J Dent Res* **53**(2)**:** 491-494.

Yamazaki H, Margolis HC (2008). Enhanced Enamel Remineralization under Acidic Conditions in vitro. *Journal of dental research* **87**(6)**:** 569-574.

Yao Y, Grogan J, Zehnder M, Lendenmann U, Nam B, Wu Z, *et al.* (2001). Compositional analysis of human acquired enamel pellicle by mass spectrometry. *Arch Oral Biol* **46**(4)**:** 293-303.

Zero DT (2006). Dentifrices, mouthwashes, and remineralization/caries arrestment strategies. *BMC Oral Health* **6 Suppl 1:** S9.

Zero DT, Fontana M, Martinez-Mier EA, Ferreira-Zandona A, Ando M, Gonzalez-Cabezas C, *et al.* (2009). The biology, prevention, diagnosis and treatment of dental caries: scientific advances in the United States. *J Am Dent Assoc* **140 Suppl 1:** 25S-34S.

Publications

Mohammed Sabar Al-Lami; Chris van der Walle; Clive G. Wilson. Preparation of amorphous calcium phosphate stabilised by acid hydrolysed carboxy methyl cellulose fractions. [Poster presentation]. In: 3rd PharmSciFair 2011, Prague, Czech Republic.

Mohammed Sabar Al-Lami; Chris van der Walle; Clive G. Wilson. Preparation of amorphous calcium phosphate stabilized by hydrolyzed casein as an alternative to casein phosphopeptides. [Poster presentation]. In: PharmaSci 2011. Nottingham, UK.